OBSERVATIONS ON THE ULTRASTRUCTURE OF HUMAN TUMORS WITH PARTICULAR REFERENCE TO THE ROLE OF TRANSMISSION ELECTRON MICROSCOPY IN TUMOR DIAGNOSIS

Volume 1

Bruce Mackay, M.B., Ch.B., Ph.D.

Emeritus Professor of Pathology, The University of Texas M.D. Anderson Cancer Center, Houston, Texas, U.S.A.

A Thesis submitted for the degree of Doctor of Medicine
The University of Edinburgh
2003

I declare that this thesis had been composed entirely by myself and that this is my own work except where I have indicated the contribution of others.

Professor Bruce Mackay

March 2003

Abstract

The advent of the electron microscope opened up for exploration a realm of biological structure far beyond that visible with the light microscope. Results from the study of normal cells and tissues came rapidly and were often spectacular. Application of the technique in pathology was slower to develop, but ultimately it became clear that early hopes for its potential as a diagnostic tool would not be realized. In certain areas of surgical pathology, transmission electron microscopy provided significant contributions, and for some decades it was a valuable and widely used diagnostic method, but its practical value diminished as newer procedures, notably immunohistochemistry, were introduced and their use burgeoned. The most fertile field for the application of electron microscopy in service pathology has been the study of tumors, and my experience with its use in a large comprehensive cancer center over a thirty year period is the basis for the thesis. During this time, over 35,000 specimens were accessioned for electron microscopy, most of them neoplasms. Many of the specimens were examined when they were received in search of information to clarify a problem diagnosis, and the collection became a resource from which I drew material for elective studies on particular types of tumors. I have conducted projects alone and with the participation of staff colleagues, department fellows, or visiting scientists. Findings were frequently reported in the literature and presented at scientific meetings in the United States and other countries.

The thesis begins with a brief account of the historical development of diagnostic electron microscopy. Practical considerations in the procurement and handling of specimens are then discussed. The major part of the thesis is an account and analysis of contributions that electron microscopy has provided in the study and diagnostic evaluation of human tumors, arranged under anatomic systems and structured around data from observations that I have made myself or with collaborators. Pertinent findings from a selection of my personal publications are briefly summarized and some are illustrated in order to demonstrate the breadth and variety of the information on tumor ultrastructure that electron microscopy has provided during the years that I have had the opportunity to apply the technique. The work of others in the field is frequently cited.

The thesis concludes with a discussion of the role of diagnostic electron microscopy in surgical pathology. I review practical considerations and detail how the effective use of electron microscopy in a surgical pathology department is enhanced by efficient organization, optimal utilization of technical facilities, integration with other routine diagnostic activities of the department, and liaison with clinical services. I contend that transmission electron microscopy has revealed much valuable data on the structure of normal and neoplastic cells, clarified the classification of certain categories of tumors, yielded insight into histogenesis, elucidated appearances seen in routine light microscopic sections and smears, facilitated correlation of morphology with immunohistochemistry, provided an often invaluable aid in the solution of diagnostic dilemmas, served as an effective resource in the instruction of pathologists in training, and enhanced presentations and publications on surgical pathology topics. The application of electron microscopy in surgical pathology is limited by economic considerations and a dearth of pathologists experienced in ultrastructural studies, but it continues to be a valuable resource in the examination and diagnosis of human tumors, and in research and education in pathology.

Introduction

The topic of the thesis is the fine structure of human neoplasms as it is revealed by the transmission electron microscope. I review a selection of original observations which I have made, alone or in collaboration, over a thirty year period, and use the findings to assess the role of electron microscopy in the study and diagnosis of tumors. I include a discussion of practical aspects of diagnostic electron microscopy based on my experience with its application in a large comprehensive cancer hospital.

My interest in electron microscopy began at the University of Edinburgh where I learned and used the technique as a postgraduate student in the department of anatomy, and I continued to apply it whenever there was an opportunity during subsequent training in surgery and pathology. In 1969, I received a position as staff pathologist at the University of Texas M.D. Anderson Cancer Center in Houston, Texas, with responsibilities in diagnostic surgical pathology, research, teaching and administration, and I developed and directed a diagnostic electron microscopy section which continues to be active now that I have retired.

My initial intention for this thesis was to present a comprehensive review of tumor ultrastructure, but it became necessary to modify the plan as the field expanded over the years. Instead, I have selected from my personal publications material which I believe collectively demonstrates the great diversity of ultrastructure that is encountered among human tumors, and which serves to illustrate the benefits of electron microscopy as well as its shortcomings. The topics are grouped under anatomic systems, and they are listed in the Table of Contents. Observations and discussion are correlated with précis of pertinent data from the selected publications. The text is frequently anecdotal in order to convey the relevance of observations at the time the work was performed. Since the field of study is so extensive, only a representative group of figures could be included, and with a few exceptions they illustrate ultrastructure. The text includes a short account of the historical development of diagnostic electron microscopy, views and recommendations concerning practical considerations in the application of the technique in a clinical setting, and my assessment of the past and current roles of transmission electron microscopy in the study and diagnosis of human tumors. Publications cited in the text, including some of my own that are not among those summarized, are numbered consecutively as superscripts and listed in the Bibliography. "Electron microscopy" is frequently abbreviated to EM in the text.

I performed the ultrastructural studies described in the thesis alone or with staff colleagues, department fellows, or visiting observers who participated under my direction. I was solely responsible for the EM portion of almost every project, and I took all the electron micrographs that are included in the thesis. In the few published studies in which a coworker did a major part of the practical work, this is made clear in the text. I have generally given residents and fellows precedence among the list of authors of my publications. Material was procured within our hospital or received for consultation, and is from the collection of over 35,000 electron microscopy specimens that have been accessioned for diagnostic study or research. Most of the tissue specimens for ultrastructural study were fixed at the time of procurement in buffered glutaraldehyde. A few were received in formalin, and on rare occasions tissue was recovered from paraffin. All but a few of the illustrations in the thesis were printed directly from negatives. Where a negative had been lost or damaged, I scanned micrographs from my publications. Approximate magnifications are given for the electron micrographs although I favor the practice of omitting numerical magnifications because they can be inaccurate and are usually unnecessary for biological material: publishers frequently manipulate the size of submitted figures without changing the magnifications, and many electron microscopes are only calibrated occasionally if at all. I believe that incorporation of a micron marker when it is needed is more meaningful.

I am deeply indebted to the many persons who have helped me by procuring tissue specimens, participating in the investigative studies, or performing technical procedures. Many of my publications correlate findings from electron microscopy with those from immunoperoxidase studies, and I am grateful to Dr. Nelson Ordonez, Chief of the Section of Immunohistochemistry, for our many years of collaboration and his immunohistochemical contributions to our joint publications. I planned, wrote, typed and printed the thesis and prepared, printed and mounted the illustrations.

Development of diagnostic electron microscopy

The pioneer in the development of electron lenses was Ernst Ruska, working at the Technical University in Berlin in the early part of the 20th century. Even before the electron microscope became commercially available in 1929, there was speculation concerning the impact that the instrument might have in science and medicine. Ernst Ruska[1] recounts that "my brother, Helmut Ruska, as a medical student, had already become clearly convinced that many sub-light microscopic agents of disease could perhaps now be made visible, and that cells ought to show the sub-light microscope structures, a knowledge of which must surely be valuable for the understanding of cell function". Most of the scientists whom the Ruskas consulted did not share this optimism, and skepticism, borne largely of ignorance, persisted for decades. Thus, Rosai[2] could write in 1981: "When I began my training in pathology some fifteen years ago, the possibility that this technique could contribute to the understanding and diagnosis of human tumors was not generally accepted by pathologists. Some people thought that the technique was too cumbersome and expensive; others had the strange attitude that it was somehow demeaning for such a wonderful method to be used for something as trivial as a microscopic diagnosis; still others felt that this technique was unnecessary as long as highly competent and experienced surgical pathologists were available to examine the hematoxylin-eosin sections".

The first electron microscopes were extremely primitive by today's standards, and many years elapsed while procedures for preserving, processing and sectioning tissues were developed and gradually improved[3-5]. A buffered solution of glutaraldehyde became the standard fixative, generally followed by post-fixation with osmium tetroxide to enhance image contrast in the electron beam, and methacrylate gave way to epoxy resin as an embedding medium. To cut suitably thin sections of the hard tissue blocks, glass knives were initially used but they were later replaced by more costly but much more durable diamond knives. Solutions of salts of heavy metals were prepared to stain the sections and improve contrast. As these advances were taking place, technical aspects of the instrument including resolution and ease of use were greatly improved.

The advent of the electron microscope rapidly revolutionized morphologic studies and produced dramatic advances in anatomy and biology. Application in pathology progressed more slowly. Before the value of the technique in pathology could be adequately assessed, it was necessary that many pathologists have access to electron microscopes, and for them to use the instrument to study a wide range of specimens of diseased tissues. The process took decades, but it eventually became apparent that most of the common problems in surgical pathology could still be performed adequately using the conventional optical microscope. For certain specimens, however, the great increase in resolution provided by the electron microscope proved invaluable. Use of EM in the assessment of renal biopsies became standard practice, and contributions in the study of various non-neoplastic lesions were identified[6-8]. Ultimately, the most extensive role of EM in diagnostic pathology emerged as the study of neoplasms[9-12].

The use of EM as a diagnostic tool was limited by a number of factors. The instrument was costly, and adding to the expense of setting up a laboratory were the need for elaborate facilities including a dedicated room fitted out for the microscope itself, ancillary equipment including ultramicrotomes and diamond knives, and skilled technical help. Inevitably, most units were located in large hospitals and medical centers where they could be shared by researchers. Pathologists without direct access to a facility could readily send their specimens to such a facility for consultation.

In the past two decades, the extent to which the electron microscope is used in surgical pathology has diminished greatly, for a number of reasons. One is the burgeoning application of immunoperoxidase techniques which often provide the same diagnostic information as can be obtained with EM. There is obvious benefit in a method which can be applied in any laboratory using commercial reagents and interpreted by every pathologist. Performance of immunohistochemistry also supplements the revenue of the laboratory while diagnostic EM is rarely cost-effective. Despite the expense of reagents and some risk of misinterpreting findings, immunohistochemistry soon replaced EM as a complement to routine light microscopy in the approach to diagnostic problems in most laboratories. Economic factors also came into play. The emphasis on cost-containment in medicine in the United States tended to limit the use of EM to situations where it could be anticipated that the results would be of significant value in patient care, thereby justifying levy of a charge to the patient. With the reduction in use of the electron microscope as a diagnostic tool, and the resulting diminution in workload and revenue, many laboratories found that an EM diagnostic service could no longer be maintained.

A further reason for the limited use of diagnostic EM has been a shortage of pathologists trained in ultrastructural pathology. Only a small minority of residents/fellows are exposed to practical EM in the course of their training, and the minimal experience they obtain does not equip them to study and evaluate diagnostic specimens. Some laboratories employ non-medical personnel to perform the EM on diagnostic specimens, but work of this nature can no more be effectively performed by a non-pathologist than can the interpretation of light microscopic sections or cytologic smears. The assessment of tumor specimens with the electron microscope should be carried out by a pathologist who is competent in routine surgical pathology and sufficiently knowledgeable about tumor ultrastructure to be able to detect and evaluate criteria that are relevant in differential diagnoses, and who can in addition correlate the pathology findings with available clinical and radiological data.

The consequence of these exacting requirements is that EM diagnostic services are now confined almost exclusively to large hospitals and medical centers.

Specimen procurement and processing

In this section, material and methods that have been used in my EM service are described and discussed.

Most of the tissue specimens for EM that I have studied were obtained in the ideal environment of the frozen section laboratory. At the M.D. Anderson Cancer Center, this is an extensive facility located within the operating room complex. A pathologist and pathology fellows staff it during the day and are on call at nights and during weekends. The specimens are often carried to the laboratory by the surgeon for intraoperative consultation, or they are delivered by a nurse or orderly. Since the specimens are usually received promptly, preservation of the portion taken for EM is as a rule extremely good. Specimens

from wards and clinics are also hand-carried to the frozen section laboratory for immediate or elective evaluation, but some of the latter are fixed in formalin. Most tissue specimens submitted from outside the hospital are formalin-fixed and they are sent wet or in paraffin, but a small percentage are submitted specifically for EM in glutaraldehyde.

The importance of obtaining good material for diagnostic EM can not be overemphasized. While it is generally possible to obtain some information from the ultrastructural study of a specimen that has been fixed in formalin, or even of material that has been recovered from a paraffin block, the superior quality of glutaraldehyde-fixed tissue is immediately evident from the crisp cellular detail and sharply defined relationships among tissue components, and it invariably reveals more extensive and accurate data.

The idea that pathology residents automatically know how to correctly take specimens for EM is a false assumption. If they adopt the same practice as is used for routine light microscopy, the results will range from poor to disastrous. A walnut-sized lump of tumor nestling in a small amount of fixative solution may be provided for the ultrastructural study and the EM technician must attempt to salvage useable tissue by shaving the surface and ignoring the possibility of drying artifact. Residents need to be instructed at the beginning of their rotation in the department in how to select and handle material for EM. If most of the specimens are procured at a particular location, as for example in the frozen section laboratory, it is also beneficial to instruct the technicians in that area on how the tissue should be handled. In the event that a clinician wishes to procure a specimen specifically for EM, detailed instructions on how to select, handle and preserve the tissue should be provided, and it may be simpler and more effective to have an experienced technician on hand at the time of the procedure if this is feasible. A core needle biopsy can simply be dropped into the fixative, but an open biopsy or larger specimen requires prompt and efficient attention. Most clinicians have little appreciation of the importance of careful and rapid handling of tissue specimens for EM.

There is an advantage to having a source of small specimen bottles containing buffered glutaraldehyde available wherever tissue specimens are grossed within the pathology department, and to maintain a supply in wards and clinics if specimens are obtained in these locations. Each specimen bottle should be labeled in order that the accession number can be written on it at the time the specimen is obtained, or an addressograph label can be affixed. Brief instructions on how to take solid tissue for EM can be printed on the specimen bottle label and they should include the information that it is not necessary to refrigerate the specimen bottle after the specimen has been placed in it. The risk of the bottle being placed in a freezer is in this way obviated. The strength of the solution of buffered glutaraldehyde can range from 1% to 4% but 2% is widely used. The type of buffer is not of great importance for pathology specimens and phosphate or cacodylate are popular. Since the shelf life of active buffered glutaraldehyde is relatively short, the supply of specimen bottles should be replenished and unused bottles replaced at intervals of not longer than two weeks.

The tissue for EM must of course be representative, and it should be selected as soon as possible following excision, handled gently to avoid crushing artifact, and immersed in fixative immediately to minimize distortion from air drying. The majority of specimens taken for EM are from solid tumors. When tissue is obtained from a large resection, it should be selected as soon as the specimen is received since the blood supply was interrupted some time earlier and the surface has probably been subjected to air-drying effect. Some resected specimens sit in a container in the operating room for a considerable time before being brought to the pathologist. Even minor degrees of deterioration in the tissue structure are conspicuous at the ultrastructural level.

Residents often ask what criteria should be followed in deciding whether to take tissue for EM while working in the frozen section laboratory, and the short answer is that material should be obtained whenever there is a possibility that ultrastructural study might be useful in the course of the diagnostic evaluation or prove instructive academically. An indication can often be perceived when a frozen section is examined, or the pathologist or clinician may know from reports on earlier accessions that the diagnosis is liable to be difficult. It takes less than a minute to take and record a specimen for EM, and in the frozen section room a technician will generally perform the documentation. Small index cards listing the information that should be provided (patient's name and hospital number, pathology accession number, site of specimen, 'diagnosis' versus 'interest') ought to be kept available beside the supply of glutaraldehyde-containing specimen bottles, and the card accompanies the specimen to the EM laboratory.

When material is to be selected from a solid specimen for EM, it is often possible to identify viable areas while inspecting the cut surface, but the gross appearance can be misleading, especially with recurrent tumors and following therapy. If there is concern that the selected tissue might not be suitable, a frozen section or a smear or touch preparation can be examined to confirm that tumor is present and is of acceptable quality for ultrastructural evaluation.

Crushing artifact can greatly detract from the value of a tissue specimen and even render it worthless. Some degree of distortion is evident in light microscopic sections of small biopsies taken for routine light microscopy, but even slight tissue damage is obvious when the tissue is examined with the electron microscope. A specimen that would otherwise have been suitable can be rendered useless by poor handling. Squashing of the tissue can be produced by rough manipulation or while slicing it with a blunt blade. Drying effect will inevitably be present if the material for EM is taken from a surface that has been exposed for some minutes. A fresh cut surface must be opened before the tissue is taken, and the specimen for EM should be gently sliced from the surface, letting the sharp knife blade do the work and keeping the slice less than a millimeter in thickness. A thin tapering wedge is acceptable since the EM technician can select from the thinner areas. The severed slice can be lifted on the knife blade till it is over the specimen bottle and gently pushed off to fall into the fixative solution. It should not be held in forceps, nor should it be minced into small pieces. A thin slice will fix adequately as the fixative penetrates from both sides, and it can then be diced into small cubes without fear of crushing or drying.

In order to harvest undistorted cells for ultrastructural study from certain types of specimens, they must be procured and processed in special ways. From experimentation over a period of time, the following methods were preferred for use at the M.D. Anderson Cancer Center.

Solid tissue.

A thin slice or wedge of tissue is fixed in 2% buffered glutaraldehyde and embedded in epoxy resin. Semi-thin sections are cut with glass knives and stained with methylene blue for evaluation with the light microscope. Thin sections are cut with diamond knives and stained with uranyl acetate and lead citrate. (Reichert ultramicrotomes were preferred, and the electron microscopes used in the studies described in the thesis were Zeiss EM9S, Phillips EM10, and JEOL 1200EX instruments).

Fine needle aspiration biopsy (FNA).

There has been a steady increase in the use of fine needle aspiration biopsies as the primary material for evaluation of a suspected neoplasm. Initial results using these preparations for

EM were extremely disappointing, with low yields of pertinent tissue and distortion so severe that the study could be of no value. With the cooperation of cytology colleagues, I therefore experimented with procedures designed to improve the yield and quality of the preparations, and the method that we finally adopted was described in the following report.

Mackay B, Fanning T, Bruner JM, Steglich MC. Diagnostic electron microscopy using fine needle aspiration biopsies. Ultrastructural Pathology 11:659-672, 1987.

We conducted a series of experiments with cells aspirated form rat liver to investigate the feasibility of using physiologic solutions as holding media. Cells were placed in a several solutions for intervals of 15 minutes to one hour then spun down to form pellets which were fixed in glutaraldehyde and processed for EM. Without exception, these procedures produced changes in the fine structure of the liver cells that were at least obvious and often severe. Much of the damage was to mitochondria and other intracytoplasmic membranes, but after longer exposures, cell membranes and nuclei were also distorted. Normal saline was particularly prone to cause structural devastation.

A frequent problem with fine needle aspiration biopsy specimens is heavy contamination by erythrocytes. To investigate the possibility of removing contaminating blood cells from a specimen, aspirates of rat liver were hemolysed for 10 or 30 seconds with distilled water, 2 M urea, or 0.8 M NaCl: isotonicity was promptly reestablished with buffer. Hemolysing agents were effective in reducing the number of erythrocytes but at the expense of damage to the cellular structure. Gradient centrifugation in a Ficoll medium provided cells with acceptable preservation of their fine structure, but it was technically difficult or impossible to recover the desired cells when they were few in number.

The most reproducible method we could find to harvest undistorted tumor cells from fine needle aspiration biopsies was based on the technique advocated by Akhtar et al[13] in which the cells are first fixed then passed through a fine filter. In our modification of Akhtar's procedure, the aspirate is promptly expressed from the syringe into a vial containing 10 ml of buffered 2% glutaraldehyde and the container is gently agitated to prevent clotting and maintain dispersion of the cells. After one hour, any floating material is withdrawn using a Pasteur pipette, transferred to buffer, and processed as specimen A. The remainder of the specimen is poured into the barrel of a syringe which is attached to a 25 mm Gelman syringe-type filter holder containing a 25 mm diameter circle of 20 micrometer Spectra/Mesh N (nylon) woven filter screen (Fisher Scientific). Circular filters of the desired size are prepared by placing a sheet of the nylon screen on a clean firm cutting surface and striking it with a metal punch. The specimen is allowed to pass through the screen by gravity. Vial and syringe are then rinsed with buffer and filtration of this washing solution can be aided by gentle pressure on the plunger of the syringe if needed. It does not appear to be beneficial to repeat the procedure more than once. The screen is then lifted off the surface of the filter by grasping it by the edge with fine forceps and it is placed in a specimen bottle containing 10 ml of buffer and agitated gently to dislodge the cells. The filter is removed and the specimen is spun down at 1500 rpm for 5 minutes in a conical glass tube. Depending on its size, the pellet is processed as a single EM tissue block or divided into more than one block. The pellet may remain intact during processing but if it breaks up it is recentrifuged at the end of that solution change. This is specimen B. Semi-thin sections of the plastic embedded material are examined and areas of a block containing groups of cohesive cells are preferred to isolated cells when both are available.

Advantages of FNA are prompt scheduling, convenience for the patient, low morbidity and rapid reporting. The accuracy of positive and negative findings by light microscopy is high but evaluation can be hindered by the small amount of material and by the customary fragmentation of the specimen which tends to obscure or obliterate architectural features that would provide useful clues in tissue sections. Even with ideal preparations, the classification of a tumor can not always be achieved, and cell blocks may not be available to provide light microscopic sections. It can then be helpful to have input from EM. An indication that EM might be of value in a particular case may come from clinical data or an earlier specimen, or it can often be recognized when perusing the rapid smear performed at the time of the FNA procedure to confirm that the specimen is representative.

The fine needle aspirate can be directly expressed into fixative and this will result in good preservation and little loss of material, but disadvantages are the common presence of necrotic debris and often large numbers of erythrocytes. Sparse tumor cells are then likely to be lost within a sea of red cells. The filtration procedure has in our experience yielded cells suitable for evaluation in most of the specimens so processed. When the cells are sparse, multiple semi-thin sections may have to be examined in order to detect a suitable area of a tissue block from which to cut thin sections.

Bone marrow aspiration biopsy.

If a heparinized bone marrow aspirate is placed in glutaraldehyde and then centrifuged, peripheral blood cells will greatly outnumber the other cells that are present making it difficult or impossible to locate the cells of interest for study. The preferred method is to centrifuge the heparinized aspirate in a hematocrit tube then remove the buffy coat using a fine pipette and slowly express it into buffered glutaraldehyde: if done carefully, the cells remain together in a wormlike coil which can be sliced into small pieces once fixed. An elegant but technically more demanding procedure is to centrifuge the aspirate in a tube of larger bore and then to remove the overlying plasma and gently layer fixative on top of the buffy coat. After it has fixed, the disc can be dislodged with a mounted needle and sliced into small cubes. Gradient separation of different cell types can then be detected in the semi-thin sections.

Core bone biopsy

Decalcifying agents produce severe damage to the structure of cells, and those in a core bone biopsy may not be evaluable after being immersed in EDTA. Though technically feasible, it is inconvenient to have to thin-section undecalcified bone for EM. The preferred procedure is to immediately place the core biopsy in glutaraldehyde. When it has fixed, it is possible under a dissecting microscope to dislodge the contents of the marrow spaces using pointed forceps or a hypodermic needle, and they can then be spun down and processed in the same way as solid tissue specimens.

Body fluid

If an effusion is not frankly bloody, it is centrifuged to provide a pellet of cells which is then fixed in glutaraldehyde. When the effusion is hemorrhagic, many of the blood cells can be removed by brief hemolysis followed by rinsing in buffer. A brief episode of mild hemolysis will cause minor damage to cell structure but it is an acceptable compromise because of the concentration of tumor cells that is achieved. The pellet obtained following centrifugation is fixed and processed as for solid tissue. Specimens of urine and cerebrospinal fluid can be centrifuged but the yield of cells is consistently meager and it may

be necessary to add a drop of agar to the centrifuged deposit to keep the cells together while they are processed.

Tissue processing

It is technically feasible to fix and hand-process tissue for EM in less than five hours, but frequent solution changes are needed and the procedure is labor-intensive requiring virtually constant attention by a technician so it is not suitable for routine use in a busy department. Automated tissue processors for EM specimens are available but the time required for set-up and cleaning only justifies their use when at least a moderate number of specimens are to be processed. Few laboratories have this volume of EM accessions on a regular basis. Surgical pathology specimens should be processed without waiting to learn whether they will be required for diagnostic study, since that decision is not as a rule made before the routine light microscopic slides have been examined, and is often deferred until immunohistochemistry has been performed. It is consequently useful to have the EM tissue embedded so that the blocks can be sectioned as soon as a request for diagnostic study is received. In this way, a verbal report from the pathologist performing the EM can be provided within two hours. A printed report and selected micrographs follow later. In my laboratory, EM tissue was routinely processed on the day after it was received and the blocks were allowed to polymerize overnight, thereby being ready for sectioning the following morning. A diagnostic report could routinely be issued within 48 hours of the time of accession of the specimen.

Specimens taken from tumors for EM may yield from one to many cubes of tissue, each smaller than 1 mm in size, and some discretion is needed in deciding how many blocks of tissue should be placed in the standard pointed-tip embedding capsules. My experience has been that it suffices to place up to five tissue blocks in capsules, and to embed up to fifteen more in an inverted plastic specimen bottle cap. On the few occasions in which the initial five blocks do not prove adequate, tissue can be recovered from the reserve supply by sawing or punching the pieces from the disc and reembedding them in capsules. Any extra tissue is retained in glutaraldehyde in the original labeled specimen bottle: none of the accessioned material is ever discarded until the case has been completed.

Section preparation

The first step in the EM study of a specimen is to examine sections of the plastic-embedded tissue with the light microscope. Sections are prepared from two blocks taken from the embedding capsules: more are cut if needed but in many instances it is not found to be necessary. The procedure is routine but is summarized here. Semi-thin sections are usually cut with glass knives and they are roughly one micrometer thick and may be referred to as semi-thin sections, or as "thick" sections to contrast them with the much thinner sections used for the EM. They may also be called "blue" sections because the dye that is used to stain them is commonly methylene blue or toluidine blue. In the staining of semi-thin sections, the plastic is not removed. A section is placed on a drop of water on a glass microscope slide which is then laid on a hot place, and the section adheres as the water evaporates. When a drop of stain is placed on the heated section, the staining process takes only seconds. Good preservation and virtual absence of shrinkage result in improved tissue architecture and cellular detail compared with that seen in routine paraffin sections, and significant diagnostic information can often be gleaned from the semi-thin sections.

The stained semi-thin sections should be studied by the pathologist who will perform the EM and by the technician who will cut the thin sections, ideally doing this together using a multi-head light microscope in order to agree on the most suitable block and how it should be

trimmed prior to cutting the thin sections. For the evaluation of a tumor, a representative thin section from one block is usually sufficient, but occasionally it is necessary to section more than a single block. The method for staining the thin sections is a routine procedure in an EM laboratory. The grid bearing the thin sections is inverted on a drop of each stain solution on a paraffin sheet for five minutes. The staining should be performed within a closed cabinet to minimize contamination from dust in the air. The stained grid is laid, section side up, on fresh filter paper (at the edge of which the specimen and grid numbers have been written in pencil) in a covered small petri dish and allowed to dry before it is introduced into the electron microscope.

Tumors of the skin

The tumors discussed in this section are squamous cell carcinoma, neuroendocrine carcinoma, and melanoma.

Squamous cell carcinoma

A primary cutaneous squamous cell carcinoma can usually be recognized by routine light microscopy since the tumor cells resemble those of the normal epidermis, and there is a corresponding similarity at the ultrastructural level. The tumor in figure 1, which was extensively infiltrating the lower lip of a 12-year-old boy with xeroderma pigmentosum, is well differentiated and a typical example. The cells have round to angular profiles and considerable quantities of cytoplasm that contains dense bundles of keratin filaments. The filaments help the cell to resist deformation, and they are able to maintain the integrity of the tissue through their connections with the attachment sites that hold the cells together[14]. Cell junctions between squamous cells are desmosomes, and where the cells are in contact with the basal lamina they are hemidesmosomes. Small numbers of gap junctions have been identified in squamous cell carcinoma[15], but the desmosomes dominate visually. Irregular clefts intervene between neighboring squamous cells and the desmosomes are located at the tips of slender protrusions of the peripheral cytoplasm (figure 2). These connections between the cells correspond to the "intercellular bridges" of the light microscopist.

Squamous cell carcinoma serves to illustrate how ultrastructural features that characterize normal cells are progressively lost in malignancy. The classic appearance is also altered in a number of uncommon variants of squamous cell carcinoma and EM reveals details of the structural changes that have taken place. Dedifferentiation and variation in tumors account for the broad spectrum of morphology with which the electron microscopist is confronted, and are largely responsible for difficulties in differential diagnosis. As a squamous cell carcinoma dedifferentiates, there is a gradual loss of the distinctive squamous features. Tonofilaments become sparse and ultimately disappear. Desmosomes are reduced in number and size, and their mature structural characteristics are lost resulting in paired subplasmalemmal densities on adjacent cells. Accompanying these changes are the cytologic alterations familiar to the light microscopist including loss of cytoplasm and organelles, increase in irregularity of cell and nuclear profiles, chromatin clumping, and prominence of nucleoli. As the cell attachments become primitive and ultimately disappear, cohesion between neighboring cells is lost and gaps of increasing size and irregularity form among the cells (figure 3). A basal lamina may still be detected after the tumor has become invasive[16], but by this time it is generally incomplete[17], and it is not usually evident in the less differentiated and metastatic neoplasms.

In some invasive squamous cell carcinomas, the cells alter from their usual round to polygonal shape and become fusiform, and this spindle cell transformation can make it difficult to distinguish the carcinoma from a soft tissue neoplasm so the term sarcomatoid carcinoma is often used. The diagnosis of a spindle cell neoplasm of the skin may be uncertain from routine light microscopy[18] and it is facilitated by ultrastructural evidence that the neoplastic cells contain tonofilaments and are connected by desmosomes[19] (figure 4). Since these features are only seen in some squamous cell carcinomas, EM is not always helpful: the presence of primitive cell junctions is not by itself a reliable indicator of squamous differentiation. Now that immunoperoxidase techniques are available, staining for cytokeratin is commonly used to resolve the issue, and it is necessary to keep in mind that the occasional malignant soft tissue neoplasm is keratin-positive.

A variant of cutaneous squamous cell carcinoma which can simulate adenocarcinoma in hematoxylin/eosin sections has been called an adenoid or pseudoglandular form[20]. EM has shown that light microscopic simulation of glandular differentiation may be produced by more than one type of structural change. Keratin is not always evenly distributed and it can form a dense aggregate in one area of the cytoplasm (figure 5) that are visible as eosinophilic foci in hematoxylin/eosin-stained paraffin sections[21, 22]. The cells may have large numbers of filopodia and few desmosomes and these surface projections are particularly conspicuous when cells separate (figure 6). Vacuoles are not common in squamous carcinoma cells, but if they are numerous and confluent, a signet-ring appearance can result[23] (figure 7). Vacuoles have also been seen in basal cell carcinoma[24]. A rare cause of electron-lucent zones in squamous cells is accumulation of cytoplasmic glycogen: the tumor in figure 8 originated in the skin of the thumb and metastasized first to axillary lymph nodes and then to brain, and when cells from all three locations were compared by EM, only those in the brain metastasis contained vacuoles. The cytoplasm may also appear optically clear in routine light microscopic sections when lysosomes accumulate in the course of degenerative changes[25].

Keratin and desmosomes are seen in skin tumors other than squamous cell carcinoma. Both are found in cutaneous basal cell carcinomas (figure 9) though not with the consistency or to the degree seen in squamous tumors. Keratin is plentiful in some adnexal tumors (figure 10), but other features are as a rule also present indicating differentiation towards particular adnexal structures.

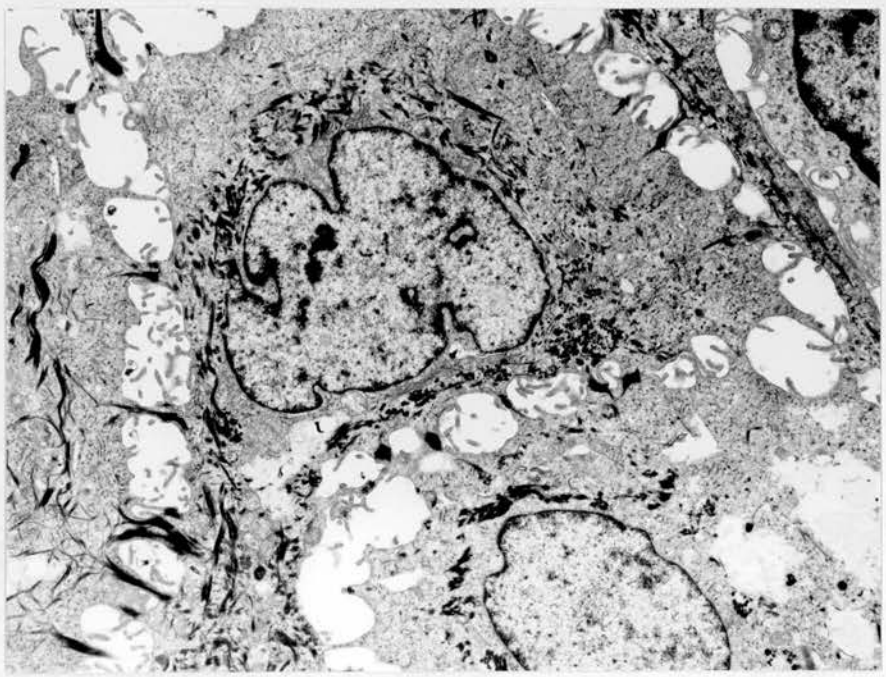

Figure 1. Squamous cell carcinoma of lip. The cells of this well-differentiated tumor contain moderate amounts of keratin and they are connected by frequent desmosomes. x 5,700.

Figure 2. Same tumor as figure 1. The desmosomes connect finger-like protrusions that bridge the gap between the two cells. Keratin filaments insert on the desmosomes. x 17,000.

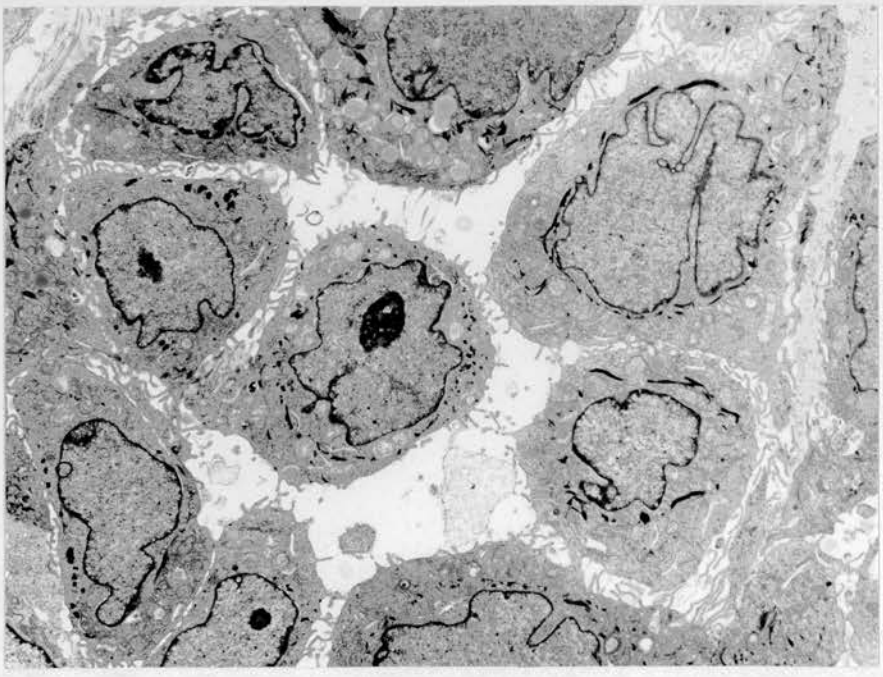

Figure 3. Squamous cell carcinoma. A poorly differentiated cutaneous tumor. Very few desmosomes are present and the cells are losing cohesion. x 3,200.

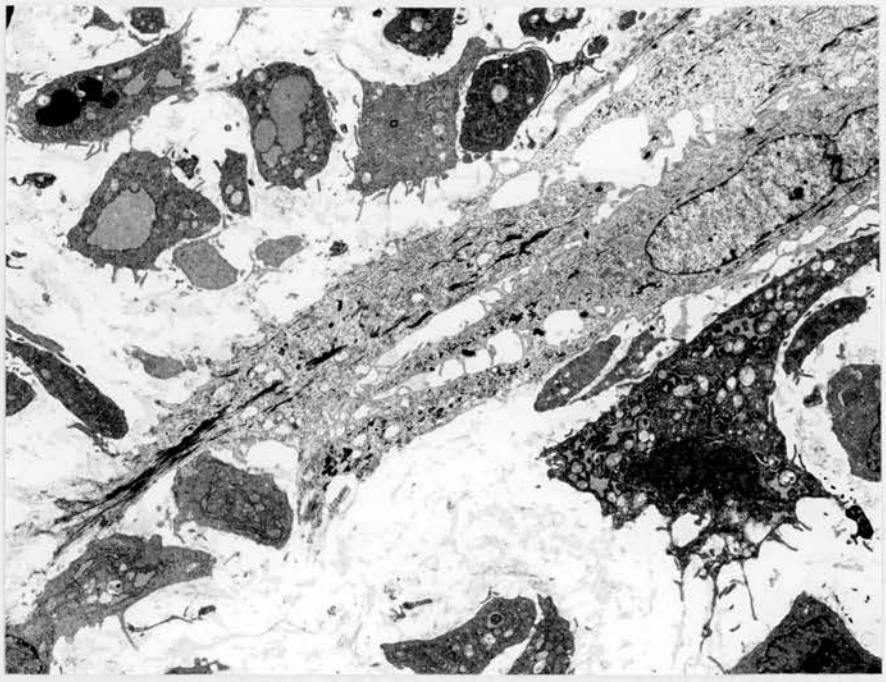

Figure 4. Sarcomatoid squamous cell carcinoma of skin. Keratin filaments are present in the elongated cells and there are occasional desmosomes. x 3,700.

Figure 5. Squamous cell carcinoma of skin. Aggregates of keratin were visible in hematoxylin/eosin-stained paraffin sections as eosinophilic inclusions. x 19,000.

Figure 6. Squamous cell carcinoma. In this preauricular skin lesion, desmosomes were infrequent and keratin was not seen, but many filopodia projected from the cell surfaces. x 10,600.

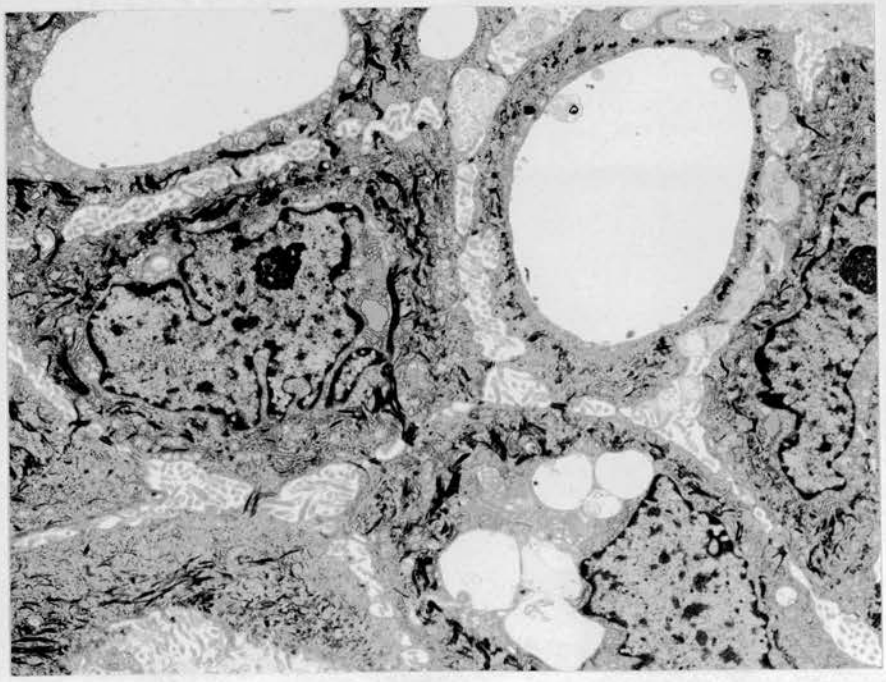

Figure 7. Squamous cell carcinoma. Many cells in this cutaneous tumor contained vacuoles. x 5,200.

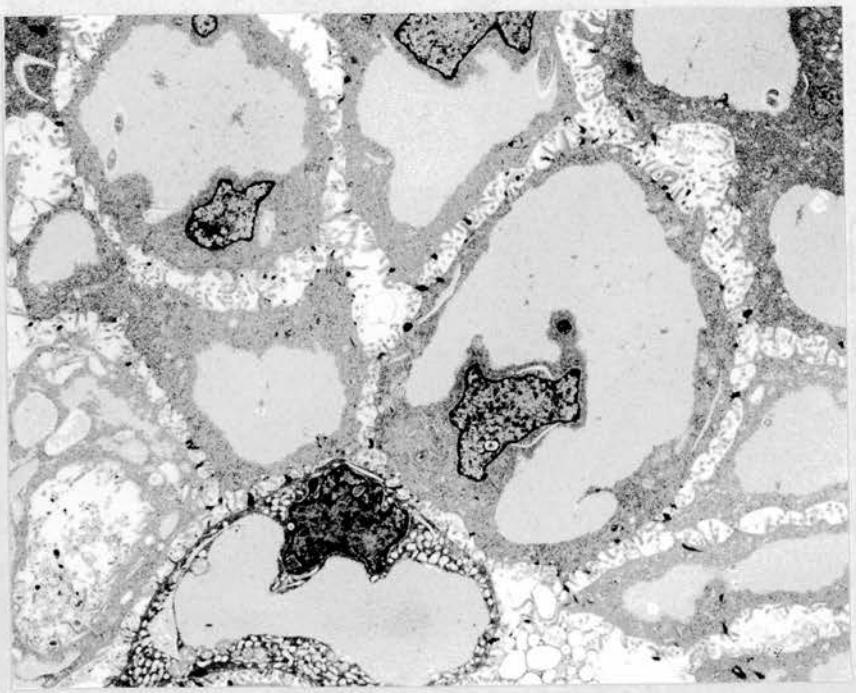

Figure 8. Squamous cell carcinoma of skin, metastatic in brain. The cells contain extensive glycogen. x 4,700.

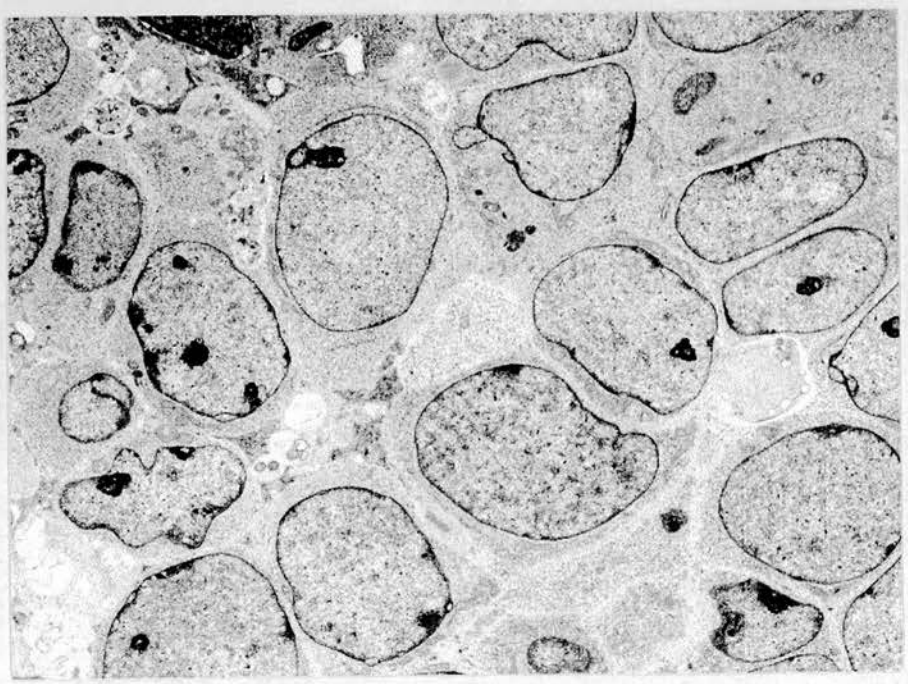

Figures 9. Basal cell carcinoma. The cells and nuclei have smooth profiles and fine chromatin. x 3,200.

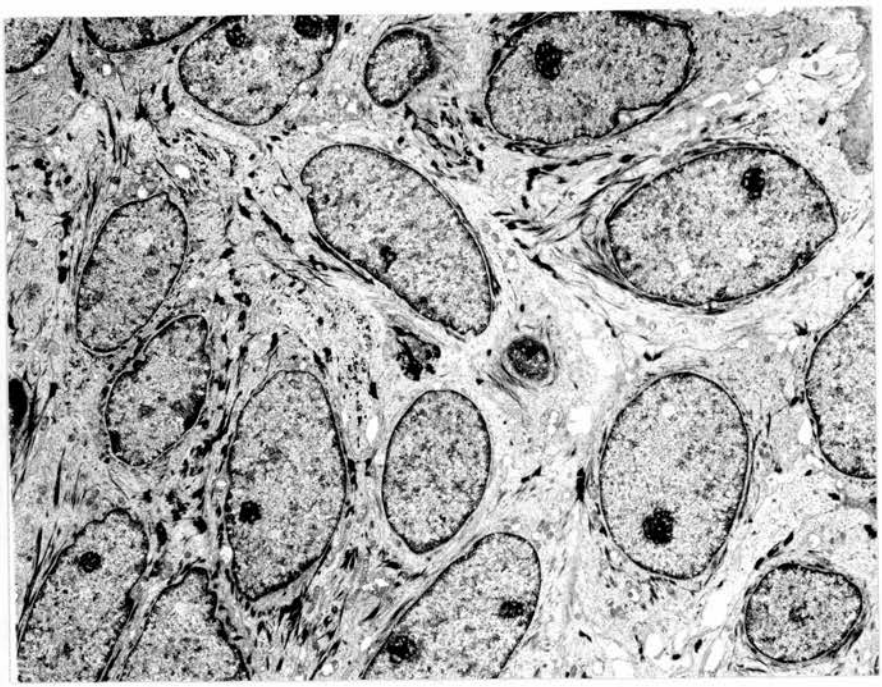

Figure 10. Adnexal carcinoma. Keratin is plentiful in the cells. x 3,400.

Neuroendocrine carcinoma

In 1976, with two colleagues, I published nine cases of small cell tumors in which I had observed by EM what appeared to be neural features with some resemblance to those seen in pediatric neuroblastomas. The youngest patient was 15 when his primary tumor presented in the nasal cavity, and the oldest was 72, so I used the umbrella designation 'adult neuroblastoma' for the nine tumors although there were clearly clinical and some structural differences among them.

> **Mackay B. Luna MA. Butler JJ. Adult neuroblastoma. electron microscopic observations in nine cases. Cancer 37:1334-1351, 1976.**
> Nine patients whose ages ranged from 18 to 72 had small round cell neoplasms which were found on EM to have some of the ultrastructural features seen in neuroblastomas of childhood including small cell size, sparse cytoplasm and organelles, and dendritic processes containing small dense-core, membrane-limited granules. The primary tumor was retroperitoneal in one patient. In a second patient, liver and bone metastases were present and the primary site was not determined. The tumor presented in a peripheral location in the other seven patients (leg in 2, buttock in 1, head and neck in 4) and all seven tumors spread to regional lymph nodes. One of the two tumors that arose in the nasal cavity displayed ultrastructural evidence of olfactory differentiation.

Three of the nine tumors presented in the skin and there was no indication that tumor was present elsewhere. A fourth tumor could also be classified as neuroendocrine carcinoma of the skin. I was teaching the histology course at the University of Texas Medical School at the time and was familiar with an illustration in the textbook[26] of the epidermal cell described by Merkel in 1865[27]. The Merkel cell is part of the dendritic cell population of the

epidermis, and studies suggest that it has a role as a slowly adapting mechanoreceptor involved with mediating the sense of touch[28]. Four years earlier, Toker had reported five small cell skin tumors which he named trabecular carcinomas, and he suggested sweat gland origin[29]. As we gathered and studied more cases, it was apparent that these were the same tumors although a trabecular pattern was not common in our series. Tang and Toker reported three additional cases in 1978 with the observation that they contained membrane-bound granules[30]. The tumor is now frequently referred to as Merkel cell carcinoma.

Silva EG, Mackay B. Neuroendocrine (Merkel cell) carcinomas of the skin. an ultrastructural study of nine cases. Ultrastructural Pathology 2.1-9, 1981.
Nine neuroendocrine carcinomas of the skin were examined by light microscopy and EM. The average age of the seven males and two females was 57 years. Seven of the tumors arose in the head and neck. Contact with the epidermis was only seen in two cases. Three tumors recurred locally, and in seven patients regional nodal metastases developed. Three patients died from disseminated disease. The dominant ultrastructural characteristic was the tumor cell processes which contained granules that were mostly 100 to 120 nm in diameter. Granules accumulated within the processes and only a few were visible in the cell body. In contrast, in normal Merkel cells that were examined, granules were present in considerable numbers within cell body and processes.

Ro JY, Ayala AG, Tetu B, Ordonez NG, el-Naggar A, Grignon DJ, Mackay B. Merkel cell carcinoma metastatic to the testis. American Journal of Clinical Pathology 94:384-389, 1990.
Two cases of clinically detected testicular metastases from Merkel cell carcinoma were reported. They were the first to occur at this site. One patient was a 73-year-old white man in whom a Merkel cell carcinoma of the upper lip had been treated one year earlier by local excision followed by radiation. Multiple subcutaneous and liver metastases subsequently developed, and the right testis was also involved. The skin primary in the second patient, a 47-year-old white male, was on the left elbow, and a year after it had been resected, a right testicular metastasis was detected followed two months later by involvement of the left testis.

Neuroendocrine carcinoma of the skin is composed of small cells with round to oval nuclei that have smooth profiles, fine dispersed chromatin, and rather small nucleoli. There is often little to be seen in the thin layer of cytoplasm other than free ribosomes and occasional mitochondria (figure 11). Cell junctions can usually be found but they tend to be scattered and small, and they are more likely to be desmosome-like than mature desmosomes. There are few if any visible tonofilaments. A similar appearance is seen in metastases (figure 12). A perinuclear aggregate of fine filaments is sometimes observed in many of the cells (figure 13) and when present it correlates with the distinctive punctate staining for keratin seen by light microscopy in immunoperoxidase preparations. The dendritic processes vary greatly in number and they may be sparse, requiring some searching before one is detected. A fortunate plane of section shows a process arising from a cell (figure 14). The processes are more likely to be cut in cross or oblique section and they tend to form small clusters that separate neighboring cells: their presence disrupts the uniform spacing of the nuclei (figure 15). Microtubules are occasionally detected in the processes but they are rarely numerous and are often absent. The small dense granules are of neuroendocrine caliber, being around 100 nm in diameter, and they are much more numerous in the processes (figure 16). These are the typical appearances, present to varying degrees in the primary tumors and also visible in many nodal and distant metastases, although the cell and nuclear shape may be more irregular in metastases.

Our early clinical studies of neuroendocrine carcinoma of the skin were facilitated by EM confirmation that the tumor was indeed neuroendocrine, although with experience it became possible to at least strongly suspect the diagnosis by routine light microscopy. The monotonous distribution of cells in the primary tumor, often separated from the overlying epidermis by an uninvolved band of superficial dermis, was helpful. However, in 19% of our cases, the epidermis over the tumor has been ulcerated. We encountered cases that had earlier been interpreted as basal cell carcinoma, both in primary and metastatic sites. At least 10% of our tumors contained foci where the cells had lost cohesion, simulating a lymphoma. Immunoperoxidase demonstration of chromogranin A, the major protein in granules of the diffuse endocrine system, can be helpful.

> **Silva EG, Mackay B, Goepfert H, Burgess MA, Fields RS. Endocrine carcinoma of the skin (Merkel cell carcinoma). Pathology Annual 19 Part 2:1-30, 1984.** Observations on the histopathology and clinical behavior of 67 cases of cutaneous neuroendocrine carcinoma were reported, with data from EM study of 45 of the tumors. All areas of the head and neck were involved but only 3% (2 cases) were on the scalp. The tumor did not often arise in the trunk but two were on the midback. It did not occur on the palm and only one involved the sole. Three patients were under the age of 40 and 73% were male. One patient was black. Twenty-seven tumors were under 1 cm and 26 were between 1 and 2 cm.

The 67 cases in this paper, published in 1984, brought the total number reported to over 200. Local recurrence was documented in 39% of our cases, after an average interval of 4.5 months, and the tumors had a tendency to spread to regional lymph nodes while the primary was small. Nodal extension was seen in 78% of the patients whom we were able to follow. The growth characteristics of the tumor cells have been studied in nude and athymic mice and the tumors recapitulated their aggressive behavior and retained histopathologic features of the primary skin tumors[31]. Before making the diagnosis of a primary or metastatic neuroendocrine carcinoma of the skin, the possibility of a metastatic small cell tumor from another site must be ruled out.

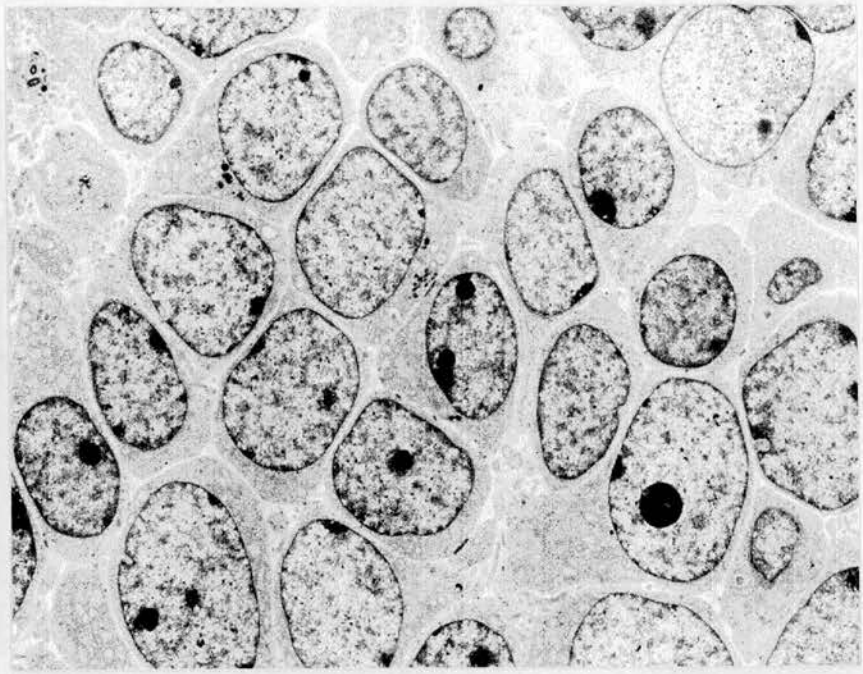

Figure 11. Neuroendocrine carcinoma of skin. The cells are small with sparse cytoplasm. x 3,900.

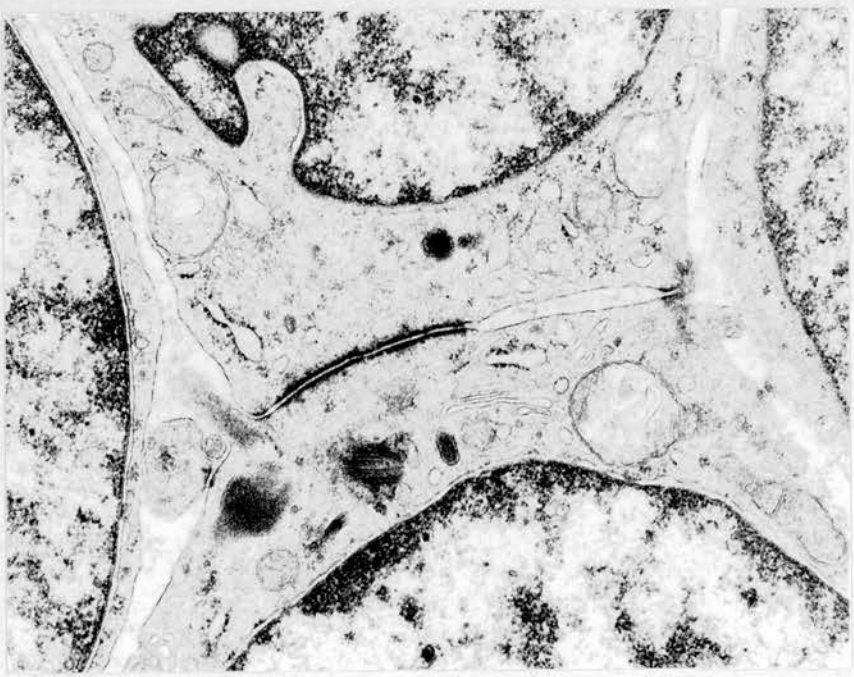

Figure 12. Neuroendocrine carcinoma of skin, metastatic to testis. Cell junctions are present. x 11,400.

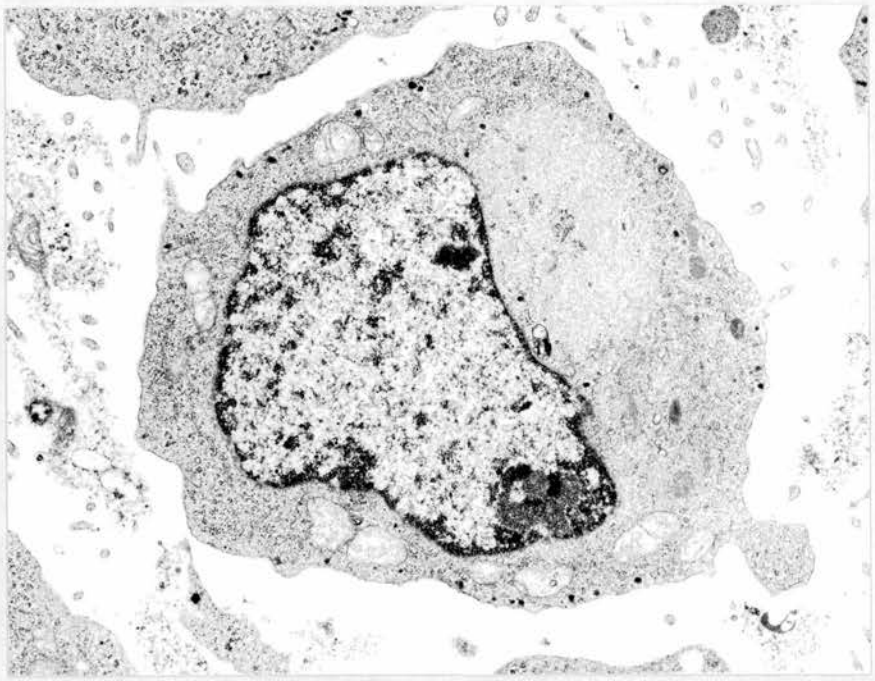

Figure 13. Neuroendocrine carcinoma of skin. The cell contains a paranuclear cluster of filaments. x 8,800

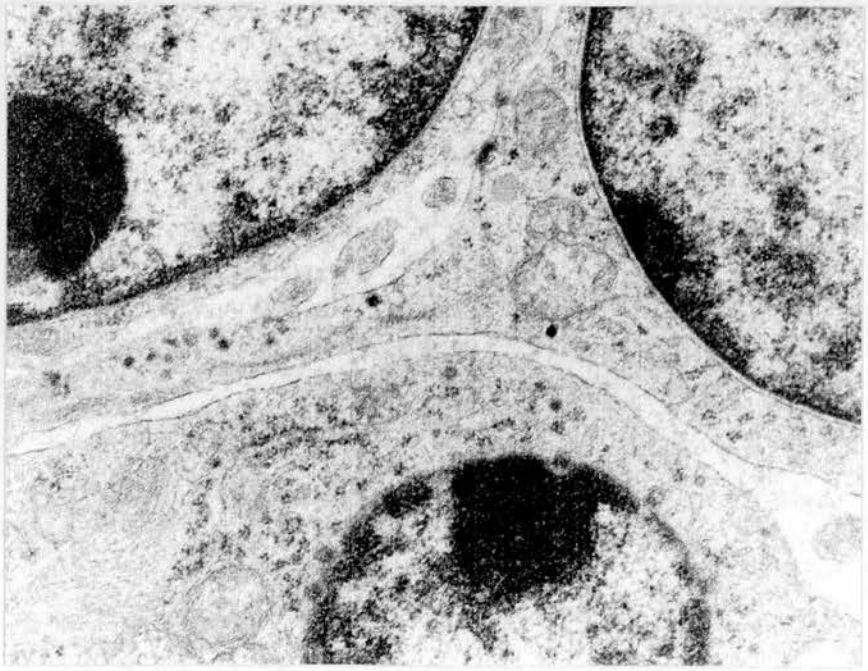

Figure 14. Neuroendocrine carcinoma of skin. A dendritic process contains a few small dense-core granules. x 11,700.

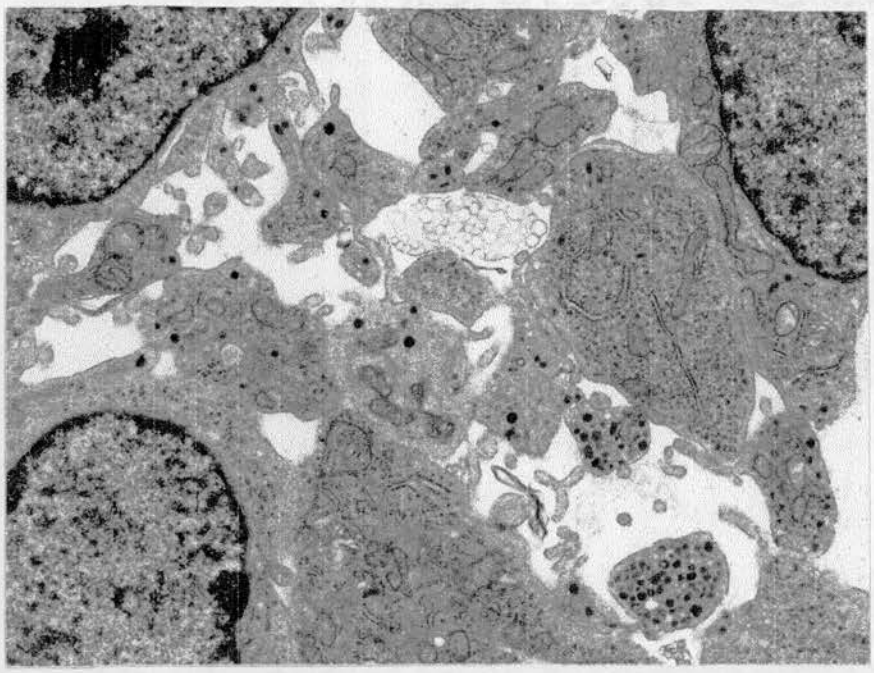

Figure 15. Neuroendocrine carcinoma of skin. A cluster of cross-sectioned dendritic processes. x 8,400.

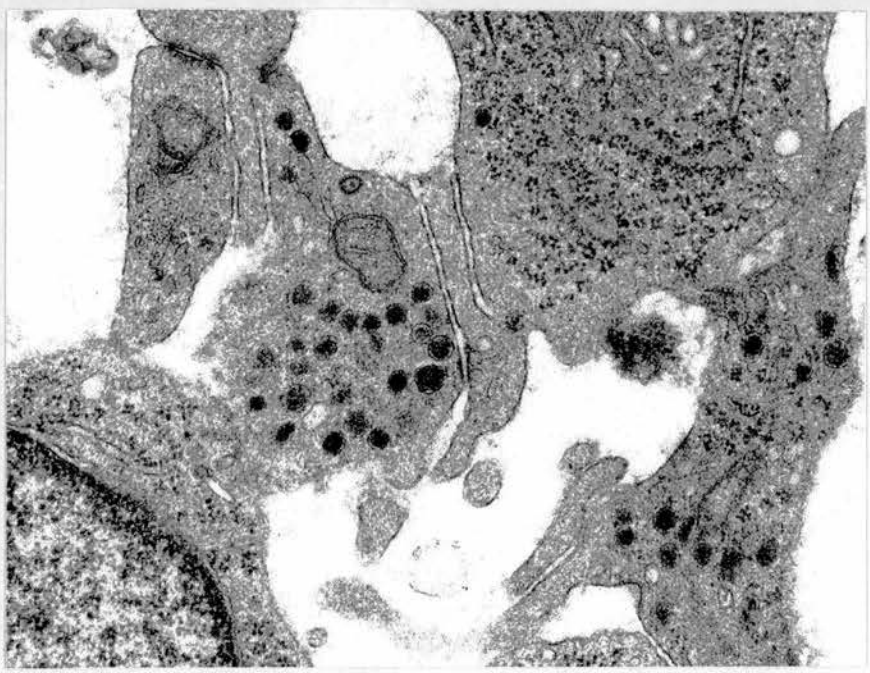

Figure 16. Neuroendocrine carcinoma of skin. The cell processes contain small membrane-bound granules. x 21,000.

Several of our cases of neuroendocrine carcinoma of the skin occurred together with or at the site of prior excision of a squamous cell carcinoma prompting a study of a possible relationship between the two tumors.

Gomez LG, DiMaio S, Silva EG, Mackay B. Association between neuroendocrine (Merkel cell) carcinoma and squamous carcinoma of the skin. American Journal of Surgical Pathology 7:171-177, 1983.

Among 32 neuroendocrine carcinomas of the skin, 11 were from patients with previous or concomitant squamous carcinoma. In two cases, the squamous and neuroendocrine carcinomas were admixed but each preserved its identify and transition between them was not seen. The diagnosis of neuroendocrine carcinoma was confirmed in each case by EM.

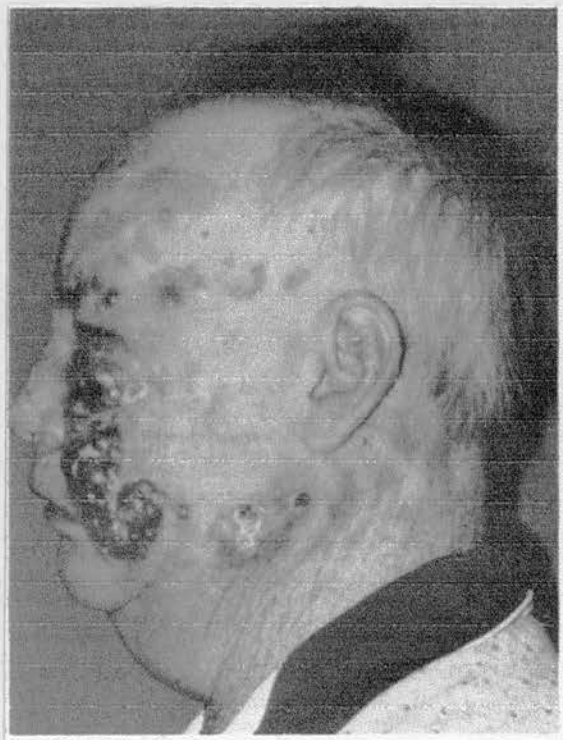

FIGURE 1
Case 7. A 56-year-old male with multiple squamous carcinomas of the face developed a neuroendocrine carcinoma anterior to a skin graft in the preauricular region.

FIGURE 2
Case 8. A 73-year-old male, who had had multiple squamous carcinomas of the face and ear, developed two fungating lesions over the cheek. Both were neuroendocrine carcinomas.

The two patients shown were elderly males who had undergone excision of squamous cell carcinomas of the facial skin and they subsequently developed multiple protuberant nodules of neuroendocrine carcinoma. In one, the tumor nodules surrounded a preauricular skin graft. A different patient whom we studied was a truck driver who was referred for management of a tumor of the buttock that had been biopsied and diagnosed as squamous cell carcinoma. Wide excision confirmed the presence of invasive squamous cell carcinoma, but a more extensive small cell tumor underlying the squamous neoplasm was shown by EM to be a neuroendocrine carcinoma, and both tumors metastasized to the same inguinal lymph node. The 34% concurrence of the two neoplasms in this series of 32 patients suggested a common carcinogenetic influence on two distinct precursor cells.

Melanoma

Metastatic melanoma enters into many differential diagnoses because of its morphologic diversity[32], and a primary skin tumor is not always found since it can regress spontaneously. Until immunohistochemical procedures became commercially available, EM was often used to investigate suspected melanoma, and the task was usually labor-intensive and resulted in many successes and some failures. There are still occasional cases of metastatic melanoma where EM is useful since the immunostaining findings are not always definitive. In a small subset of melanomas, S-100 protein is either not fully expressed or is below the level that can be detected by routine immunohistochemistry[33], and keratin may be present[34]. An interesting correlation between light and EM came from a report of post-embedding immunogold electron microscopy which revealed that HMB-45 antigen was exclusively localized to stages I and II melanosomes in the cytoplasm of neoplastic melanocytes, whereas it was detected mainly on stages II and III melanosomes in melanocytes from fetuses and infants[35].

Nevus cells, which have been described as "simply melanocytes"[36], share many structural features with melanoma cells, and the suggestion has been made on the basis of EM studies that dysplastic nevi fill the biological gap between benign nevocellular nevi and malignant melanomas[37]. The number and appearance of the melanosomes are too variable to be used as distinguishing criteria as the nevus cells in figures 17 and 18 illustrate.

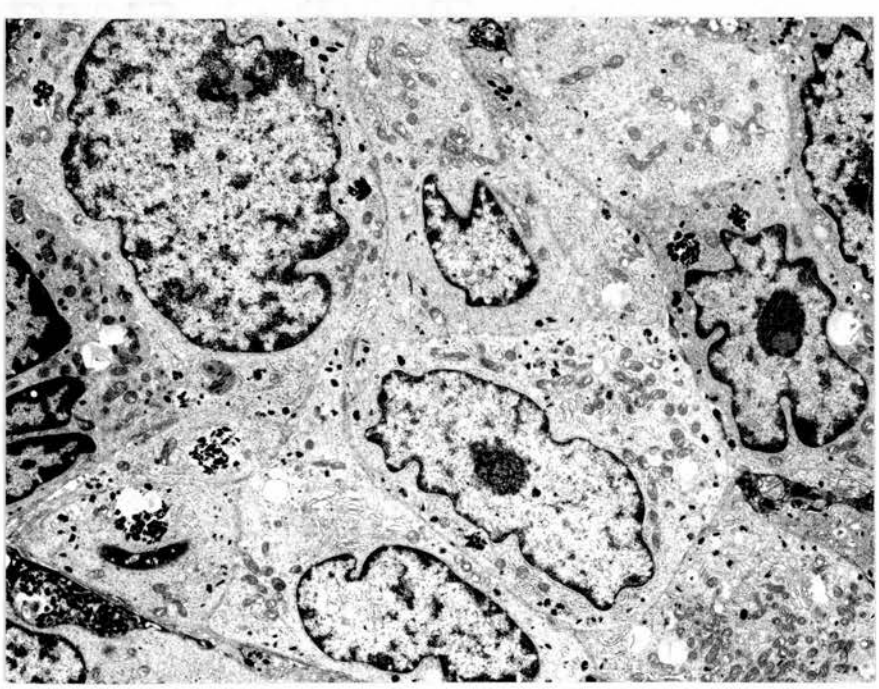

Figure 17. Compound nevus of conjunctiva with sparse melanosomes. x 4,000.

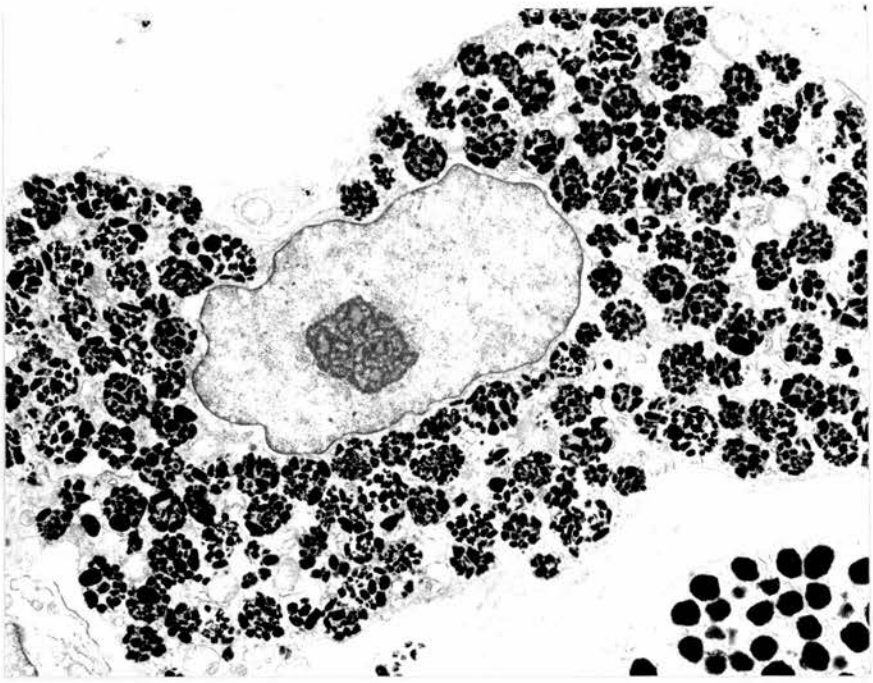

Figure 18. Blue nevus of scalp. The cell contains many clusters of melanosomes. x 5,400.

Distinction between melanoma and a benign nevus was aided by EM in the following case.

Steinberg JM, Gillespie JJ, Mackay B, Benjamin RS, Leavens ME. Meningeal melanocytoma with invasion of the thoracic spinal cord. A case report. Journal of Neurosurgery 48:818-824, 1978.

A 71 year old woman noted the insidious onset of diminishing sensation over the right half of her body extending downward from the upper thorax. She also noticed progressive weakness of her left leg. A myelogram revealed an intradural, extramedullary lesion at the T3 level. A thoracic laminectomy of T2-4 was performed and it revealed a black-pigmented neoplasm located on the left antero-lateral aspect of the spinal cord, densely adherent to both the dura and the cord surface. A subtotal excision was performed and post-operative radiation was given. The appearance of symptoms of recurrent tumor three years later led to a second operation through the original incision. The spinal cord was widened and pigmented tumor had separated the cord into two halves. The tumor was not encapsulated but most of it was removed and the patient was able to ambulate well with the aid of a walker one month after surgery.

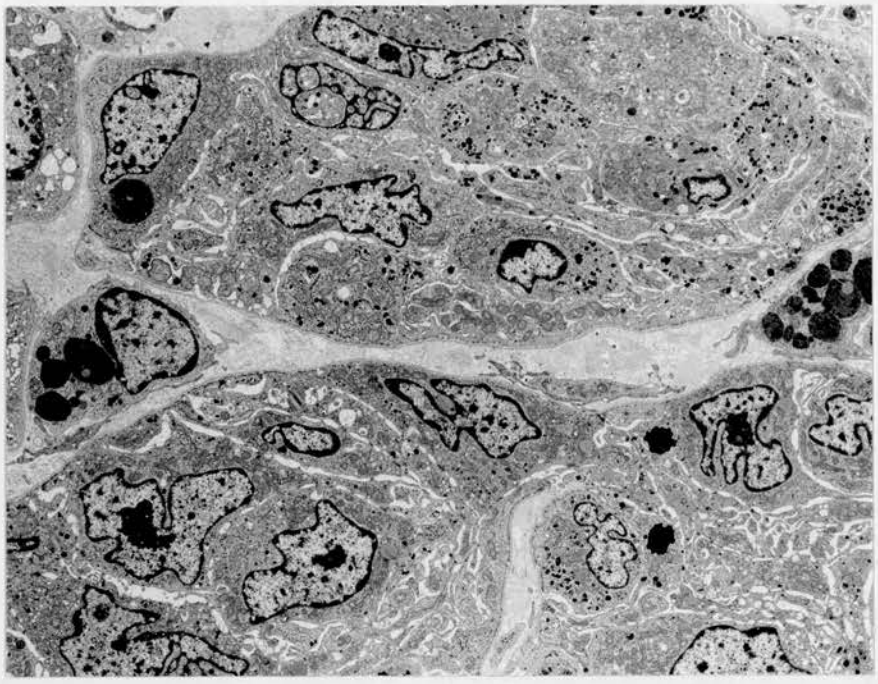

Figure 19. Melanocytic tumor of meninges. The tumor cells form sharply defined clusters. x 2,800.

Melanin-containing neoplasms of the meninges are uncommon. They include primary melanoma of the meninges, metastatic melanoma to the meninges, and the infrequently reported entity that has been called pigmented meningioma, melanocytic meningioma, meningeal melanocytoma, and cellular blue nevus of the meninges[38, 39]. The ultrastructural features of the tumor we reported argue for its being benign. It does not possess the unique cell shapes seen in a true meningioma (page 259). The relatively large groups of tumor cells were consistently well circumscribed (figure 19). The fact that they were bordered by an intact basal lamina also supports their being benign, though a study has shown that nests of melanoma cells, like those of nevi, are surrounded by basement-membrane material containing type IV collagen and laminin, and loss of basal lamina is not considered by the authors to be mandatory for melanoma invasion or even metastasis[40]. The clinical context provides a strong indication that our meningeal tumor was benign since a primary leptomeningeal melanoma is almost invariably fatal from rapid growth and spread to sites within the nervous system.

A primary cutaneous melanoma is a good source for the study of the ultrastructure of neoplastic melanocytes (figure 20). They are round cells with dendritic processes, a central nucleus, sparse organelles as a rule, and varying numbers of melanosomes displaying stages of maturation from vacuoles (type I melanosomes), to type II premelanosomes with their distinctive fine periodicity, to type III premelanosomes in which the deposition of pigment progressively obscures the barred framework, to the mature (type IV) melanosome.

Abnormalities in the number and structure of melanosomes have been described in malignancy[41], including greater numbers and irregularities in the matrix, but it is doubtful that these could be used as diagnostic criteria. Nuclear pseudoinclusions are often seen in melanocytic lesions but again they can not be depended on to distinguish between malignant melanoma and benign melanocytic lesions, although it has been claimed that they are useful

in distinguishing melanocytic from non-melanocytic tumours[42]. Nucleoli are typically prominent in melanomas (figure 21), and one investigator[43] found that in benign nevus cells the nucleoli displayed a compact ribonucleoprotein distribution whereas in melanoma cells the nucleoli were large with an irregular, nucleolonema-like ribonucleoprotein distribution and numerous small fibrillar centers.

The diagnosis of a suspected metastatic melanoma can be difficult by routine light microscopy, and before the immunohistochemical era, EM was often helpful. The possibility of melanoma may not be suspected from light microscopy when the tumor is myxoid[44] or is composed of clear[45] or signet-ring[46] cells. A spectrum of ultrastructural morphology has been described in metastatic melanoma[47]. The diagnosis may be suggested by the observation at low power that irregular dense bodies are present in the cytoplasm, but a number of objects can present the same appearance including the ubiquitous lysosome and identification of type II premelanosomes is necessary to confirm the diagnosis (figure 22). Rarely, maturation arrest in melanoma cells may result in only early premelanosomes being formed and these vacuoles are empty, or they may contain small linear densities which must be scrutinized in search of periodicity. As noted above, the presence of a basal lamina does not rule out a diagnosis of melanoma[48], but visible basal lamina is in my experience uncommon in metastases.

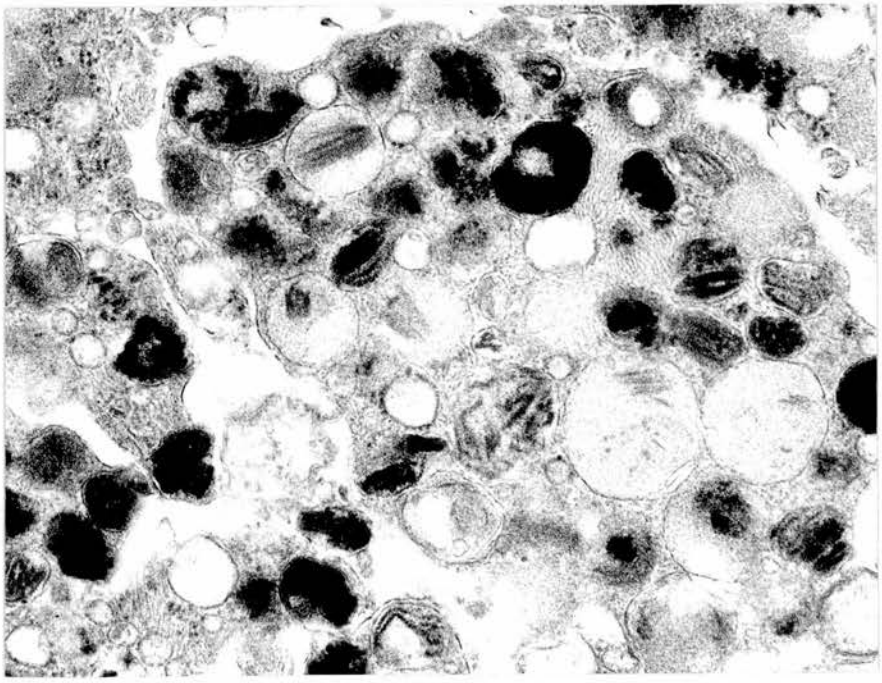

Figure 20. Malignant melanoma of skin, primary configuration. Within the processes of the melanoma cells, there are many melanosomes at various stages of maturation. x 32,000.

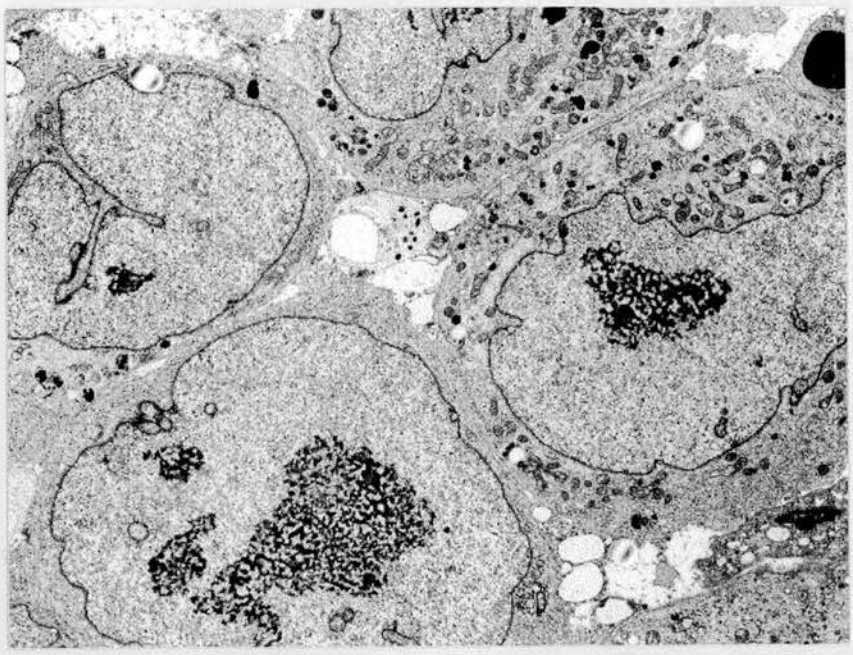

Figure 21. Metastatic melanoma. The cells have large nuclei with prominent nucleoli. x 8,100.

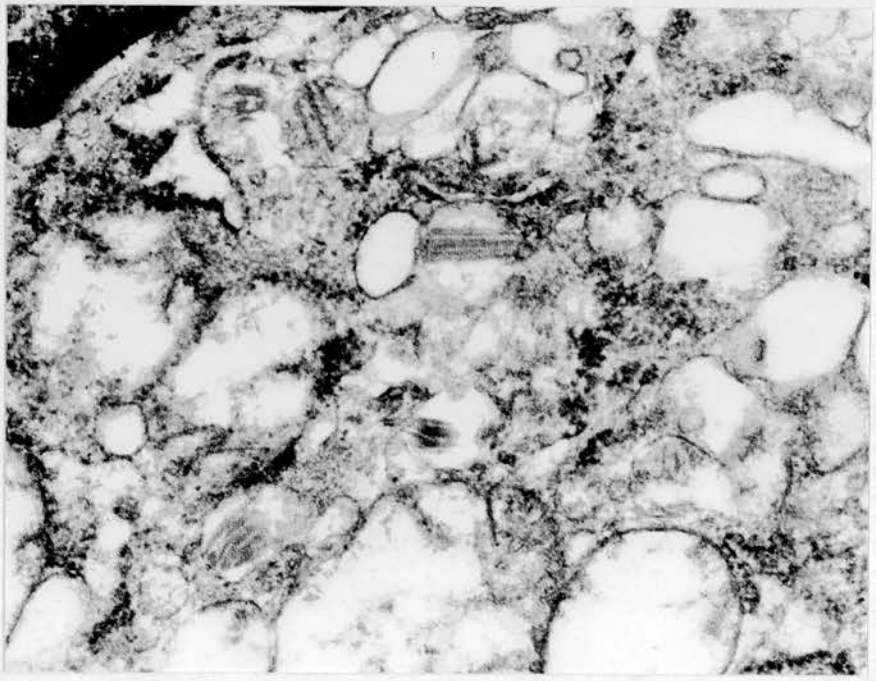

Figure 22. Metastatic melanoma in lung, poorly preserved, with rare premelanosomes. x 40,000.

A diagnosis of melanoma should never be made on the basis of EM findings alone since tumors other than melanoma can contain melanosomes, mature and immature[49], including basal cell[50] and squamous cell[51] carcinomas. A tumor can also become secondarily colonized by melanocytes[51] as the following case illustrates.

> **Lloreta-Trull J, Ordonez NG, Mackay B. Pigmented carcinoma of the breast.: an ultrastructural study. Ultrastructural Pathology 24:109-113, 2000.**
> A pigmented lesion on the skin of a breast removed for carcinoma was thought to be a primary melanoma by routine light microscopy but immunohistochemistry and EM established that carcinoma cells were present in the upper dermis where they intermingled with a proliferation of melanocytic cells. The carcinoma cells possessed desmosomes and intracytoplasmic lumens, and melanosomes were present in their cytoplasm. The melanocytic cells were melanocytes and melanophages and they were often intimately draped around the tumor cells.

The skin tumor in this patient was a dermal extension of the underlying breast carcinoma, and the tumor cells contained melanosomes which they had obtained through intimate association with the non-neoplastic pigmented cells. In normal skin, squamous cells have not been shown to synthesize melanin but normal keratinocytes frequently contain a few melanosomes which they acquire by passive transfer from the dendritic epidermal melanocytes.

A variety of appearances can be seen by EM in primary and metastatic melanomas. In the course of examing a large number of cases, I came across some distinctive variants. The mitochondria may contain tubular cristae (figure 23) but the cells do not have zones of smooth endoplasmic reticulum and confusion with a metastatic steroid-forming tumor is unlikely. In a balloon cell melanoma, there are many vacuoles and some melanosomes (figure 24), and although it is generally believed that this appearance in a melanoma represents a degenerative change, immunohistochemical and EM findings have suggested that these are metabolically active melanocytic cells[52]. The presence of microtubules within cisternae of the endoplasmic reticulum of melanoma cells creates a striking appearance.

> **Mackay B, Ayala AG. Intracisternal tubules in human melanoma cells. Ultrastructural Pathology 1:1-6, 1980.**
> (This article earned a certain measure of distinction in being the first paper in the first issue of a journal that has been the source of many original ultrastructural observations.) Two cases of metastatic melanoma were described in which the cells contained geometric arrays of microtubules within cisternae.

The microtubules produce a unique look both at low magnification (figure 25) and at higher power once details of the individual microtubules become visible. They are evenly spaced in rows (figure 26) and most of the microtubules are hollow but a few have dense interiors. A helical pattern can be discerned in longitudinally sectioned microtubules (figure 27). Intracisternal microtubules are not a common finding in melanoma[53]. I estimate that they have been present in fewer than 5% of the cases I have examined. They are occasionally encountered in small numbers in other tumors, but are only seen in abundance in some extraskeletal myxoid chondrosarcomas where they do not display the geometric pattern seen in melanoma (page 241).

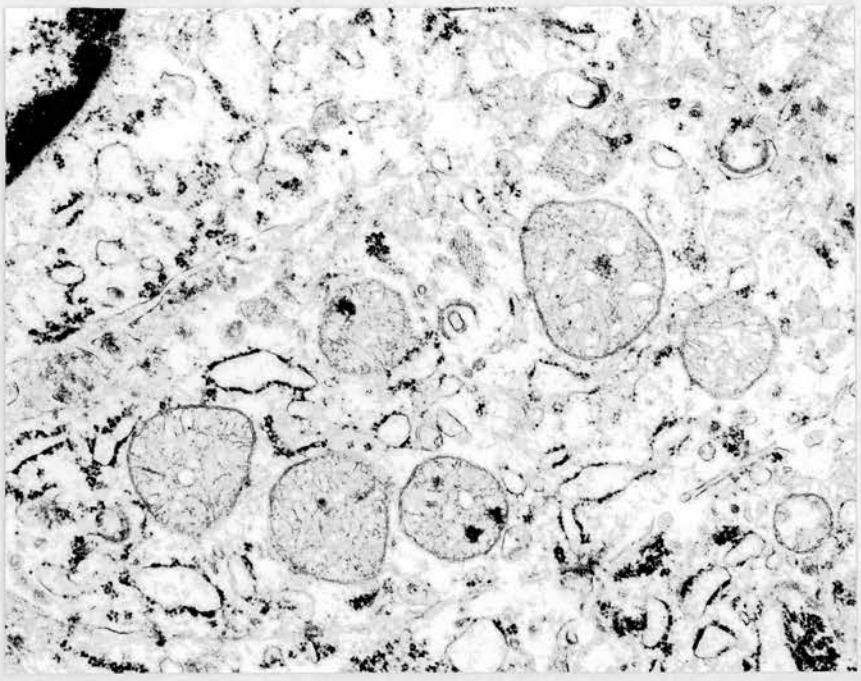

Figure 23. Metastatic melanoma. The mitochondria have some tubular cristae. x 21,000.

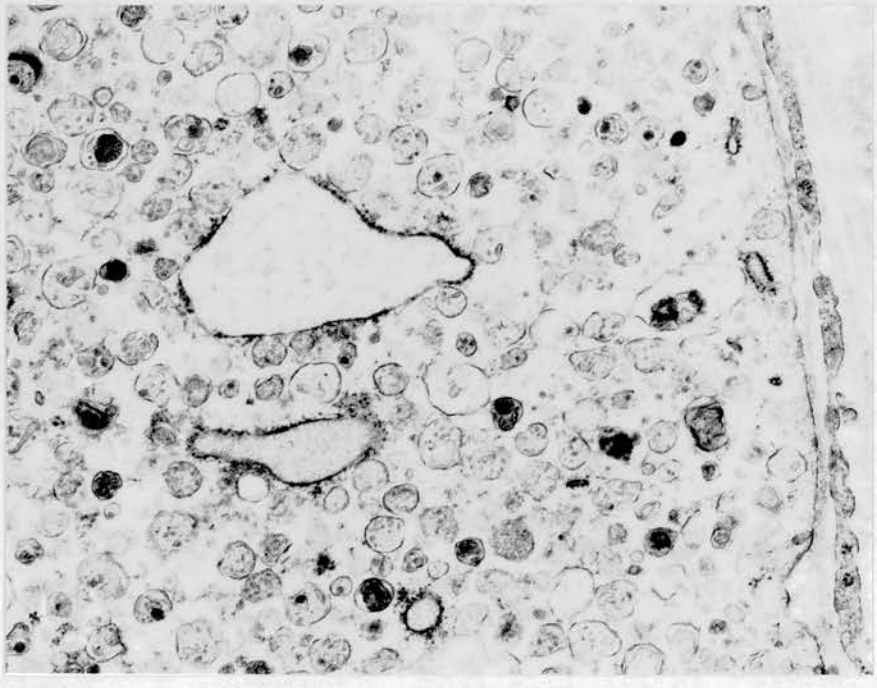

Figure 24. Balloon cell melanoma. At this magnification, melanosomes are indistinguishable from lysosomes. x 17,400.

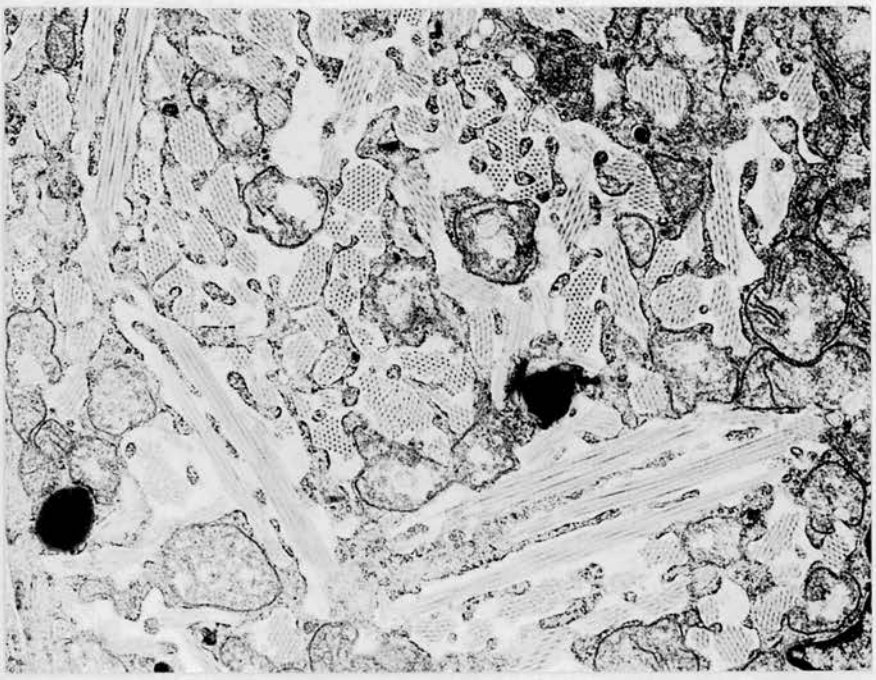

Figure 25. Metastatic melanoma. The cisternae contain large numbers of microtubules. x 12,800.

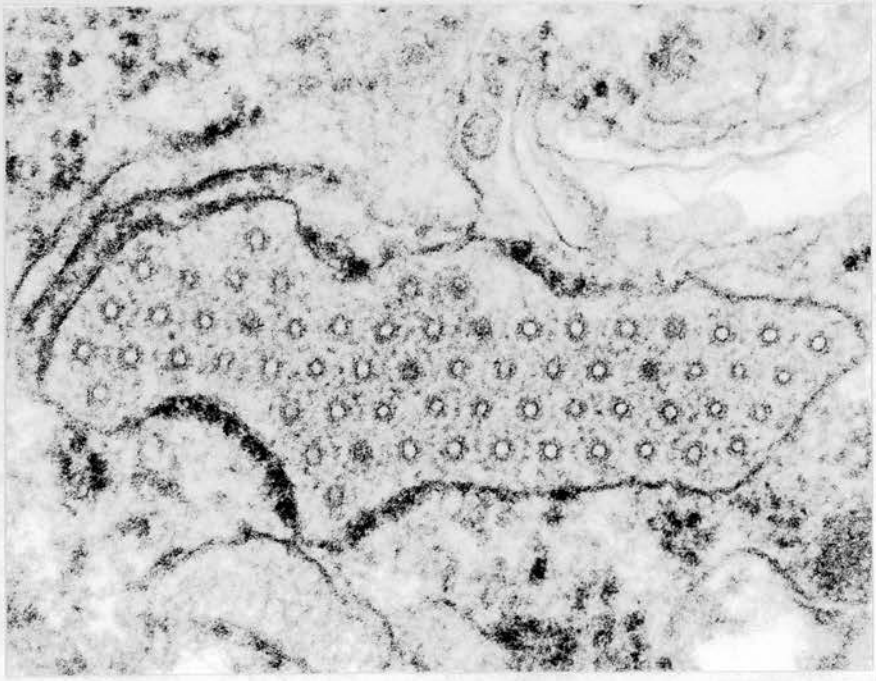

Figure 26. Metastatic melanoma. The intracisternal microtubules form a geometric array. Some have solid interiors. x 90,000

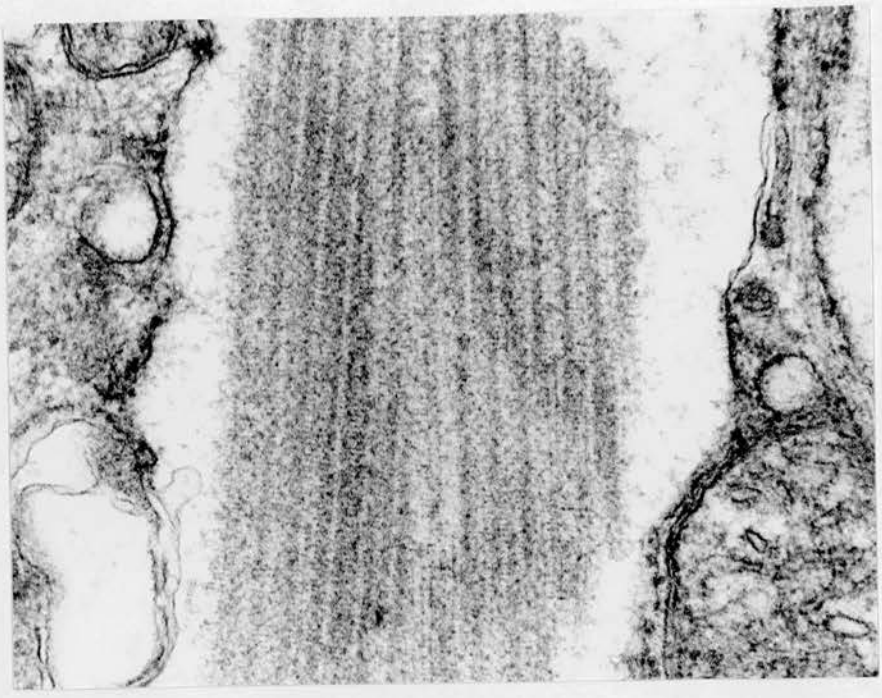

Figure 27. Metastatic melanoma. Intracisternal microtubules have a helical periodicity. x 53,000

When a melanoma arises in an extracutaneous site, EM may suggest or confirm the diagnosis. The tumor has been reported in a number of mucosal locations[54, 55].

> **Yamashina M, Mackay B, Ordonez NG, DuBrow R. Ultrastructural diagnosis of melanoma from an endoscopic biopsy. Ultrastructural Pathology 11:465-472, 1987..**
> An endoscopic biopsy of the small intestine showed the presence of pleomorphic tumor cells within the mucosa. Carcinoma was suspected, but EM revealed premelanosomes within the neoplastic cells. Tumor was not found elsewhere and the presumption was that the tumor had arisen in the wall of the intestine.

Soft tissue is a well-established site for a primary melanoma. EM studies of cases led to the recognition that these were indeed tumors of melanocytes[56] and not sarcomas of tendons or aponeuroses as had initially been suspected[57].

> **Benson JD, Kraemer BB, Mackay B. Malignant melanoma of soft parts. an ultrastructural study of four cases. Ultrastructural Pathology. 8(1).57-70, 1985.**
> Four cases of melanoma presenting in soft tissues were studied. Clinical data favored this being the primary site in each patient. Two consistent ultrastructural observations were large dense nucleoli in many of the cells and occasional premelanosomes. Multinucleated cells were found in one tumor.

The large, dense nucleoli are a prominent feature by EM (figure 28) and they are conspicuous in routine light microscopic sections. Premelanosomes are not abundant and may require a search for their detection (figure 29). Scattered multinucleated cells in one case were S-100 positive and they contained dense bodies that suggested melanosomes (figure 30) but type II premelanosomes could not be identified. Precursor cells of a

melanoma arising in soft tissues have presumably become misplaced in the course of their embryonic migration from neural crest to skin, during which time they may be pluripotential cells[58].

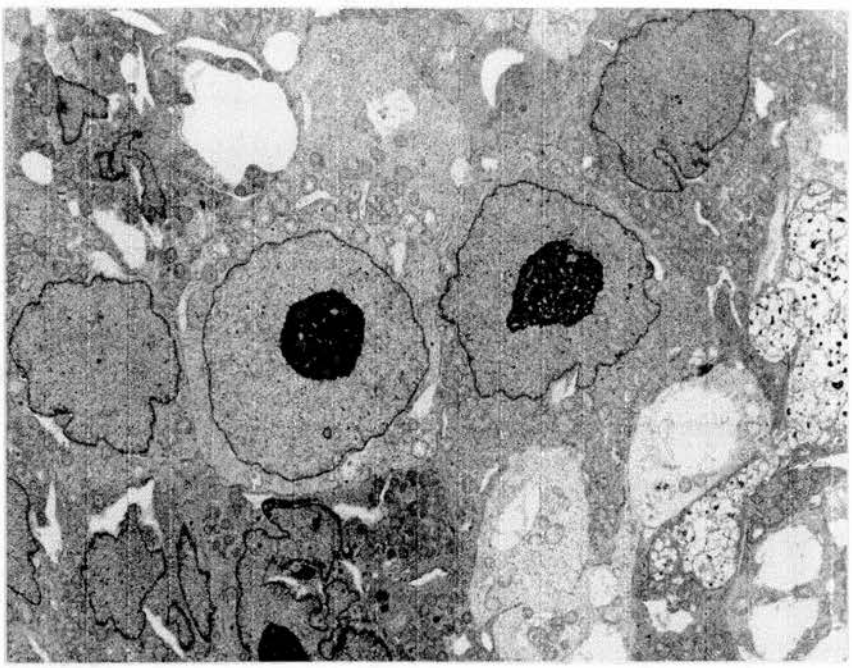

Figure 28. Melanoma, primary in soft tissue, with prominent dense nucleoli x 3,100.

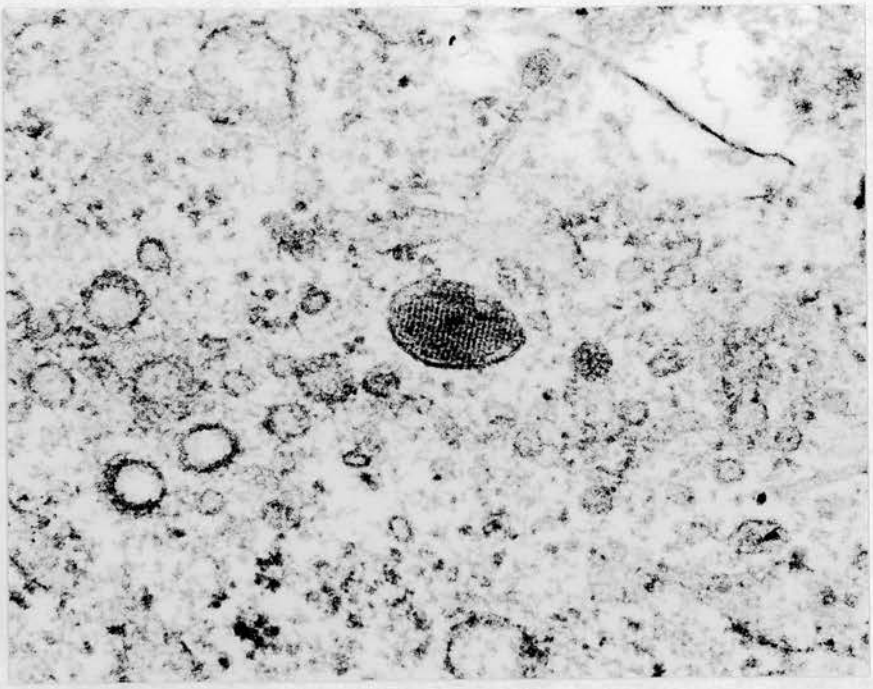

Figure 29. Melanoma of soft parts. A premelanosome from the tumor shown in figure 28. x 68,000

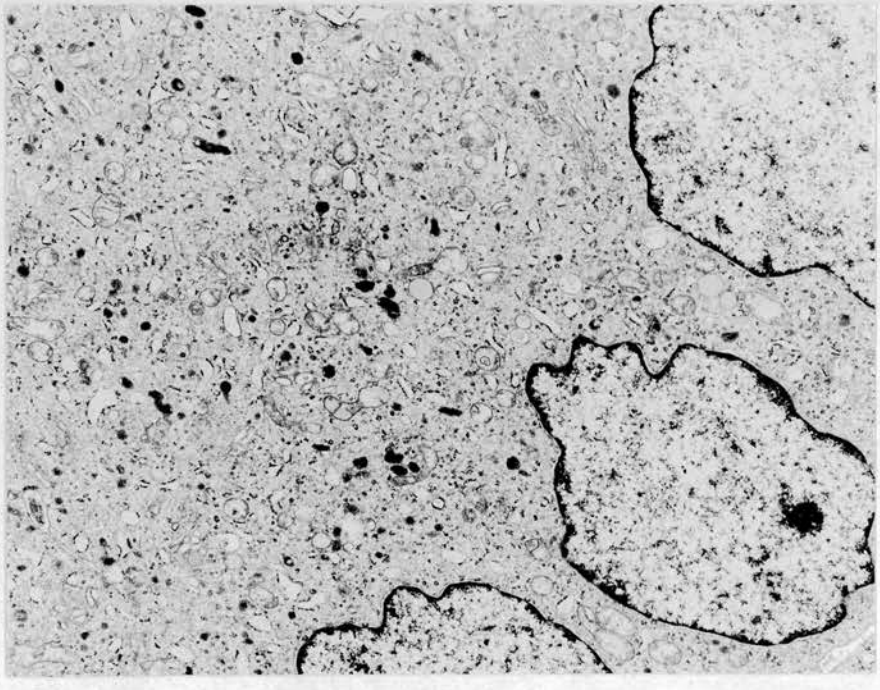

Figure 30. Same tumor as figure 28. Part of a multinucleated cell containing dense bodies suggestive of melanosomes. x 19,000.

A melanoma may undergo spindle cell transformation. While viewing several cases, primary and metastatic, with the electron microscope, I made the serendipitous observation that the cells resembled those of a schwann cell tumor, and we reported six cases to draw attention to this finding, using the descriptive designation 'neurosarcomatous transformation of melanoma'.

> **DiMaio SM, Mackay B, Smith JL, Dickersin GR. Neurosarcomatous transformation in malignant melanoma. An ultrastructural study. Cancer 50:2345-2354, 1982.**
>
> Six cases diagnosed by light microscopy as desmoplastic melanoma had common ultrastructural features which were interpreted as evidence of schwann cell differentiation. The cells formed thin parallel bundles and they had long, slender cytoplasmic extensions that contained microtubules. Premelanosomes were not found in any of the tumors.

By routine light microscopy, the cells of this tumor can closely resemble fibroblasts, and it is difficult to detect the grouping of the spindle cells in paraffin sections though the bundles are obvious in electron micrographs (figure 31). The cells and their processes cluster to form thin fascicles that participate in the radial growth phase of the tumor and are separated by intervening zones of fibroblasts and collagen. The long cell processes resemble those of benign schwann cell tumors, but they are closely apposed within the little fascicles (figure 32) and vestiges of basal lamina are only found on the outside of a bundle.

Desmoplastic malignant melanoma is an uncommon variant in which the invasive tumor is associated with fibroplasia[59, 60], and EM may be useful to clarify the diagnosis[61]. The pathogenesis of the desmoplasia remains obscure. A variant of desmoplastic melanoma that exhibits a distinctive neural or schwannian appearance of the amelanotic spindled melanocytes was given the name 'neurotropic melanoma'[62], but a distinction has appropriately been made between neurotropism and neural transformation and these manifestations may be seen separately or together[63]. Ultrastructural evidence of schwannian differentiation has been confirmed by others[61, 64]. This variant may have a better prognosis than conventional melanomas of similar depth of invasion[65], but it can be mistaken for fibrosis in routine histological sections and as a result some tumors are more advanced by the time the diagnosis is established. Since schwann cells and melanocytes are both of neural crest origin[66], it is not surprising that their fine structural features sometimes overlap. Elongated cytoplasmic processes surrounded by basal lamina material have been described in nevi[67], and occasional peripheral nerve sheath tumors are melanotic[68].

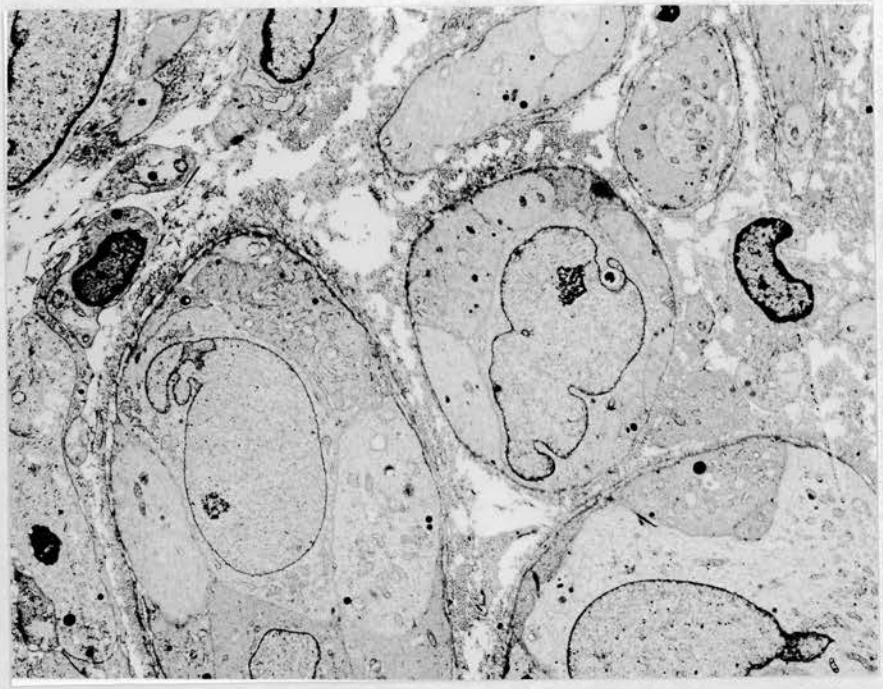

Figure 31. Melanoma of skin with neural differentiation. The slender bundles of tumor cells are transversely sectioned. x 4,400

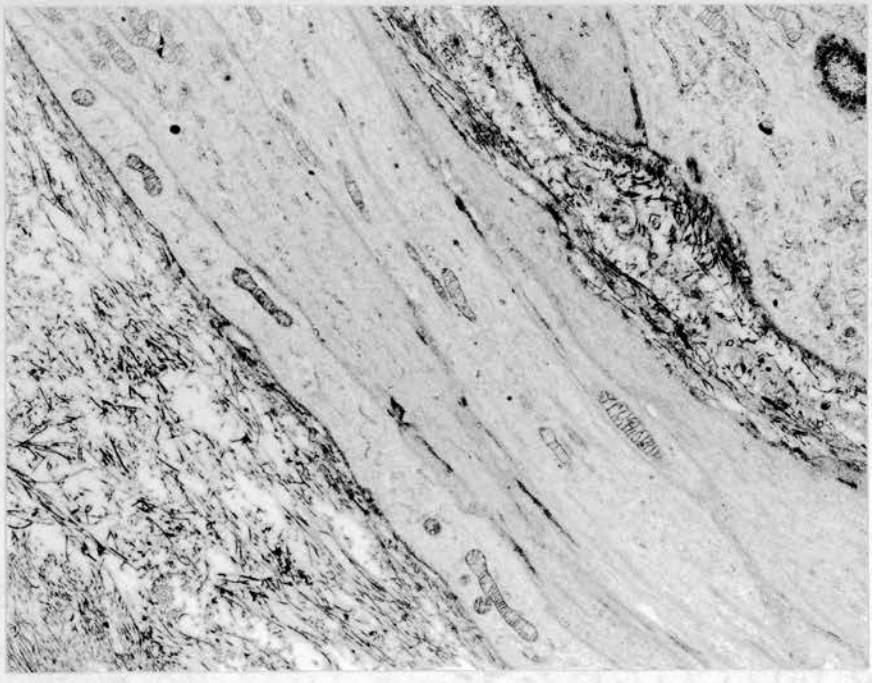

Figure 32. Same tumor as figure 31. A bundle of processes is shown in longitudinal section. x 4,800.

Tumors of the head and neck

The tumors discussed in this section are nasopharyngeal angiofibroma, nasal adenocarcinoma with enteric differentiation, olfactory neuroblastoma, and myoepithelioma.

Nasopharyngeal angiofibroma

The final year of my pathology residency was spent in the University of Washington Hospitals program at Seattle, Washington. A head and neck surgeon, Dr. Joseph Walike, approached me with a request to use EM to study the problem of often excessive blood loss that occurred during biopsy and resection of juvenile nasopharyngeal angiofibromas. He was particularly interested in the efficacy of pre-operative estrogen therapy and wanted to know details of structural changes that took place within the tumor. Our report of one case was followed by a review of his surgical experience together with EM observations on a second case

> **Walike JW, Mackay B. Nasopharyngeal angiofibroma: light and electron microscopic changes after stilbesterol therapy. Laryngoscope 80:1109-1121, 1970**
> A 12-year-old boy had a history of recurrent severe epistaxis over an 8 month period. On examination, a reddish mass was seen filling the right choana and nasopharynx, and radiologic studies revealed the presence of a large nasopharyngeal mass, predominantly on the right side and extending into the pterygo-maxillary fossa, forcing the thin posterior wall of the maxillary sinus anteriorly. A wedge of the tumor was removed and processed for light and electron microscopy. The patient received 5 mg of oral stilbesterol daily for the next 30 days. The 8 by 6 cm tumor was then completely removed. It involved the sphenoid sinus and the ethmoid complex and extended into the right pterygomaxillary fossa. Blood loss was estimated at 800 cc, and the patient's recovery was uneventful. The pathology findings are described below.

> **Walike JW, Mackay B. Management of nasopharyngeal angiofibroma. Transactions of the American Academy of Ophthalmology and Otolaryngology 76:1346-1353, 1972.**
> This was a report of Dr. Walike's surgical experience with more than twenty patients who received preoperative stilbesterol therapy, including details on one in whom the tumor was studied by light and electron microscopy before and following therapy and surgical resection. The structural changes that occurred in the tumor were the same as those seen in the previous case. Blood loss during the procedures rarely exceeded 800 ml., even in large tumors with pterygomaxillary extension.

Prior to this study, it had been recognized for many years that these benign lesions might spontaneously regress as the patients passed into adulthood, and in 1959, Schiff[69] postulated that the tumors possess a relative hormonal dependency. He demonstrated histologic maturation in four of the tumors using androgen and estrogen treatment in two cases each, and found that estrogen produced the greater response. The contribution of EM in our study was to show details of the maturation process in the vascular and connective tissue components. In the pre-therapy biopsies, the tumors contained many small branching vessels lined by plump endothelial cells which tended to obscure the lumens. The stroma was relatively loose in texture with scattered fibroblasts and poor organization of collagen fibrils. Following therapy, the vessels were more widely spaced, the lining cells were flatter, and lumens were more circular in cross section. Stromal cells were further apart and evenly distributed, and the intervening collagen fibrils formed dense interlacing fascicles. Within

the fibroblasts, precollagen and smooth muscle myofilaments were conspicuous after therapy, but pericytes and mast cells did not alter in appearance or frequency.

The changes in the tumor following stilbesterol administration dramatically reduced the amount of blood loss during surgical resection. The appearance of the vessels modified to some extent, but the basic vascular ultrastructure was not significantly altered and pericytes were as numerous in the before and after specimens. The alterations in the stroma were more significant since it transformed from a loosely textured tissue with haphazardly distributed collagen fibrils and quiescent fibroblasts to become dense and organized with sparse ground substance, intersecting collagen bundles, and actively synthesizing fibroblasts which contained abundant tropocollagen and showed transformation to myofibroblasts by the presence of peripheral smooth muscle myofilaments. While some clinicians have been hesitant to administer hormonal therapy to prepubescent boys, a five-year follow-up of hormonally treated patients revealed no abnormalities of growth, development, or sexual potency[70]. Although a recent report using electron microscopy has suggested that nasopharyngeal angiofibroma is a vascular malformation[71], the clinical behavior would seem to justify viewing it as a neoplasm, and it is so classified in the latest World Health Organization classification of soft tissue tumors[72]. The cells do not show marked deviations in their ultrastructure from corresponding normal cells, but this is also the case in an aggressive fibromatosis (pages 173-175), a lesion that can be responsible for serious morbidity.

An intriguing observation in our study of nasopharyngeal angiofibromas was the presence of dense bodies within nuclei of the stromal fibroblasts.

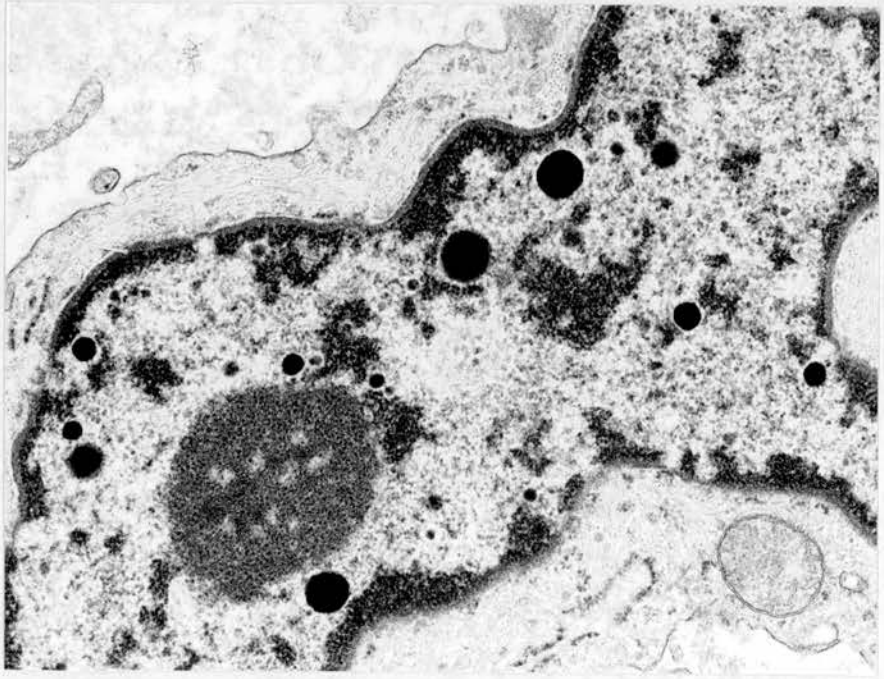

Figure 33. Nasopharyngeal angiofibroma. The stromal cell nucleus contains perichromatin granules and a thin fibrous lamina. x 10,000.

The intranuclear dense granules (figure 33) appear to be consistently associated with this tumor, and they can be as large as 400 nm. Ghadially coined the term giant perichromatin granules[73], and enzymatic digestions carried out on thin sections and staining procedures for nucleoproteins have shown that they represent tightly bound RNA-protein complexes and that they do not contain DNA[74]. The nucleus may have a prominent fibrous lamina adjacent to the inner membrane of the nuclear envelope (figure 33). This structure is found in a variety of normal and pathological cells[75] and appears to be a meshwork of lamin filaments[76].

Adenocarcinoma with enteric differentiation

Unlike the endoderm-derived epithelium of the laryngobronchial tree, the Schneiderian mucosa that lines the nose and paranasal sinuses is formed from ectoderm, accounting for some of the variability seen among tumors of the surface epithelium or duct system in the upper airway. Differentiated adenocarcinomas of the nasal cavity and paranasal sinuses of non-salivary type do not usually have notable ultrastructural features, but an exception is the rare adenocarcinoma of the nasal cavity displaying enteric differentiation

> **Batsakis JG, Mackay B, Ordonez NG. Enteric-type adenocarcinoma of the nasal cavity. An electron microscopic and immunohistochemical study. Cancer. 54:855-860, 1984**
> A primary adenocarcinoma of the left nasal cavity in a 67-year-old man was well differentiated by light microscopy. The patient had a long history of springtime allergies. EM revealed that the tall columnar cells possessed microvilli with microfilaments cores and glycocalyceal granules. Goblet cells were interspersed with cells containing a variety of dense-core granules similar to those seen in Paneth and enterochromaffin cells.

The light microscopic appearance of the tumor is shown in figure 34. The cells were tall with mostly basal nuclei, and uniform, straight "picket-fence" microvilli clothed the apical surfaces (figure 35). This construction is a characteristic of the columnar cells of the gastrointestinal tract, and its occurrence in an adenocarcinoma will suggest that the tumor has arisen in the gut. Each microvillus contains a slender bundle of microfilaments that extends down into the apical cytoplasm to combine with other rootlets and create a web of filaments which inserts into the zonula adherens of the junctional complex. Small glycocalyceal vesicles are embedded within amorphous material between the microvilli. There are a number of other sites in which a primary adenocarcinoma can present these features including lung (bronchioloalveolar adenocarcinoma) so their presence is not a consistently reliable indication that a tumor originated in stomach or intestines. This nasal cavity tumor contained goblet cells (figure 36), scattered cells with relatively large exocrine-type granules comparable to those seen in Paneth cells, and many cells in which small granules of differing caliber in the basal cytoplasm (figure 37) were identical to those of enterochromaffin hormone-producing cells. Immunoreactivity for five gastrointestinal-type hormones was demonstrated. The tumor thus possesses ultrastructural properties that are seen in adenocarcinomas of the gastro-intestinal tract and in particular the small intestine.

Figure 34. Adenocarcinoma with enteric differentiation, nasal cavity. Hematoxylin and eosin.

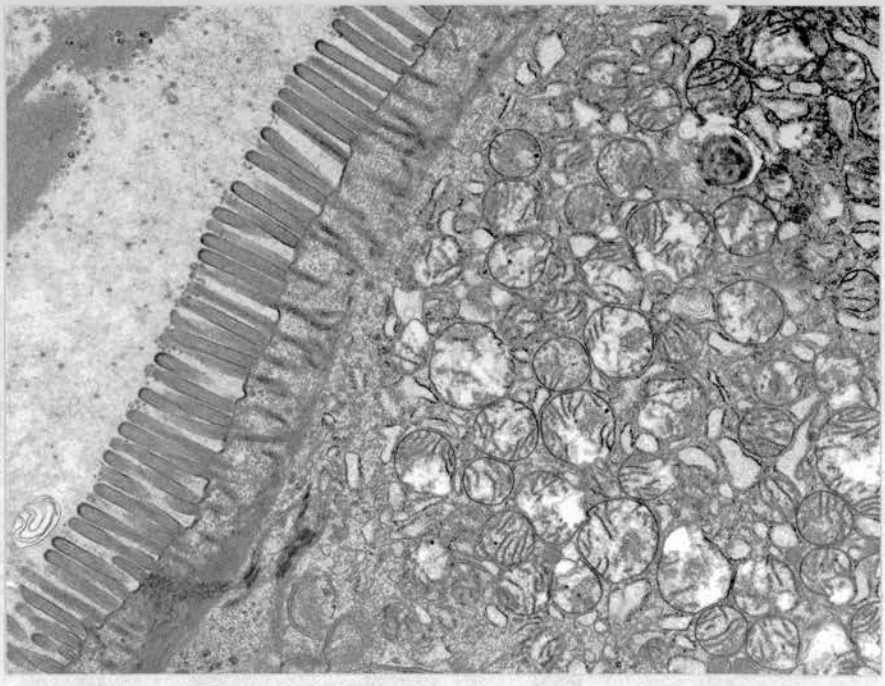

Figure 35. Same tumor as figure 34. The cell has an array of straight uniform apical microvilli containing microfilament cores. x 21,000.

Figure 36. Same tumor as figure 34 showing a goblet cell. x 6,500.

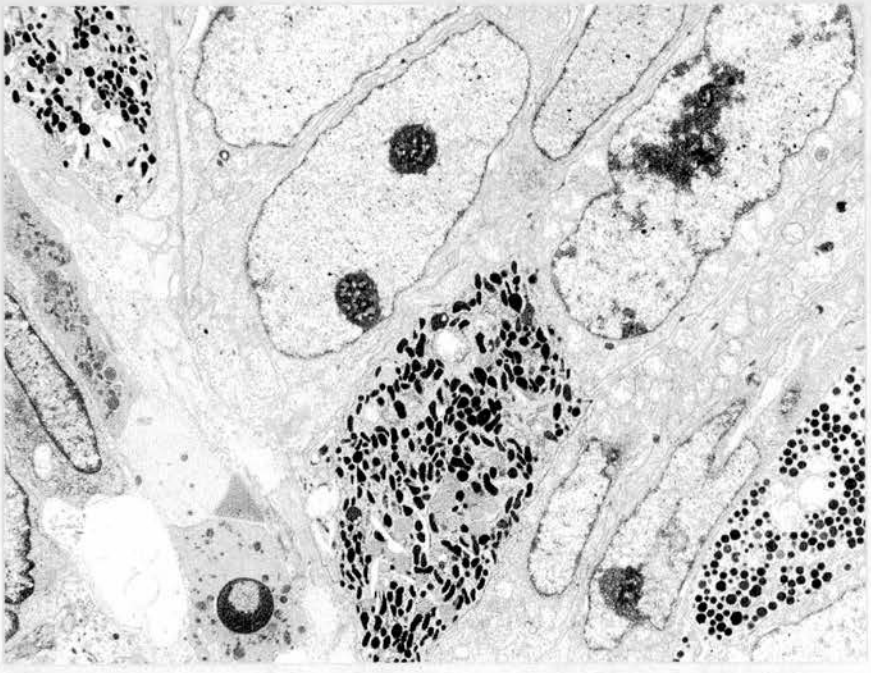

Figure 37 Same tumor as figure 34. Endocrine granules of varying shape can be seen within tumor cells. x 9,100.

Olfactory neuroblastoma

A neuroblastoma arising in the nasal cavity or its immediate vicinity is commonly called an olfactory neuroblastoma, but my experience has been that true olfactory differentiation is only rarely expressed in neoplasms. In the paper on adult neuroblastomas referred to earlier in connection with neuroendocrine carcinoma of the skin (page 21), a tumor with olfactory differentiation was among the nine reported cases and it is shown in figures 38a – c. The patient was 15 years of age when the primary tumor was removed, and three years later he underwent a regional cervical lymph node dissection to remove metastatic tumor which was histologically identical to the original accession.

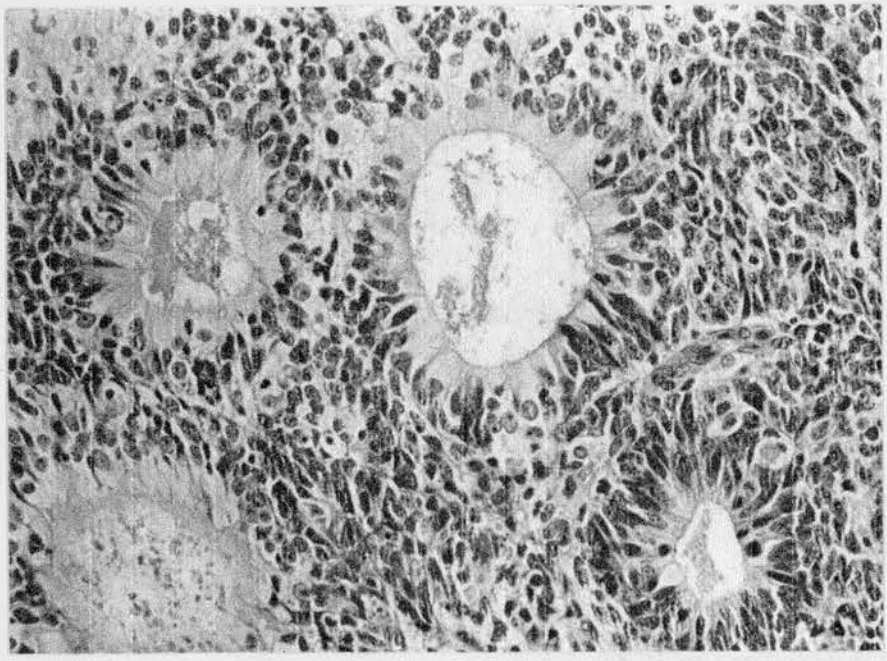

Figure 38a. Olfactory neuroblastoma, metastatic in cervical lymph node. Hematoxylin and eosin.

Figure 38b. Same tumor as figure 38a. An olfactory vesicle protrudes into a gland lumen. x 15,500.

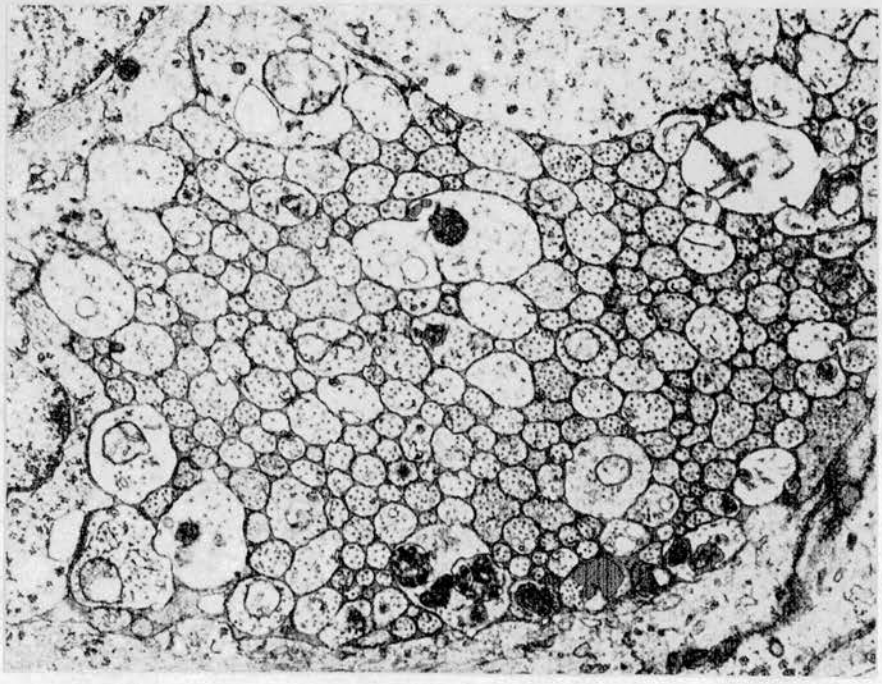

Figure 38c. Same tumor as figure 38a. A bundle of slender dendritic processes. x 15,200.

In a more recent case of olfactory neuroblastoma, the tumor showed similar features but neuroepithelial cells and their apical vesicles were clustered. The dendritic processes were again slender, forming compact bundles with few dense-core granules.

Griego JE, Mackay B, Ordonez NG, Langford L, Batsakis JG. Olfactory neuroblastoma. Ultrastructural Pathology 20:399-406, 1996.
A neuroblastoma arising in the nasal cavity of a 66-year-old male invaded the frontal sinus and extended into the cranial cavity. In light microscopic sections, zones of small ovoid cells merged with gland-like spaces bordered by columnar cells that were strongly immunoreactive to epithelial markers. Within the sheets of small cells, focal immunoreactivity for synaptophysin and chromogranin was demonstrated. EM confirmed the presence of olfactory differentiation and the three figures that follow show the light microscopic appearance and the detailed structure of the gland-like foci.

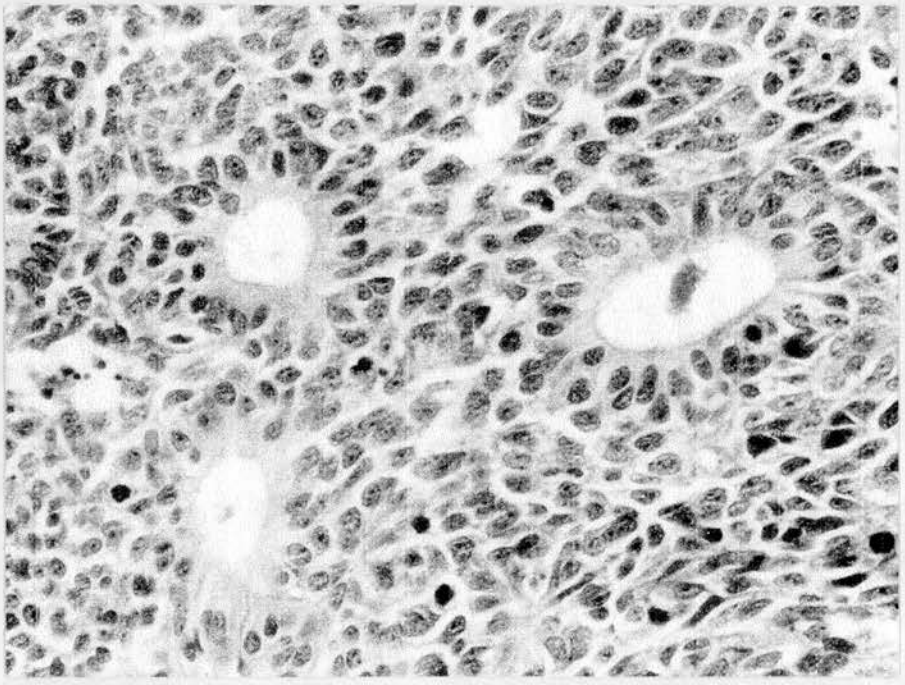

Figure 39. Olfactory neuroblastoma. Small gland-like structures are bordered by columnar cells which merge imperceptibly with surrounding small cells. Hematoxylin and eosin.

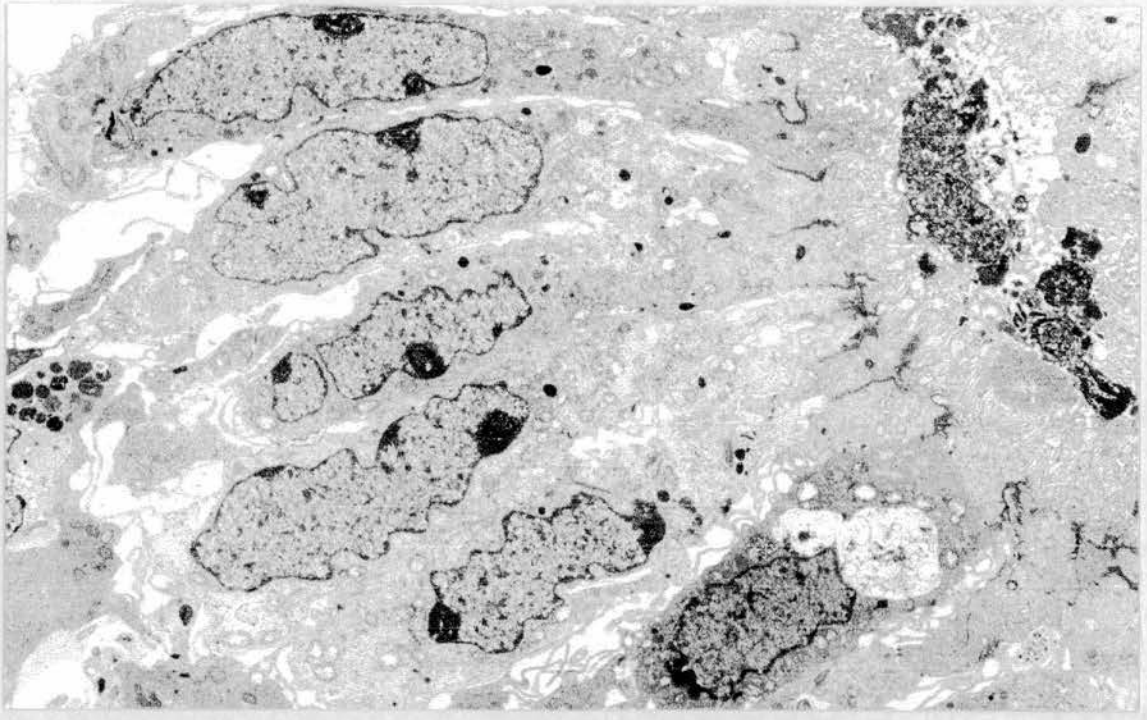

Figure 40. Same tumor as figure 39. Columnar cells bordering a lumen have basal nuclei but no basal lamina. Apical microvilli project into the lumen which contains structureless electron-dense material. x 4,300.

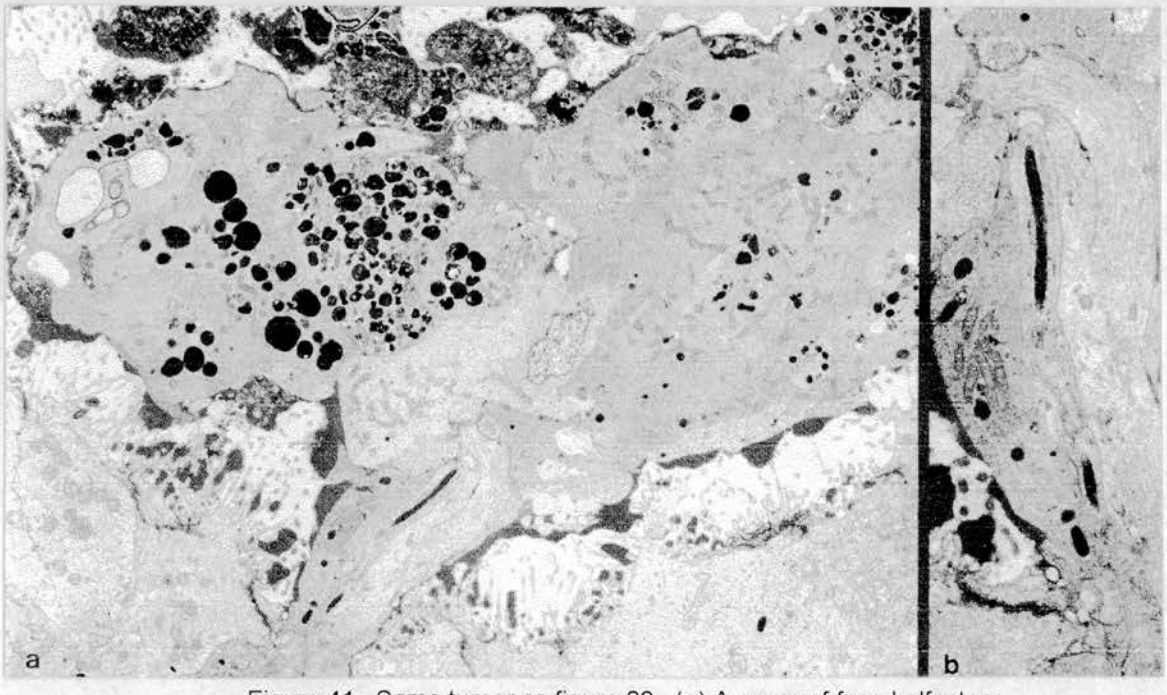

Figure 41. Same tumor as figure 39. (a) A group of fused olfactory vesicles forms a bulbous expansion within a lumen. x 3.200. (b) Detail of part of figure 40a. The stalk of the expansion is made up of several dendrites that contain longitudinally aligned microtubules. x 9,000.

The glandular lumens in the first case were well defined but the surrounding tall cells with basal nuclei were not sharply demarcated from sheets of small round to ovoid cells filling the areas between the lumens (figure 38a). The sine qua non of olfactory differentiation at the ultrastructural level is the presence of olfactory vesicles protruding into lumens and one is shown in figure 38b. In the tumors, these vesicles contain some dense-core granules but I have not observed cilia comparable to those found on vesicles of normal olfactory neuroepithelial cells. The slender basal processes of neuroepithelial cells are present in the tumors, and they group to form bundles (figure 38c) which in the normal individual would combine further and pass through the cribriform plate to reach the olfactory bulb. Most of the neoplastic columnar cells do not have an olfactory vesicle or basal lamina but they do have many irregular microvilli and these cells correspond to the sustentacular cells of normal olfactory mucosa.

The second case had similar histology (figure 39) and again the periphery of a gland-like structure was not sharply defined. EM showed that the columnar cells did not rest on a basal lamina (figure 40) and almost all the cells were of sustentacular type. The sparse neuroepithelial cells were clustered and figure 41a shows olfactory vesicles combining to form a mushroom-shaped expansion that protrudes into a lumen. In the thin stalk of this aggregate, the closely apposed stems of cytoplasm contain microtubules (figure 41b).

The great majority of neuroblastic tumors arising in the nasal cavity do not show evidence of true olfactory differentiation, but some have considerable numbers of dendritic processes that cluster and may occupy more extensive domains than the cell bodies. The caliber and granule content are quite variable. Figure 42 shows processes from one case.

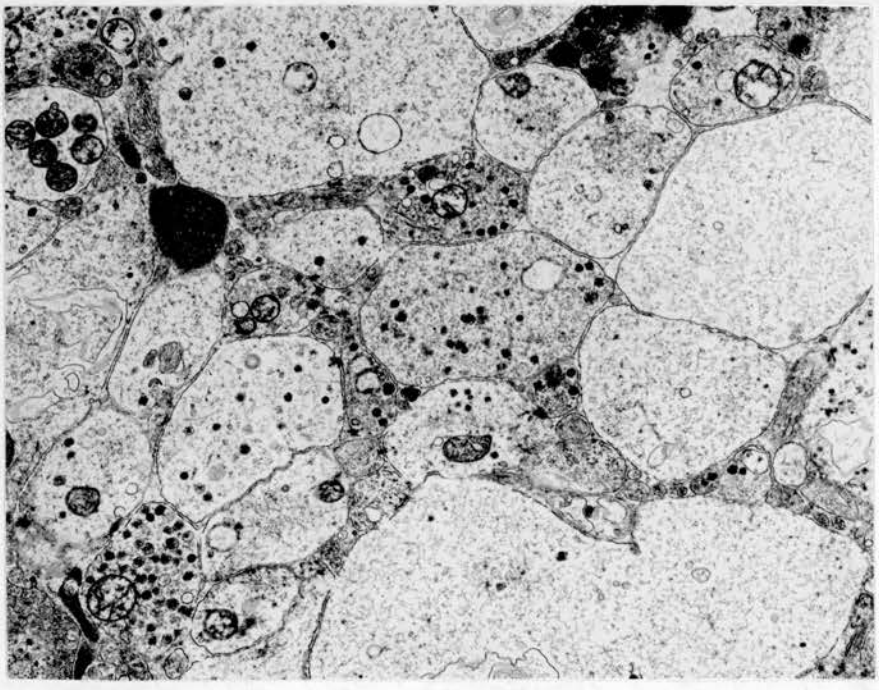

Figure 42. Neuroblastoma from the nasal cavity. Tumor cell processes are closely packed and they vary in diameter and granule content. x 23,000.

The possibility that the extent of the processes might have prognostic significance was studied by morphometric analysis performed on low-magnification electron micrographs. The morphometry was performed by Dr. Josep Lloreta.

> **Lloreta-Trull J, Mackay B, Troncoso P, Ribalta-Farres T, Smith T, Khorana S. Neuroendocrine tumors of the nasal cavity: an ultrastructural and morphometric study of 24 cases. Ultrastructural Pathology 16:165-175, 1992.** Twenty-four small-cell nasal tumors with neuroendocrine differentiation were identified by EM. Morphometric analysis of electron micrographs was used to determine the areas occupied by the tumor cell bodies and by their dendritic processes.

The apparatus used for the morphometry study is shown in figure 43. The procedure for each tumor was to trace outlines on low magnification electron micrographs as illustrated in figure 44. Statistical analysis was limited by the small number of cases, but a positive correlation was demonstrated between the dendritic area index (total dendritic area divided by total cell area) and the survival of the patients. EM studies of small cell nasal tumors indicate that separation into olfactory neuroblastomas, neuroblastomas without true olfactory differentiation, and neuroendocrine carcinomas is feasible[77, 78].

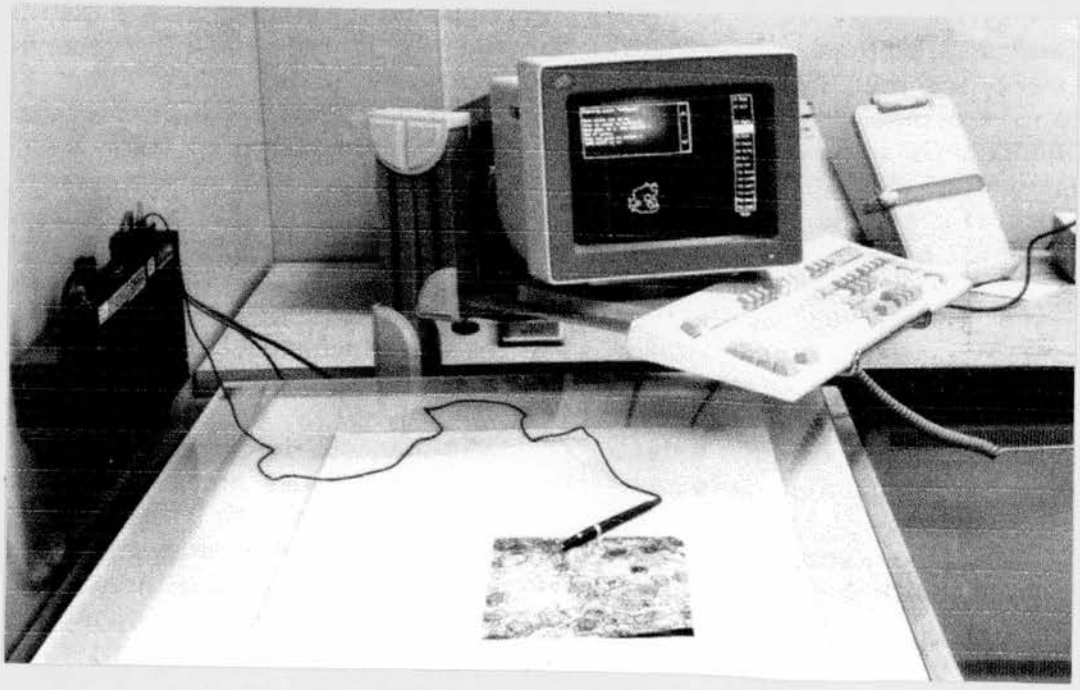

Figure 43. The morphometry apparatus

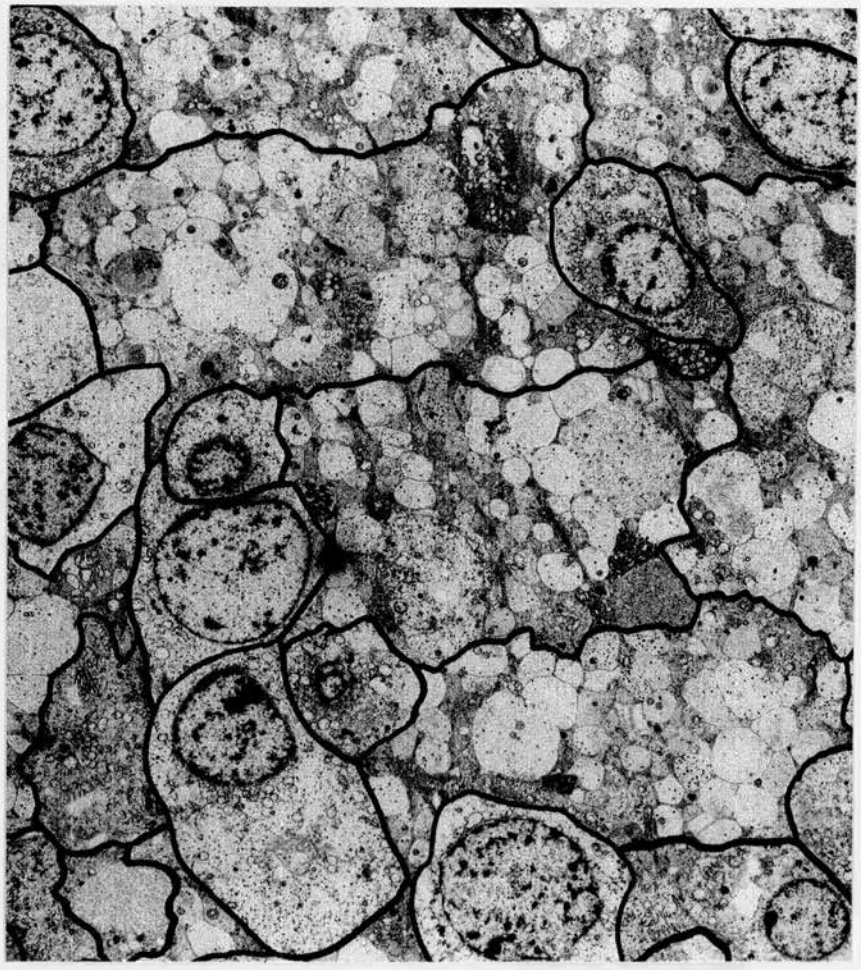

Figure 44. Outlines of cell bodies and groups of processes have been marked on the electron micrograph (the morphometric analysis was performed by Dr. Josep Lloreta).

One tumor that arose in the para-nasal tissues of a 15 year old female had been diagnosed as neuroblastoma, but it was unusual by EM which confirmed the presence of neuroblastic features but also revealed a component of melanocytic cells. The presence in the tumor of both neuroblastic (figure 45) and melanocytic (figure 46) cells is not compatible with the impression that the tumor was a typical neuroblastoma, and a well defined basal lamina was identified (figure 45). Rather, the combination of the two elements suggests a melanotic neuroectodermal tumor[79]. However, most of these tumors occur in the first year of life[80], and although rare examples in adult patients have been reported, they are widely regarded as misdiagnoses[81]. The interpretation is nevertheless favored by the findings from EM.

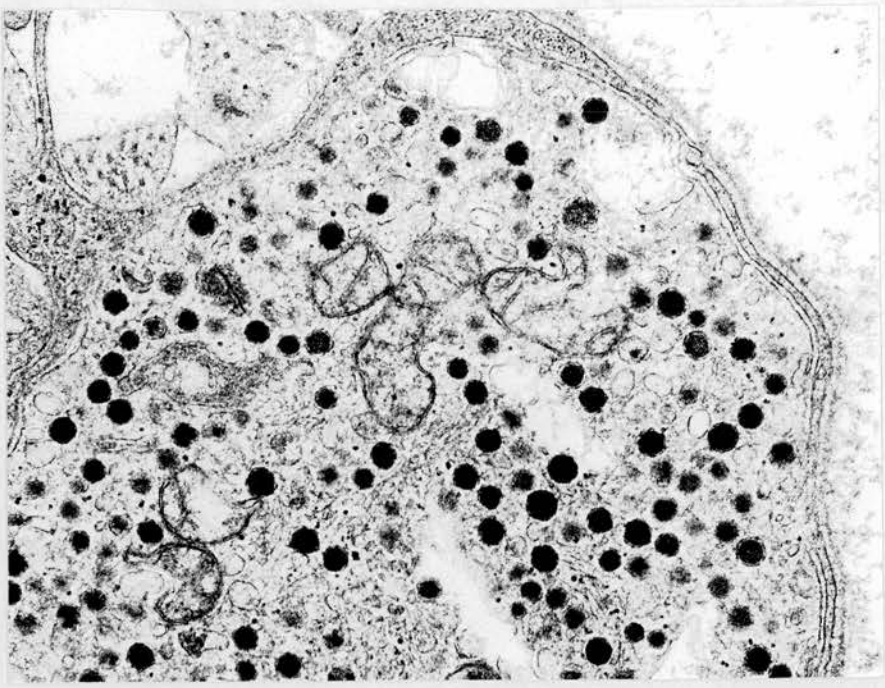

Figure 45. Possible pigmented neuroectodermal tumor. Neuroblastic differentiation is evident and a basal lamina appears intact. x 14,000.

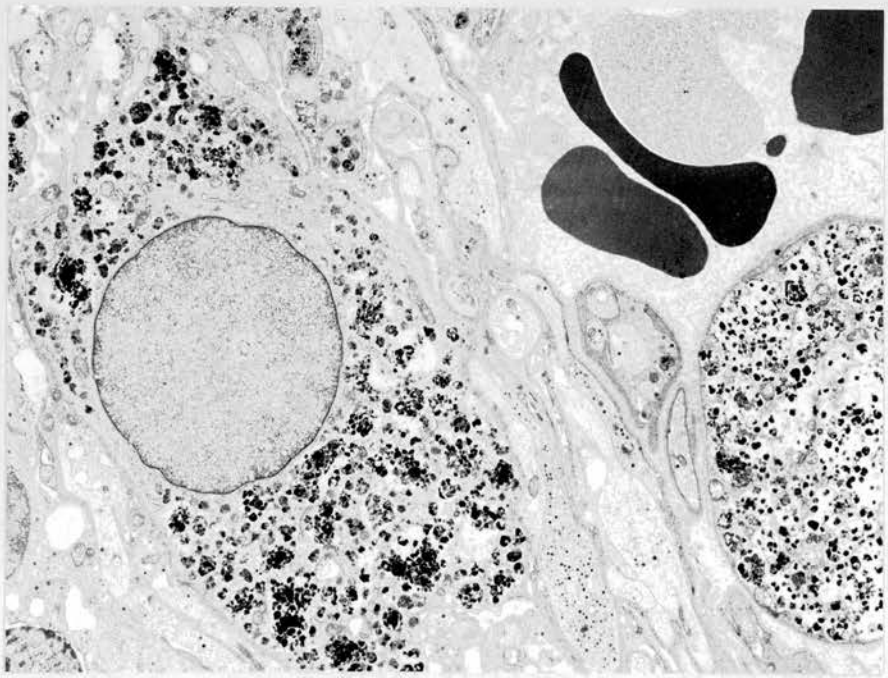

Figure 46 Same tumor as figure 45. Cells contain numerous melanosomes. x 3,200..

Myoepithelioma

The diversity of subtypes in salivary gland tumors, as well as the range of histomorphology within any one subtype, is unparalleled in any other human tumor, and this and their relative infrequency cause diagnostic problems for pathologists[82]. EM has a limited role in the diagnosis of primary salivary gland tumors, but it has been of value in elucidating appearances seen by routine light microscopy[83] including the extent of participation of myoepithelial cells. Four classic types of salivary gland tumors are illustrated here.

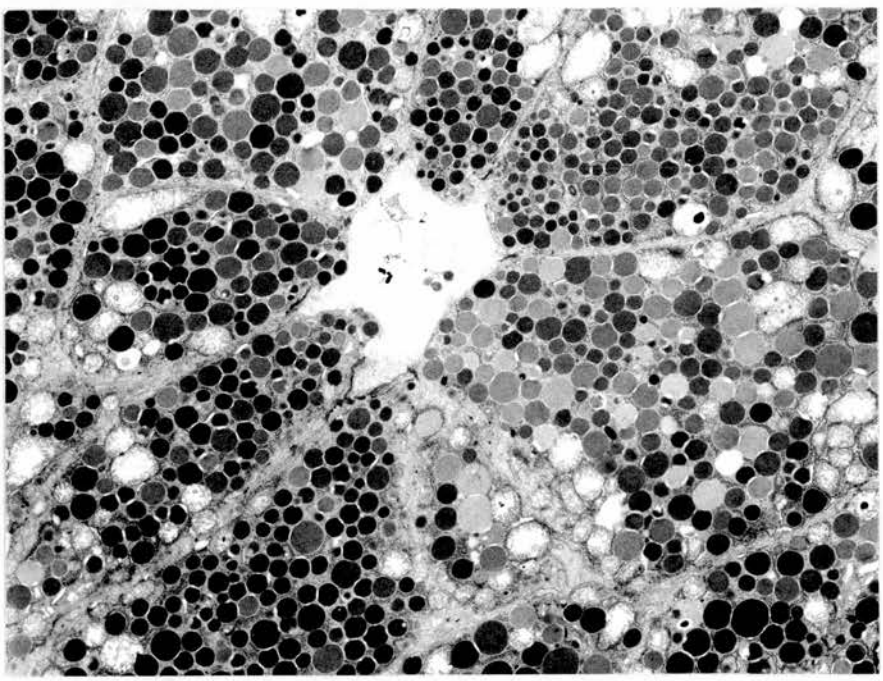

Figure 47. Acinic cell carcinoma of parotid gland. Cells containing large granules surround a small lumen. x 4,700.

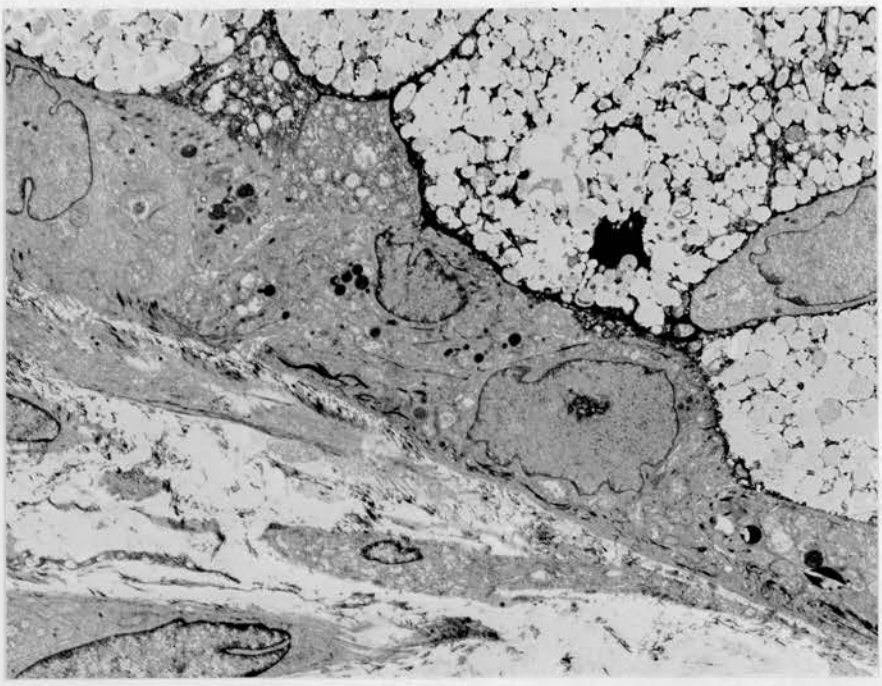

Figure 48. Mucoepidermoid carcinoma of submandibular gland. Epithelial cells containing sparse keratin lie beneath mucus-forming cells. x 4,200.

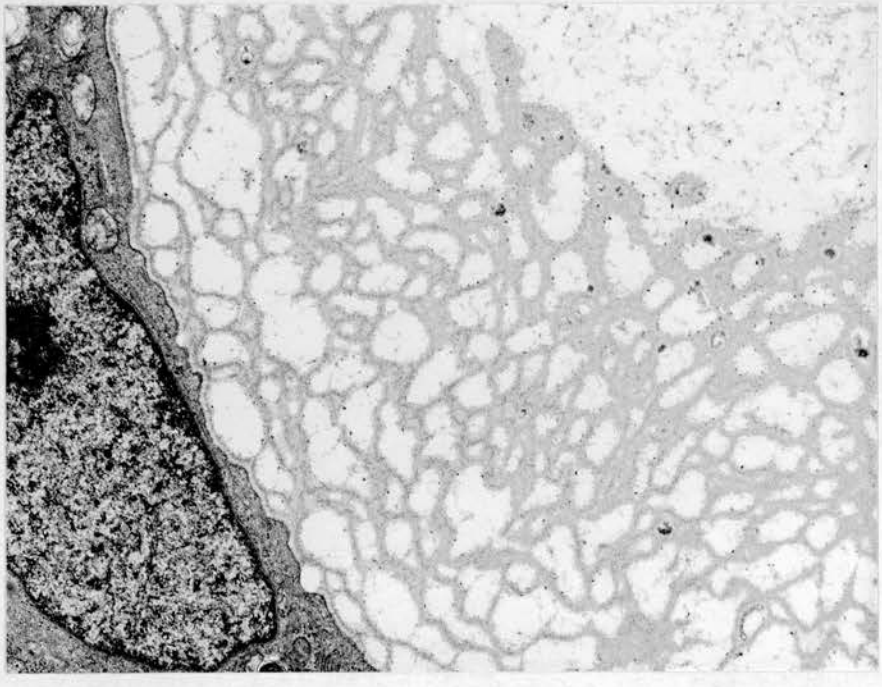

Figure 49 Adenoid cystic carcinoma of parotid gland showing marked replication of basal lamina. x 7,800.

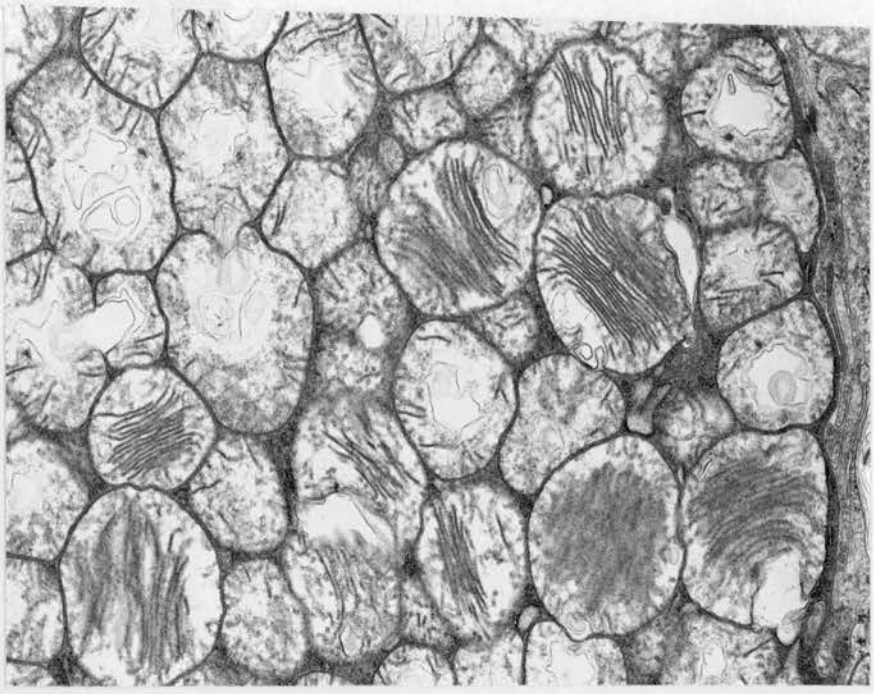

Figure 50. Warthin's tumor of parotid gland. The cell is packed with mitochondria that have elaborate cristal patterns. x 14,200.

The dominant feature in an acinic cell carcinoma is the many large granules within the cytoplasm (figure 47). These are typical exocrine-type granules measuring at least 600 nm in diameter, and they have round dense cores within a tightly applied limiting membrane. Stratification of epithelial and mucin-forming cells can be seen in Mucoepidermoid carcinomas with a variety of appearances possible at the ultrastructural level depending on the degree of keratinization in the epithelial cells, the amount of mucin that is present, and the degree of admixture of transitional forms. In the area of the tumor shown in figure 48, the transition between the epithelial and mucin forming strata is fairly abrupt. Marked replication of basal lamina material accounts for the hyaline material seen by light microscopy in adenoid cystic carcinoma[84] (figure 49). Warthin's tumor is a classic source of oncocytic cells packed with mitochondria, many of which have unusual patterns of their cristae (figure 50).

Myoepithelial cells are a basic component of the secretory units of salivary gland tissue, enveloping the acinar cells and small ducts with their cell processes, and they occur as a component of the common tumors[85, 86]. They have been called basket cells, although with their radiating arms of cytoplasm they more closely resemble starfish than baskets. In human salivary tissue, myoepithelium is not limited to the acinar-intercalated ductal system but extends to the intra- and extralobular striated ducts[87]. As a pathology resident, I collaborated in a study of the relationship of peripheral nerves to myoepithelial cells.

> **Harrop TJ, Mackay B. Electron microscopic observations on myoepithelial cells and secretory nerves in rat salivary tissues. Journal of the Canadian Dental Association 34:481-488, 1968..**
> In rat salivary glands, myoepithelial cells and their cytoplasmic extensions lay within the basal lamina of acini and small ducts, separated by an interval of about 200 A from adjacent secretory cells. The myoepithelial cells contained slender bundles of

microfilaments. Unmyelinated axons were numerous in the connective tissue between acini. Axons containing granular vesicles approximated to but did not penetrate the basal lamina overlying myoepithelial cells. In contrast, axons were present within serous acini, separated from the secretory cells by a gap of about 150 A. The observations suggested that sympathetic nerves contact myoepithelial cells of mucous acini and that most axons in serous acini are parasympathetic.

Neoplastic myoepithelial cells can assume a wide range of appearances[88, 89], and the presence of myoepithelial differentiation in salivary gland tumors is not always obvious by light microscopy. The myoepithelial cells may coexist with epithelial cells producing a clearly recognizable biphasic pattern[90], but if only myoepithelial cells are present, the diagnosis may not be obvious. This is illustrated by reports on two benign tumors.

Luna MA, Mackay B, Gamez-Araujo J. Myoepithelioma of the palate. Report of a case with histochemical and electron microscopic observations. Cancer 32:1429-1435, 1973.

A submucosal mass in the left side of the hard palate of a 30 year old female had been present for five years, slowly increasing in size. It was resected, and was found to be located in the submucosa. The tumor was solid and unencapsulated, measuring 4.5 cm in greatest dimension. By light microscopy, it had a uniform composition with slender spindle-shaped cells in closely packed interlacing bundles. The cytoplasm contained many slender filaments and there were frequent mature desmosomes between the cells. An epithelial component could not be identified and the tumor was classified as a benign myoepithelial cell tumor (myoepithelioma).

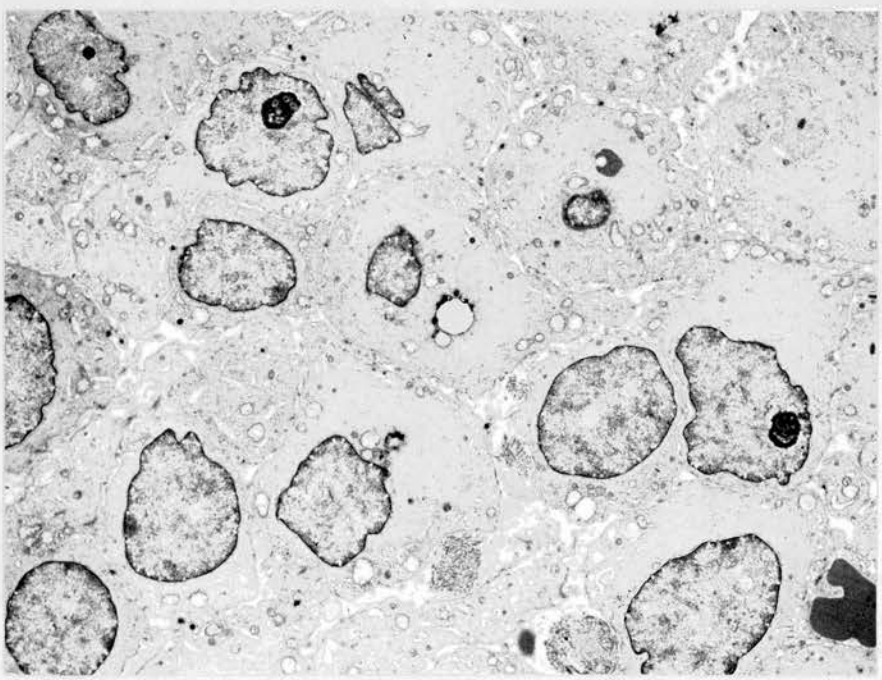

Figure 51. Myoepithelioma of palate. The spindle cells are cross-sectioned. Much of their cytoplasm was occupied by filaments. x 3,000.

Myoepithelial tumors can display a multiplicity of histologic patterns and cellular features, and epithelioid, plasmacytoid, spindle, and clear cell types have been described[91]. They may therefore present difficulties in diagnosis and cellular varieties can be misinterpreted as malignancies[92]. The cells in the tumor of the palate (figure 51) had a hyaline appearance by light microscopy because of the diffuse filaments occupying most of their cytoplasm. Myoepithelioma is an unusual tumor at this site and reported cases have also contained plasmacytoid or spindle cells[93, 94]. The histologic complexity of these neoplasms is due to the ability of the neoplastic ductular myoepithelial cell to modulate its morphologic appearance and intermediate filament composition, and to produce large amounts of matrix substances[95].

Mackay B. Ordonez NG. Batsakis JG. Goepfert H. Pleomorphic adenoma of parotid with myoepithelial cell predominance. Ultrastructural Pathology 12:461-468, 1988.
A 43-year-old woman presented with a parapharyngeal mass that was initially interpreted as a soft tissue sarcoma with neural differentiation. EM and immunohistochemistry led to a diagnosis of pleomorphic adenoma with myoepithelial cell predominance.

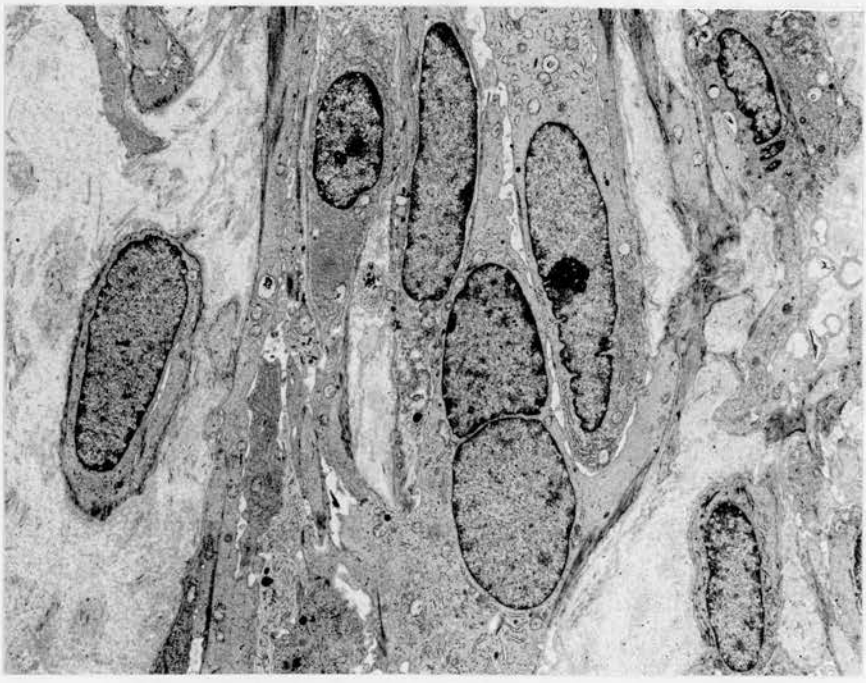

Figure 52 . Pleomorphic adenoma of parotid gland with myoepithelial cell predominance. The dense bundles of filaments in this field are smooth muscle myofilaments. x 3,400.

The deep lobe of the parotid gland forms the lateral wall of the parapharyngeal space and a pleomorphic adenoma may present in this location. In one study of 42 lesions of the parapharyngeal space, 17 (40%) were neurogenic and 16 (38%) were salivary gland tumors[96]. The tumor we report was composed of fascicles of spindle cells which initially suggested a malignant peripheral nerve sheath tumor. EM revealed the presence of keratin

filament bundles and smooth muscle myofilaments (figure 52), and both were often seen in the same cell. Immunoperoxidase staining demonstrated keratin and smooth muscle positivity.

Small cell carcinomas of parotid gland

Pure small cell carcinomas are uncommon salivary gland neoplasms. We reported three cases from the parotid gland to show that ductal and neuroendocrine types occur and that the neuroendocrine features can persist in metastases.

> **Kraemer BB, Mackay B, Batsakis JG. Small cell carcinomas of the parotid gland. A clinicopathologic study of three cases. Cancer 52:2115-2121, 1983.** Three small cell carcinomas arising in the parotid gland were reported. EM showed that two were neuroendocrine tumors. The fine structure of the third tumor indicated intercalated duct cell differentiation from the absence of neuroendocrine granules and processes and the presence of frequent desmosomes.

Figure 53. Small cell carcinoma of parotid gland. The series of long desmosomes indicates ductal differentiation. x 12,000.

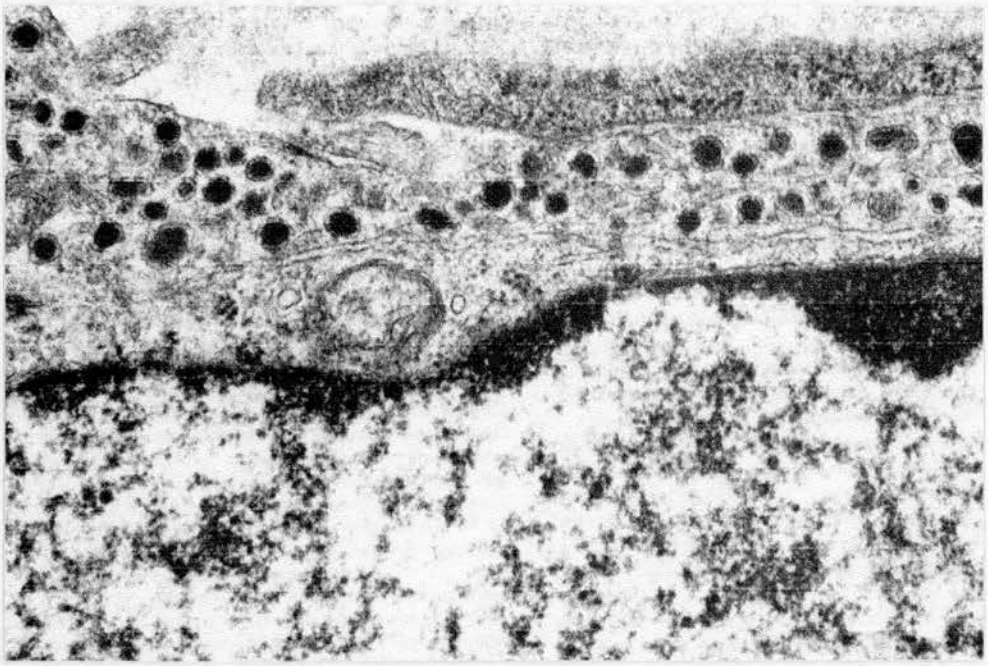

Figure 54. Small cell carcinoma of parotid gland. A cell process contains many dense-core granules of neuroendocrine caliber. x 35,000.

This report provided evidence that two distinct types of small cell carcinomas can arise in salivary glands. In one of the three tumors, small cells were connected by series of mature desmosomes with tonofilaments that were only visible alongside the desmosomal densities (figure 53). In the other two tumors, the cells had very few cell junctions and those that were present were small and primitive in construction. In both tumors, dendritic processes contained numerous membrane-bound dense-core granules, most of which were between 100 and 120 nm in diameter (figure 54). One of the two tumors was primary and the other was diagnosed from an inguinal metastasis. Only a minority of small cell tumors of the parotid show neuroendocrine differentiation by EM[97], though immunohistochemical markers may reveal its presence in additional cases[98]. In an ultrastructural study of eight small cell tumors arising in major salivary glands, only one showed evidence of dense-core granules[99]. The possibility of metastasis from a primary skin tumor should be considered when assessing the differential diagnosis of a small cell parotid tumor: one of the nine tumors reported as adult neuroblastomas (page 21) was a cutaneous neuroendocrine carcinoma that had spread to a parotid lymph node.

Tumors of the respiratory system

The lung tumors discussed in this section are adenocarcinoma, small cell carcinoma, carcinoid tumor, and as examples of the uncommon tumors, sclerosing hemangioma, epithelioid hemangioendothelioma, and alveolar adenoma. Mesothelioma is also discussed.

The clinical importance of lung and pleural tumors and the often dismal results of therapy were inducements for me to conduct correlated light and electron microscopic studies on a large number of cases, and I had the opportunity to work with Study Groups including the International Association for the Study of Lung Cancer (IASLC), and to participate in the preparation of the 3rd Edition of the WHO classification of lung and pleural tumors[100]. Many of my observations were illustrated and discussed in a book on the pathology of lung cancer[101], and a number of publications[102-106].

Adenocarcinoma of lung

In addition to the basic morphologic features common to most differentiated adenocarcinomas, some lung adenocarcinomas show cellular specializations that correlate with their light microscopic subclassification. The breadth of histopathology that exists among lung tumors is in part the result of variations between subtypes, and heterogeneity, with various admixtures of adenocarcinoma, squamous cell carcinoma, and undifferentiated large cell carcinoma, can often be recognized by routine light microscopy[107] and at the ultrastructural level[108, 109].

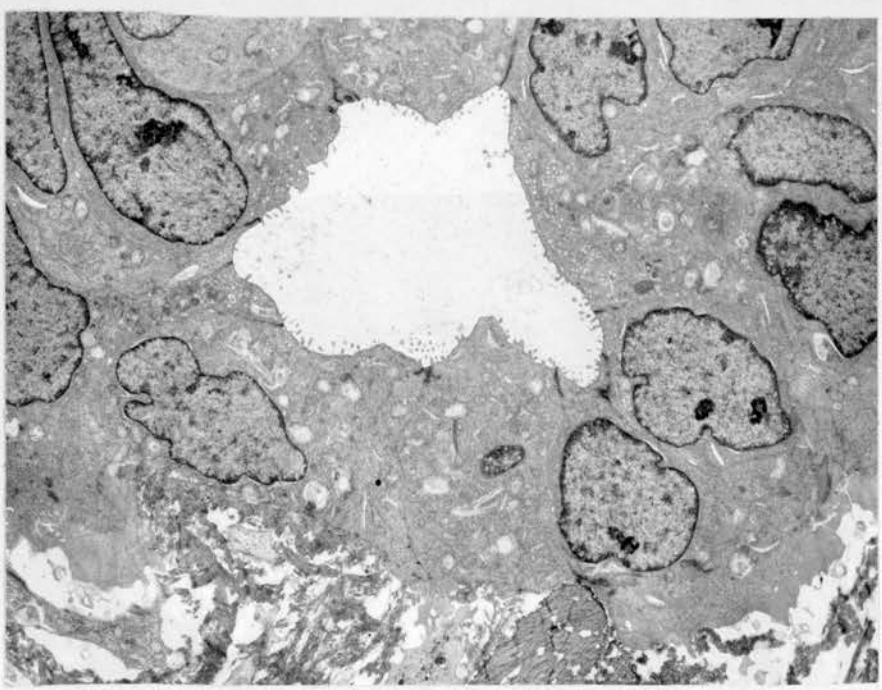

Figure 55. Adenocarcinoma of lung, well differentiated. Tumor cells with irregular microvilli surround a small lumen. x 4,400.

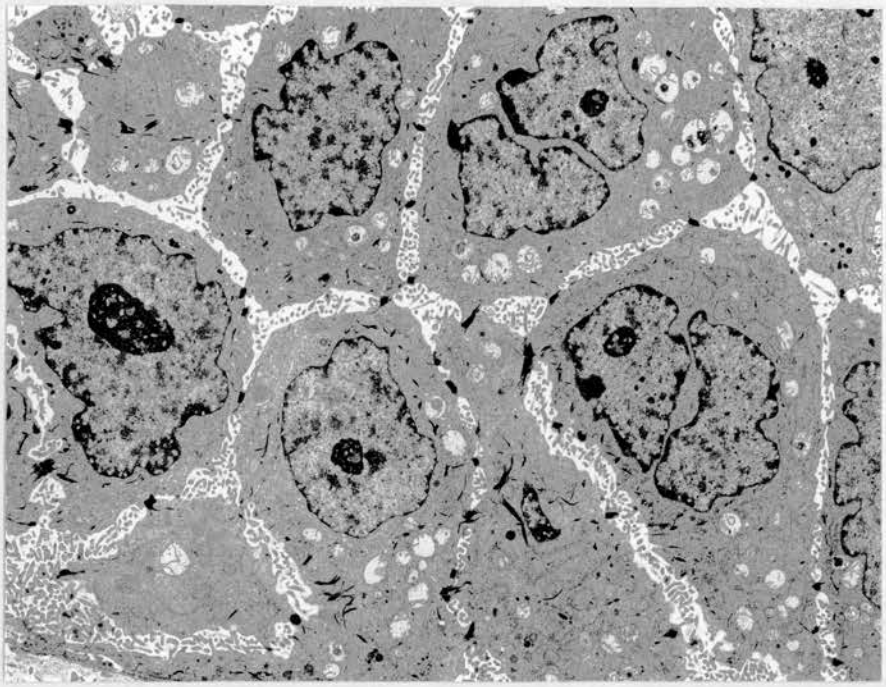

Figure 56. Squamous cell carcinoma of lung, well differentiated. Desmosomes are present in moderate numbers but keratin is not abundant. x 4,700.

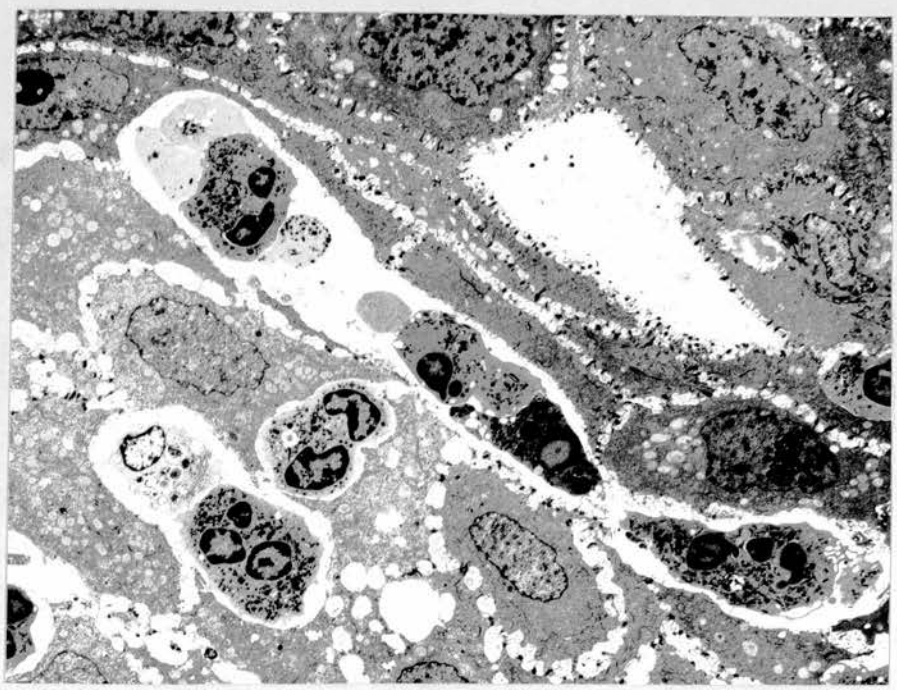

Figure 57. Squamous cell carcinoma of lung, moderately differentiated. Loss of cohesion among the cells simulates gland formation. Invasion by neutrophils is occurring. x 3,800.

Gland formation is the hallmark of acinar type adenocarcinomas and the number, size and shape of the glandular lumens (figure 55) show a rough correspondence to the level of differentiation both by light and electron microscopy. The number and length of the microvilli on the apical cell surfaces is quite variable and does not relate closely to the size of the lumens: they can be luxuriant in very small lumens, or sparse and irregular. When mucin is present, it tends to accumulate in the apical cytoplasm in columnar cells, but is diffuse in the uncommon signet ring cells. Glycogen often forms small lakes which can be distributed throughout the cell. Squamous cell carcinomas in the lung are similar in their fine structure to the same tumors in skin and other locations, but the cells may be more closely apposed resulting in a lack of 'intercellular bridges' for the light microscopist, and keratin is usually less abundant compared with skin tumors (figure 56). As with the cutaneous tumors, the amount of keratin and number and maturity of the desmosomes diminish with loss of differentiation, but the degree of development of these features does not consistently correspond to the light-microscopic assessment of the level of differentiation. Sampling can influence this descrepancy. In a tumor classified by light microscopy as adenosquamous carcinoma, there is generally a fairly good separation of the glandular and squamous components and the appearance by EM will again be influenced by the area selected for study. True admixtures of the two lines of differentiation[110] are sometimes seen in an EM thin section, but this appearance can be simulated when loss of cohesion occurs among cells of a squamous tumor, creating an illusion of gland formation that is heightened by filopodia projecting into the lumen (figure 57). A more intimate juxtaposition among different cell types in non-small cell lung carcinomas is a relatively common EM finding, with keratin-forming and mucin-producing cells in the same cluster. These observations indicate that a rigid separation of adenocarcinoma and squamous cell carcinoma of the lung is often impossible. Many tumors show mixed differentiation at the ultrastructural level that is not detected in paraffin sections.

Figure 58. Bronchioloalveolar adenocarcinoma. Apical cytoplasm projects into the lumen. The cytoplasmic granules are mostly supranuclear. x 3,900.

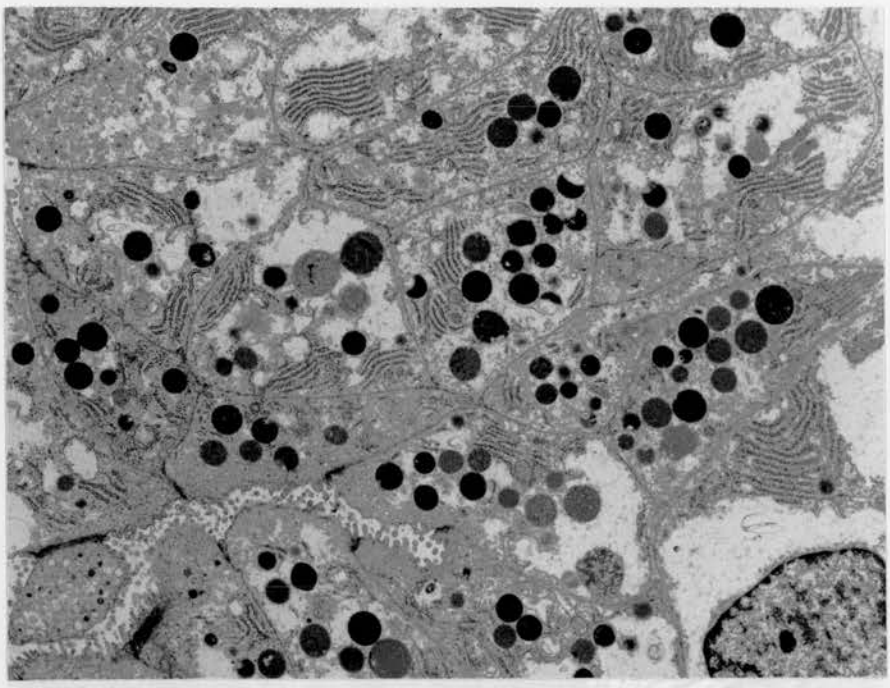

Figure 59. Bronchioloalveolar adenocarcinoma. The plane of section passes through the apical cytoplasm of several tumor cells and demonstrates the large round granules and amorphous mucin. A small slit of lumen is visible. x 6,100.

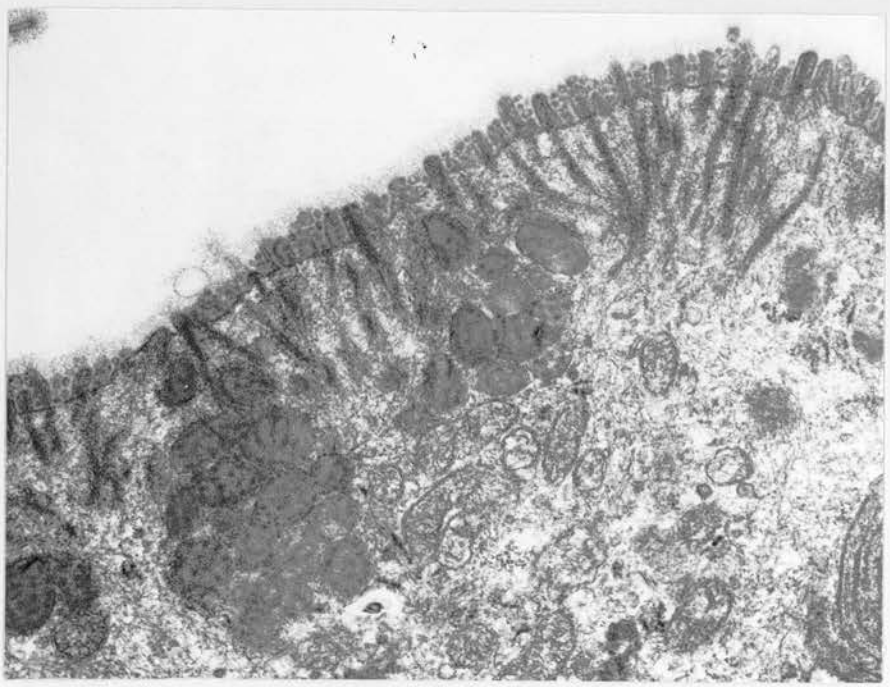

Figure 60. Bronchioloalveolar adenocarcinoma. Microfilaments from the microvilli extend down into the apical cytoplasm. There are many glycocalyceal granules between the microvilli. x 13,200.

Figure 61. Bronchioloalveolar adenocarcinoma. Fan-like clusters of tumor cells rest on the alveolar framework. The cells contain apical mucin granules. x 3,500.

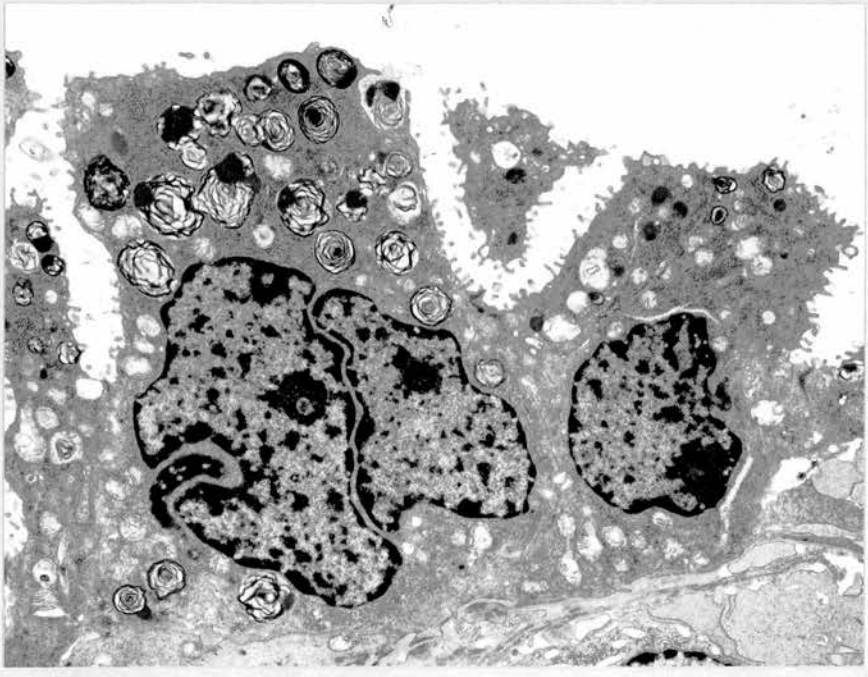

Figure 62. Bronchioloalveolar adenocarcinoma. Cells in this tumor contain lamellar bodies. x 5,300.

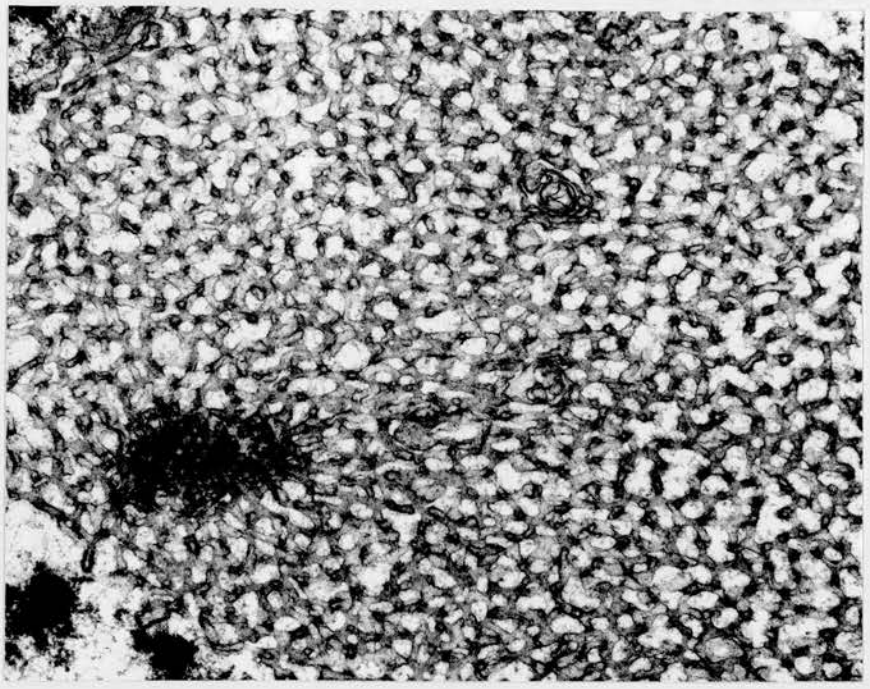

Figure 63. Bronchioloalveolar adenocarcinoma. Part of an intranuclear inclusion. x 44,000.

Bronchioloalveolar adenocarcinomas frequently show Clara cell differentiation[111], characterized by the projection of the apical cytoplasm into the lumen (figure 58) and the presence of dense granules of exocrine caliber in the apical cytoplasm (figure 59). One or two dense granules of this type are a frequent finding in cells of many poorly differentiated lung adenocarcinomas but their significance is uncertain. Mucin is often present alone or together with the granules, and it can occupy much of the cytoplasm. In some bronchioloalveolar adenocarcinomas, the microvilli have microfilament cores like those of gastrointestinal tract cells (figure 60). A fan-like pattern of tall columnar cells attached to the alveolar framework is striking by both light microscopy and EM (figure 61). Lamellar bodies like those of type 2 pneumocytes (figure 61) are quite uncommon in the neoplastic cells: when they are present in moderate numbers, staining for surfactant should be positive[112, 113]. I have only seen one Clara cell tumor that contained an admixture of ciliated cells. A few of the tumors contain distinctive nuclear inclusions made up of branching tubules that are continuous with the inner layer of the nuclear envelope (figure 63).

The following case of bronchioloalveolar adenocarcinoma was unique in that the tumor contained myoepithelial cells.

Dekmezian R, Ordonez NG, Mackay B. Bronchioloalveolar adenocarcinoma with myoepithelial cells. Cancer 67:2356-2360, 1991.
A papillary lung carcinoma resected from a 58-year-old woman contained both Clara cells and myoepithelial cells. It recurred in the lung and tumor was not detected in other sites.

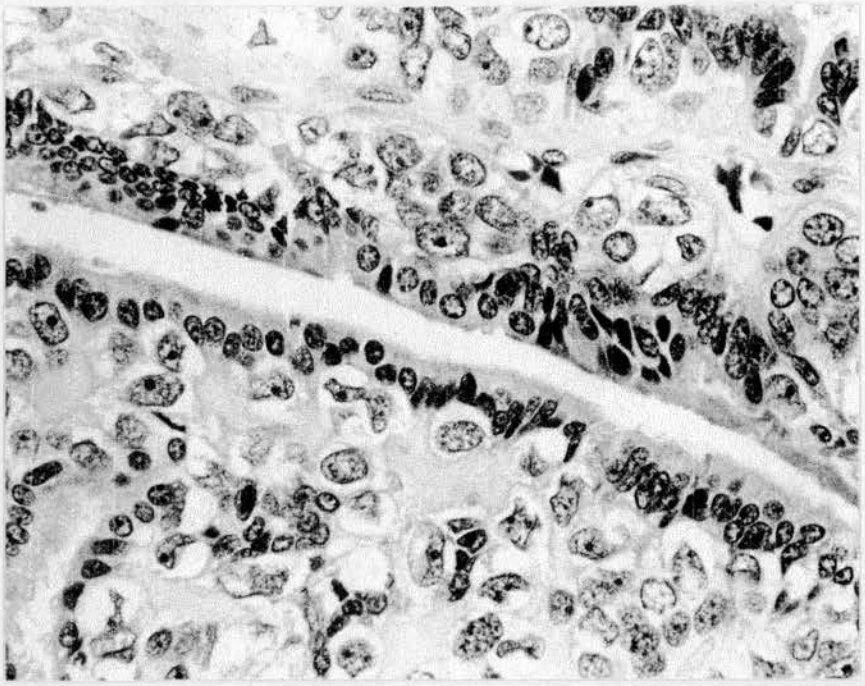

Figure 64. Bronchioloalveolar adenocarcinoma with myoepithelial cells. Hematoxylin and eosin.

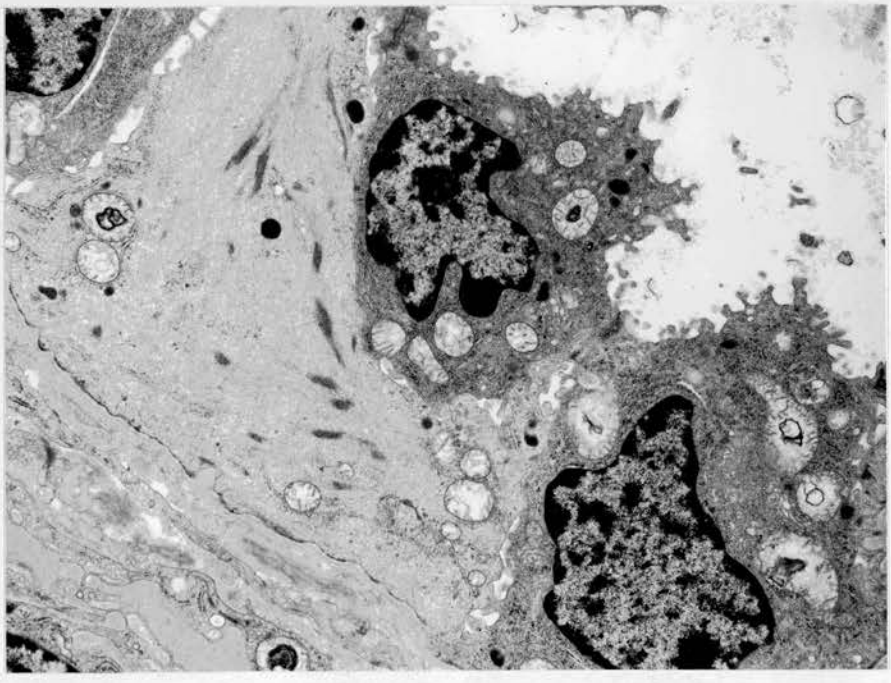

Figure 65. Same tumor as figure 64. A myoepithelial cell underlies epithelial cells. x 7,300.

By light microscopy, two types of cells could be seen throughout the tumor (figure 64). EM confirmed that the more superficial cells were Clara cells though many of them had sparse granules (figure 65). The deeper cells were rich in smooth muscle myofilaments and they rested on a basal lamina. The immunohistochemical features of the Clara cells (positive for keratin and surfactant) and myoepithelial cells (positive for S-100 protein and smooth muscle actin) were consistent. Myoepithelial cells had not previously been reported in bronchioloalveolar adenocarcinoma. This tumor recurred within the lung, and tumor was not detected in other locations. A pure myoepithelioma of the lung is rare[114], but myoepithelial cells can be present in mixed and mucoepidermoid tumors of bronchial gland or tracheal origin[115-117]. A comparable juxtaposition of surface secretory cells containing exocrine granules with underlying myoepithelial cells occurs in epithelial-myoepithelial cell tumors of the salivary glands[118], and we have seen one case that metastasized to the lung from parotid and continued to display replication of basal laminar material, a feature that was absent in the primary lung tumor[119].

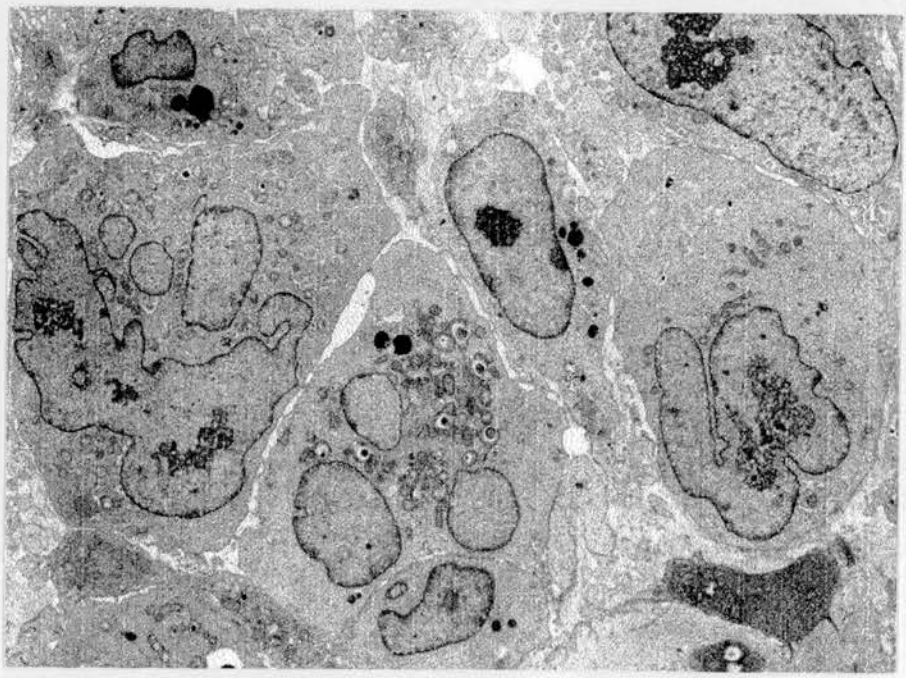

Figure 66. Large cell undifferentiated carcinoma of lung, pleomorphic variant. x 3,300.

The specialized structural features of glandular and squamous cells are progressively lost as a lung carcinoma dedifferentiates[120], but they continue to be visible in many cases by EM when they are no longer seen by routine light microscopy. In particular, small acini with a few microvilli are often found. This minimal level of differentiation has not been shown to have prognostic significance. Tumors that can not be identified as either glandular or squamous are designated undifferentiated large cell carcinomas, and the number so classified will be significantly smaller in series studied by EM. The cells can be uniform or pleomorphic. In the former subtype, nuclei can have smooth profiles but the closely packed cells are larger than those of a small cell carcinoma and they have prominent nucleoli and more frequent organelles. Cell junctions tend to be sparse and primitive, and then loss of cell cohesion occurs. A pleomorphic form of undifferentiated large cell carcinoma may be entirely made up of bizarre cells, or they may form a component of an otherwise

differentiated carcinoma. Pleomorphic cells (figure 66) are more frequently seen in adenocarcinomas than in squamous tumors and they are often large with multilobated or multiple irregular nuclei

Small cell lung carcinoma

Most biopsy specimens sent for electron microscopy to confirm a diagnosis of small cell lung carcinoma are from metastatic sites and they are prone to crushing artifact.

Nuclei in small cell lung carcinoma are typically to ovoid with smooth profiles and fine dispersed chromatin (figure 67) . The surrounding rim of cytoplasm is narrow and cells are closely packed. Cell junctions do occur thought they may be scattered, and they can be small desmosomes devoid of tonofilaments, or more primitive subplasmalemmal densities. Organelles are always sparse and cytoplasmic extensions (figure 68) are uncommon. The dense-core granules are only found with ease in about one third of the tumors, and after a search in a further third, while some do not contain granules. The granules are small, under 120 nm in diameter, and they are membrane-bound with round dense cores. Being of neuroendocrine caliber, they are smaller, as well as less numerous than those of many though not all pulmonary carcinoid tumors. I have observed similar fine structure in small cell carcinomas of the trachea[121] and larynx[122]. Rarely, small granules of this type are seen in a large cell lung tumor corresponding to the large cell neuroendocrine carcinoma described by Travis[123, 124].

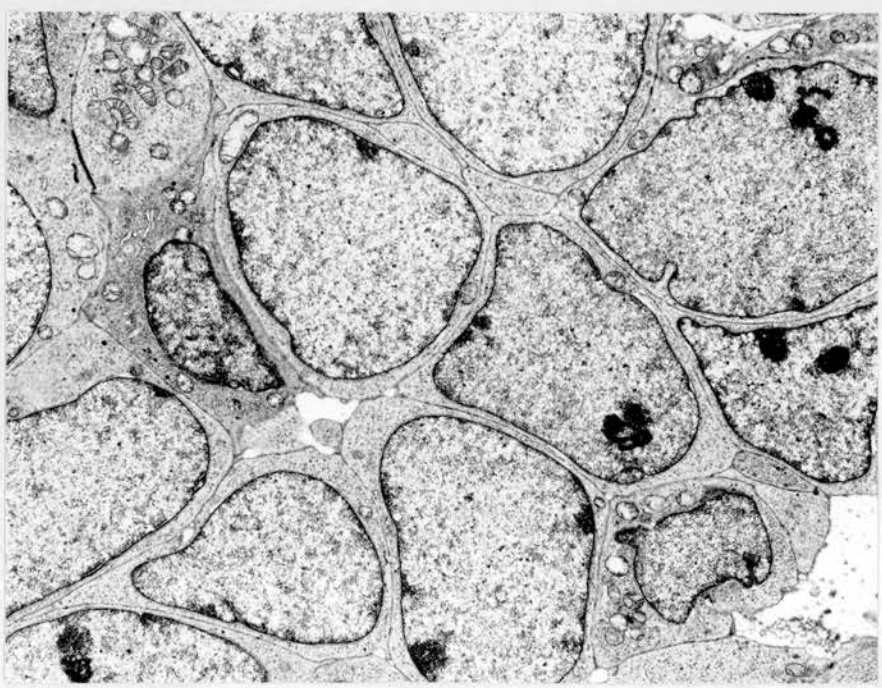

Figure 67. Small cell lung carcinoma. The cells are closely apposed but cell junctions are infrequent. The sparse cytoplasm contains a paucity of organelles. Nuclear profiles are smooth and the fine chromatin is dispersed. x 4,100.

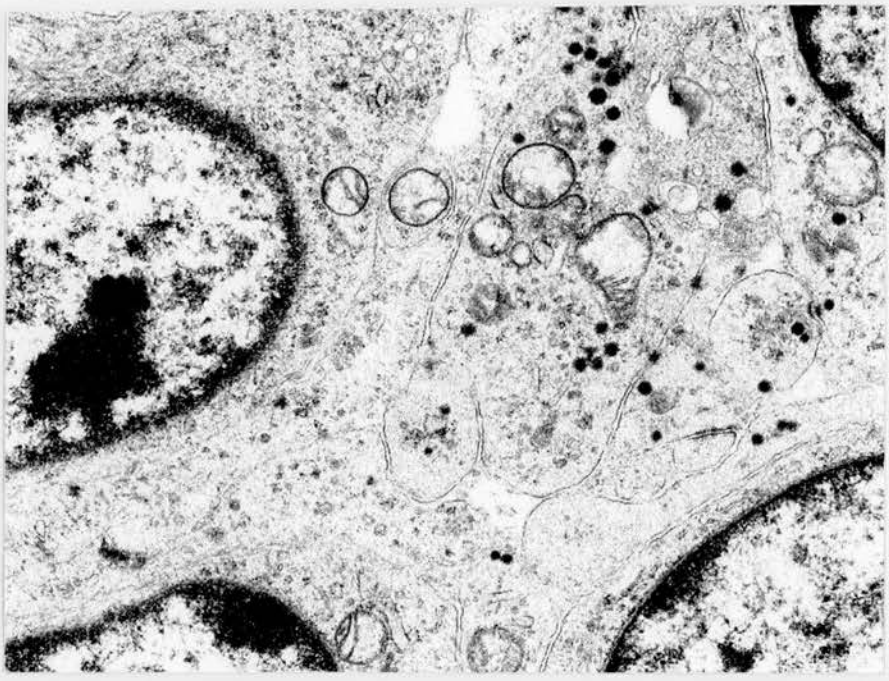

Figure 68. Small cell lung carcinoma. The aggregate of cell processes is an unusual finding. Small dense-core granules are present. x 7,200.

At the time I began studying small cell carcinomas of the lung with the electron microscope, it was standard practice to attempt to subdivide the tumors into intermediate and small cell categories on the basis of their appearance in routine light microscopic sections. After examining many cases, I found no justification from EM for the use of this terminology. Small round or ovoid cells could predominate in a particular tumor, but mixtures were the rule and sampling influenced the choice of subtype. In one study, nuclear size was not found to be a reliable indicator of prognosis[125], and there did not appear to be any clinical data to support the practice. I shared this information with the pathology group of the International Association for the Study of Lung Cancer (IASLC) of which I was a member, and revision of the existing classification was advocated.

Hirsch FR, Matthews MJ, Aisner S, Campobasso O, Elema JD, Gazdar AF, Mackay B, Nasiell M, Shimosato Y, Steele RH. Histopathologic classification of small cell lung cancer. Changing concepts and terminology. Cancer 62:973-977, 1988.

The recommendation was made that the current classification of small cell lung carcinomas be replaced by the following scheme. 1: Small cell carcinoma – this subtype includes most of the tumors previously included in the oat cell and intermediate subtypes, and more than 90% of untreated small cell lung carcinomas fall into this category. 2: Mixed small cell/large cell carcinoma – a subtype containing a spectrum of cell types ranging from typical small cell lung carcinoma to larger cells resembling those of large cell carcinoma. 3. Combined small cell carcinoma – a subtype in which typical small cell elements are intimately admixed with areas of differentiated squamous cell or adenocarcinoma.

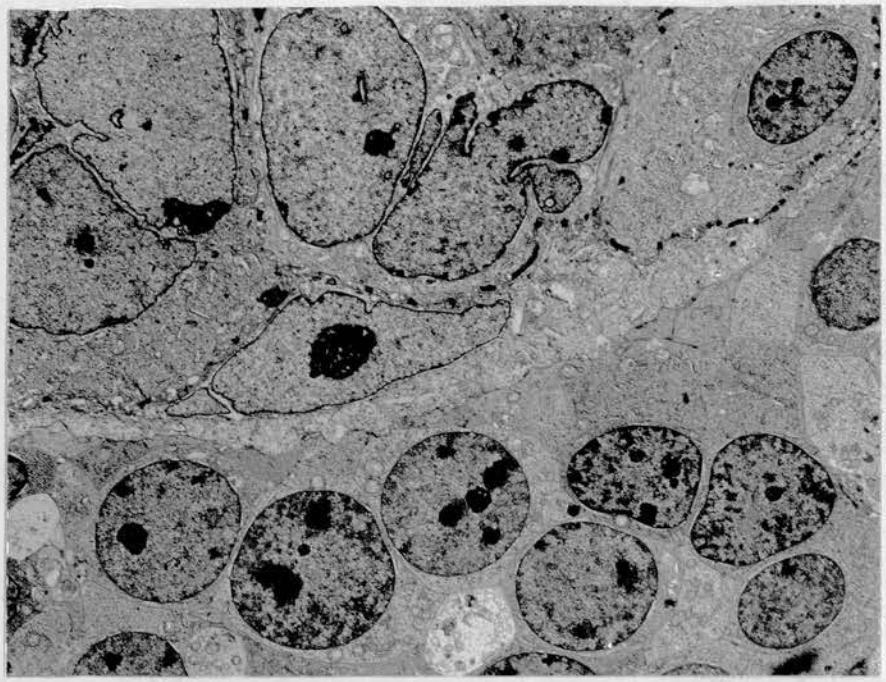

Figure 69. Combined small cell carcinoma. Small cells abut against a nest of squamous cells. x 3,200.

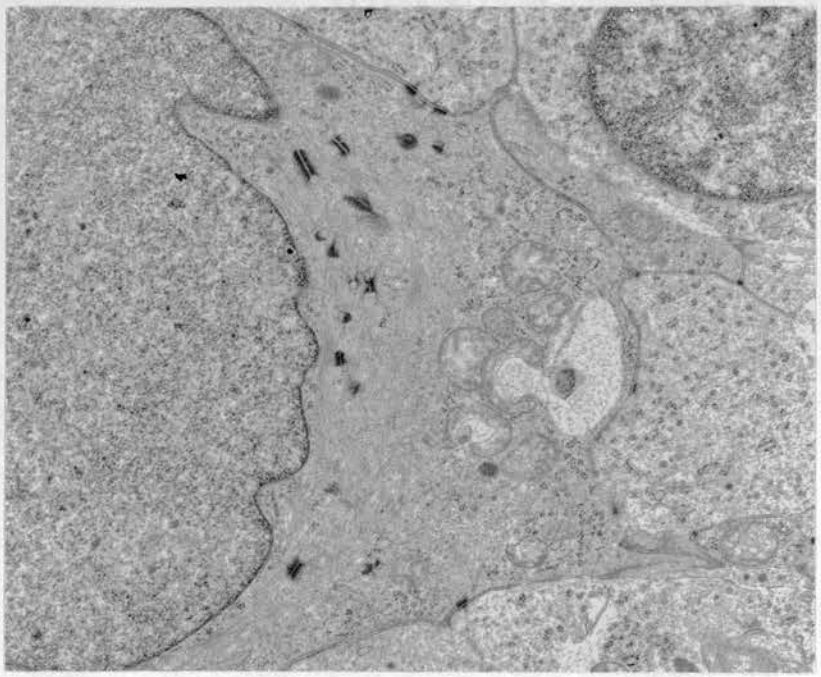

Figure 70. Same tumor as figure 69. Desmosomes lie free within the cytoplasm of a squamous cell. x 8.100.

I had not seen a convincing example of a mixed small cell/large cell carcinoma by EM and was of the impression that tumors so designated by routine light microscopy were poorly preserved. This subtype was omitted from the 3rd WHO classification of lung neoplasms, and the only variant of small cell carcinoma is thus the combined form. An example in which the differentiated component was squamous cell carcinoma is shown in figure 69. Small desmosomes linked small cells, and larger desmosomes were present between the squamous cells, and where small and squamous cells were in contact, they were connected by the small desmosomes (figure 70) indicating that the small cells had taken the initiative in their formation. A curiosity was the presence of detached desmosomes lying free within the cytoplasm of a number of the squamous cells (figure 70).

A continuous row of small cells can often be found resting on the basal lamina in bronchial mucosa (figure 71) and they presumably function as reserve cells with at least the potential for squamous differentiation. Goblet and other taller cells have to squeeze between them to reach the basal lamina (figure 71). These basal cells do not contain neuroendocrine-type secretory granules so it is not possible to argue from the ultrastructure that they are the progenitors of small cell lung carcinoma. Scattered true endocrine cells are in contrast larger and triangular in cross section, and they contain abundant granules (figure 72).

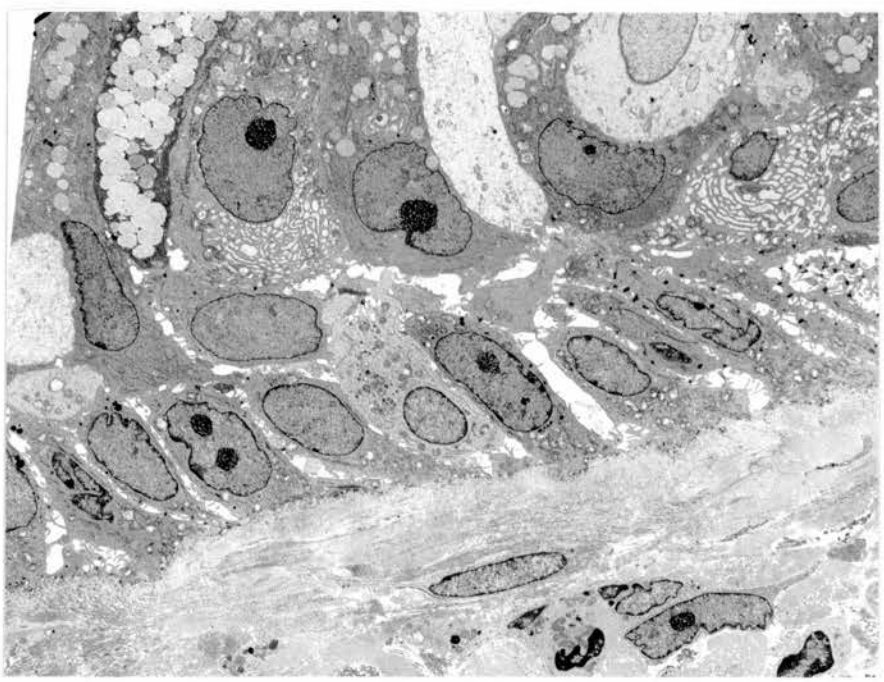

Figure 71. Normal bronchial mucosa. A row of small basal cells rests on the basal lamina. x 3,400.

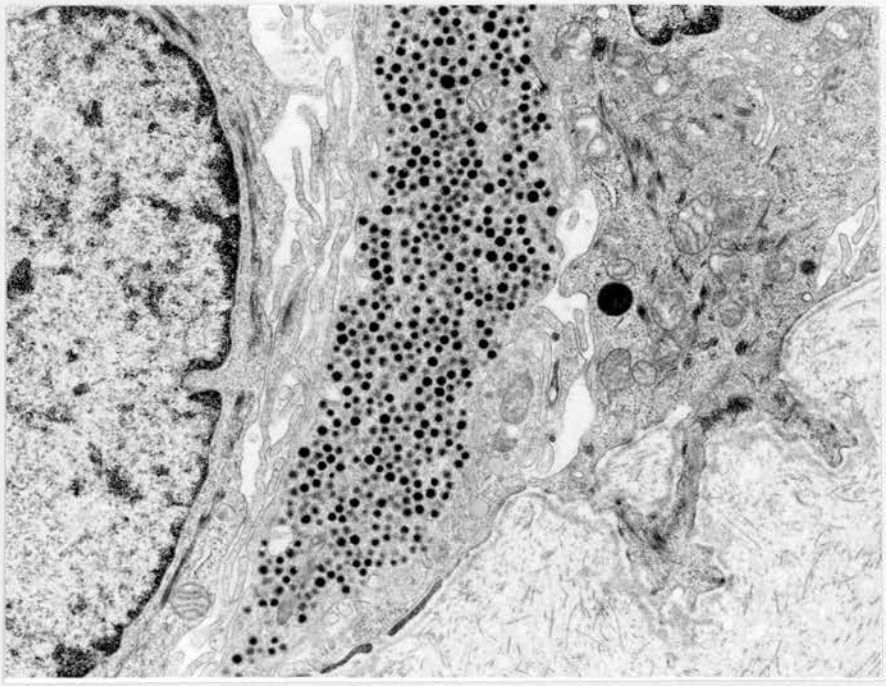

Figure 72. Normal bronchial mucosa. An endocrine cell contains many secretory granules. x 7,400.

Carcinoid tumor

Carcinoid tumors in the lung do not overlap structurally with other subtypes to the degree that this occurs in the other common lung tumors, although an atypical or poorly differentiated carcinoid can resemble a small cell carcinoma. The appearance of carcinoid tumors of the lung in light microscopic sections is as a rule sufficiently characteristic to allow a firm diagnosis although atypical forms show a range of appearances. A distinction between carcinoid and small cell lung cancer is usually possible by electron microscopy though there some difficult cases[126].

Compared with small cell lung carcinomas, cells of carcinoid tumors have more cytoplasm and their nuclei are larger with greater clumping of the chromatin. The cells are polygonal when packed in sheets, or in some tumors they are elongated, and they contain moderate numbers of organelles. A small number have scattered myoepithelial cells. The granules in a particular tumor fall with in a narrow range of diameters, but they can be up to 350 nm (figure 73), which is still distinctly smaller than exocrine granules like those of Clara cells, and they can be as small as 120 nm which is within the range seen in small cell lung carcinomas. In a small percentage of lung carcinoids, the granules are angular (figure 74), but in most they are spherical. The granules in the spindle cell carcinoid tumor shown in figure 75 are towards the small end of the range of diameters found in lung carcinoids and they are inconspicuous at low magnification. Granules are again small in the tumor in figure 76 (the larger densities are lysosomes). Myoepithelial cells were present in this tumor and one is visible in the figure, inside an incomplete basal lamina. Small lumens with some microvilli are quite common (figure 77). If the cells contain well-defined aggregates of filaments (figure 78), granules are then mixed with the filaments (figure 79). Therapy can induce filament formation [127].

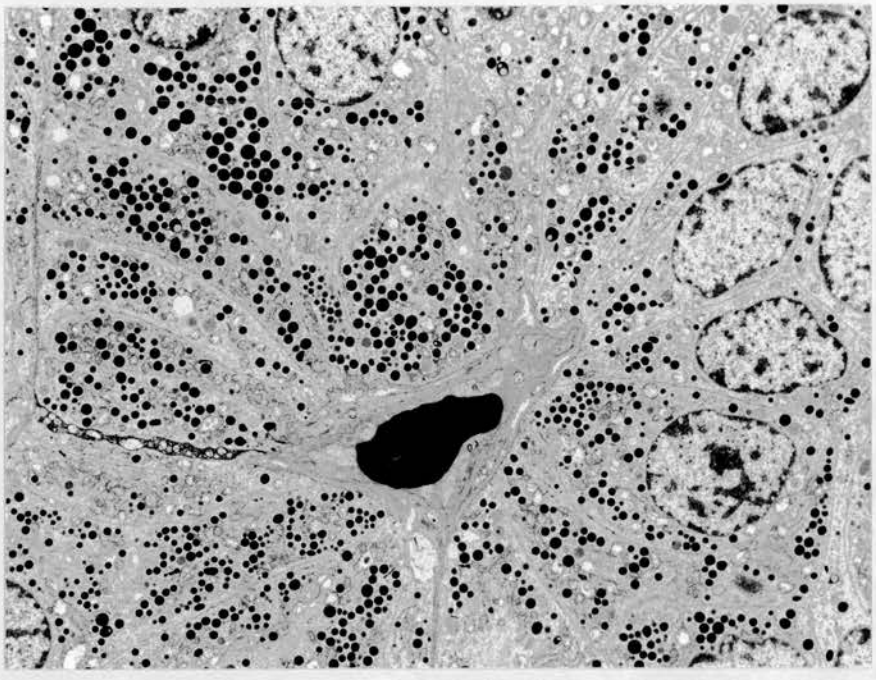

Figure 73. Carcinoid tumor of lung. Cells rich in granules surround a capillary. x 3,800.

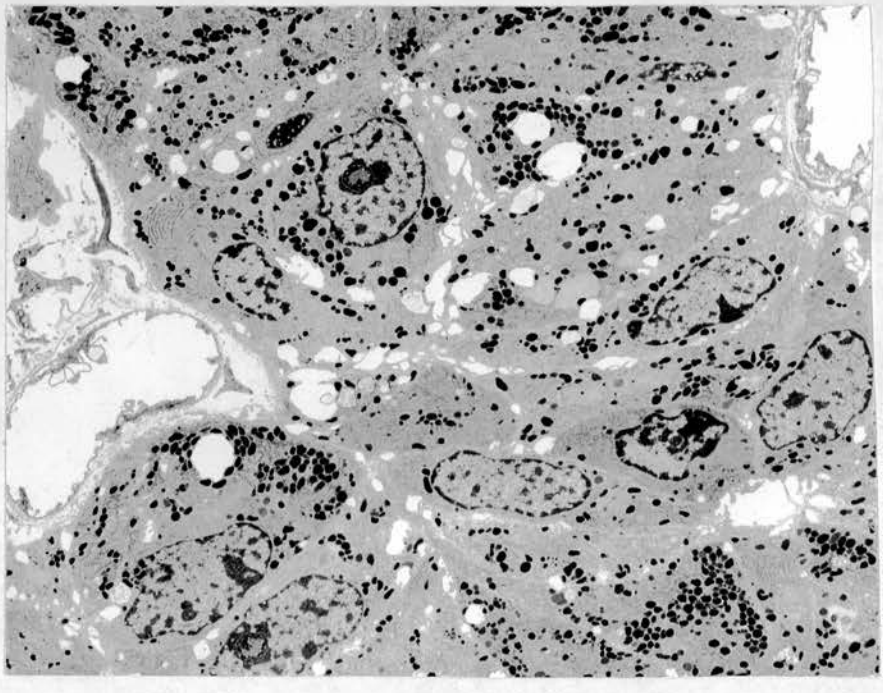

Figure 74. Carcinoid tumor of lung with pleomorphic granules. x 4,000.

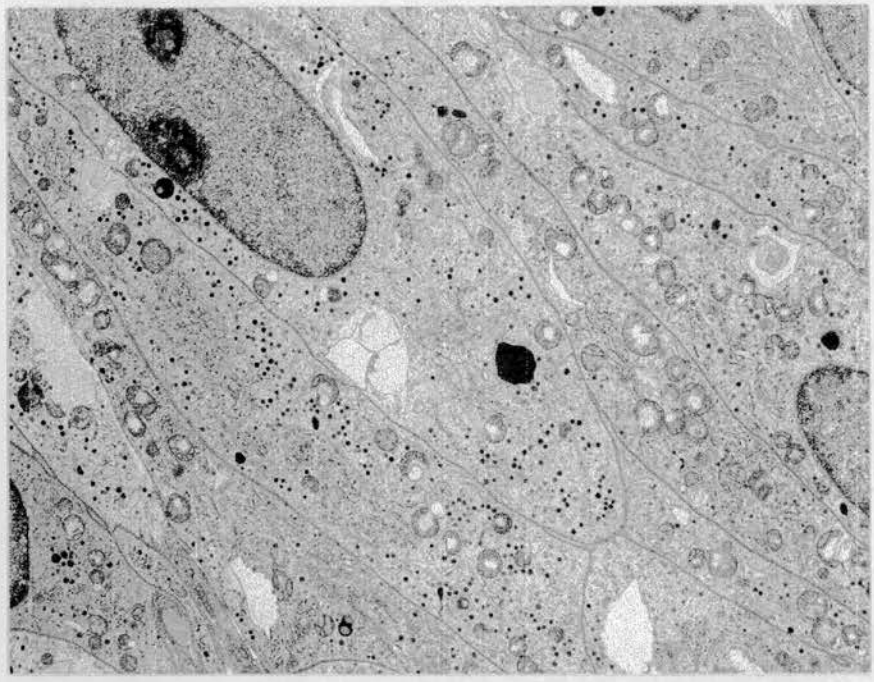

Figure 75. Carcinoid tumor of lung, spindle cell variant. The granules are small. x 4,300.

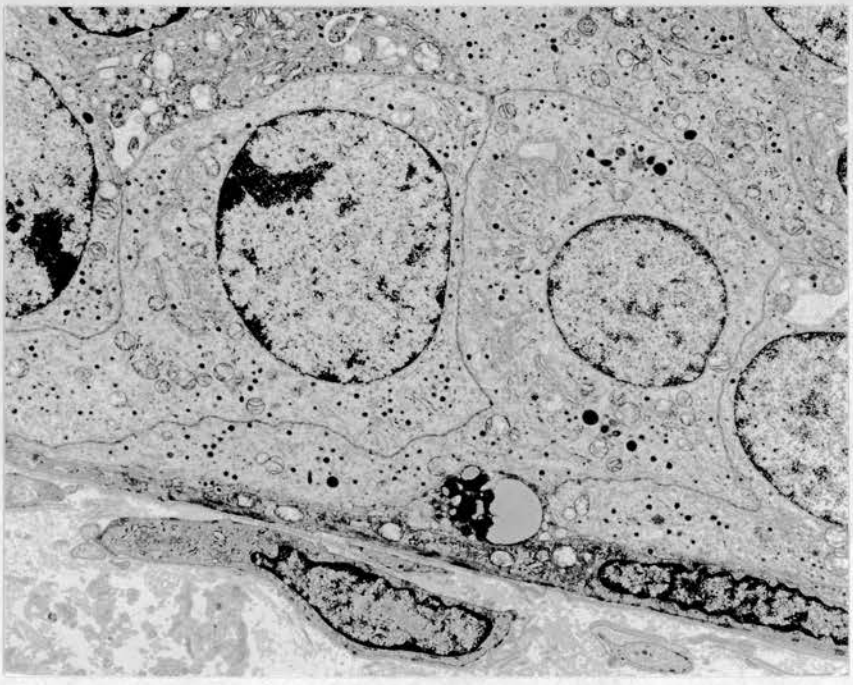

Figure 76. Carcinoid tumor of lung. The granules are small. A myoepithelial cell lies on the basal lamina. x 6,200.

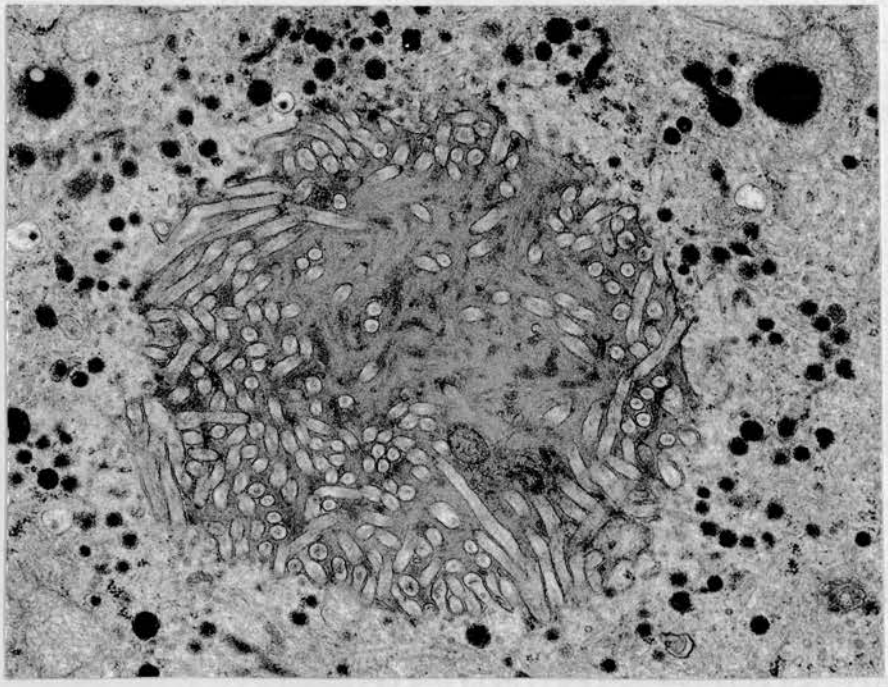

Figure 77. Carcinoid tumor of lung. Small granules surround an intracytoplasmic lumen. x 11,700.

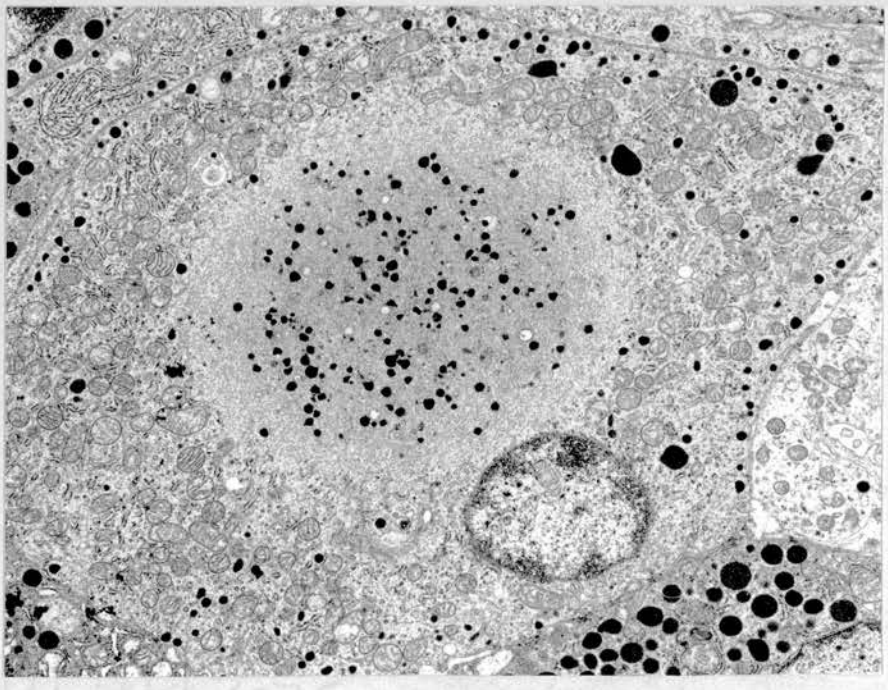

Figure 78. Carcinoid tumor of lung. An aggregate of cytoplasmic filaments is present and moderate numbers of mitochondria are present. x 6,900.

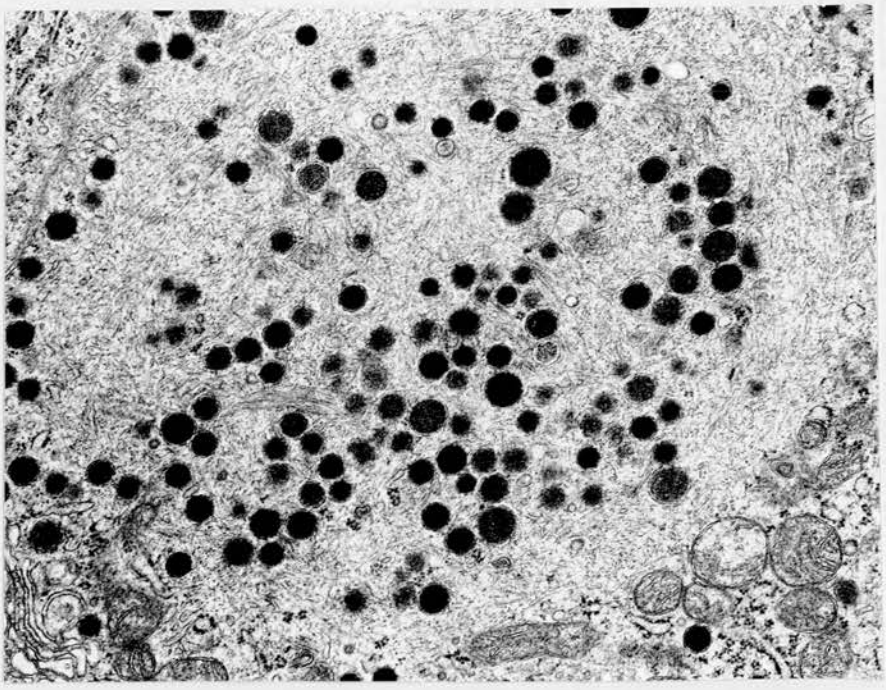

Figure 79. Same tumor as figure 78 showing filaments and granules. x 12,000.

Attempts have been made to demonstrate differences among the subtypes of lung cancer on the basis of the size, shape, and detailed appearance of the cells and their nuclei, and they have revealed considerable overlap in nuclear size[128]. Measurements of this type made by light microscopy using formalin-fixed tissue in paraffin sections can be quite unreliable because of the limited precision of the technical method and shrinkage and distortion in the tissue. In contrast, electron micrographs of well-preserved tissue show very little distortion and they are ideal for this purpose. Cases that I had accumulated and studied were used in a correlated ultrastructural and morphometric analysis of a series of differentiated lung tumors, and some of the findings were included in the following report

Mackay B, Ordonez NG, Bennington JL, Dugan CC. Ultrastructural and morphometric features of poorly differentiated and undifferentiated lung tumors. Ultrastructural Pathology 13:561-71, 1989.

The morphometric study was performed on differentiated examples of primary lung tumors and included 39 adenocarcinomas, 15 squamous cell carcinomas, 11 undifferentiated large cell carcinomas, 33 small cell carcinomas, and 44 carcinoid tumors. All the tumors had been fixed in 2% glutaraldehyde and embedded in epoxy resin. Thin sections were photographed at a magnification of x1,000 to provide enough negatives for at least 50 intact cells from each tumor. Prints were prepared on 8 x 10-inch photographic paper at a constant magnification. The maximum and minimum cell and nuclear diameters, cell and nuclear areas, and cell and nuclear perimeters were measured from the electron micrographs by means of an image cytometer. To facilitate the measurement of the cell features, the outlines of cells and nuclei which I selected were traced on transparent white paper to give high-contrast images. The tracings were scanned with a high-resolution video camera, and each cell and its nuclear image were digitized by a Leitz TAS Plus Image Analyzer and

processed to yield a total of 16 morphometric tumor cell features, including maximum and minimum cell and nuclear diameters, and cell and nuclear areas and perimeters. This phase of the work, with statistical analysis of the data, was performed in coauthor Dr. James Bennington's laboratory in San Francisco. The University of California at Los Angeles BMDP-P2D statistical program was used to tabulate the tumor cell measurements and to extract statistical descriptors from the tumor cell features, including the mean, median, interquartile range, and log of the standard deviation.

TABLE 1 Mean Values and Standard Deviations for Statistically Derived Tumor Descriptors for Each Tumor Group

	Maximum cell diameter		Minimum cell diameter		Maximum nuclear diameter		Minimum nuclear diameter		Cytoplasmic area		Nuclear area		N:C ratio[a]	
Tumor type	Mean	SD	Mean	SD	Mean	SD	Mean	SD	Mean	SD	Mean	SD	Mean	SD
Adenocarcinoma	16.6	2.8	10.4	1.7	9.3	1.0	6.5	0.79	116	37	45	11.0	0.42	0.09
Squamous cell carcinoma	15.0	3.1	9.6	2.2	9.0	0.94	6.2	0.88	98	47	41	11.0	0.47	0.09
Undifferentiated large cell carcinoma	14.8	1.8	9.9	1.3	9.1	9.1	6.3	0.64	98	22	43	9.0	0.46	0.06
Small cell carcinoma	11.0	1.6	7.3	0.8	7.8	1.0	5.4	0.60	55	12	30	6.0	0.58	0.17
Carcinoid	12.0	1.6	7.7	1.2	7.2	7.0	5.0	0.56	63	18	26	6.0	0.44	0.05

[a]Ratio of nuclear to cytoplasmic area.

As the figures in the table demonstrate, there is considerable overlap in cell and nuclear size and area among the different types of lung carcinoma, and an absolute separation of large cell from small cell carcinoma or carcinoid tumor could not always be made from these criteria. The heterogeneity that is common among large cell lung tumors contributes to the variability. The analysis showed the ratio of nuclear to cytoplasmic area in small cell carcinomas to be 0.58 compared with 0.44 for carcinoid tumors, and when the standard deviations were taken into account, the two overlapped. The morphometric data were used for linear stepwise discriminant analysis of the statistical tumor cell descriptors to classify the 142 tumors into the five diagnostic categories used in the original classification of these tumors (large cell neuroendocrine carcinoma was not included in the study). The power of the classification was subsequently tested with the unbiased jackknife protocol, yielding an optimum combination of five descriptors (mean of maximum cell diameter, interquartile range of minimum nuclear diameter, median of the ratio of nuclear to cytoplasmic area, log standard deviation of cell area, and log standard deviation of nucleolar diameter), and it was found that 63% of the tumors were classified into the diagnostic groups to which they had originally been assigned by light microscopy. 11% were misclassified as small cell carcinoma, 8% as carcinoids, 7.6% as undifferentiated large cell carcinoma, 13% as squamous cell carcinoma, and 6% as adenocarcinoma. When small cell carcinomas and carcinoids were considered a single group, the accuracy in classifying one of the tumors into this group was 88%.

Uncommon lung tumors

Approximately 2% of primary lung tumors are not the common carcinomas or carcinoid tumors, and EM provided some original information on these tumors and can aid in their identification, but has done little to clarify persisting problems of histogenesis. The reported cases were from three institutions. M.D. Anderson cases are illustrated here.

> **Hammar S, Troncoso P, Yowell R, Mackay B. Use of electron microscopy in the diagnosis of uncommon lung tumors. Ultrastructural Pathology 17:319-351, 1993.**
> Ten uncommon tumors presenting in the lung were reported with electron microscopic observations. Cases 1, 2, 3 and 5 were examples of epithelioid hemangioendothelioma, and case 4 was a sclerosing hemangioma

The cell of origin of sclerosing hemangioma of the lung remains a mystery but mesothelial derivation has been ruled out from the ultrastructural findings. The cells in the cellular zones have an epithelial appearance (figure 80) with moderate numbers of rather primitive cell junctions and irregular peripheral projections that look like microvilli (figure 81), but without obvious squamous or glandular differentiation. They do not display neuroendocrine characteristics.

Epithelioid hemangioendothelioma of the lung was initially thought to be a form of bronchioloalveolar tumor because of its growth pattern (figure 82). Its histopathology is virtually identical to that seen in the same tumor occurring in liver and soft tissues. Electron microscopy is sometimes useful as the diagnosis can be overlooked and the tumor misinterpreted as a carcinoma or mesothelioma. Many of the cells contain diffuse zones of fine filaments (figure 83).

Alveolar adenoma has been a poorly characterized entity. I had the opportunity to participate in a clinical and light microscopic study of 17 cases and I consulted on the electron microscopy of the two cases in which this was performed but did not contribute the micrographs that were included in the paper[129]. The tumors were coin lesions on chest radiographs in asymptomatic patients except for one with cough. Each tumor was well demarcated and the mean size was 2.2 cm. Multiple cystic spaces were lined by type 2 pneumocytes with a smaller number of type 1 cells and no Clara cells.

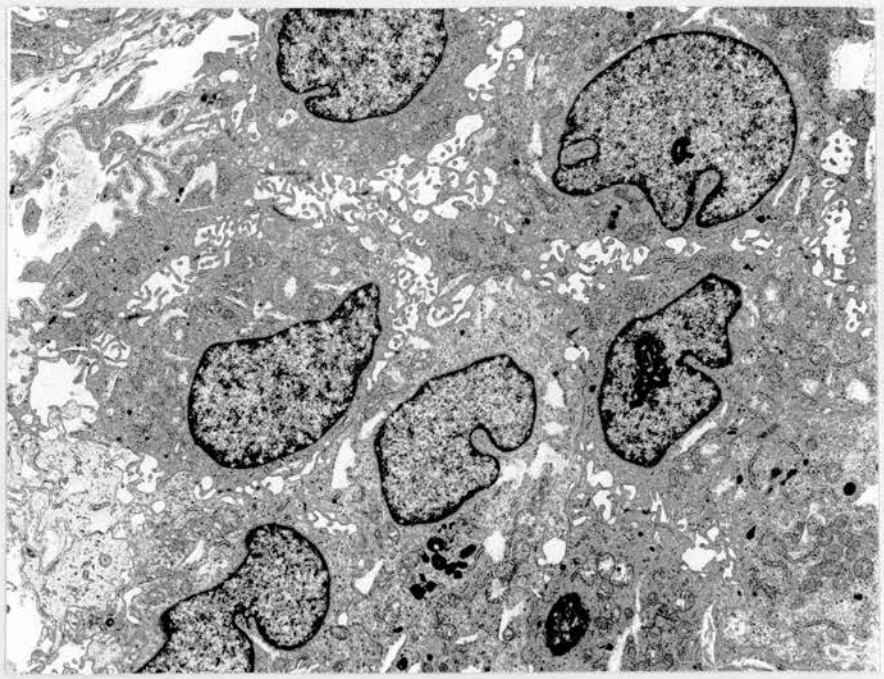

Figure 80. Sclerosing hemangioma of lung. Cellular area showing slender gaps between cells. x 4,300.

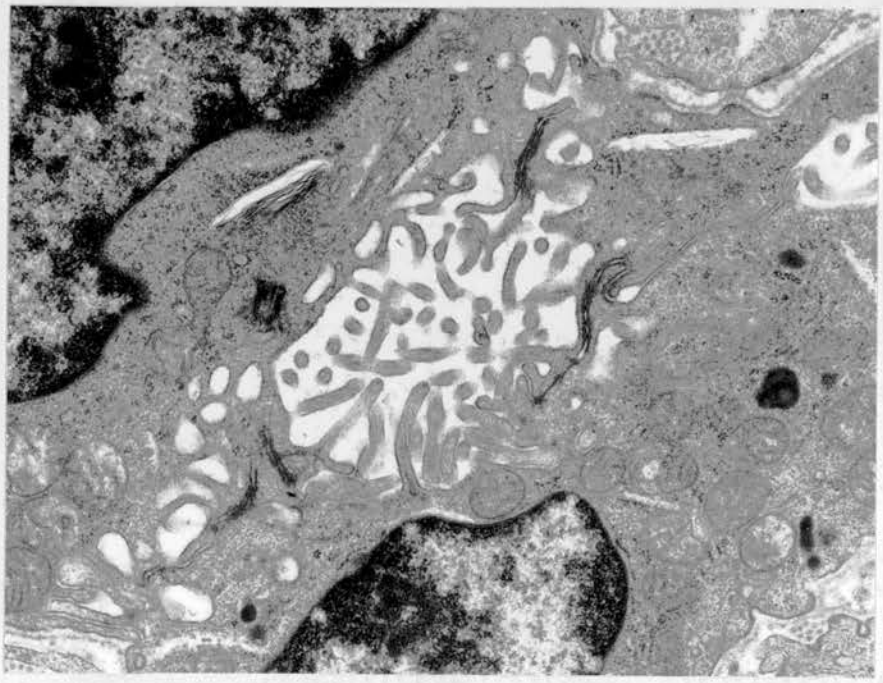

Figure 81. Same case as figure 80. Microvilli project into a gap between cells, and tight junctions connect neighboring cells. x 9,700.

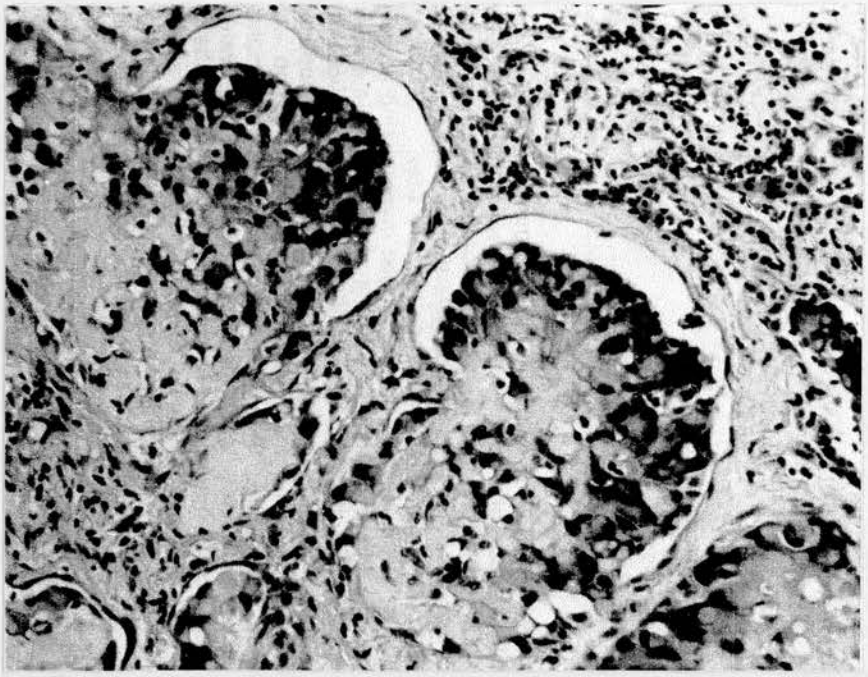

Figure 82. Epithelioid hemangioendothelioma of lung. Hematoxylin and eosin.

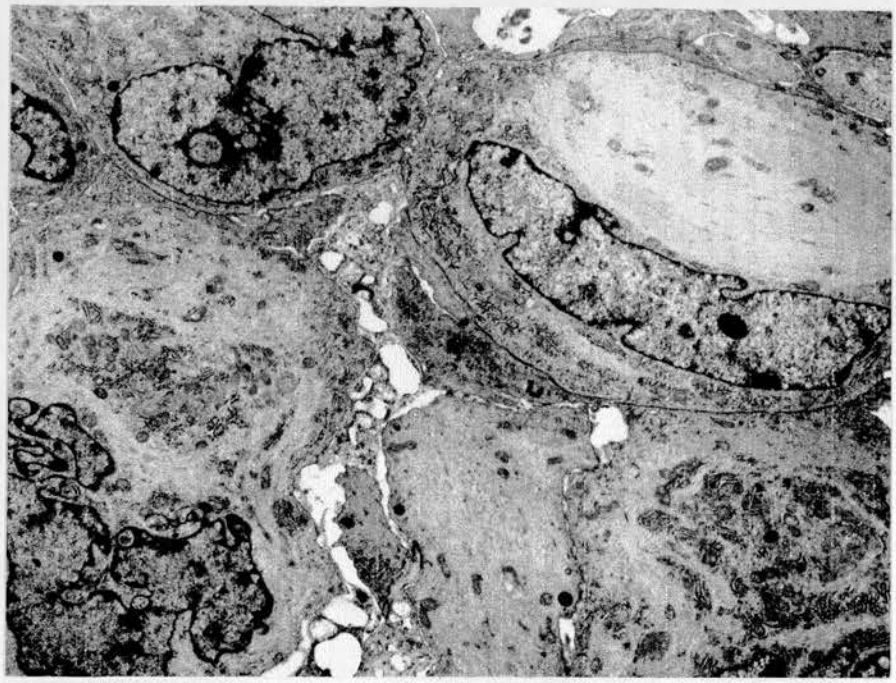

Figure 83. Same tumor as figure 82. The cells contain extensive zones of fine filaments. x 8,300.

Mesothelioma

The poor prognosis of mesothelioma, and pressure to provide a firm diagnosis because of medico legal implications, have prompted pathologists to request electron microscopy on pleural tumors that might otherwise have been reported by routine light microscopy, and as a result the ultrastructure of mesothelioma has been examined more thoroughly than that of most tumors.

> **Ordonez NG, Mackay B. The roles of immunohistochemistry and electron microscopy in distinguishing epithelial mesothelioma of the pleura from adenocarcinoma. Advances in Anatomic Pathology 3:273-293, 1996.**
> Points made in this review included the following. The incidence of mesothelioma is increasing in the United States and other countries. Most mesotheliomas are pleural and epithelial. The differential diagnosis is usually with an adenocarcinoma from the lung or a more distant source. Histochemical stains are of limited value. The usual approach is to perform a battery of immunohistochemical stains, and/or electron microscopy if tissue is available. The relative merits of the two techniques to discriminate between epithelial pleural mesothelioma and adenocarcinoma were reviewed and it was concluded that there is no consistently reliable approach, but a carefully selected and cautiously interpreted group of immunostains will often strongly favor one or other tumor, while EM is usually but not always diagnostic.

There is no consistently reliable method to distinguish between mesothelioma and adenocarcinoma by light microscopy, although one or other tumor may be strongly favored. Histochemical stains are of limited value since both tumors can contain glycogen or mucin[130]. Immunoperoxidase studies will often suggest one or other tumor[131]. The contribution of electron microscopy ranges from confirming the diagnosis to at the other extreme offering no aid as is the situaiton with some poorly differentiated tumors. It can be particularly difficult and may be impossible to distinguish isolated adenocarcinoma cells from those of a mesothelioma in effusion specimens, and while EM may offer some useful information[132], reactive and neoplastic mesothelioma cells in effusions can look identical by electron microscopy, and single cells from a metastatic adenocarcinoma may have long thin microvilli and be indistinguishable from mesothelial cells.

The most distinctive feature of mesothelioma cells is the luxuriant microvilli (figure 84) which are long, slender, undulating and often branching, and they lack microfilament cores or rootlets (figure 85). Attempts to measure the microvilli in order to compare them with those of adenocarcinomas are not technically feasible since the microvilli curve in and out of the plane of section, and the exercise is unnecessary as visual inspection is adequate. If the tumor cells are closely packed, the layer of microvilli will appear distinctly thicker than that customarily seen in adenocarcinoma. Occasionally, mesothelioma cells contain intracytoplasmic lumens. Cell junctions are often mature desmosomes, and when they are long they favor mesothelioma over adenocarcinoma[133]. Some tumors have loosely grouped filaments in the perinuclear cytoplasm but they are nonspecific in appearance. Dense bundles of keratin should suggest a carcinoma. In some well-differentiated mesotheliomas, the neoplastic cells recapitulate the architecture of normal mesothelium by forming sheets a single layer thick that rest on a basal lamina. The lamina is, however, often incomplete. Cells in these sheets may be higher than they are wide, but uniformly tall columnar cells should suggest adenocarcinoma.

A feature of normal mesothelium that is often seen in the well-differentiated tumors is the presence of clefts between the lateral borders of neighboring cells: they can be seen in the

epithelial component of a mixed mesothelioma in figure 86. It may be that in normal serous membranes the presence of these gaps allows for rapid passage of material from the lumen of the serous cavity to capillaries beneath the basal lamina. Peritoneal mesotheliomas have similar ultrastructural features to the pleural tumors. The profusion of microvilli on cells of a peritoneal mesothelioma is evident in figure 87, and gaps between adjacent cells on this tumor can be seen in figure 88. The so-called cystic variant of mesothelioma that occurs in the peritoneum is not clearly neoplastic[134, 135] (figure 89) and is rarely encountered in the pleura.

Cases of possible mesothelioma sent for diagnostic EM are often the less differentiated tumors that can not be confidently identified by light microscopy, and they tend to be made up of a diffuse population of cells with poorly developed junctions and no specific surface or cytoplasmic features. While EM may help in categorizing such a tumor[136-138], it is not always successful and there are occasions when the diagnosis remains undecided.

Mesothelium is structurally an epithelium and mesothelioma is an epithelial neoplasm[139]. During the preparation of the 3rd WHO classification of lung and pleural tumors, the light microscopists in the group insisted on using the designation "epithelioid mesothelioma", but heeded the remonstrances of the three pathologists with expertise in electron microscopy and added "epithelial mesothelioma" as a synonym.

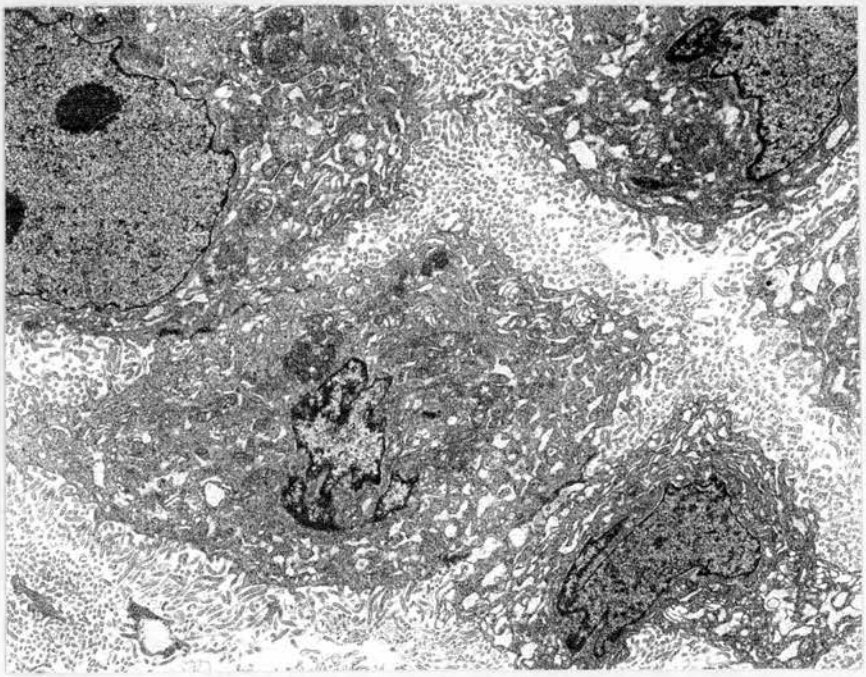

Figure 84. Mesothelioma of pleura. Copious long microvilli occupy gaps between tumor cells. x 4,400.

Figure 85. Mesothelioma of pleura showing long slender microvilli that curve and often branch. x 28,000.

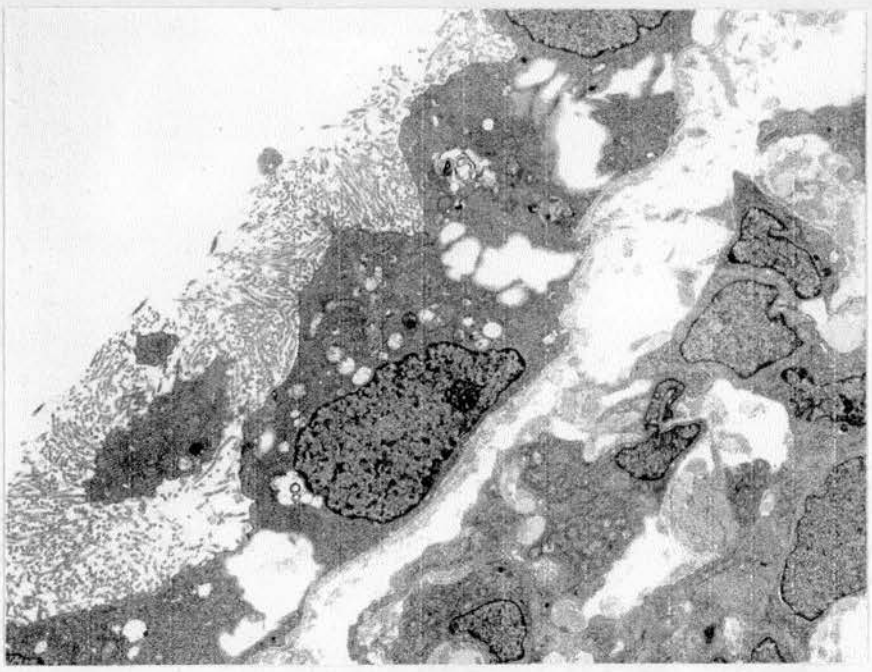

Figure 86. Mesothelioma of pleura, mixed cell type. The epithelial tumor cells are forming a single layer and they have long microvilli. Clefts separate the lateral borders of these cells. Deep to the epithelial layer, some of the mesenchymal tumor cells can be seen. x 4,200.

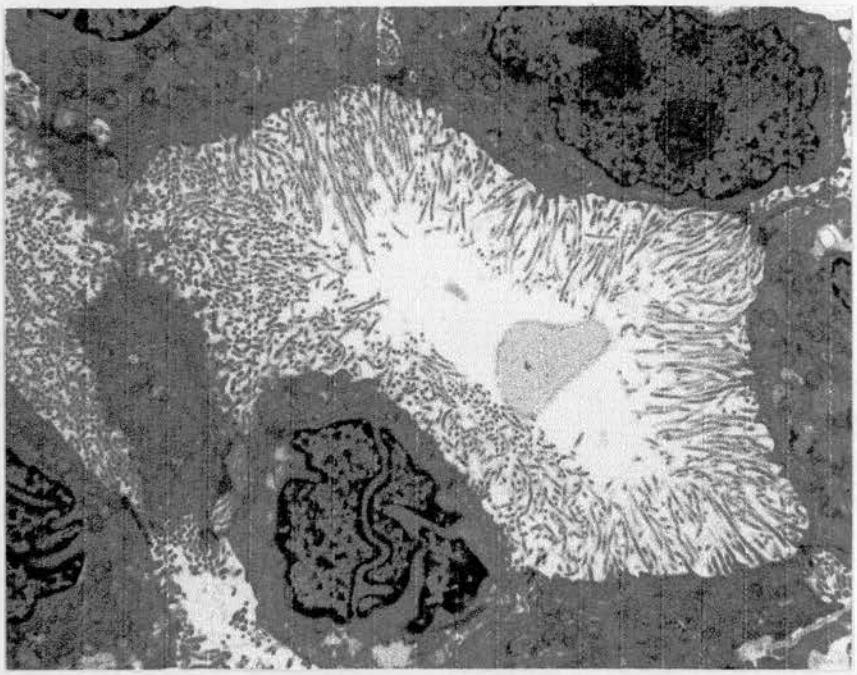

Figure 87. Mesothelioma of peritoneum showing the long microvilli. x 4,000.

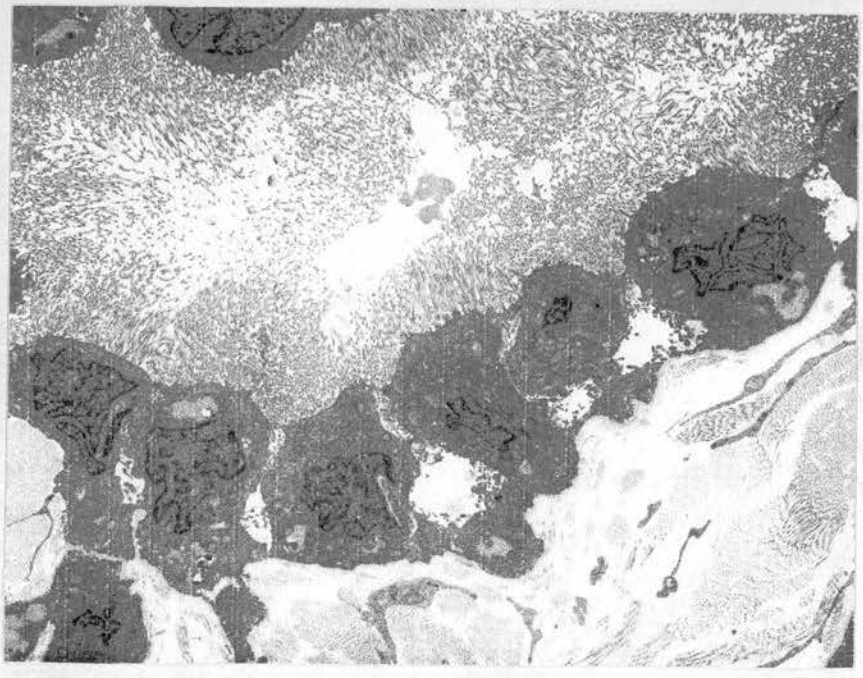

Figure 88. Same tumor as figure 87 to demonstrate clefts between cells. x 3,600.

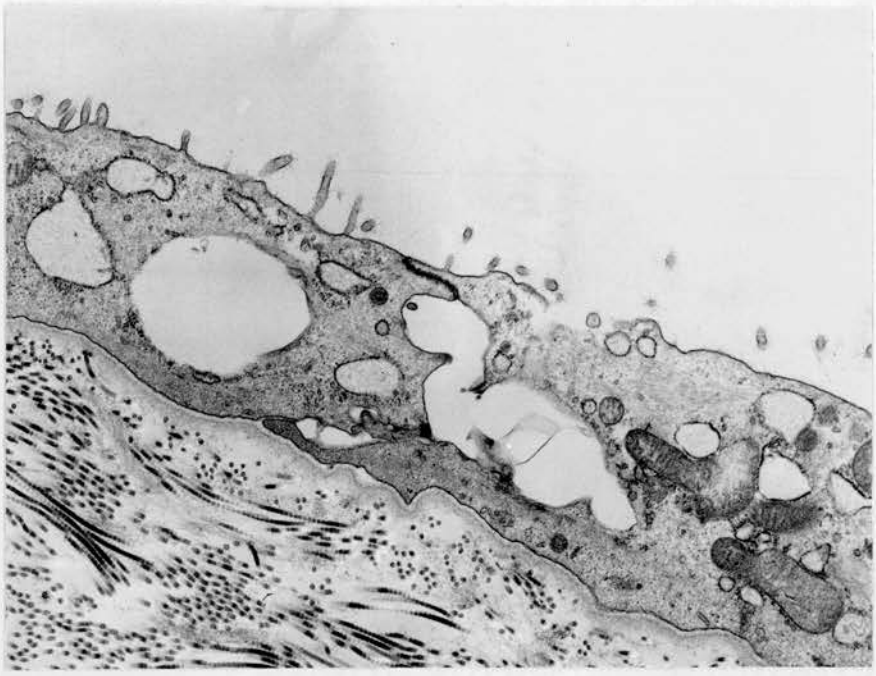

Figure 89: Cystic mesothelioma of peritoneum. The cells had only a few short microvilli but intercellular clefts were present. The basal lamina is continuous. x 4,400.

Occasionally, a mesothelioma is composed of cells that have optically clear cytoplasm in paraffin sections.

Ordonez NG, Mackay B. Glycogen-rich mesothelioma. Ultrastructural Pathology 23:401-406, 1999.
One case is described. This variant is uncommon but important to recognize since it is readily confused on routine light microscopy with other clear cell tumors involving the pleura. EM and immunohistochemical studies can be helpful in establishing the correct diagnosis.

Ordonez NG, Myhre M, Mackay B. Clear cell mesothelioma. Ultrastructural Pathology 20:331-336, 1996.
Multiple nodules on the left parietal pleura of a 74-year-old man were broad-based and plaque-like, ranging in size from 0.1 to 2 cm. The cells had optically clear cytoplasm. Immunohistochemistry and EM identified the tumor as an epithelial mesothelioma. The cells contained large numbers of vesicles.

The occurrence of uncommon variants of mesothelioma stresses the need for caution in the interpretation of pleural tumors. Glycogen can be plentiful in mesothelioma cells (figure 90). A combination of EM and a small selection of the more reliable immunostaining procedures[140] offers the best chance to reach a correct conclusion and enable the identification of unusual forms of mesothelioma.

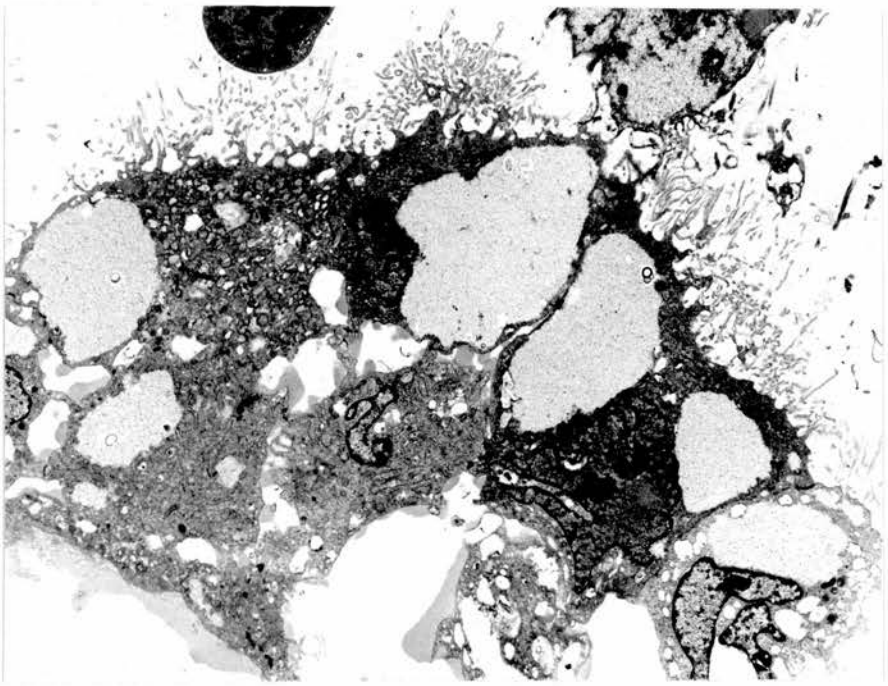

Figure 90. Extensive lakes of glycogen in cells of a pleural mesothelioma. x 4,800.

Tumors of the alimentary system

Tumors discussed in this chapter are stromal tumors of the gastrointestinal tract, carcinomas of the liver, and acinar cell, islet cell, small cell, and solid and papillary tumors of the pancreas.

Carcinomas and endocrine tumors arising from the gastrointestinal tract are usually identified without difficulty by routine light microscopy. Typical examples are illustrated.

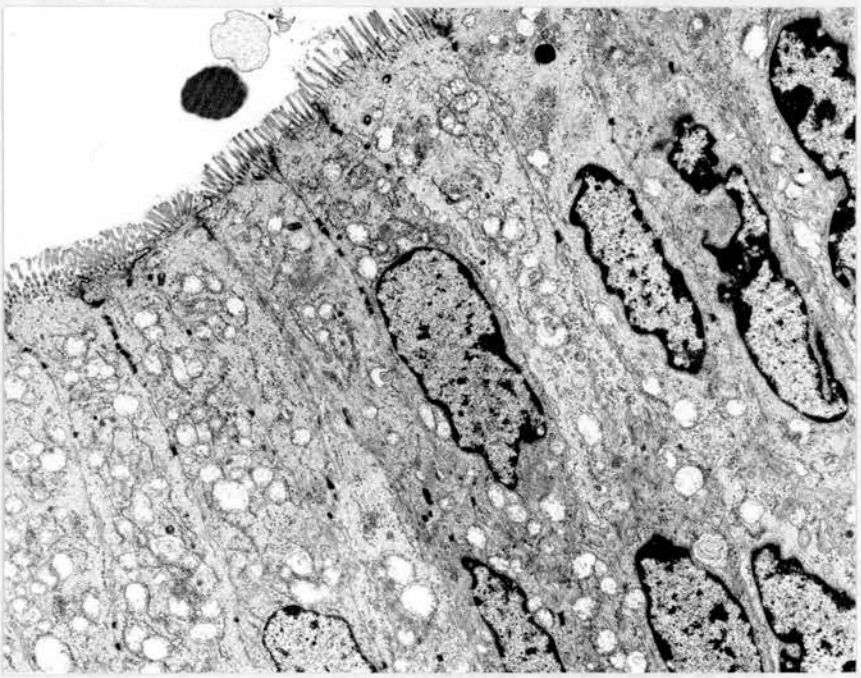

Figure 91. Adenocarcinoma of stomach, well differentiated. The tall columnar cells have straight microvilli. x 4,200.

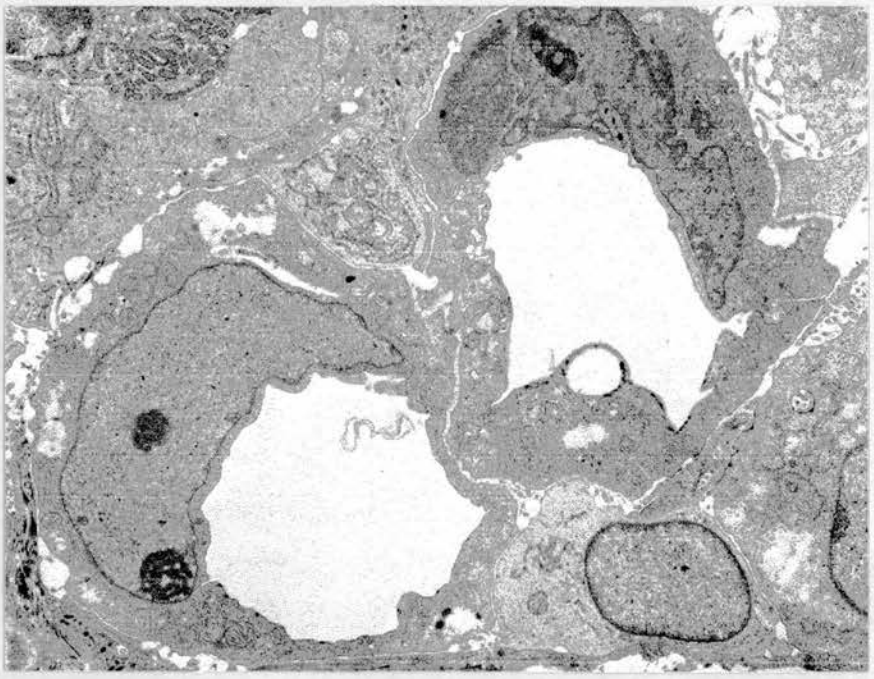

Figure 92. Carcinoma of stomach. Signet ring cells in a cervical lymph node metastasis. x 6,300.

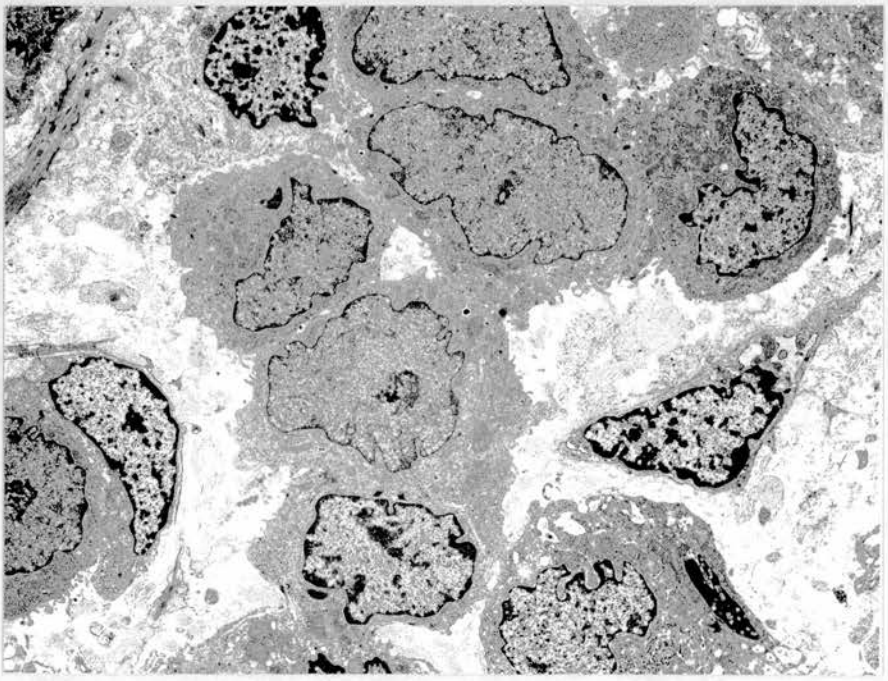

Figure 93. Small cell carcinoma of colon. At low magnification, the cells show a tendency for apposition. x 3,900.

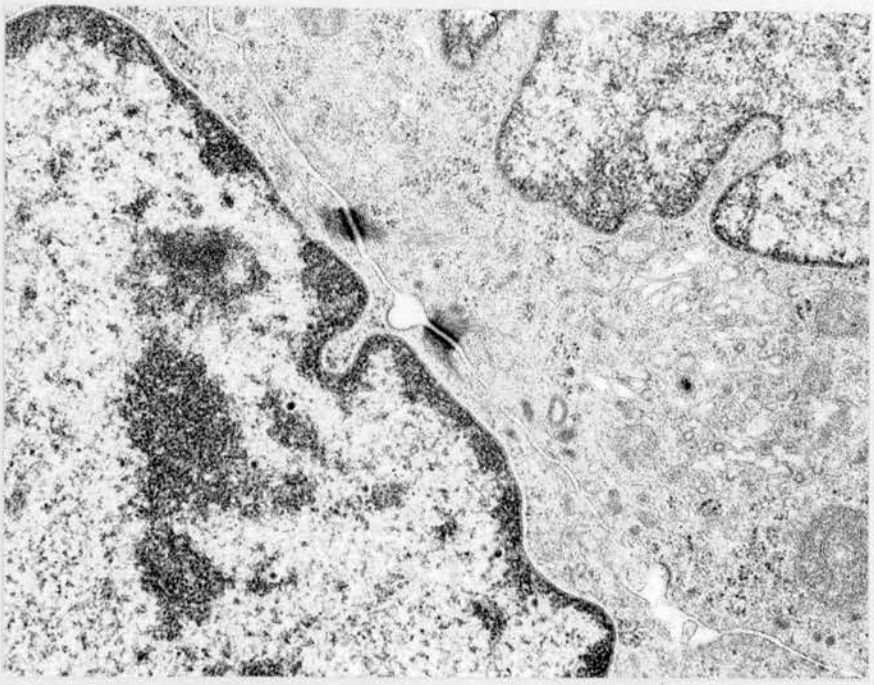

Figure 94. Same tumor as figure 93. Desmosomes connect the tumor cells. x 9,500.

Features of gastrointestinal adenocarcinomas tumors at the ultrastructural level have already been discussed and illustrated with the example of adenocarcinoma of the nasal cavity with enteric differentiation (page 64). A widely held impression during the early days of diagnostic electron microscopy was that microfilament cores within microvilli were specific for gastrointestinal tumors. The idea has been disproved, and microvilli of this type have been illustrated here in bronchioloalveolar adenocarcinomas (figure 60). When they are detected in a metastatic tumor, gastrointestinal tract will be the first site to consider in the search for a primary tumor, but other possibilities can not be excluded. The cells of a well differentiated adenocarcinoma of the stomach are tall and closely apposed and they have moderate numbers of the common organelles. Quantities of mucin may be present. The apical microvilli are straight and uniform and they contain microfilament cores that are barely detectable at low magnification (figure 91). Adjacent cells are joined by a few desmosomes along their length, and at the lumen margin by junctional complexes. In the signet ring cell variant, the round cells contain a vacuole that is often filled with mucin, but the central cavity may be a membrane-limited lumen and appear empty in fixed tissue (figure 92). A true small cell carcinoma is uncommon in the gut: figure 93 shows one from the small intestine in which the cells are often in contact, and at higher power, are connected by small but mature desmosomes (figure 94).

Endocrine tumors of the gastrointestinal tract have close similarities in their fine structure with tumors of polypeptide-forming endocrine cells in other locations including lung carcinoids.

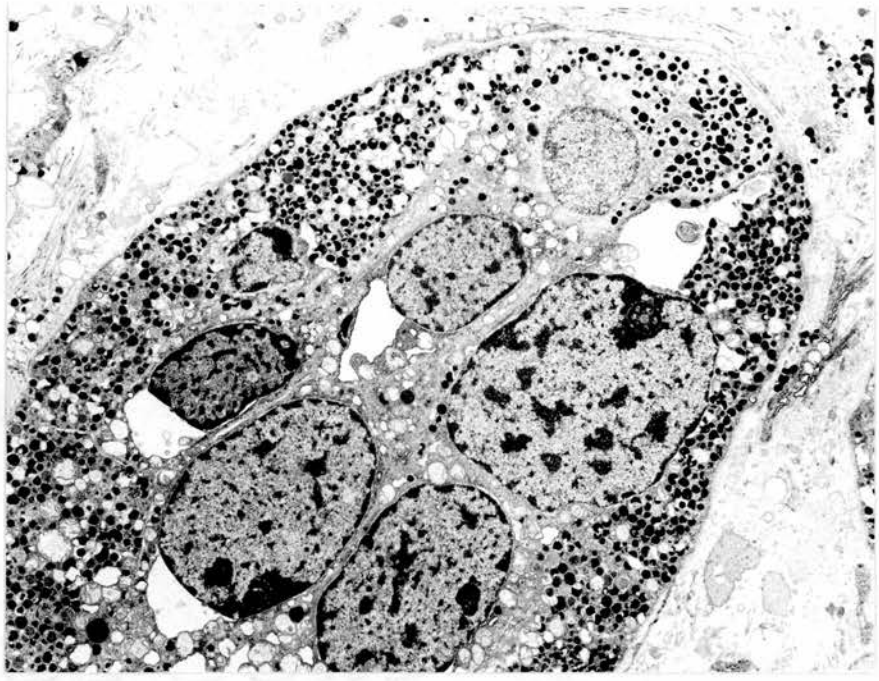

Figure 95. Carcinoid tumor of small intestine. A well-demarcated cluster of cells. x 3,100.

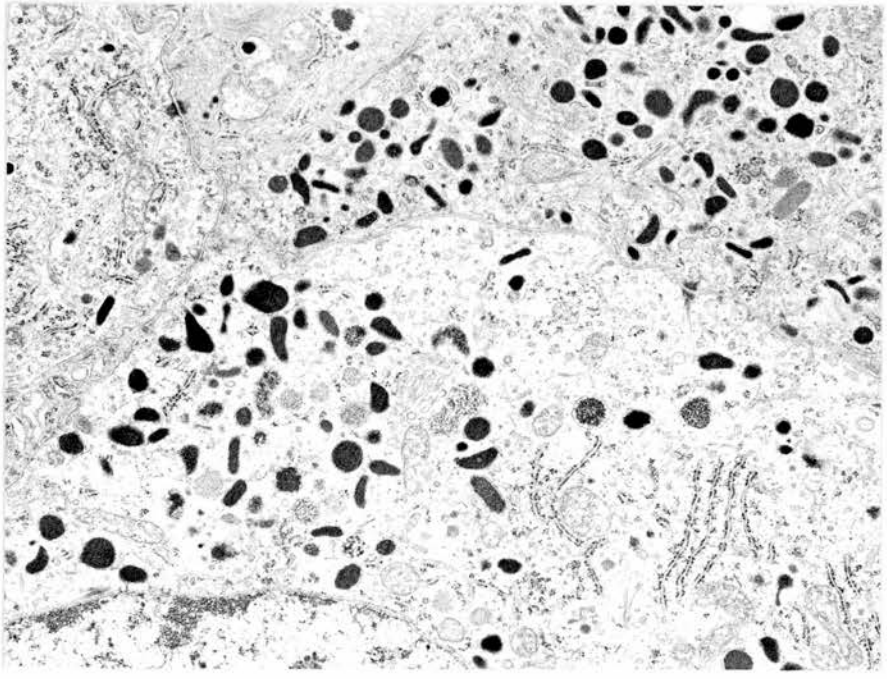

Figure 96. Carcinoid tumor of small intestine with pleomorphic granules. x 14,000.

Many endocrine granules are the rule in differentiated tumors of the enterochromaffin cells, and the small intestinal tumor in figure 95 is typical. All the cells in the compact group contain numerous granules that are consistently round. More variation in granule size, to the point where many are ovoid or angular, is a common finding in the small intestinal tumors (figure 96). Variants include mixed endocrine/exocrine tumors and which show more variety in granule size from one cell to the next than do the pure tumors. While a particular amine or peptide may predominate, most gut carcinoids are multihormonal[141].

Stromal tumors of the gastrointestinal tract

In an early study of a group of gastrointestinal stromal tumors with the electron microscope, I was surprised to find that smooth muscle differentiation was not a common occurrence. A later expanded study confirmed that this was the case and revealed a few tumors with neural features .

> **Weiss RA, Mackay B. Malignant smooth muscle tumors of the gastrointestinal tract. An ultrastructural study of 20 cases. Ultrastructural Pathology 23:.231-240, 1981.**
> Twenty malignant soft tissue tumors arising from the stomach or intestine were studied by light microscopy and EM. All the tumors had been considered to be of smooth muscle origin when they were studied in paraffin sections. Ten were spindle cell neoplasms and ten were epithelioid. By EM, only five tumors possessed smooth muscle features. A sequence of dedifferentiation could be traced among the tumors from those with well developed smooth muscle features to tumors that were totally devoid of differentiating features. None of the epithelioid tumors contained myofilaments. Neural tumors were not identified in this group of cases.

A subsequent expanded study confirmed these findings and revealed a few tumors with neural features. Among the 50 gastrointestinal stromal tumors, 25 arose in the stomach (20 malignant, 5 benign), 14 in the small intestine (all malignant), and 11 in the large intestine (11 malignant, 1 benign). By light microscopy, most of the tumors were spindle cell neoplasms, but epithelioid areas were present in 14 of the sarcomas and 1 benign tumor and they predominated in 3 sarcomas. Only one third of the tumors contained cells with smooth muscle features and these were often poorly defined and confined to scattered cells. Immunostaining for desmin was positive in 13 tumors including 9 sarcomas and correlated with the presence of plentiful myofilaments in 10 cases, 7 of them sarcomas. Smooth muscle myosin was positive in 19 tumors including 16 sarcomas, and 11 (9 sarcomas) showed ultrastructural evidence of smooth muscle differentiation. S-100 protein immunoreactivity was found in 9 tumors (7 sarcomas) and 4 (3 sarcomas) had neural features by EM. The sarcomas displayed an aggressive behavior with a mean survival time of 37 months (gastric), 41 months (small intestine) and 40 months (large intestine).

Figure 97. Malignant stromal tumor of colon with prominent smooth muscle differentiation. x 4,000.

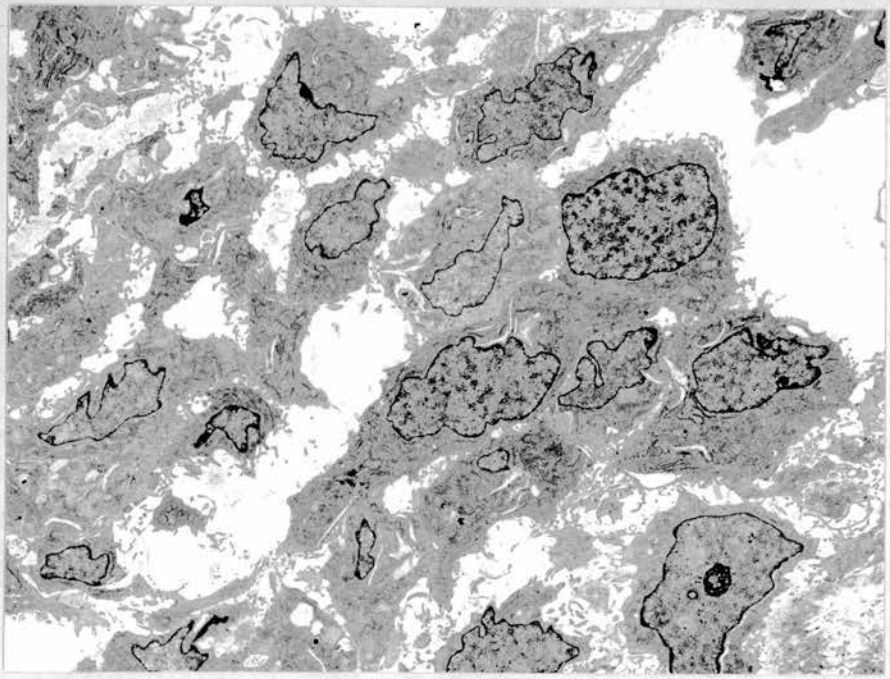

Figure 98. Malignant stromal tumor of stomach. The small cells do not show any architectural pattern. x 2,900.

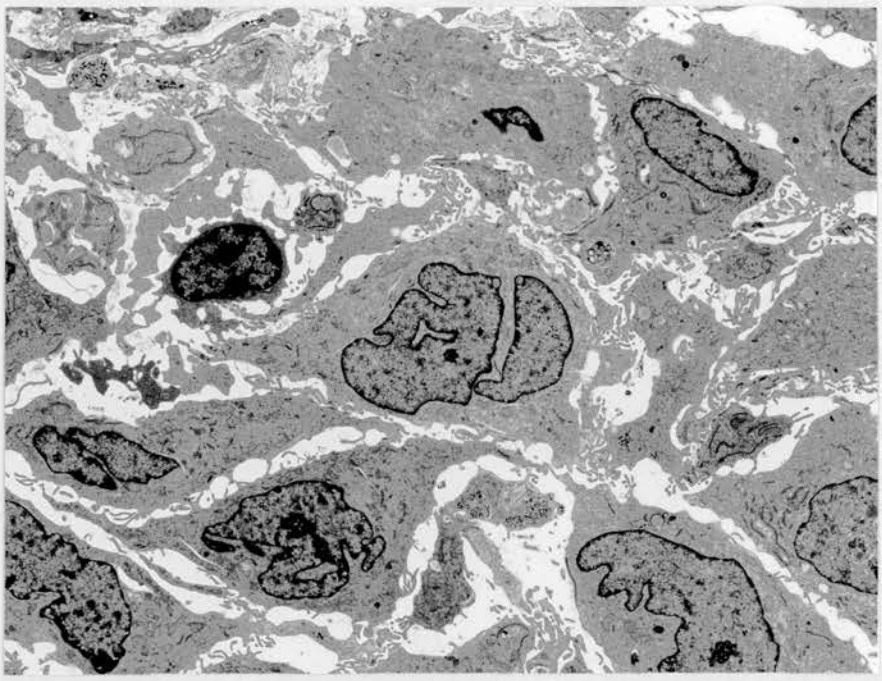

Figure 99. Malignant stromal tumor of small intestine. The cells ranged in shape from polygonal to angular to elongated. x 4,500.

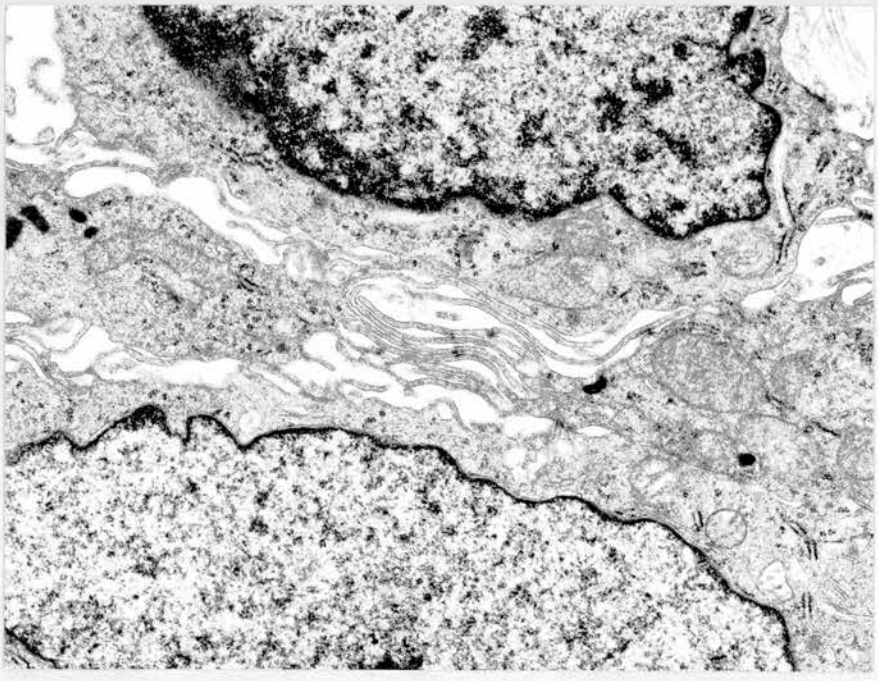

Figure 100. Malignant stromal tumor of small intestine. Slender filopodia-like extensions were present on many cells. x 10,200.

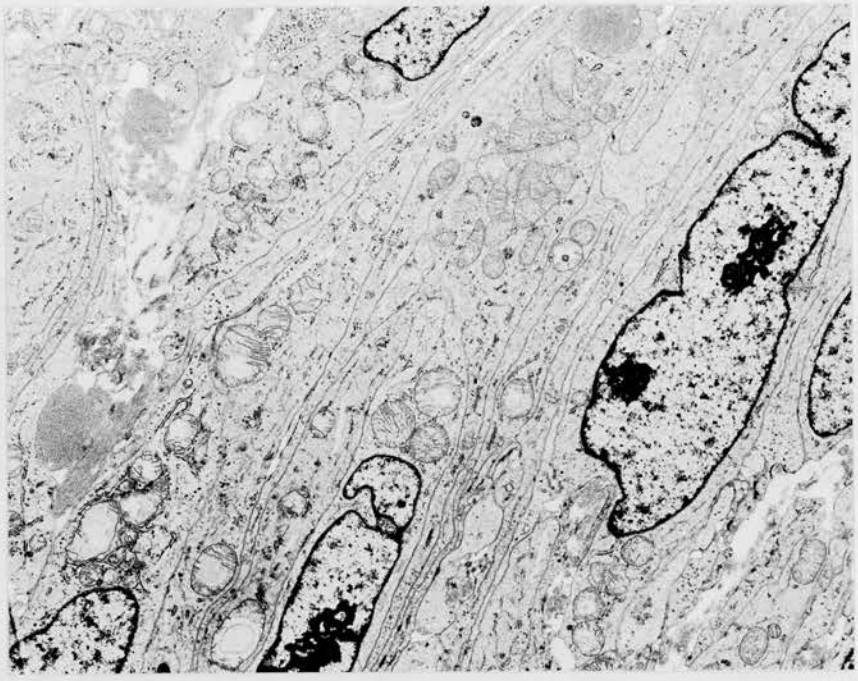

Figure 101. Malignant stromal tumor of jejunum with neural features. The elongated cells and their long straight extensions are intimately apposed. x 4,900.

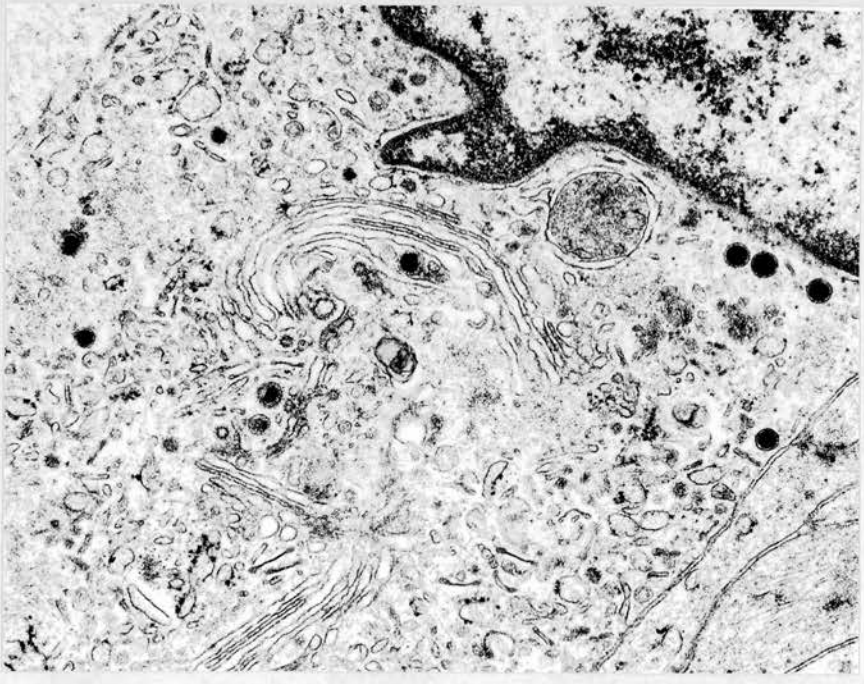

Figure 102. Malignant stromal tumor of distal ileum. In this tumor with neural differentiation, small dense-core granules could often be found in the vicinity of the golgi complex. x 23,000.

Since our first report was published, there has been considerable interest in stromal tumors of the gastrointestinal tract. Ultrastructural observations have established that there is a spectrum of differentiation ranging from tumors with obvious smooth muscle features to ones in which where they are poorly developed, to undifferentiated tumors in which they are completely absent. The tumor in figure 97 was relatively well differentiated by light microscopy and the smooth muscle myofilaments seen by EM were confidently anticipated. The nuclear inclusions in this tumor are unusual. Our observations suggest that smooth muscle myofilaments will be found in approximately one third of cases though perhaps only in scattered cells. In tumors that have undergone epithelioid transformation, it is unlikely that evidence of smooth muscle differentiation will be detected by EM. Mazur and Clark[142] used EM to study 12 tumors which had been called smooth muscle neoplasms by light microscopy, and only two, one benign and one malignant, contained cytoplasmic myofilaments of smooth muscle type. The tumors that make up the dedifferentiated end of the morphologic spectrum do not possess ultrastructural characteristics that would allow them to be placed in one of the defined subcategories of soft tissue sarcomas. Most of the cells in the tumor of the stomach in figure 98 were small and round by light microscopy and none had distinctive characteristics. More frequently, the cells are larger and angular to elongated (figure 99), and it is common to find slender projections on the cell surface that look like long filopodia (figure 100).

Nine of our 50 tumors, seven of them sarcomas, were positive with immunostaining for S-100 protein, but only four (three from small intestine and one gastric) showed convincing ultrastructural evidence of schwann cell differentiation. In figure 101, cytoplasmic extensions were particularly long and they tended to run in parallel. The tumor in figure 102 had a similar appearance and small dense-core granules were present in and around the golgi complex. S-100 protein is not a totally reliable method with which to detect neural differentiation as two of our cases were also immunoreactive with smooth muscle markers and one contained smooth muscle myofilaments. Hjermstad et al[143] found that 5% of a series of 170 gastrointestinal tract tumors which appeared to be of smooth muscle type with routine stains were positive for S-100 protein. Erlandson et al[144] classified their 56 tumors as 42.9% smooth muscle tumors (4 leiomyomas, 9 spindle cell and 8 epithelioid leiomyosarcomas, and 3 mixed spindle cell and epithelioid leiomyosarcomas); 37.5% gastrointestinal autonomic nerve tumors, 47.6% of which arose in the small intestines; 8.9% mixed leiomyosarcoma/neurogenic tumors; and 10.7% undifferentiated gastrointestinal stromal tumors (GIST) that were not otherwise specified. Tumors thought to be derived from the enteric plexus were originally called plexosarcomas[145], but the term gastrointestinal autonomic nerve tumor (GANT) is now popular, distinguishing the neural neoplasms from the more common GIST. The presence of synapse-like structures containing dense core neurosecretory granules measuring 100-200 nm, and 40-60 nm endocytoplasmic vesicles has been advanced as evidence that most gstrointestinal stromal tumors of neurogenic origin are derived from the myenteric nerve plexus[146]. There were no features of smooth muscle, schwannian or perineurial differentiation in the 10 cases of GANT studied with EM by Segal et al[147], and these authors described as characteristic features elaborate smooth endoplasmic reticulum enmeshed with intermediate filaments, pleomorphic mitochondria with lamellar cristae, mitochondrial-RER complexes, confronting RER cisternae, and circumscribed collections of stromal "skeinoid" fibers.

Variations that occur in the gastrointestinal stromal tumors include varying degrees of epithelioid transformation, an event that is not exclusive to tumors of the alimentary tract: it can for example occur in uterine[148] and retroperitoneal[149] leiomyosarcomas. The GIST may have a myxoid matrix[150], and oncocytic[151] and signet ring[152] forms have been reported.

A flow-cytometric study on tumors from 58 of our patients including many that we had analyzed by electron microscopy gave the following results[153]. Aneuploid DNA patterns were found in 43 cases (74%) including 33 (77%) that were histologically malignant and 10 (23%) in the indeterminate category. DNA ploidy pattern was significantly correlated with mitotic count (<5/10 HPF versus > or = 5/10 HPF, P = 0.04), and histologic grade (malignant versus indeterminate, P = 0.02). DNA content was not related to tumor size, site, or histologic patterns (epithelioid versus spindle). Survival was significantly correlated with DNA content (P < 0.001), histologic grade (indeterminate versus malignant, P = 0.02), and mitotic rate (<5/10 HPF versus > or = 5/10 HPF, P = 0.01). Multivariate regression analysis showed that DNA ploidy is an independent parameter in predicting the clinical outcome for patients with gastrointestinal stromal neoplasms.

Liver cell carcinoma

Carcinomas arising in the liver display a broad range of ultrastructural features, and it is not always possible to establish or confirm a diagnosis of primary or metastatic liver cell carcinoma by EM.

> **Ordonez NG, Mackay B. Ultrastructure of liver cell and bile duct carcinomas. Ultrastructural Pathology 5:201-241, 1983.**
> Ten liver cell carcinomas, 13 bile duct carcinomas, and 3 hepatoblastomas, the diagnoses being based on assessment by routine light microscopy, were studied by EM. A broad spectrum of ultrastructure was seen in the liver cell carcinomas and it was typical to find a large number and variety of organelles in the primary tumors, and an even greater range in specimens from metastases. The basic criterion for a bile duct carcinoma was evidence of duct formation: sparse dense bodies in a few cells were an occasional finding of uncertain significance. Cells of the three hepatoblastomas contained moderate numbers of organelles and the size and shape of the cells in each tumor were quite variable although overall they were considerably smaller than those of most liver cell carcinomas. Cell junctions in the hepatoblastomas was consistent with the epithelial nature of the tumor but liver cell origin could not be confirmed by EM.

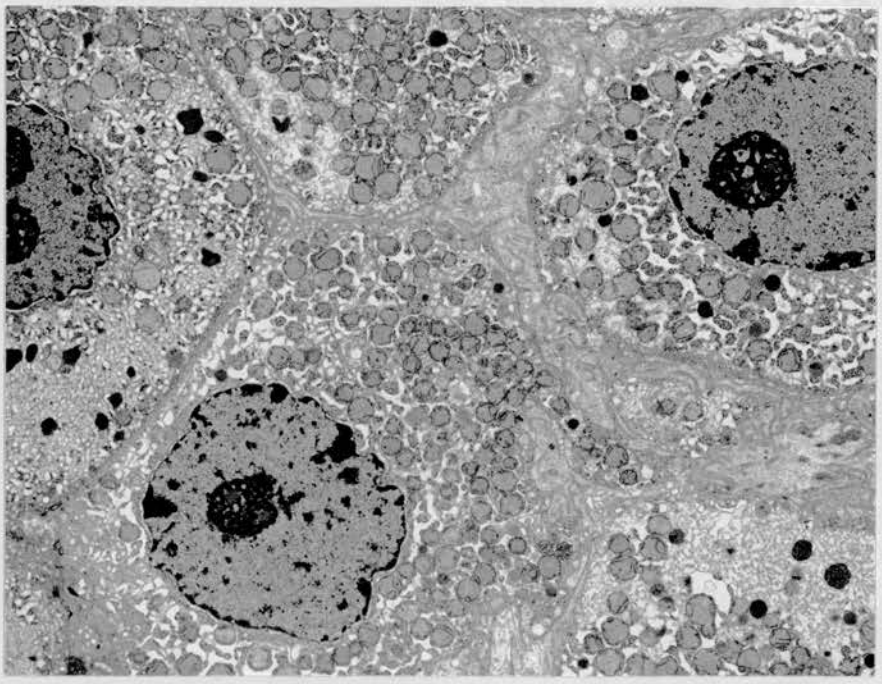

Figure 103. Liver cell carcinoma, well differentiated. There is a resemblance to normal hepatocytes. Cells are polygonal and apposed, and they contain many organelles. x 4,400.

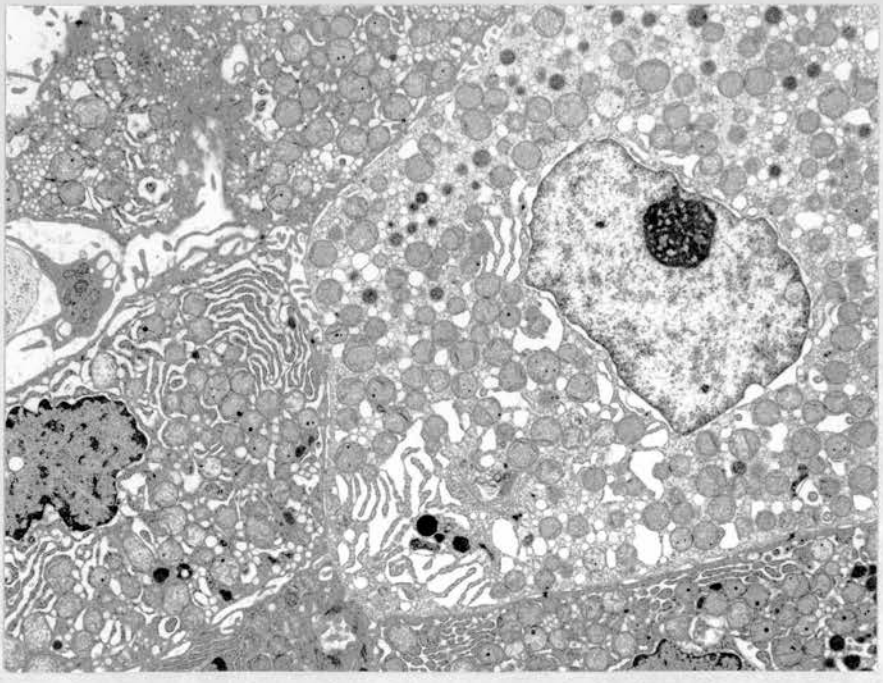

Figure 104. Liver cell carcinoma, well differentiated. Features are similar features to those in the previous figure. The organelles include many mitochondria, dense bodies, and granular and smooth endoplasmic reticulum. x 7,200.

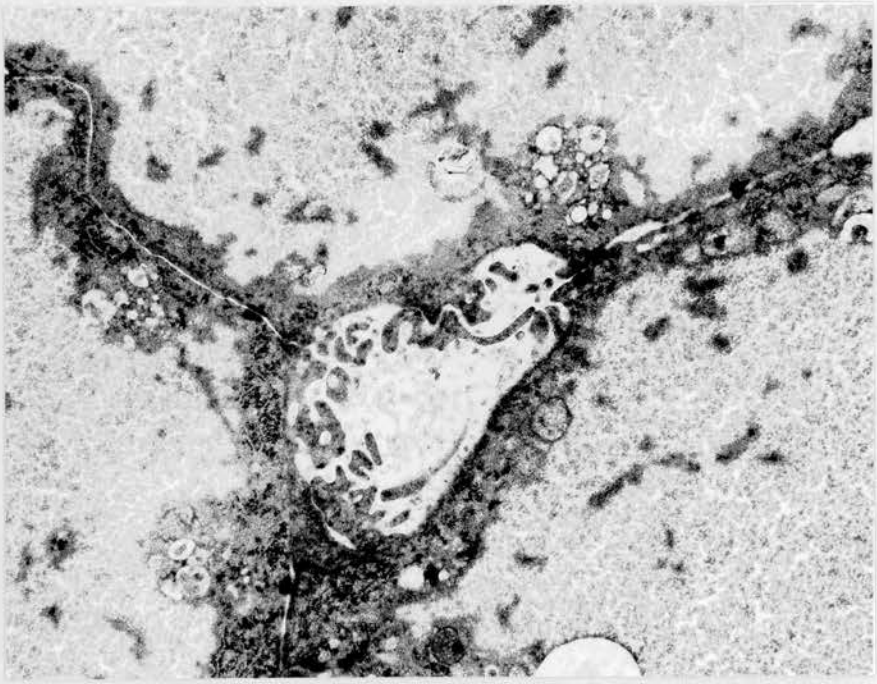

Figure 105. Liver cell carcinoma, well differentiated, showing a bile canaliculus. x 13,000.

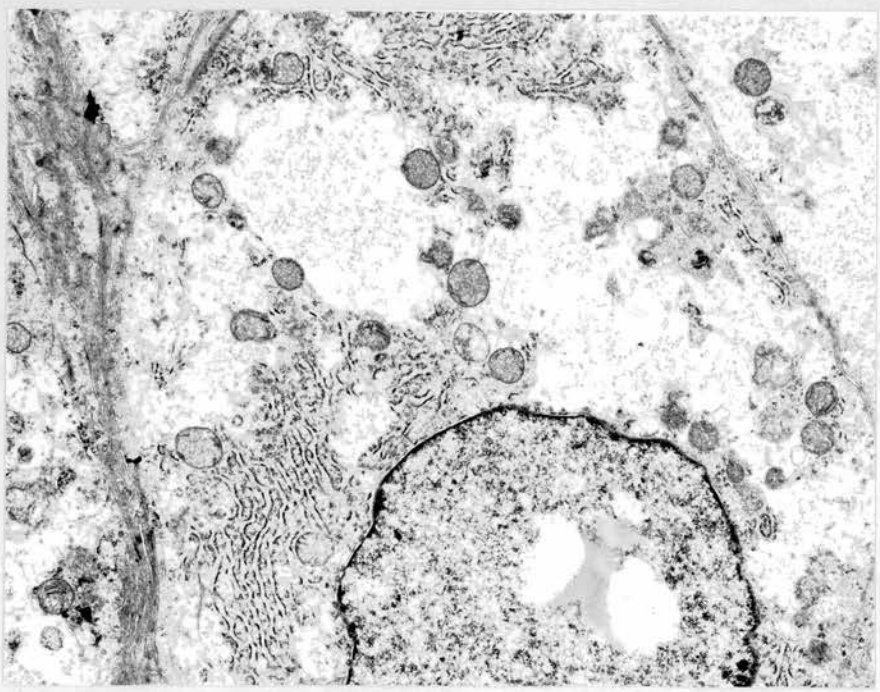

Figure 106. Liver cell carcinoma, well differentiated. Organelles were not present in large numbers but glycogen was plentiful. The nucleus contains a lipid droplet. x 8,600.

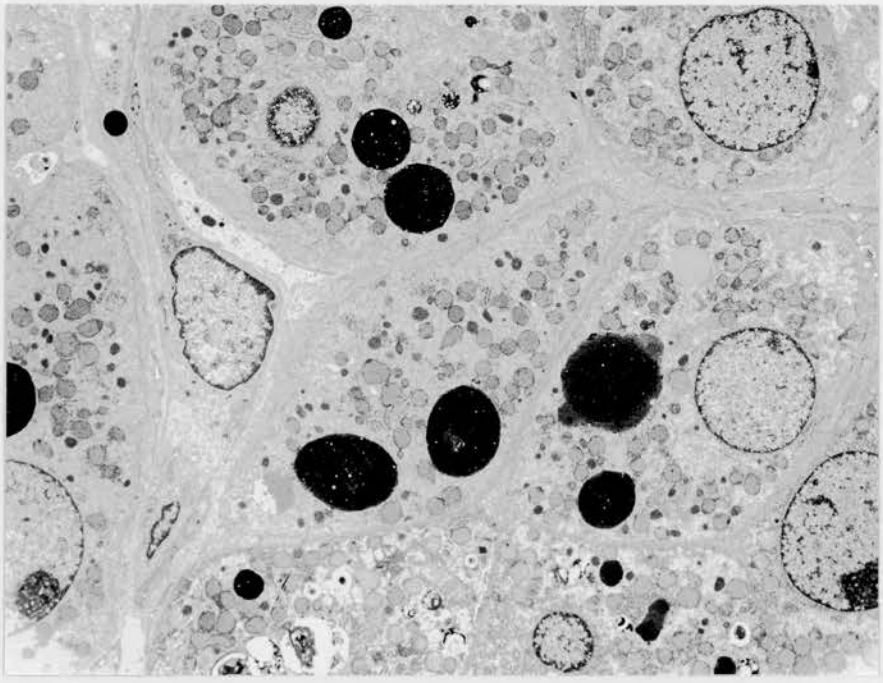

Figure 107. Liver cell carcinoma. Large dense bodies are present in the tumor cells. Staining for alpha-1-antitrypsin was positive. x 4,500.

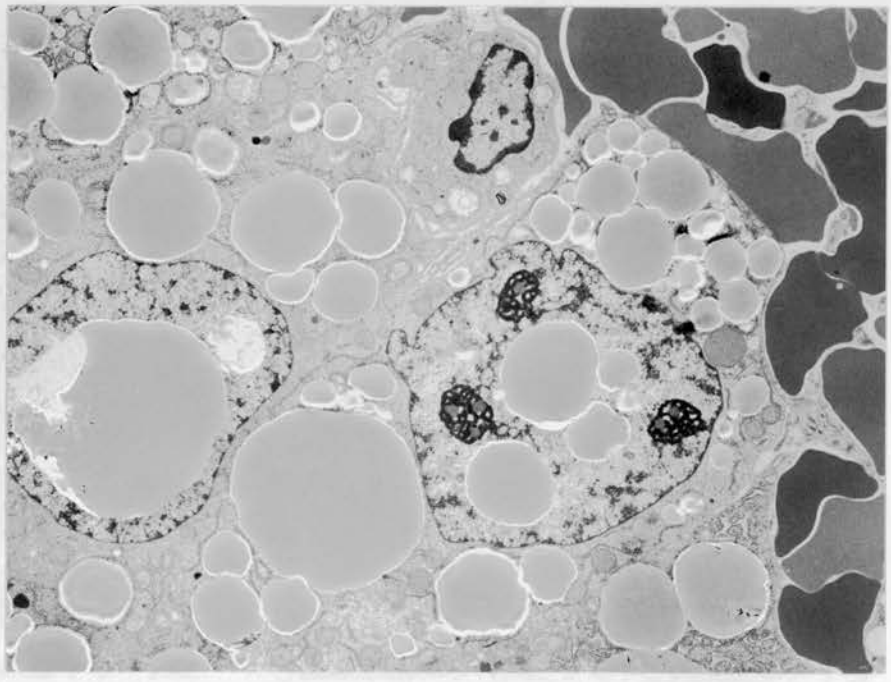

Figure 108. Liver cell carcinoma, metastatic in brain, showing marked accumulation of lipid in cytoplasm and nuclei. x 7,200.

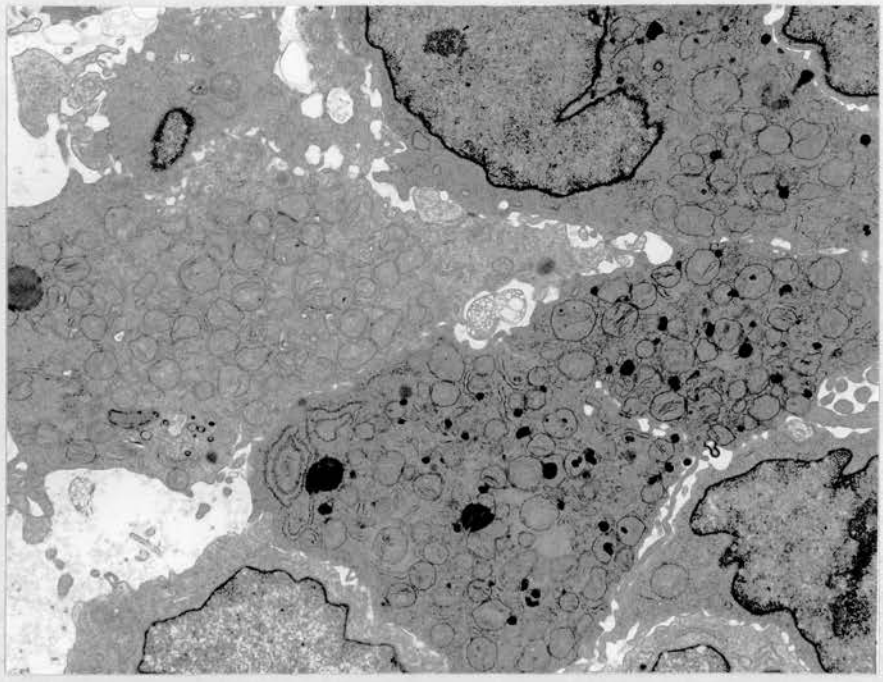

Figure 109. Liver cell carcinoma, metastatic in abdomen. The cells contain many mitochondria, some with dense inclusions. x 4,500.

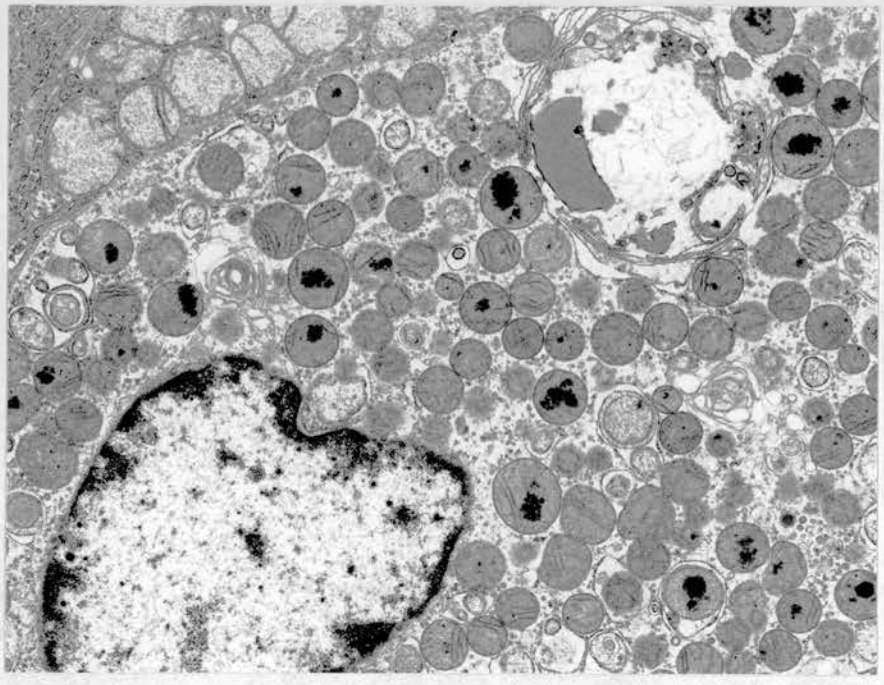

Figure 110. Liver cell carcinoma. Dense inclusions are present in many of the mitochondria. x 12,600.

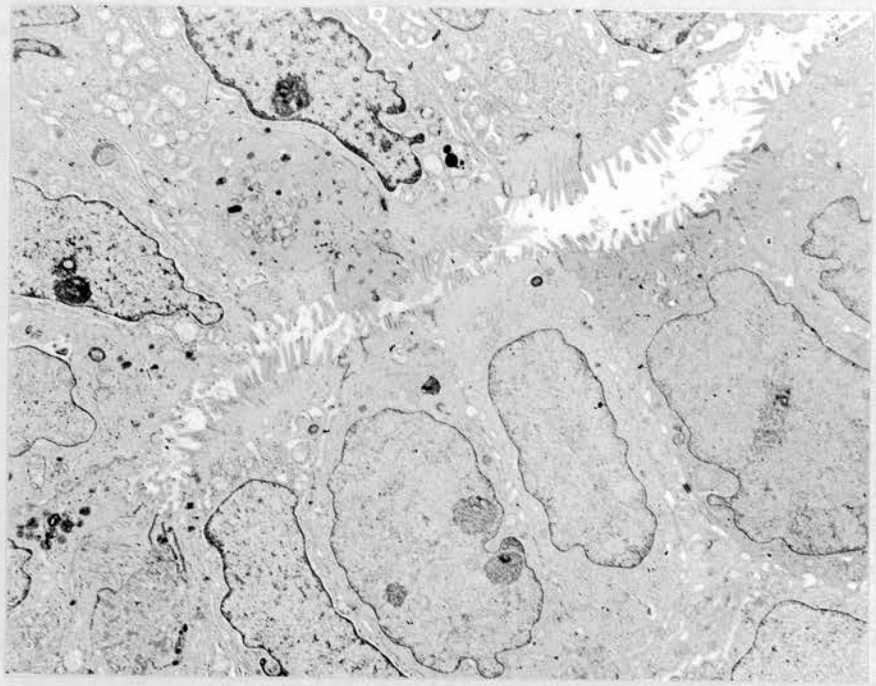

Figure 111. Bile duct carcinoma, well differentiated. The microvilli are straight and they contain microfilament cores. x 6,100.

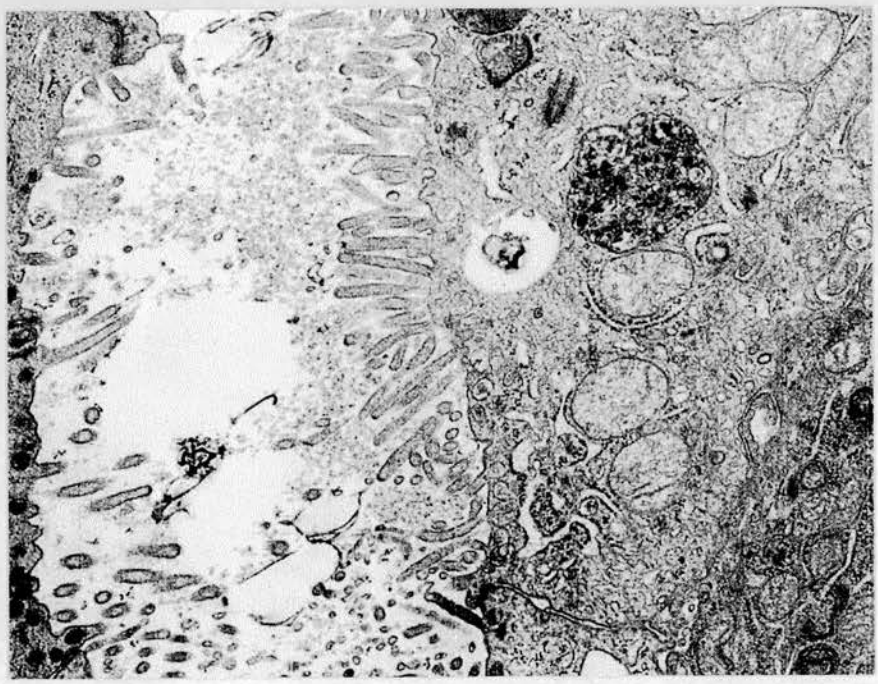

Figure 112. Bile duct carcinoma, moderately differentiated. Microvilli are irregular and they do not contain microfilament cores. x 11,800.

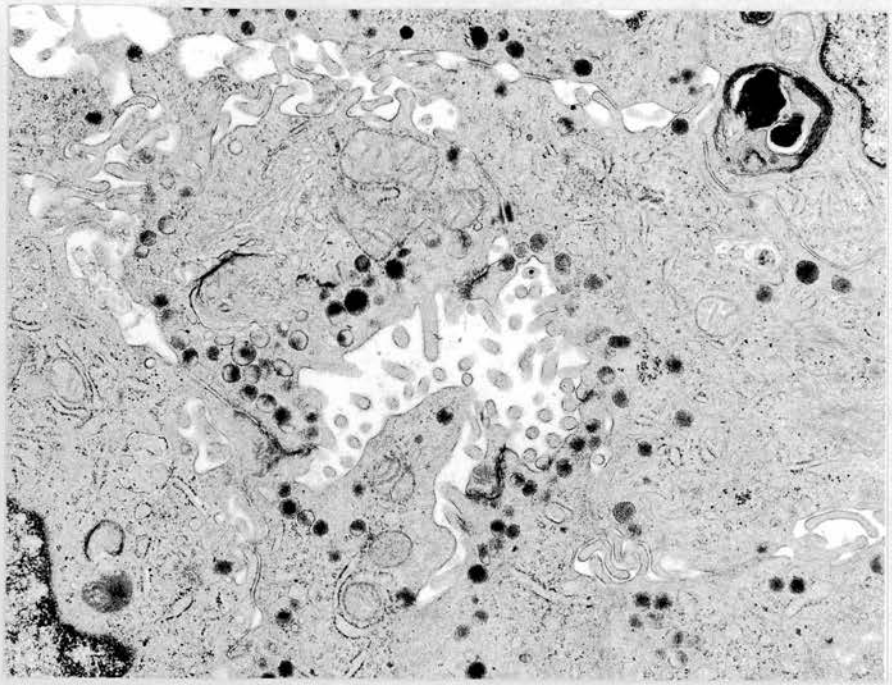

Figure 113. Bile duct carcinoma, poorly differentiated. A small lumen contains a few short microvilli and the cells are joined by vestiges of tight junctions. Small round granules surround the lumen. x 14,000.

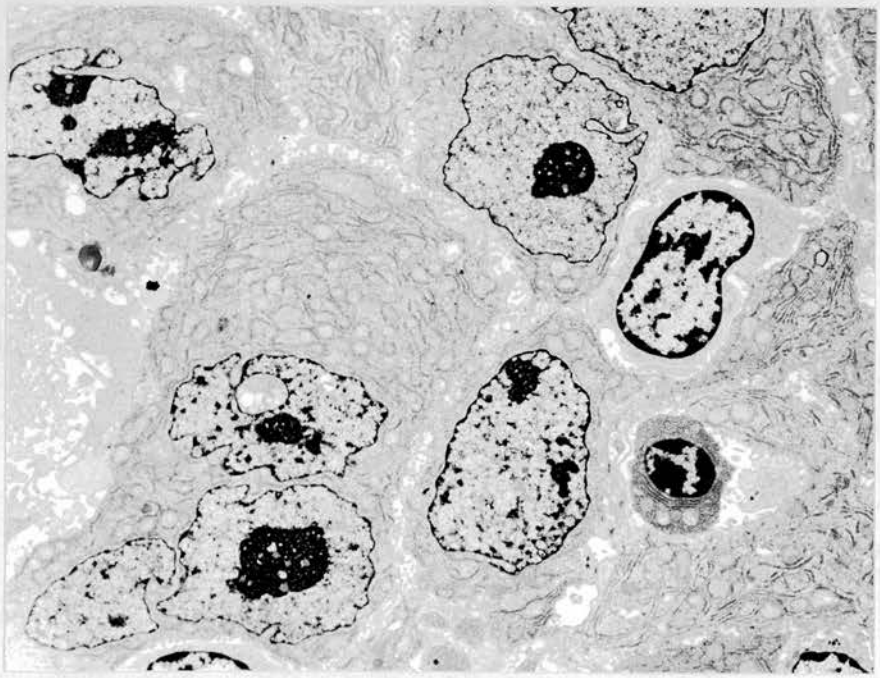

Figure 114. Hepatoblastoma, metastatic in lung. There are no discernible liver cell features. x 6,100.

The diagnosis of a primary tumor of the liver is not always an easy task for the light microscopist, and this is especially the case when the tumor is not well differentiated, or if material is scanty or distorted as may be the case with a needle biopsy. This is an area where EM can be helpful[154]. A large Japanese study confirmed that bile duct tumors are much less frequent than liver cell carcinomas[155]: among 2829 cases, 2411 were classified as liver cell carcinoma and 268 as bile duct carcinomas, while 58 were of mixed type and 69 were hepatoblastomas. Accurate subclassification is not always possible as mixed forms occur.

The cells of a differentiated liver cell carcinoma may closely resemble those of the normal liver cords (figure 103) and EM can then be diagnostic, even in a specimen from a metastatic site. A large number of organelles with a mixture of mitochondria, granular and smooth endoplasmic reticulum, and some dense bodies of varying size are the usual finding (figure 104). The differentiated carcinomas typically have a trabecular pattern, but with loss of differentiation, modifications occur on the cell surface, and in the relationship of the cells to one another and to the vessels of the tumor. There is much variation in the quantity and appearance of the cytoplasmic components and inclusions may be present. With dedifferentiation, cell junctions become smaller and fewer, the cells become separated by irregular gaps, and the cord-like arrangement is replaced by irregular groups within which loss of cohesion is evident . Extensive zones of smooth endoplasmic reticulum were not seen in the tumors that we studied, a relevant point when the differential diagnosis includes adrenal cortical carcinoma. While bile canaliculi can be found in better differentiated liver cell carcinomas (figure 105), they are distinctly fewer and less regular in their distribution and more variable in size and shape than in normal hepatic parenchyma.

The tumor cells may have clear, empty cytoplasm by light microscopy as a result of accumulation of glycogen and lipid droplets[156, 157]. Glycogen is often extensive in normal hepatocytes and it can be abundant in well differentiated liver cell carcinomas (figure 106) but progressively decreases in amount with loss of differentiation.. Cytoplasmic inclusions in liver cell carcinoma cells may be filamentous or solid. The filamentous inclusions are not membrane-limited and have some resemblance to Mallory bodies. Large electron-dense inclusions in our cases were more or less round and they varied considerably in size: this could sometimes be appreciated by light microscopy as they could be visible in paraffin sections as intracytoplasmic or occasionally extracellular bodies that were brightly eosinophilic, PAS-positive and diastase-resistant (figure 107). Alpha-1 antitrypsin staining was strongly positive in cells of the tumors containing these inclusions. Lipid is sometimes plentiful as diffusely distributed small droplets, but it is rare to find lipid in the amount seen in figure 108: the droplets vary in size and they are within the nuclei as well as cytoplasm, but this tumor was metastatic in brain. Mitochondrial hyperplasia can occur (figure 109), occasionally obscuring other organelles and producing an oncocytic neoplasm. Oncocytic hepatocellular carcinoma with numerous globular hyaline bodies was reported by Fukunaga et al[158]. Crystalline matrical inclusions are often present within elongated mitochondria in normal hepatocytes but we have only found them well developed in two tumors. However, irregular matrical densities were occasionally observed (figure 110) and some had geometric profiles so they may consist of the same material.

The space between vessel walls and adjacent tumor cells ranges from a narrow gap to a broad interval, and collagen may be observed in this space as may replication of the basal lamina of capillarized sinusoids. In the study by Haratake et al[159], thickened endothelial cells with loss of fenestrae were conspicuous features.

A frequent finding on cells lining channels in the bile duct tumors was an array of uniform, closely packed, straight microvilli with microfilament cores (figure 111). In the less differentiated bile duct carcinomas, occasional small lumens were lined by cells with shorter,

irregular microvilli that did not contain microfilaments (figure 112). The profusion of organelles seen in many liver cell carcinomas was never observed in the bile duct tumors. Small numbers of round dense bodies were seen in one bile duct carcinoma, mostly in the apical cytoplasm (figure 113), but they were much smaller than the large inclusions in liver cell carcinomas and staining for alpha-1-antitrypsin was negative. The granules were of endocrine caliber but they were mostly apical and were too few to suggest a carcinoid tumor. We did not see a convincing example of a combination of liver cell and bile duct differentiation in the cases we studied but it has been documented by light microscopy and EM[160].

The three hepatoblastomas did not show recognizable liver cell features. They were poorly differentiated tumors with some multinucleated cells and prominent nucleoli, and one (figure 114) contained cells with moderate numbers of mitochondria. Organelles and dense bodies were sparse and none of the inclusions seen in the liver cell carcinomas were found. EM reports of hepatoblastomas have confirmed that a spectrum of differentiation can be seen[161-163], supporting the hypothesis that the tumor derives from a pluripotent cell[164].

Although EM can aid in distinguishing liver cell from bile duct carcinomas, it is only reliable when the tumors are reasonably well differentiated, and conclusions from an ultrastructural study must be related to the findings on routine light microscopy because of the limited sampling in EM preparations. True mixtures of the two types are uncommon in these small specimens. EM is of more value in distinguishing between primary and metastatic tumors in the liver, particularly if the latter are neuroendocrine. Primary neuroendocrine tumors of the liver are rare, but granules have been described in the fibrolamellar variant of liver cell carcinoma[165, 166].

Acinar cell and islet cell tumors of pancreas

Acinar and islet cell tumors both contain within their cells large numbers of secretory granules, but they can nevertheless be separated from their ultrastructural features.

Osborne BM, Culbert SJ, Cangir A, Mackay B. Acinar cell carcinoma of the pancreas in a 9-year-old child. Case report with electron microscopic observations. Southern Medical Journal 70:370-372, 1977.
A retroperitoneal mass in a 9-year-old boy had been diagnosed on a biopsy specimen as lymphoma prior to his being referred. The tumor is shown in figure 115. EM showed clear cut evidence of an exocrine neoplasm. Large, dense, membrane-bound granules were present in every cell in considerable numbers establishing the diagnosis of acinar cell carcinoma of the pancreas.

Mackay B, Franzini DA, Keyes LM, Bennington JL. Retroperitoneal tumor with liver metastases in a 38-year-old female. Ultrastructural Pathology 2:183-186, 1981.
A liver biopsy from a 38-year-old woman with a retroperitoneal mass was submitted for EM. The cells contained large exocrine-type granules and extensive, often parallel cisternae of granular endoplasmic reticulum (figure 116), and a diagnosis of acinar cell carcinoma metastatic to liver was made.

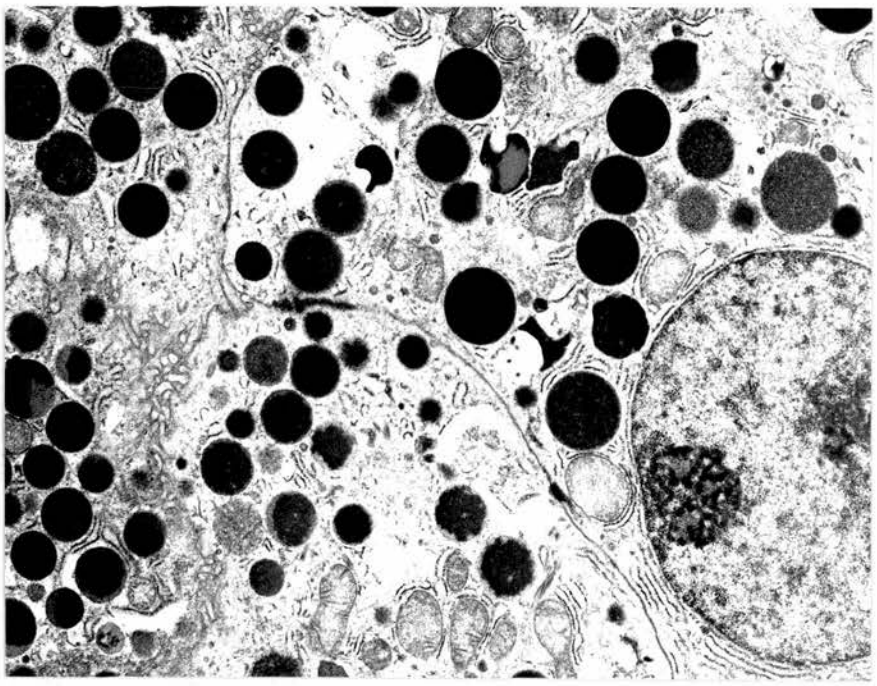

Figure 115. Acinar cell carcinoma of pancreas from a child. Large membrane-bound granules are present. x 9,600.

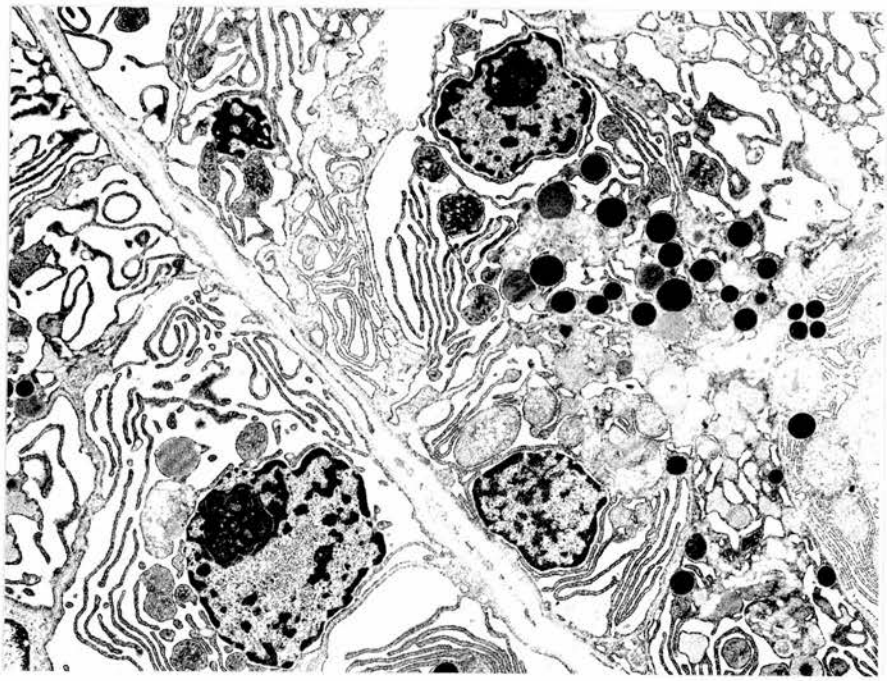

Figure 116. Acinar cell carcinoma of pancreas, metastatic in liver. In addition to exocrine-type granules, the cells contain extensive, often dilated cisternae of granular endoplasmic reticulum. x 7,400.

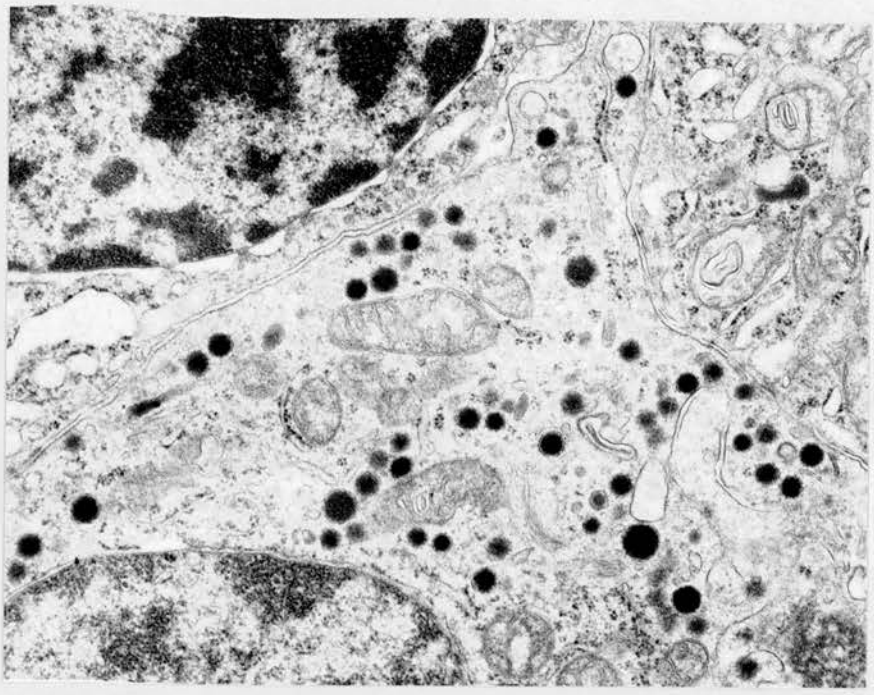

Figure 117. Islet cell tumor from the pancreas. The granules are of endocrine caliber. x 8,600.

The tumor cells may form solid sheets but small aggregates of microvilli can still be detected, sandwiched between cells as in figure 115. This retroperitoneal tumor in a young boy had been diagnosed as lymphoma. The many large granules and extensive granular endoplasmic reticulum are typical[167]. Cisternae in the cells from the liver metastasis are conspicuous because they are so extensive and dilated (figure 116), and some granules can be seen. Membrane-bound bodies containing filaments, possibly defective granules, have also been described[168]. Visually, the difference in granule size between exocrine and endocrine cells may appear to be obvious, making the distinction between an acinar cell carcinoma and an islet cell tumor easy by simple inspection of electron micrographs. The granules are clearly smaller in the islet cell tumor in figure 117 than in the previous two figures. To confirm the difference, we performed a morphometric analysis of granule caliber in acinar and islet cell tumors and confirmed that there is a distinct separation between the two neoplasms. In normal acinar cells, the diameter of the granules was 694 ±105 nm , and in acinar cell carcinomas, the figure was 648 ± 97 nm. The mean granule size in 20 islet cell tumors was 182 ± 52 nm[169]. A visual assessment should not be based on a few cells as several reports have stated that mixed exocrine and endocrine differentiation occurs in some pancreatic tumors[170-173].

Endocrine tumors occasionally have a clear cell appearance in routine sections and the following two cases illustrate that it can be from the presence of glycogen or mucin.

Guarda LA, Silva EG, Ordonez NG, Mackay B, Ibanez ML. Clear cell islet cell tumor. American Journal of Clinical Pathology 79:512-517, 1983.
A 52 year old male from Lebanon had a level III malignant melanoma on the skin of his back which was excised in his home country. Fifteen months later, he was investigated following six months of intermittent left upper quadrant pain: a mass described as suprarenal was resected and adrenal cortical carcinoma was diagnosed. Ten months later, he was referred and a recurrent mass was found involving the left kidney, spleen, body of pancreas, and diaphragm, and it was resected. The cells were predominantly clear by light microscopy and stains for glycogen were positive. EM revealed endocrine granules and correlation with the resected specimen established that the tumor was arising in the pancreas. Metastases subsequently developed.

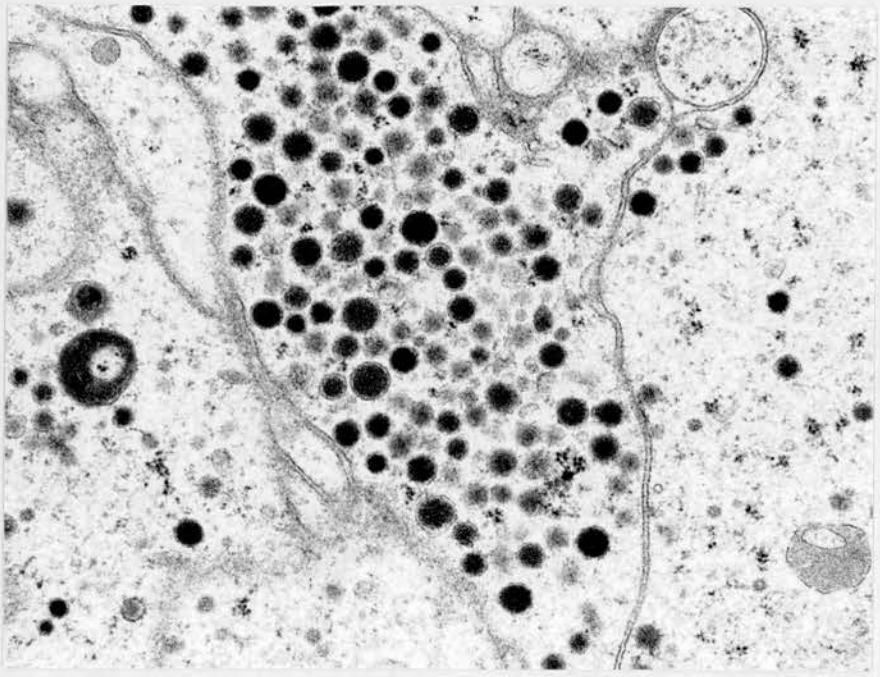

Figure 118. Islet cell carcinoma. The tumor had clear cytoplasm by light microscopy. Some cells contained considerable numbers of granules. x 15,000.

The number of secretory granules in the cells of this tumor varied but they are numerous in figure 118. Immunostaining was performed and cells positive for VIP and substance P were detected. Clear cell tumors of the endocrine system are recognized[174]. We found similar features in a clear cell carcinoid tumor of the stomach[175], and in another islet cell tumor the clear cytoplasm was attributed to intracytoplasmic accumulation of lipid[176].

Ordonez NG, Balsaver AM, Mackay B. Mucinous islet cell (amphicrine) carcinoma of the pancreas associated with watery diarrhea and hypokalemia syndrome. Human Pathology 19:1458-61, 1988.

A 62-year-old woman gave a history of several months of severe diarrhea and she was found on investigation to have hypercalcemia. CT scans showed a 4 cm tumor mass in the head of the pancreas, and at surgery, metastatic nodules were found in the liver. One of the liver nodules was biopsied and EM was performed. The tumor was a mucin-producing endocrine carcinoma, and immunohistochemical studies demonstrated numerous cells staining for pancreatic polypeptide and chromogranin. Stains for other hormonal polypeptides were negative.

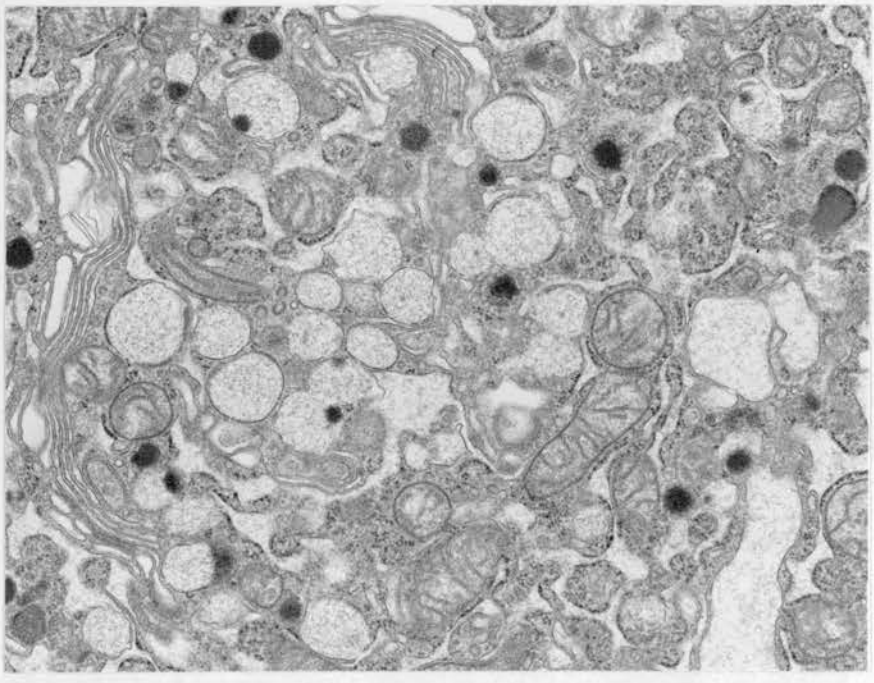

Figure 119. Amphicrine carcinoma of pancreas, metastatic in liver. The cells contain mucin droplets and granules. x 16,500.

The tumor cells contained granules of endocrine caliber and larger mucin granules (figure 119). The term amphicrine has been used for neoplasms that coexpress mucin and neurosecretory granules in the same cell population. Mucin-producing endocrine tumors include goblet cell carcinoid of the appendix and mucin producing medullary carcinoma of the thyroid. In the case we reported, a high plasma level of VIP associated with watery diarrhea, hypokalemia and a pancreatic tumor was diagnostic of the Werner-Morrison syndrome.

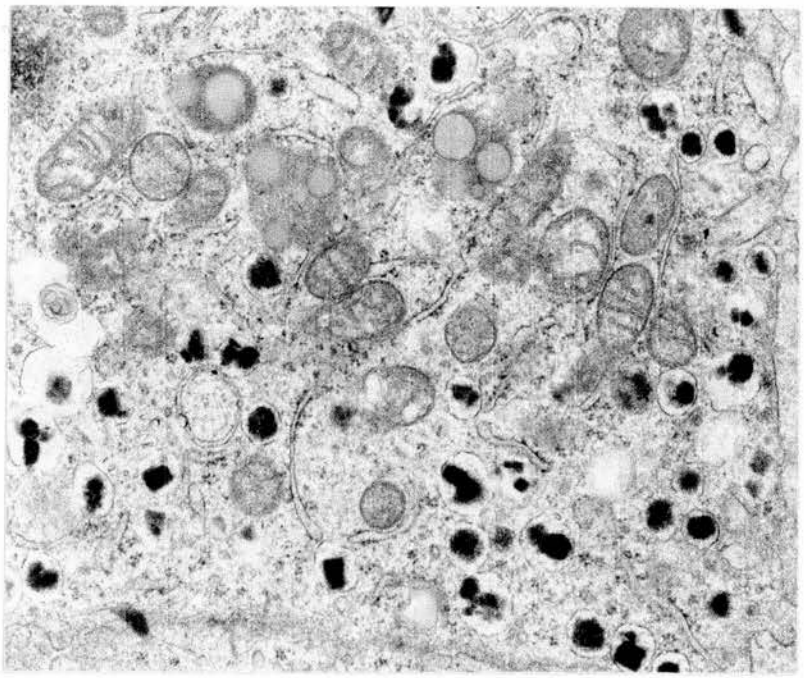

Figure 120. Islet cell tumor of pancreas. The granules have crystalline cores. x 13,800.

The islet cell tumor in figure 120 occurred in a 51 year old male and it contained endocrine granules by EM and gave a positive reaction for pancreatic polypeptide in most of the tumor cells. A few cells stained for insulin and glucagon. In this beta cell tumor, most of the granules have crystalline cores. In another islet cell tumor that we studied, EM showed intracytoplasmic inclusions which were visible as globoid structures by light microscopy and correlated with a positive immunoreaction for alpha-1-antrypsin. Reinke-like crystals were also observed[177].

Uncommon tumors of the pancreas

The two examples discussed are small cell carcinoma and the so-called solid and papillary tumor.

Ordonez NG, Cleary KR, Mackay B. Small cell undifferentiated carcinoma of the pancreas. Ultrastructural Pathology 21:467-474, 1997.
The clinical evolution, immunohistochemical profile, and ultrastructure of a tumor occurring in a 37 year old woman are described in this case report. The tumor was diagnosed as a small cell carcinoma arising in the pancreas.

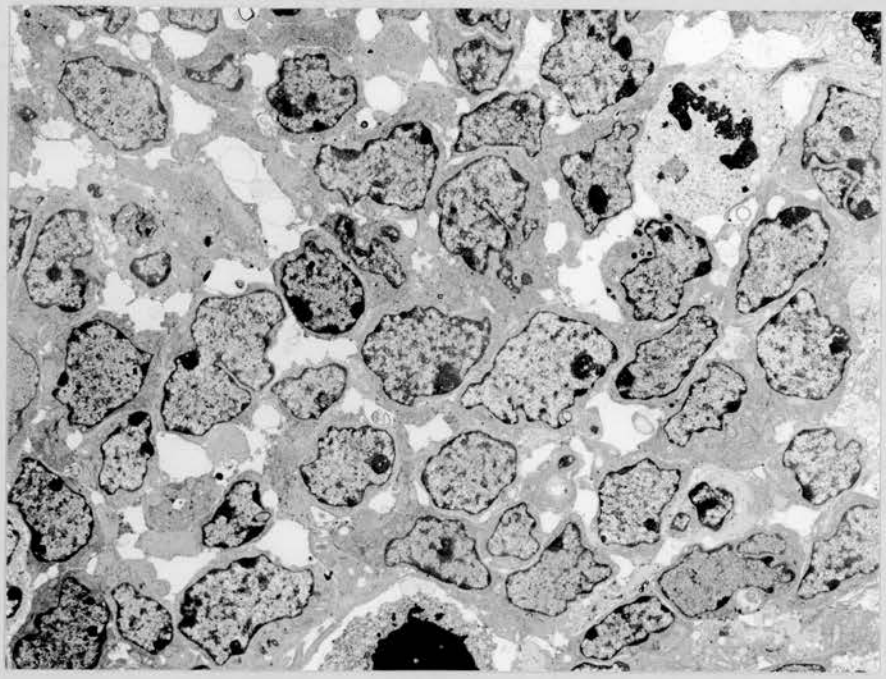

Figure 121. Small cell carcinoma of pancreas. The cells have scanty cytoplasm and irregular nuclei. x 2,400.

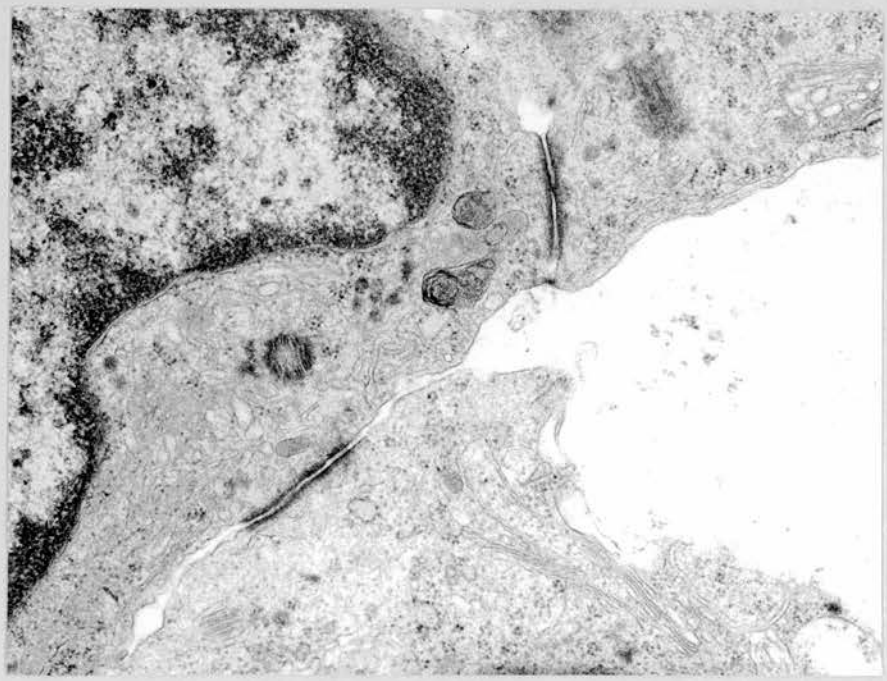

Figure 122. Same tumor as figure 122 showing desmosome-like cell junctions. x 12,000.

Small cell undifferentiated carcinoma of the pancreas is a rare neoplasm, and at the time of this report only 12 cases had previously been recorded. The tumor cells are small with irregular cell and nuclear profiles (figure 121). They were not tightly packed but were often in contact with their neighbors and cell junctions were easily found (figure 122).

De la Roza G, Cleary KR, Ordonez NG, el-Naggar A, Mackay B, Romsdahl MM. Solid and papillary tumor of the pancreas. Ultrastructural observations on two contrasting cases. Ultrastructural Pathology 21:439-447, 1997.
Two papillary and solid tumors of the pancreas were reported. Both tumors contained papillary and solid areas by light microscopy. They differed in their clinical features, ultrastructure, and biologic behavior. One tumor followed the more usual indolent course. The second patient presented with a liver metastasis and died of progressive disease in a relatively short period of time.

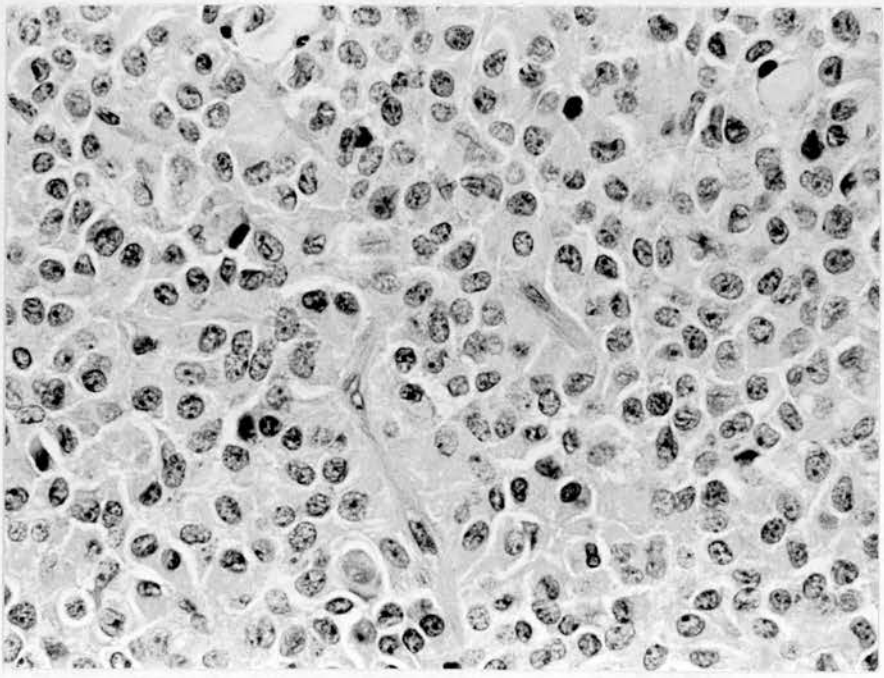

Figure 123. Solid and papillary tumor of pancreas. A solid area is shown. Hematoxylin and eosin.

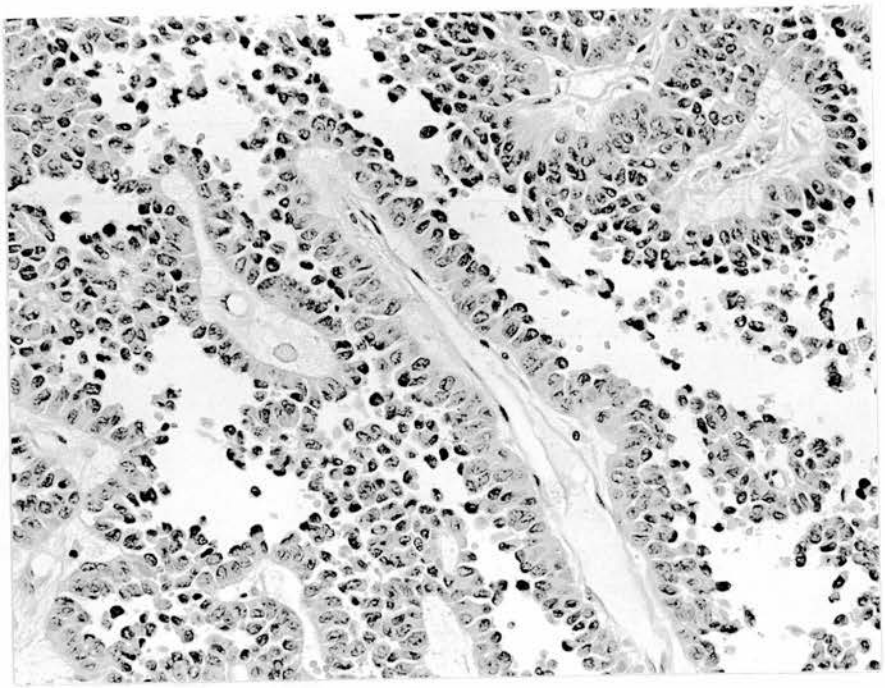

Figure 124. Same tumor as figure 123 illustrating a papillary area. Hematoxylin and eosin.

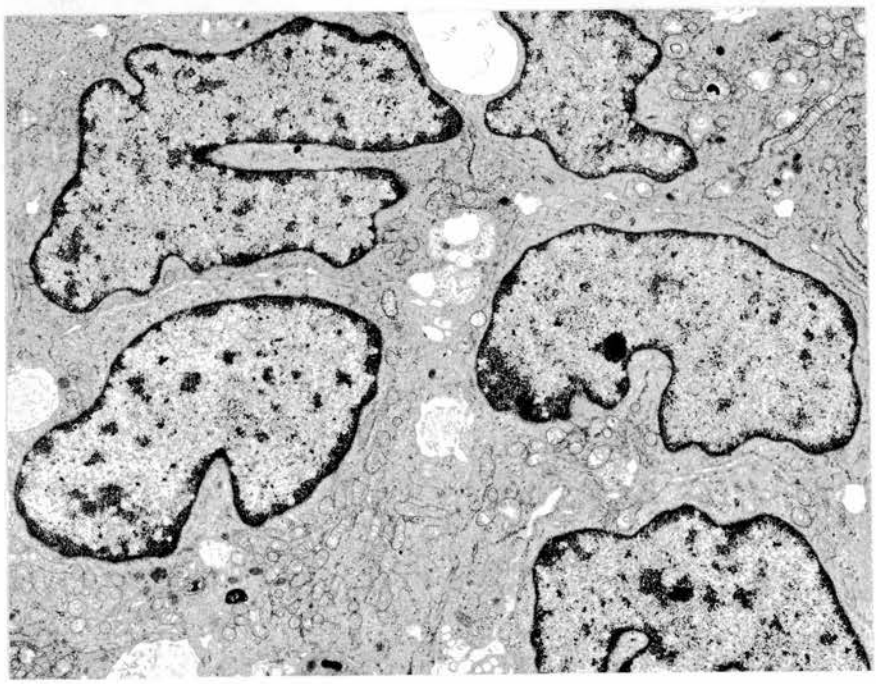

Figure 125. Solid and papillary tumor of pancreas. The closely apposed cells contain moderate numbers of organelles and they have nuclear indentations. x 6,200.

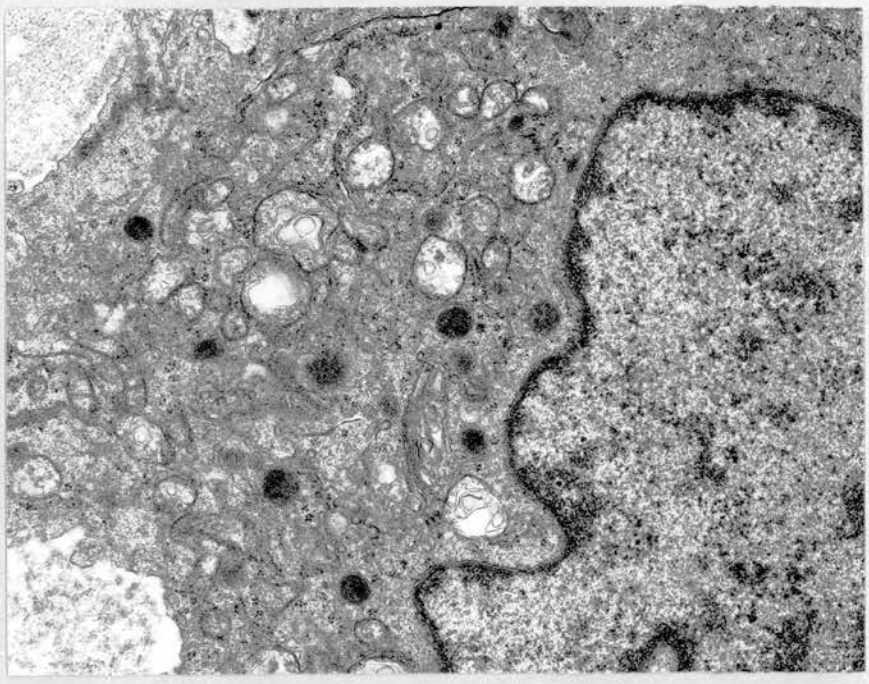

Figure 126. Solid and papillary tumor of pancreas. A few dense-core granules of endocrine caliber are present. x 14,000.

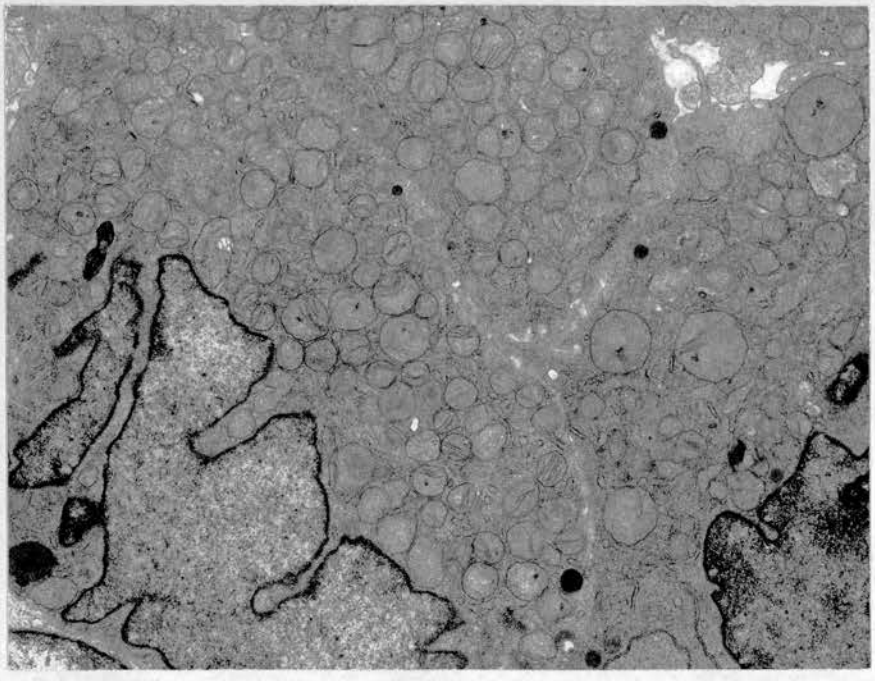

Figure 127. Solid and papillary tumor of pancreas. The many mitochondria create an oncocytic appearance. x 12,900.

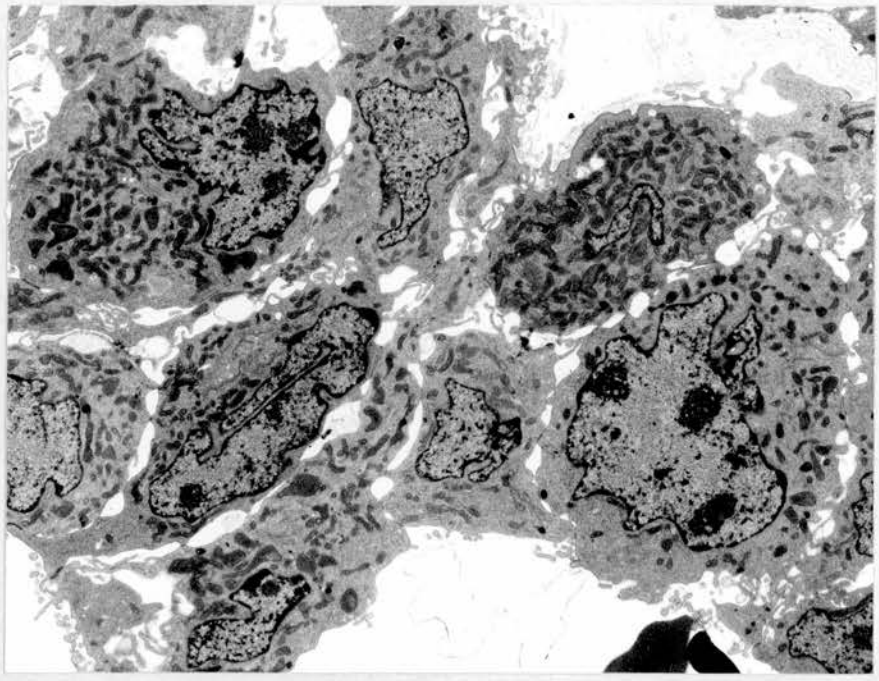

Figure 128. Solid and papillary tumor of pancreas, metastatic in omentum. The poorly differentiated cells have markedly irregular nuclear profiles. x 5,000.

The light microscopy of a solid area from one of the primary sites is shown in figure 123 and a papillary pattern from the same tumor is illustrated in figure 124. Four areas are shown to demonstrate the great variability in ultrastructure that was found between the cases, and in primary and metastatic sites from the same patient. The cells are compactly grouped in figure 125 and nuclei are indented. A few cells contained dense core granules of endocrine caliber (figure 126). The many mitochondria in figure 127 qualify the cells as oncocytic and some of the mitochondria have bizarre arrangements of their cristae. In the omental metastasis in figure 128, the cells have highly irregular nuclei and only occasional contacts with a few primitive cell junctions.

The occurrence of oncocytic cells would be compatible with the tumor possessing endocrine properties. Although the few granules we found were of endocrine caliber, others have found larger, exocrine-type granules[178]. However, granules were not found in one EM study of five cases[179]. We reported the two cases because of the variation seen by EM and others have also formed the impression from the variety of ultrastructural appearances that the tumor is derived from pluripotential cells which may be capable of differentiating into ductal or secretory cells, both exocrine and endocrine[180].

Tumors of the urinary system

The tumors discussed in this section are renal cell carcinoma, endocrine tumor of the kidney, and carcinosarcoma of the kidney.

Renal cell carcinoma

Most primary tumors of the kidney in adults fall within the spectrum of clear to granular cell renal cell carcinomas. EM has proved useful to characterize the common tumors[181], but it is particularly helpful in identifying and detailing the structure of less frequently seen renal neoplasms. The typical forms are illustrated for comparison with four variants.

> **Mackay B, Ordonez NG, Khoursand J, Bennington JL. The ultrastructure and immunocytochemistry of renal cell carcinoma. Ultrastructural Pathology 11:483-502, 1987.**
> A report of a project using light microscopy and EM to examine a series of renal cell carcinomas, both primary and metastatic, including clear cell, granular, oncocytic, and sarcomatoid types. Immunoperoxidase staining was performed on 28 sarcomatoid carcinomas to complement data already available on the common tumors. The ultrastructural study encompassed 156 primary and 69 metastatic tumors.

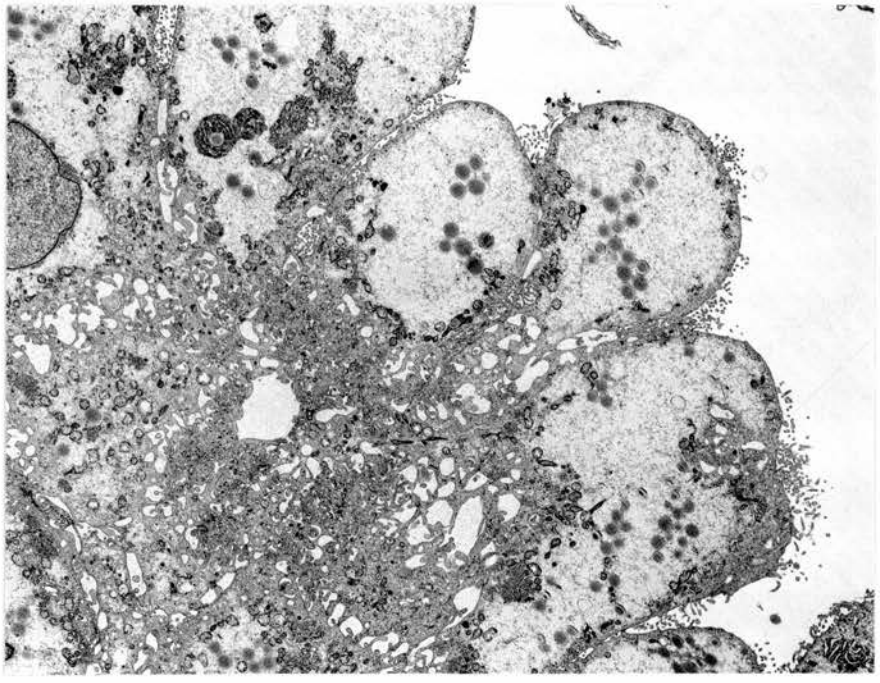

Figure 129. Renal cell carcinoma. Clear cell type: lipid droplets and lakes of glycogen occupy the apical cytoplasm. x 6,200.

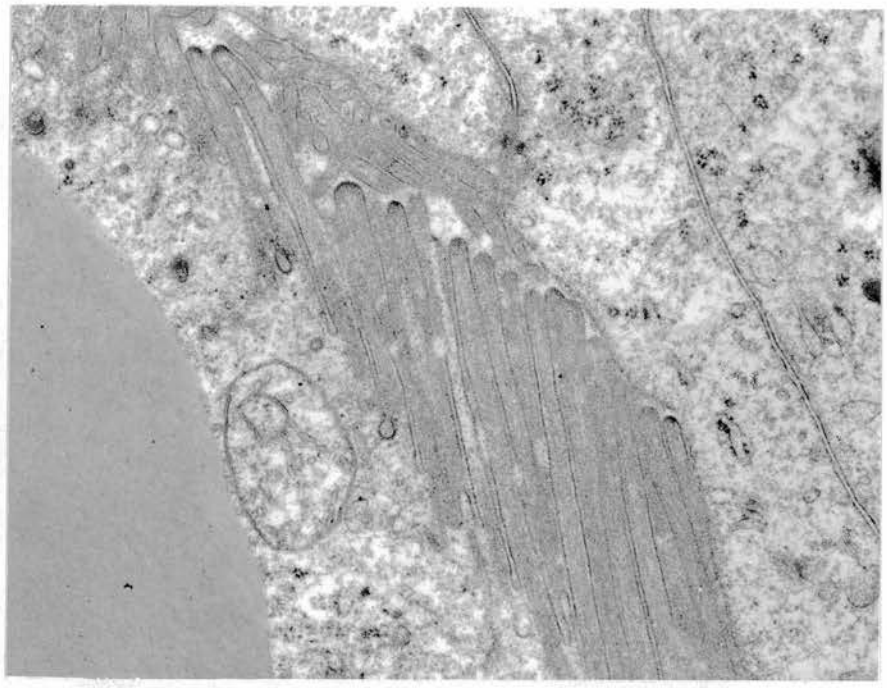

Figure 130. Renal cell carcinoma, clear cell type, metastatic in lung. The microvilli have a picket-fence pattern. Part of a large lipid droplet is visible. x 24,000.

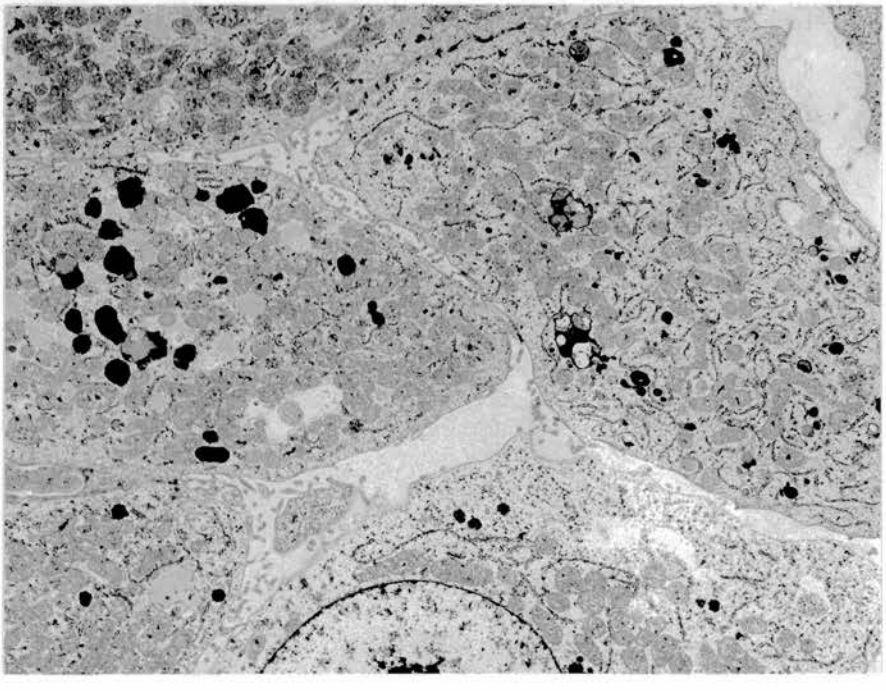

Figure 131. Renal cell carcinoma, granular cell type. The cells contain numerous organelles, some lysosomes, and little or no visible glycogen or lipid in most of the cells. x 7,500.

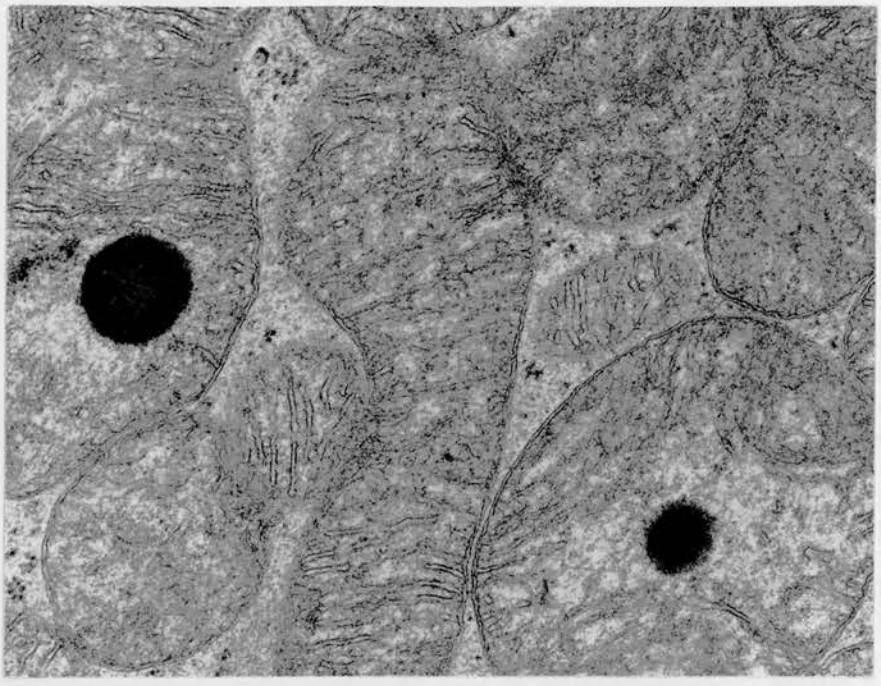

Figure 132. Oncocytic renal cell tumor. Some of the mitochondria contained large matrical densities. x 32,000.

The typical appearances of renal cell carcinomas of clear and granular cell type are illustrated here. In the clear cell type, there is abundant glycogen and varying numbers of lipid droplets that are small and uniform (figure 129). Other organelles are not usually plentiful. Histochemical procedures are not specific and are of limited value in the differential diagnosis beyond showing the presence of glycogen. Neither clear nor granular cell renal cell carcinomas contain intracytoplasmic mucin although they may have abundant glycocalyx on cell surfaces bordering tubular lumens. There are no specific immunocytochemical markers for renal cell carcinoma though again these methods may aid in narrowing a problem diagnosis. Scanty to moderate numbers of mitochondria are present in the primary tumors and their frequency is more variable in metastatic foci. Nuclei are central with smooth contours, fine chromatin, and round dense nucleoli of medium size. The periphery of the cells is often smooth with close apposition of adjacent cell membranes. On cells lining lumens or covering papillae, the apical cytoplasm may bulge into the lumen conferring a crenated profile. Microvilli are quite variable, ranging from an array of straight or slightly curved structures to a few short irregular projections (figure 129). Even in a metastasis of a poorly differentiated tumor, a uniform array of microvilli may be detected (figure 130). Cell junctions are usually small and often scattered. Lloreta-Trull et al[182] conducted an ultrastructural morphometric study of nuclear, nucleolar, and cytoplasmic features in clear cell renal cell carcinomas and concluded that nucleolar area is the most useful prognostic criterion.

In granular cell carcinomas, there are more organelles than in the clear cell tumors, and glycogen and lipid are in smaller quantities (figure 131). Many cells contain little or no visible glycogen and lipid droplets may not be evident. The organelles that are present are identical in appearance to those in the clear cell tumors. Some lysosomes are often seen in the apical cytoplasm. The basal cell membrane tends to form deep folds. Microvilli are similar in frequency to those of clear cell tumors. Although they are infrequent, unique

cytoplasmic inclusions occur: they are spherical bodies made up of concentric layers of membranes which create a laminated appearance and they are bounded by a unit membrane. Some contain fine amorphous material. They are uncommon in my experience and unusual though I question their specificity. While these are the typical findings, there is a considerable range of ultrastructure among the common renal cell carcinomas and mixed populations of clear and granular cells are common. In one study[183], tumors in half of the patients contained fewer than 5% of granular cells, and almost two thirds had less than 20% of granular cells: the latter patients had improved short-term survival but there was no correlation with long-term survival. EM has shown that cells in the chromophobe form of renal cell carcinoma contain cytoplasmic microvesicles which are 150-300 nm in diameter, and like the granular cell tumors they have a low glycogen content when compared with clear cell carcinomas[184]. The vesicles in the chromophobe tumors may be of mitochondrial origin[185], and many of the mitochochondria have tubulovesicular cristae[186].

In oncocytic renal tumors, the fine structure of the cells is dominated by the profusion of mitochondria, but the degree of mitochondrial hyperplasia varies and it can not always be predicted from paraffin sections. Most of the mitochondria are of normal size and appearance but some have slender, closely packed cristae and it is common to find within a few of them large, round matrical densities (figure 132) which are of lipid composition. Lumens and microvilli are not usually seen in a renal oncocytoma though intracytoplasmic lumens have been recorded[187]. An orderly pattern of the cells and intervening thin-walled vessels is characteristic. Origin of renal oncocytoma from the distal nephron has been suggested[188, 189].

Uncommon Renal Tumors

Four less common primary tumors of the kidney are now described. The first is a renal cell carcinoma which appeared unusual throughout most of its extent by light microscopy, and its appearance when viewed with the electron microscope was viewed as evidence of distal nephron differentiation.

> **Ordonez NG, Mackay B. Renal cell carcinoma with unusual differentiation. Ultrastructural Pathology 20:27-30, 1996.**
> A 4 cm tumor in the kidney of a 67-year-old male contained a small focus of classic renal cell carcinoma with a papillary architecture and clear cells, but most of the tumor was made up of paired sheets of cuboidal to flattened cells, and EM showed that the slender paired cords were covered by a single layer of cells with a paucity of microvilli comparable to those of the distal tubule of the normal nephron. Since most of the tumor cells were more flattened than truly cuboidal, a resemblance to cells of the loop of Henle was suggested although the greatly attenuated cytoplasm of the thin segment of the loop was not seen.

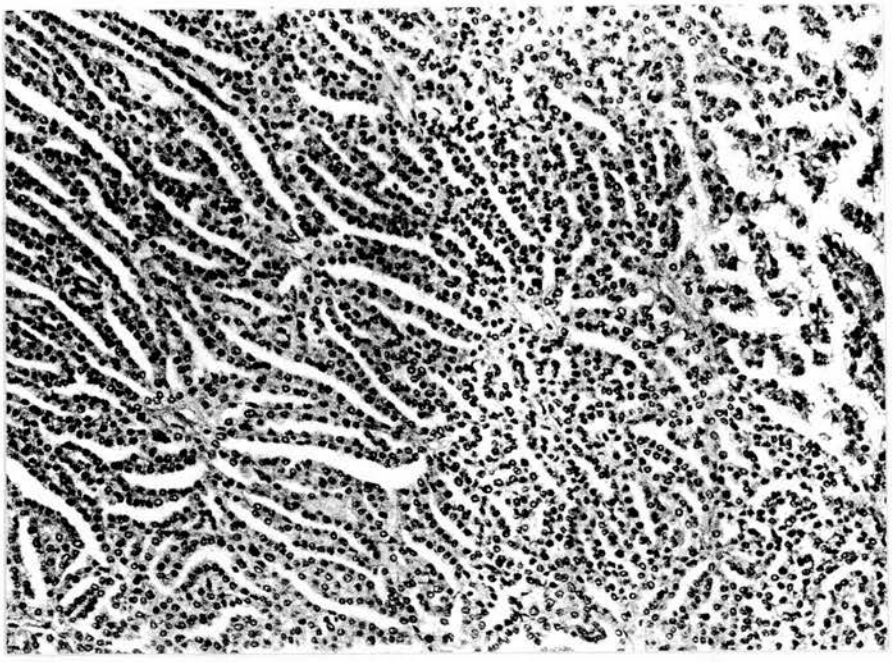

Figure 133. Renal cell carcinoma. Almost the entire tumor was made up of the principal pattern illustrated but a small focus of more typical renal cell carcinoma was present and can be seen at the left side of the figure. Hematoxylin and eosin.

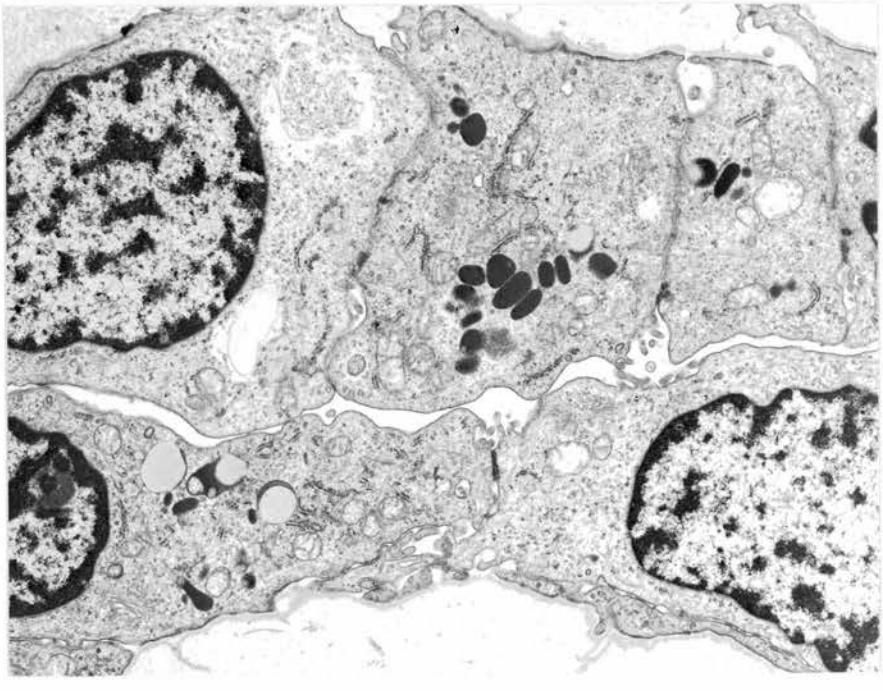

Figure 134. Same tumor as figure 133. A small part of a cord of cells is shown. There is a flattened central lumen, and an intact investing basal lamina can be identified. x 13,000.

In most renal cell carcinomas, whether clear cell or granular cell and with papillary or solid pattern, the cells show some resemblance to those of the proximal tubule of the normal nephron which are low columnar in shape with closely grouped and often straight microvilli on the apical surface. In the tumor we report, a small zone of classical renal cell carcinoma with papillary configuration and clear cells was detected, and it merged with the main pattern (figure 133 was selected to show both) which extended throughout the rest of the sections. The slender paired cords were covered by a single layer of cells (figure 134), and the paucity of microvilli is similar to what is seen in the distal tubule of the normal nephron. However, infoldings of the basal cell membrane which are prominent in normal distal tubule cells were not evident in this tumor where most of the cells were more flattened than truly cuboidal, and they thus more closely resembled cells of the loop of Henle, although the attenuated lining cells of the thin segment of the loop were not seen. He et al[190] have reported a renal tumor in a 45-year-old woman that mainly consisted of tubules formed by flat or cuboidal cells and the authors suggested that the histology mimicked lower-nephron nephrogenesis. Parwani et al[191] also postulated distal nephron segments in their EM study.

A renal cell tumor with epithelial features which did not fall within the spectrum of typical renal cell carcinomas was found to possess endocrine features by EM.

Gurley SD, Luna MA, Ordonez NG, Mackay B. Endocrine carcinoma of the kidney. Ultrastructural Pathology 21:307-310, 1997.
A 4 cm mass in the right kidney of a 43-year-old female had an endocrine appearance by light microscopy, and EM confirmed this impression: the cells contained numerous cytoplasmic granules of endocrine caliber. Unusual features were only patchy immunoreactivity for chromgranin and polarity of the granules within the tumor cells. Extrarenal extension and liver metastases were documented.

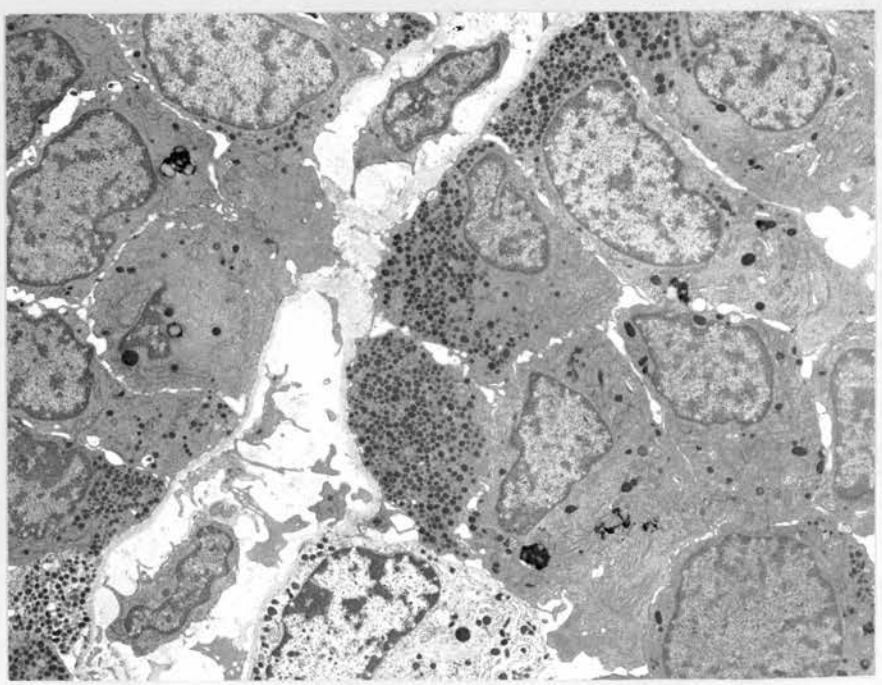

Figure 135. Endocrine tumor of kidney. Large numbers of granules are present in some of the cells. x 4,200.

Large numbers of endocrine granules were present in most of the tumor cells and they tended to congregate within part of the cytoplasm (figure 135). Primary endocrine tumors of the kidney have generally been called carcinoid tumors. In a 1983 report[192], five previous cases of primary carcinoid of kidney were found and the authors recorded a sixth. Huettner et al[193] reported the 16th case in 1991 and observed that the predominantly trabecular histology, nonreactivity with silver stains, and immunohistochemical profile of their case are common characteristics of rectal carcinoids, and they concluded that renal carcinoids are tumors of hindgut endocrine cells. One renal carcinoma with intermittent ACTH production contained neuroendocrine granules and many mitochondria[194] and resembled an oncocytic carcinoid. Smaller granules are occasionally found renal tumors. Seventeen cases of renal small cell carcinoma have been reported in the literature, approximately half showing combination with transitional cell carcinoma[195], and one from this hospital contained neuroendocrine granules[196].

A unique type of renal neoplasm with endocrine properties is the rare juxtaglomerular cell tumor.

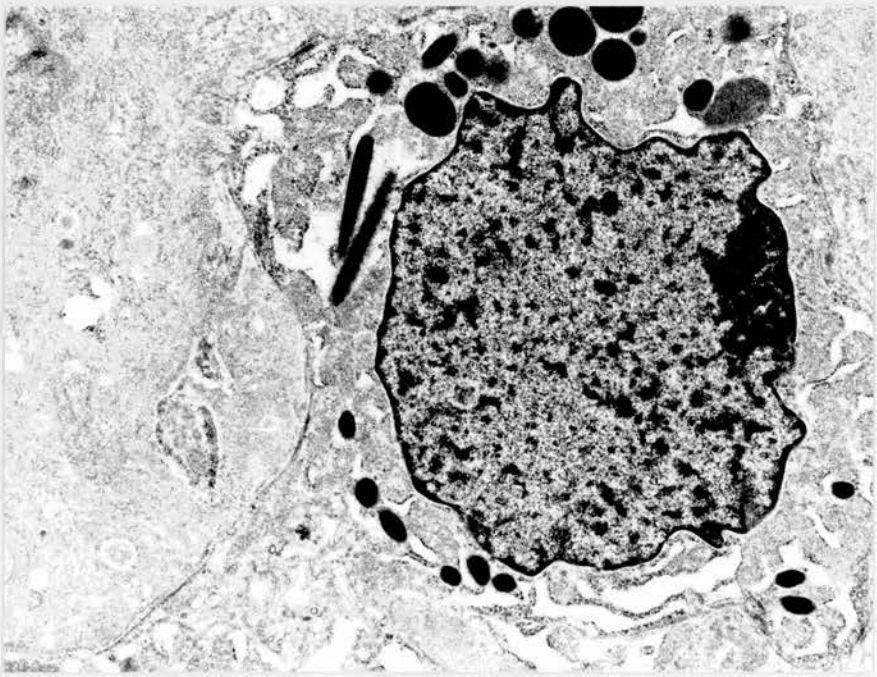

Figure 136. Juxtaglomerular renal cell tumor. The dense granules ranged from round and ovoid to needle-like. x 10,200.

The variability in size and shape of the dense granules (figure 136) and the occurrence of rhomboid, elongated and even needle-shaped bodies[197] separate this tumor ultrastructurally from other endocrine tumors. The cells are fairly uniform and mostly round, and they are arranged in cords and clusters with scattered mast cells[198]. While EM can confirm the diagnosis, it will already be anticipated if the patient is hypertensive and has high levels of plasma renin activity, but some tumors are non-functioning. The prognosis is good and symptoms may disappear after the tumor is resected[199]. EM has been advocated to exclude renal involvement by hemangiopericytoma[200].

An elongated cell from a spindle-cell renal tumor with a biphasic pattern by light microscopy is shown in figure 137.

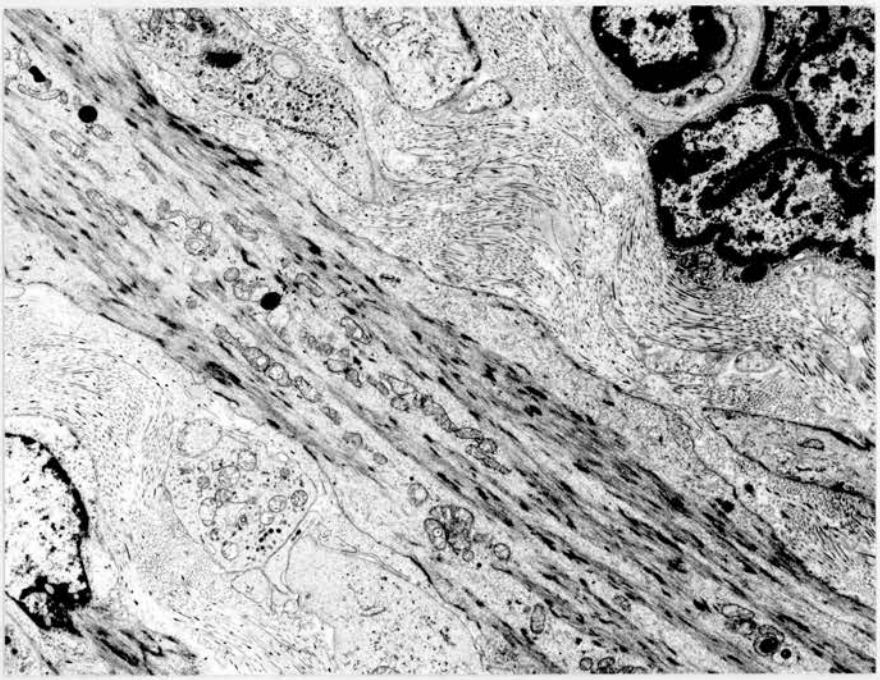

Figure 137. Carcinosarcoma of kidney. The spindle cell component was made up of cells that displayed prominent smooth muscle differentiation. x 8,400.

A sarcomatoid carcinoma of the kidney can be confused with a true sarcoma or a carcinosarcoma by routine light microscopy[201]. In a study of 28 primary renal tumors composed of both epithelial and spindle cells[202], immunostaining for keratin, desmin and smooth muscle myosin was performed, and tissue for EM was available on eight cases. Sixteen tumors were grouped as sarcomatoid carcinomas from the immunostaining findings since both the epithelial and spindle cell components were cytokeratin positive. Four tumors were not immunoreactive but EM revealed that the spindle cells were carcinomatous from the presence of many lipid droplets and lakes of glycogen. In eight tumors, only the epithelial component was keratin positive, and two of these tumors were true carcinosarcomas with leiomyosarcoma as the mesenchymal component. Immunohistochemistry is valuable in the investigation of spindle-cell tumors of the kidney[201, 203], and EM is useful for confirmation of questioned diagnoses.

Tumors of the reproductive systems

The tumors discussed in this section are small cell carcinoma of the cervix, and Paget's disease of the vulva.

A great variety of histopathology is seen among germ cell and stromal tumors of the male and female gonads but most can be classified from their light microscopic appearance with assistance from immunoperoxidase methods. EM has been useful in characterizing small cell tumors of the female reproductive system and examples from the cervix and ovary are shown here. The observations on Paget's disease are of academic interest.

Small cell carcinoma of cervix

In a report of two cases, I drew attention to the existence of a small cell tumor of the cervix that differed ultrastructurally from squamous cell carcinomas.

> **Mackay B, Osborne BM, Wharton JT. Small cell tumor of cervix with neuroepithelial features. Ultrastructural observations in two cases. Cancer 43:1138-1145, 1979.**
> Two cases of small cell carcinoma of the cervix are reported. Both lacked squamous features, and EM showed neuroendocrine differentiation in the primary tumors and metastases of both cases.

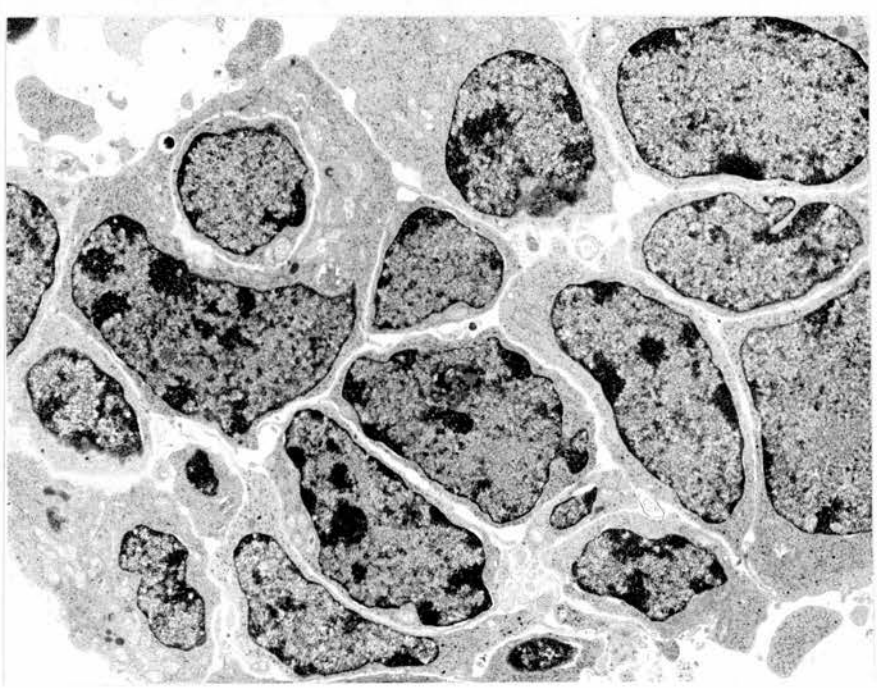

Figure 138. Small cell carcinoma of cervix. The tumor was composed of sheets of small cells with sparse cytoplasm. x 5,400.

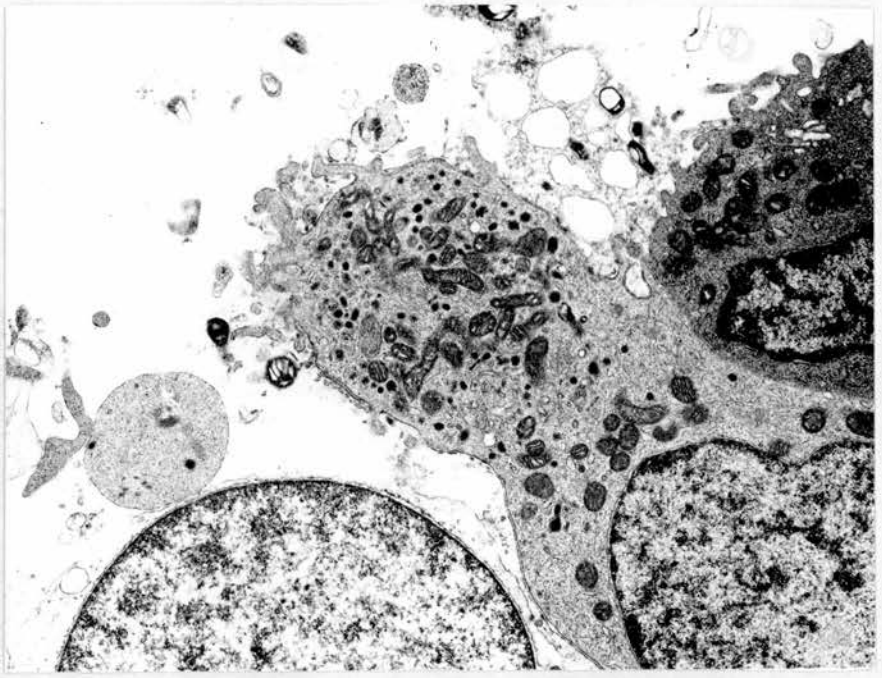

Figure 139. Same tumor as figure 138. The plane of section passes through the base of a cell process. x 8,700.

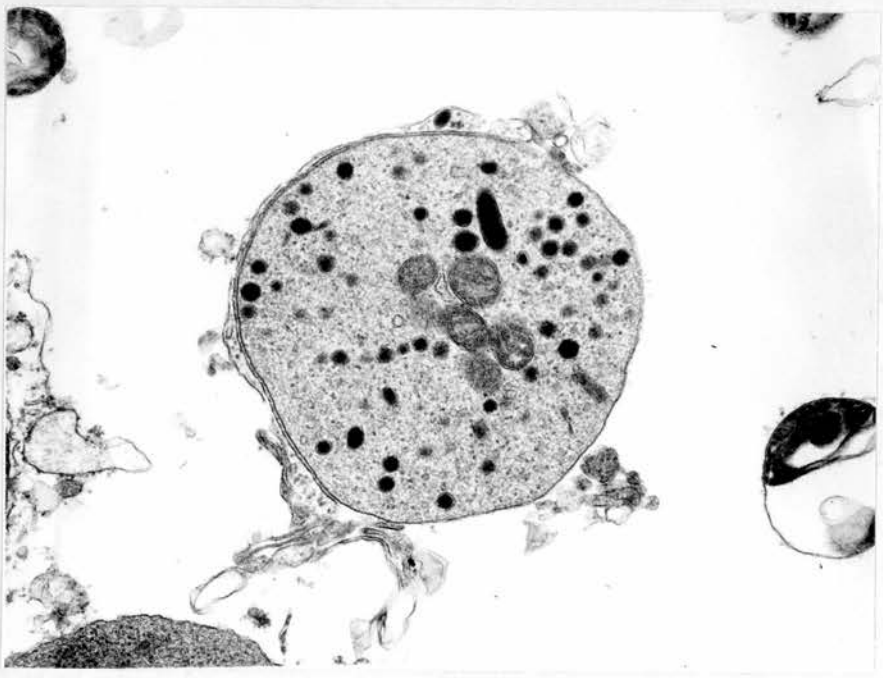

Figure 140. Same tumor as figure 138, showing granules in a cross-sectioned process. x 21,000.

Figure 141. Small cell carcinoma of cervix, metastatic in pancreas. x 4,900.

The neoplastic cells in the two cases we reported formed diffuse sheets devoid of architectural patterns in hematoxylin/eosin-stained sections. With EM, they were seen to have scanty cytoplasm and few organelles, but even when closely packed some appeared irregular, crescentic or even elongated because of the presence of dendritic processes (figure 138). It was not difficuilt to locate processes emerging from the cell bodies (figure 139) and small granules of neuroendocrine caliber were congregated within the processes (figure 140). Microtubules were present but sparse. In contrast to their abundance in processes, granules were infrequent in the cytoplasm of the cell body. These features were discernible in metastases though they were less developed and processes and granules were not always visible (figure 141).

Following the publication of this report, we identified other examples of small cell cervical carcinoma and some were combined with differentiated squamous cell or adenocarcinoma. Small cell undifferentiated carcinomas account for fewer than 5% of cervical carcinomas[204], and neuroendocrine features have been reported in cervical tumors that were considered poorly differentiated rather than undifferentiated[205]. One case of small cell neuroendocrine carcinoma of the cervix was associated with endocrine cell hyperplasia[206], and a cell line from a tumor contained neurosecretory granules and showed immunoreactivity for neuroendocrine markers[207]. This small cell tumor is different from tumors that have been called malignant carcinoids of cervix[208, 209]. Primary small cell carcinoma of the endometrium with neuroendocrine granules has also been reported[210].

The small round cell tumor of the ovary that occurs in young patients and is often associated with hypercalcemia does not possess neuroendocrine features. A case is illustrated below.

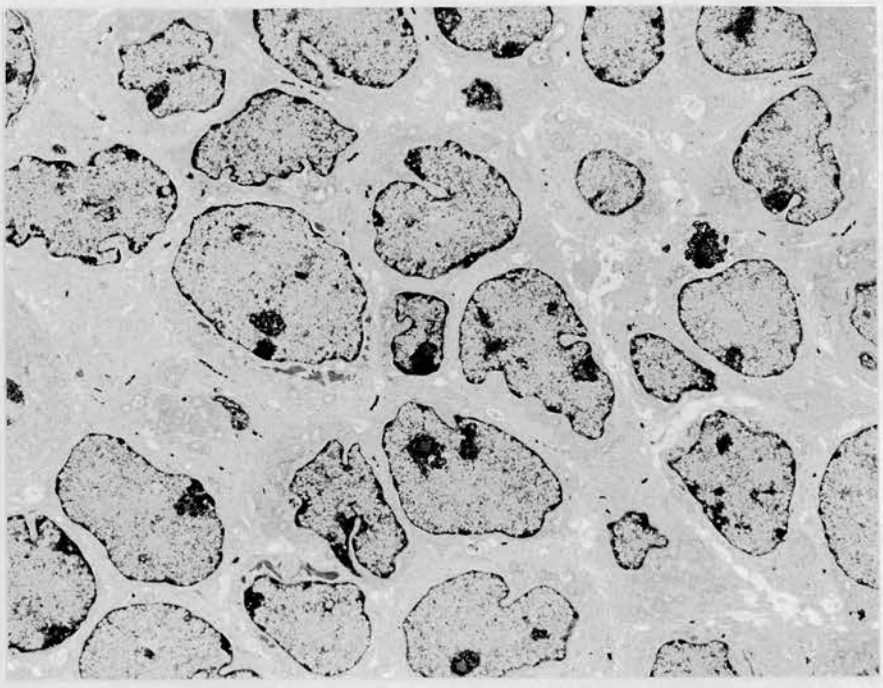

Figure 142. Small cell carcinoma of ovary in a 7-year-old girl. The cells have sparse cytoplasm and few organelles. x 3,800.

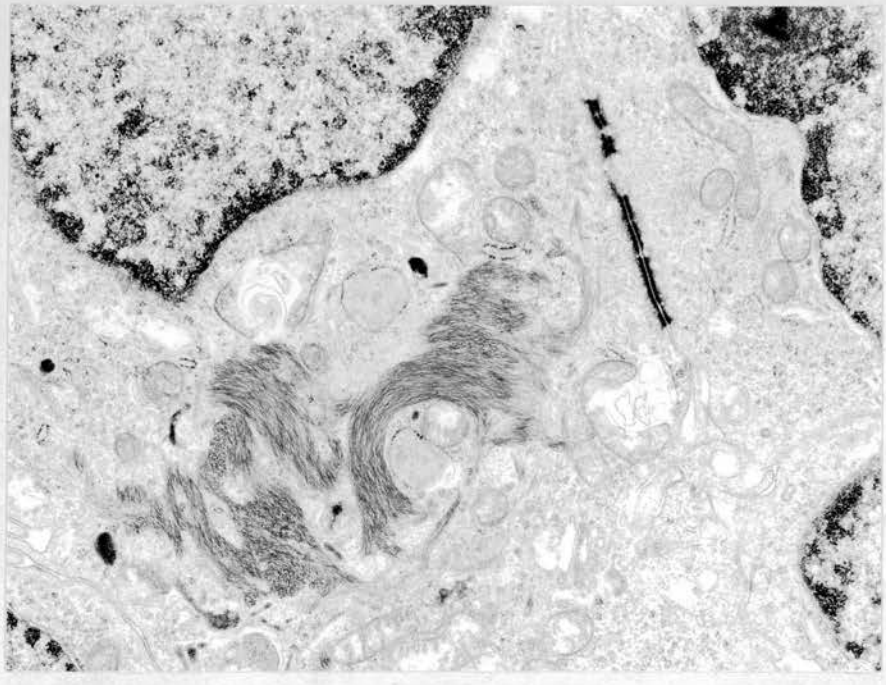

Figure 143. Small cell carcinoma of ovary. Same tumor as figure 142 showing desmosomes and filaments. x 10,200.

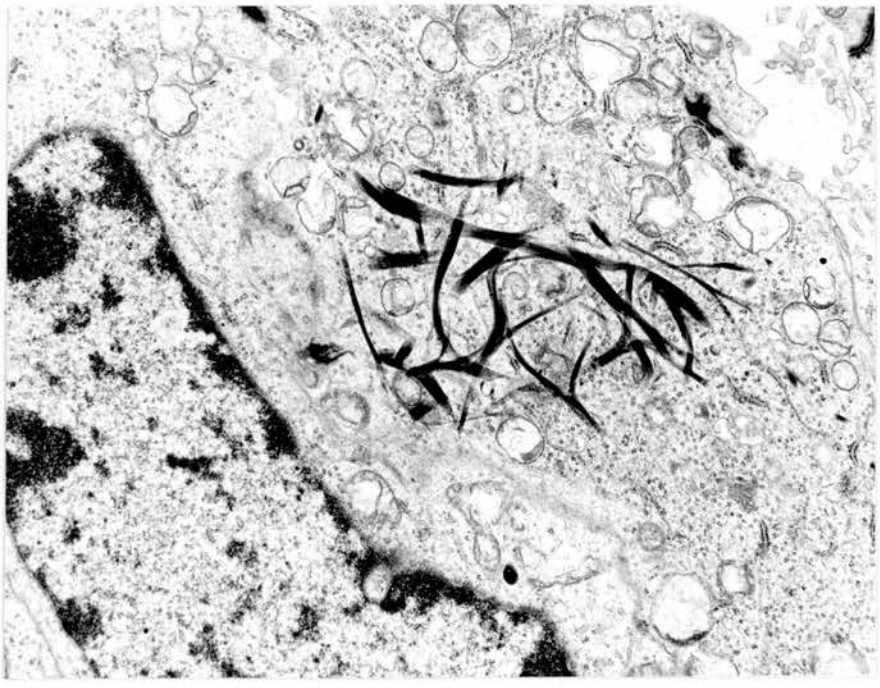

Figure 144. Small cell carcinoma of ovary. Same tumor as figure 143, from an inguinal lymph node metastasis. Small amounts of keratin were still evident. x 18,000.

The patient was a 7-year-old girl and the tumor presented as an inguinal mass and was at first thought to be Ewing's sarcoma. The EM findings were not compatible with this diagnosis and further investigation led to the detection of enlarged ovaries which were resected and were diffusely infiltrated by the same tumor. The small cells are closely packed and they have sparse cytoplasm, moderate amounts of granular endoplasmic reticulum, and somewhat irregular nuclei (figure 142), and they are connected by desmosomes with few or no tonofilaments (figure 143). Keratin filaments were present in tumor cells within the ovaries and in the metastasis (figure 144).

Since the first description of small cell carcinoma of the ovary with hypercalcemia in 1982, additional examples have been reported and a number of the tumors were studied with EM[211]. This tumor is the most common form of undifferentiated carcinoma of the ovary in women younger than 40 years and it has a poor prognosis. In addition to diffuse sheets of small cells, clusters, cords, follicles, and larger cells are sometimes seen[212, 213]. Hypercalcemia is absent in about one third of the cases[214]. If the patient is not hypercalcemic, it can be difficult to distinguish this neoplasm from other small cell tumors in the ovary including diffuse granulosa cell tumor and undifferentiated small cell carcinomas metastatic from other sites, but the tumor is diploid[215] and EM will add to the information obtained from the clinical presentation, light microscopy, immunohistochemistry[216, 217]. The histogenesis of this small cell carcinoma of the ovary is still undetermined.

Paget's disease of vulva

EM effectively documents the structural differences that exist between Paget's cells and normal vulvar epithelial cells.

Ordonez NG, Awalt H, Mackay B. Mammary and extramammary Paget's disease. An immunohistochemical and ultrastructural study. Cancer 59:1173-1183, 1987.

Twenty-one cases of Paget's disease were studied by light microscopy and EM. Eight tumors involved the nipple and 13 were extramammary, 11 of them vulvar and 2 anal. Paget's cells, regardless of their location, are adenocarcinoma cells. Intracytoplasmic mucin is scanty in the tumor cells in the nipple but typically plentiful in the extramammary locations where the cells frequently have a signet ring configuration. Paget's cells are usually large in comparison with the squamous cells, and they have a central, sometimes indented nucleus with several small nucleoli. Small granules can be found in some of the cells and microvilli are infrequently observed on the cell surface, particularly where adjacent cells enclose a cleft or lumen. Small desmosomes unite Paget's cells and similar small desmosomes are formed between Paget's cells and keratinocytes.

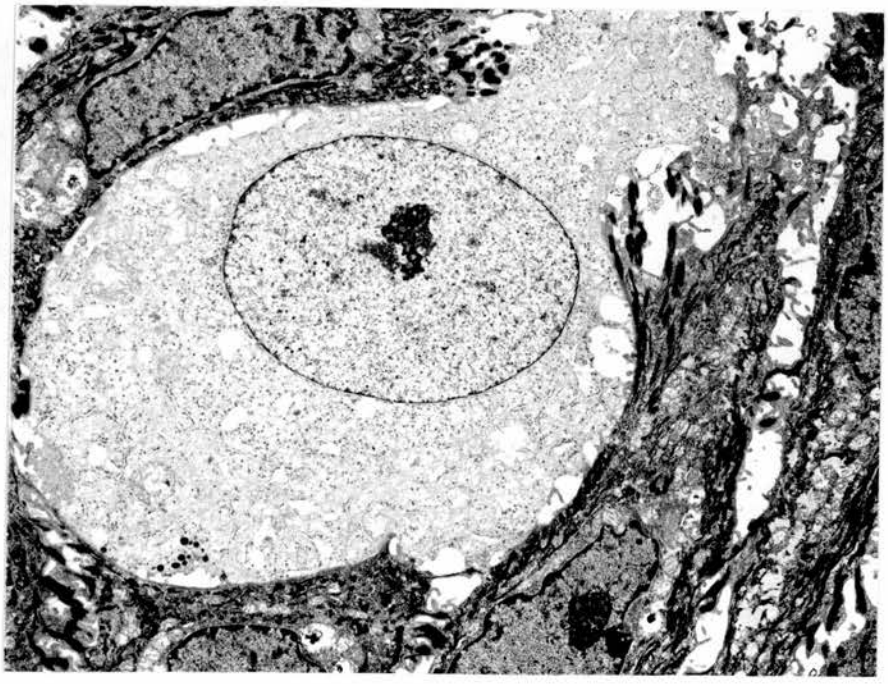

Figure 145a. Paget's disease of vulva. A neoplastic cell is surrounded by keratinocytes. x 4,300.

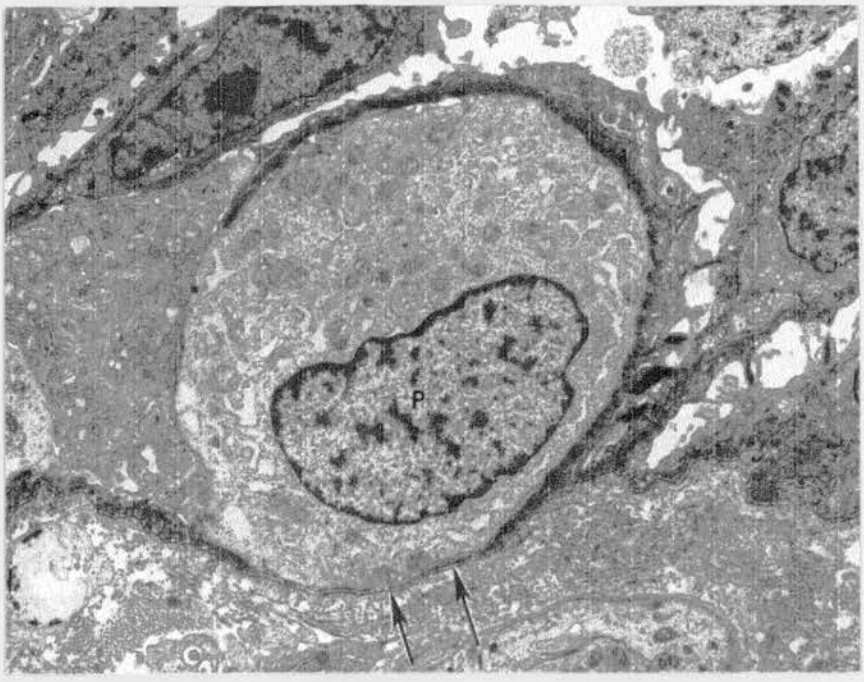

Figure 145b. Paget's disease of vulva. The tumor cell contacts the basal lamina. x 4,500.

Figure 146. Paget's disease of nipple. Small desmosomes have formed between a tumor cell (with lucent cytoplasm) and neighboring keratinocytes. x 13,000.

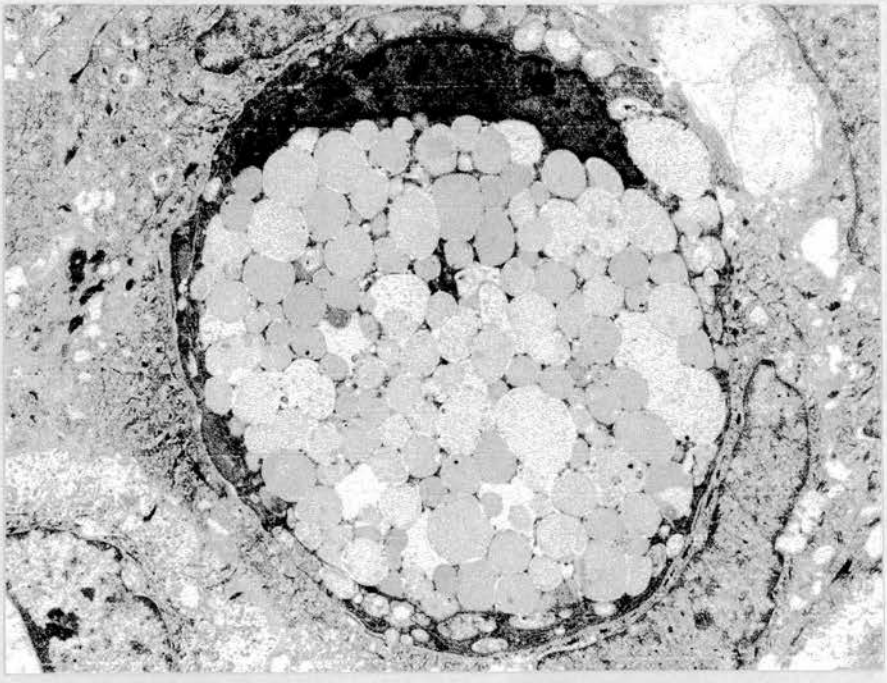

Figure 147a. Paget's disease of vulva. The tumor cell is filled with mucin droplets. x 6,100.

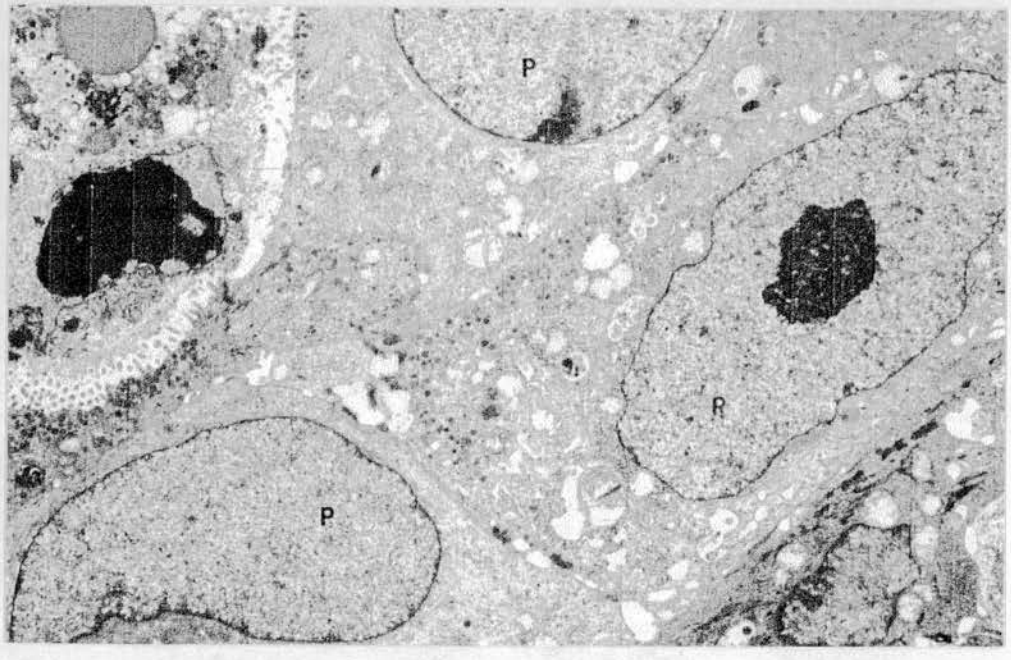

Figure 147b. Paget's cells border a small intraepithelial lumen containing debris. x 5,300.

Paget's cells look round in paraffin sections but they form tongues of cytoplasm that insinuate among the epidermal cells (figure 145a). The Paget's cells may rest directly on the basal lamina (figure 145b) without disupting it. Desmosomes that are present between Paget's cells are small with short tonofilaments, and similar small desmosomes form between Paget's cells and neighboring keratinocytes, in contrast to the larger desmosomes that connect keratinocytes to one another (figure 146). In specimens from the vulva, the Paget's cells may be filled with mucin droplets giving them a signet-ring shape (figure 146). Occasionally a small lumen is formed, bordered by cells with tight junctions and irregular microvilli (figure 147b). Keratin filaments are scanty or absent in the Paget's cells in contrast with their abundance in the surrounding keratinocytes.

It is widely believed that Paget's disease of the nipple results from involvement of the epidermis by tumor cells that have migrated from a carcinoma in the underlying breast, but the cell of origin of extramammary Paget's disease is more controversial since an underlying carcinoma often can not be identified. In five of our six mammary cases, only intraductal carcinoma was found. The sixth patient had a 6.5 cm carcinoma with axillary metastases. In two of the extramammary cases which were involving the anal canal, a rectal adenocarcinoma smaller than 2 cm, with invasion confined to the submucosa, was located at the anorectal junction and there was no documented evidence of metastases. One of the carcinomas contacted the proximal anal epithelium and a transition to signet ring Paget's cells was seen at this site. Paget's cells appear to be uniquely epidermotropic[218], spreading laterally within the epidermis while the deepest cells hug the basal lamina without showing an obvious tendency to breach it. The formation of desmosomes between Paget's cells and adjacent keratinocytes implies permanence, but desmosomes can be formed and dissolved rapidly and the small size of the tumor cell desmosomes indicates that the Paget's cells are taking the initiative in their creation. These intercellular connections should not impede migration of the cells within the epidermis and might even facilitate it by providing fulcrums for cell movement.

Tumors of the endocrine system

Tumors discussed in this sections are pituitary adenomas, small cell carcinoma of thyroid, and tumors of the adrenal cortex and medulla.

Pituitary adenoma

Granule-containing endocrine cells in tumors have the same basic fine structure with occasional distinctive features: this is briefly illustrated with adenomas of the anterior pituitary.

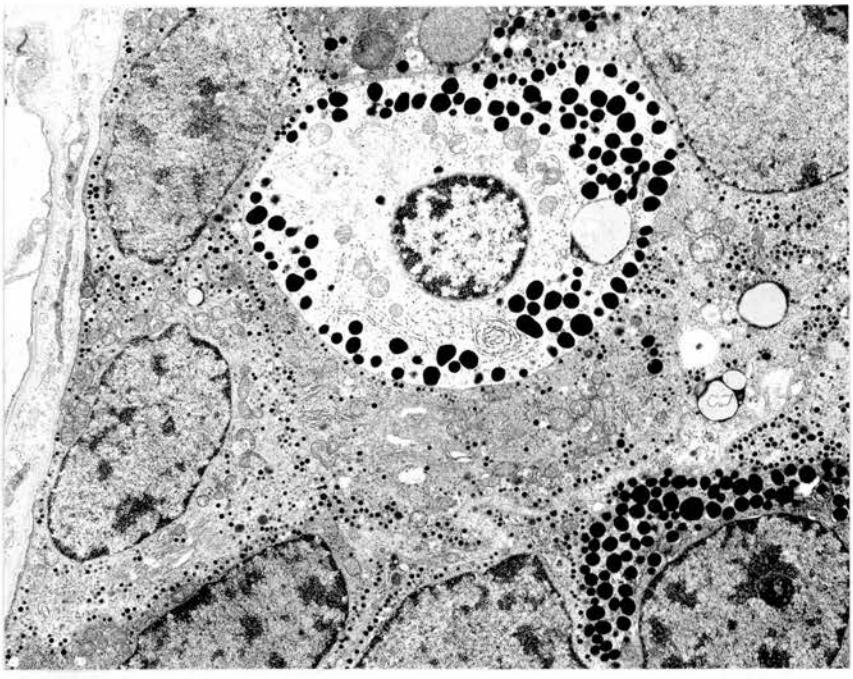

Figure 148. Anterior pituitary, normal parenchyma. The presence of different cell types is evident from the variation in granule size. x 4,900.

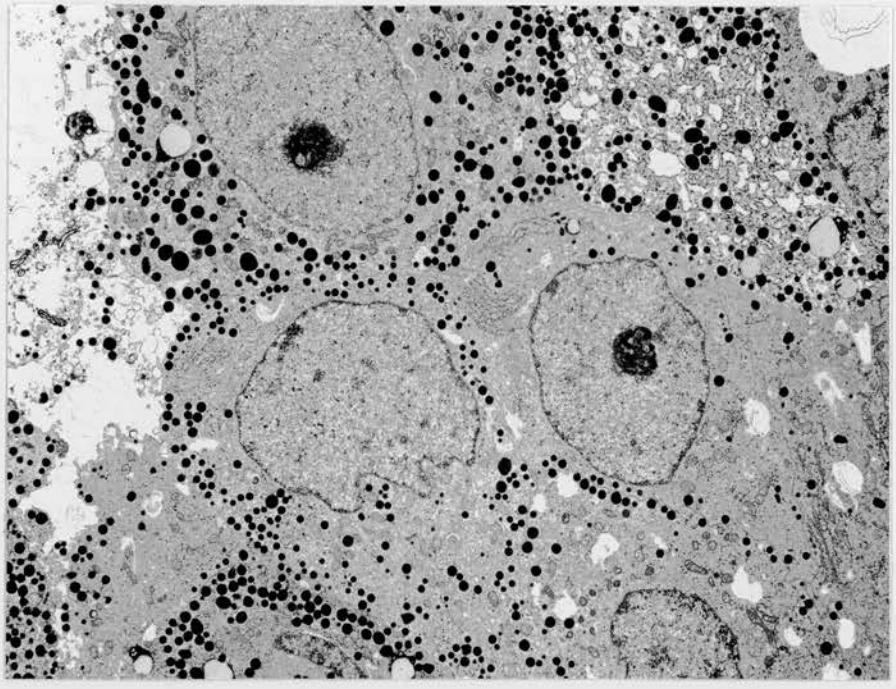

Figure 149. Pituitary adenoma producing growth hormone. The granules fall within a fairly narrow range of diameters. x 5,400.

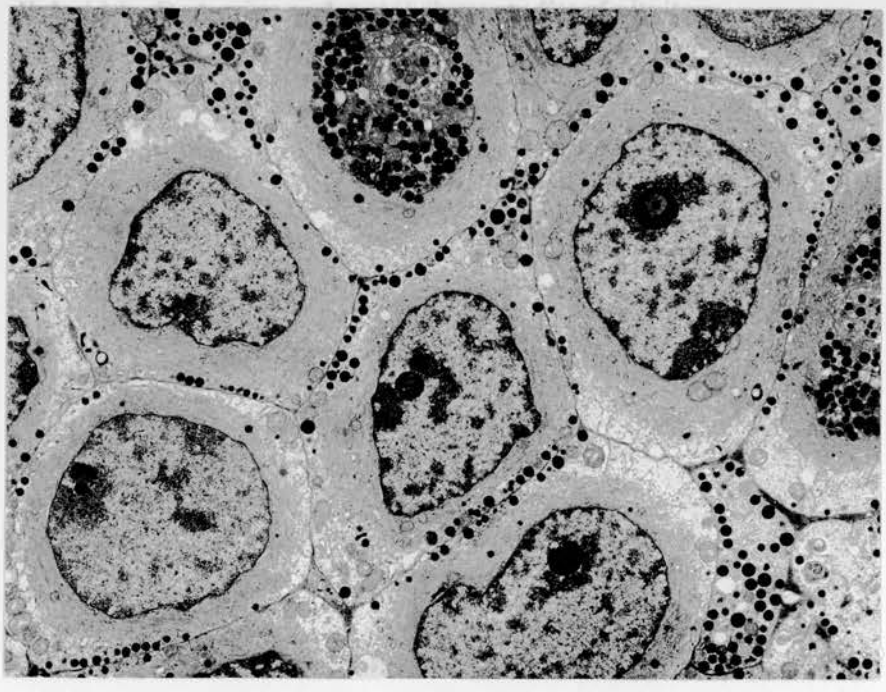

Figure 150a. Pituitary adenoma showing Crooke's change. A concentric band of filaments surrounds the nucleus and granules are at the cell periphery. x 6,300.

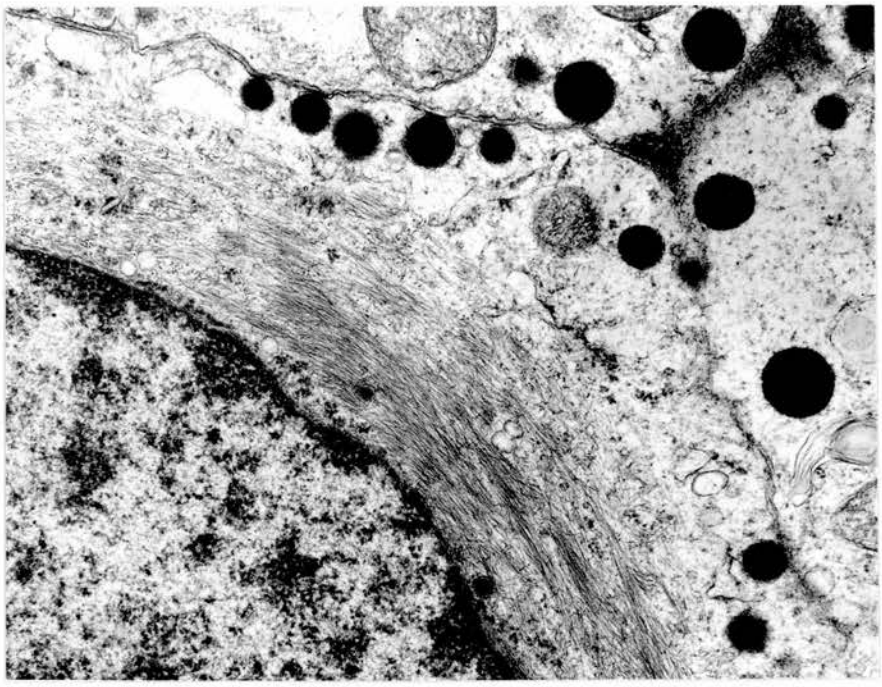

Figure 150b. Same tumor as figure 151 showing the filaments in greater detail. x 17,000.

Samaan NA, Osborne BM, Mackay B, Leavens ME, Duello TM, Halmi NS. Endocrine and morphologic studies of pituitary adenomas secondary to primary hypothyroidism. Journal of Clinical Endocrinology and Metabolism 45:903-911, 1977.
Two patients, one male and one female, with enlarged pituitary fossae had high TSH concentrations before and after stimulation with TRH. After pituitary surgery, the serum TSH levels diminished but remained abnormally high and were suppressed by administration of thyroid hormone. Both tumors were pituitary adenomas. In the female patient, suprasellar extension had occurred.

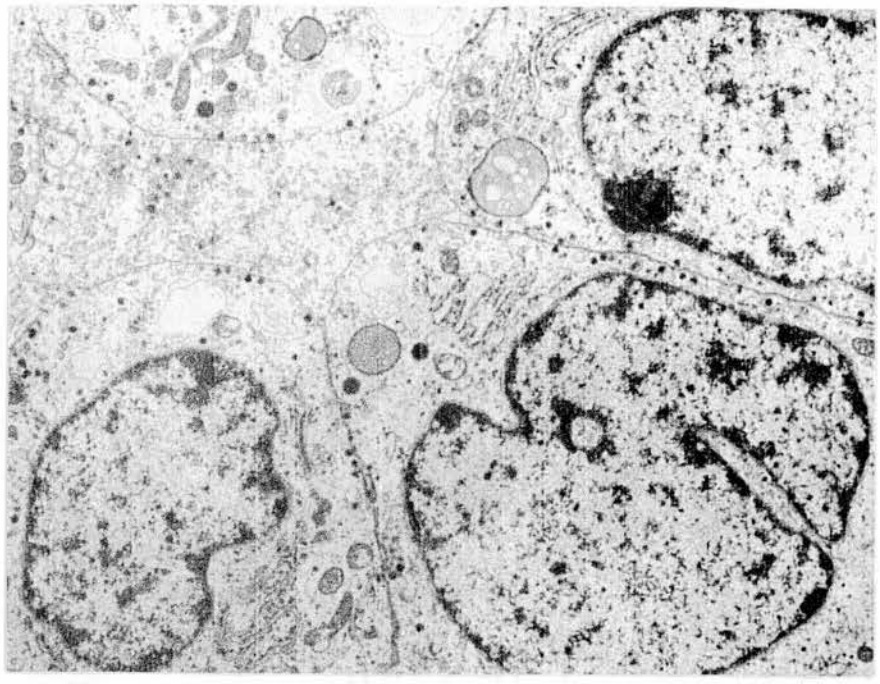

Figure 151a. TSH-producing adenoma from a 58-year-old male. x 6,800.

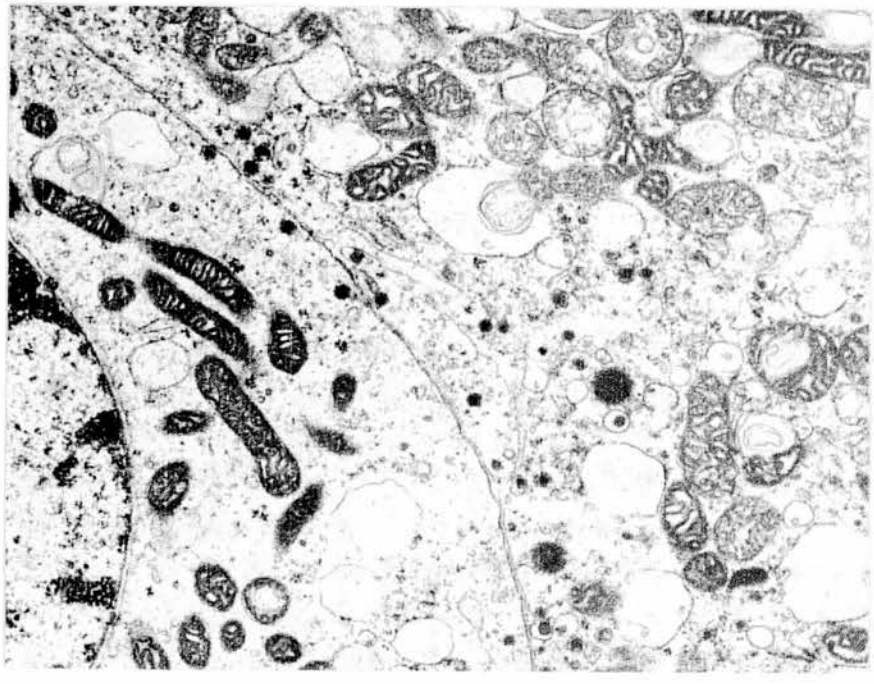

Figure 151b. TSH-producing adenoma from a 55-year old female. x 18,000.

The tissue in figure 148 was designated pituitary adenoma but the small portion taken for EM showed well preserved architecture with obvious variation in the size of the cytoplasmic granules from cell to cell. This part of the specimen was thus normal anterior pituitary parenchyma. A typical adenoma is shown in figure 149: the tumor was producing growth hormone and the cells contain numerous granules that fall within a narrow range of diameters throughout the tissue. In Crooke's change (figure 150a), the granules are similar in caliber to those in the previous figure, but they are not as numerous and are confined to the peripheral cytoplasm because the more central part of the cell is occupied by a perinuclear zone of concentric filaments (figure 150b). Crooke's hyalinization occurs in inhibited corticotrophs[219] and is seen in a minority of the corticotroph adenomas associated with Cushing's disease. In the rare TSH-producing adenoma (figures 151a and b), granules are small and few and they group underneath the cell membrane. Occasionally a granule is found outside the cell in a pituitary adenoma and extrusion of granules into the extracellular space, so-called misplaced exocytosis, is a feature of lactotrophs. Granules are often sparse in clinically non-functioning adenomas[220]. Oncocytic change can occur in a pituitary adenoma although it is in my experience uncommon, and the profusion of mitochondria displaces and obscures the granules[221]. The value of correlated immunohistochemistry and electron microscopy in the investigation of pituitary tumors has been stressed[222, 223], and the secretory products of a pituitary adenoma are often indicated by the ultrastructure, but immunohistochemistry is usually relied on to determine the functional properties of the cells. Monomorphous pituitary adenomas expressing several hormones by immunohistochemistry are common, whereas adenomas displaying multiple immunoreactivities and consisting of more than one morphologic cell types are rare[224].

Small cell carcinoma of thyroid.

> **Luna MA, Mackay B, Hill CS, Hussey DH, Hickey RC. Malignant small cell tumor of the thyroid. Ultrastructural Pathology 1:265-270, 1980.**
> A 46-year-old male presented with a large mass in the lower anterior neck that had grown rapidly over a three month period. There was clinical evidence of paralysis of the right vocal cord, the trachea was deviated to the right, and a superior vena caval syndrome was present. The mass could not be resected. Radiotherapy produced radiological evidence of regression but the tumor recurred locally and again grew rapidly.

Figure 152. Small cell carcinoma of thyroid. Cell junctions are barely visible at this low magnification. The field contains one small lumen. x 4,800.

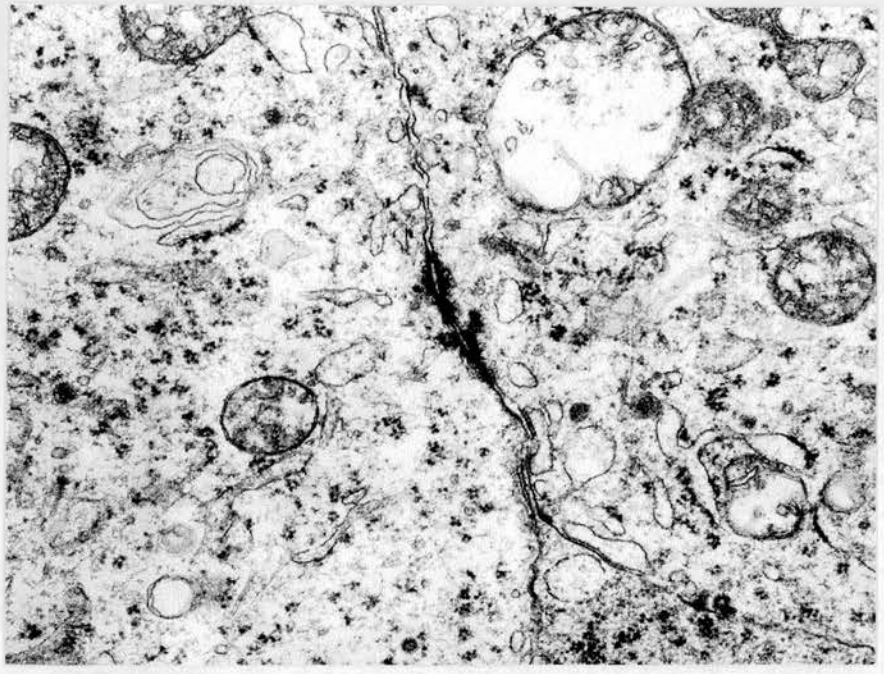

Figure 153. Same tumor as figure 152. The cell junctions were scattered and primitive in construction. x 21,000.

The combination of nuclei with smooth profiles, closely apposed cell surfaces, and sparse cytoplasm containing moderate numbers of organelles (figure 152) does not suggest a defined type of lymphoma, and cells are connected by cell junctions although they are primitive (figure 153). Clinically, the tumor was thought to be arising within the thyroid and it recurred locally without evidence of tumor elsewhere. The cells were small and they formed diffuse sheets so from the pathology findings it was labeled a small cell carcinoma of the thyroid. This case was accessioned before immunohistochemistry was available, and the prevailing view at the time was that a small cell tumor of the thyroid must be a lymphoma. The following quote is from 1985: "Undifferentiated small-cell carcinoma is a term to be discarded. Nearly all tumors so designated in the past are malignant lymphomas, small-cell variants of medullary carcinomas, or poorly differentiated (insular) carcinomas."[225, 226] There were no granules or dendritic processes to suggest a small cell variant of medullary carcinoma[227]. Study of many sections by light microscopy eventually revealed small foci of differentiated thyroid carcinoma.

Adrenal cortical carcinoma

Carcinomas of the adrenal cortex are often difficult to diagnose, particularly once the tumor has extended from the primary site. They can resemble other upper abdominal neoplasms including liver cell carcinoma, and EM is often helpful in their identification despite the complexity and variety of the ultrastructure of hepatic and adrenocortical neoplasms.

> **Silva EG, Mackay B, Samaan NA, Hickey RC. Adrenocortical carcinomas. an ultrastructural study of 22 cases. Ultrastructural Pathology 3:1-7, 1982**
> This report detailed the range of appearances seen by EM in 28 specimens of adrenocortical carcinoma from 22 patients. The distinctive features of steroid-forming cells were only present in some cells of some of the cases. Sequential specimens (up to four) from the same patient demonstrated marked changes in the tumor cell morphology as the disease progressed, including accumulation of cytoplasmic glycogen.

The distinctive ultrastructural features of steroid forming cells are smooth endoplasmic reticulum which commonly forms slender anastomosing tubules, and mitochondria with tubulo-vesicular cristae. These structural specializations were present in the majority of cells in only 13 of the 22 cases in our first study, and one or both might be seen in a particular tumor. Large mitochondrial matrical granules measuring up to 300 nm were present in several cases but were confined to scattered cells and to occasional mitochondria within these cells. In three tumors, all non functioning, larger granules were present in the cytoplasm. Lipid vacuoles were seen in significant numbers in only nine of the carcinomas. Lysosomes were found in cells in most of the tumors but were never numerous. In ten tumors, the cytoplasm of most of the cells contained numerous organelles, while a moderate number were present in eight cases, and they were scanty in the remaining four tumors. In one patient, four accessions were obtained over a period of years and they revealed a reduction in the number of organelles, diminution or loss of smooth endoplasmic reticulum and tubular mitochondrial cristae, and increase in the number of cytoplasmic lipid droplets and quantity of glycogen.

Some of these features are shown in the figures that follow. The cells are typically large with extensive cytoplasm that is often filled with organelles (figure 154a), but a marked contrast between neighboring cells is a common finding (figure 154b), and granular

endoplasmic reticulum can always be seen, often as stacks of short cisternae. Smooth-surfaced endoplasmic reticulum may form slender tubules or larger vesicles (figure 154c). Extensive zones of cells are sometimes occupied by a branching network of tubules (figure 155a), and the smooth reticulum occasionally forms concentric whorls that encircle small groups of mitochondria (figure 155b). The occurrence of crystalline aggregates within cisternae of granular endoplasmic reticulum is unusual (figure 156). The tumor in figure 157 had metastasized to the lung where the cells had a clear appearance by light microscopy and were filled with glycogen. Some adrenal cortical carcinomas are oncocytic (figure 158). While the mitochondria often have tubular cristae (figure 159), their frequency varies from cell to cell and in some tumors only the usual shelf-like cristae are seen.

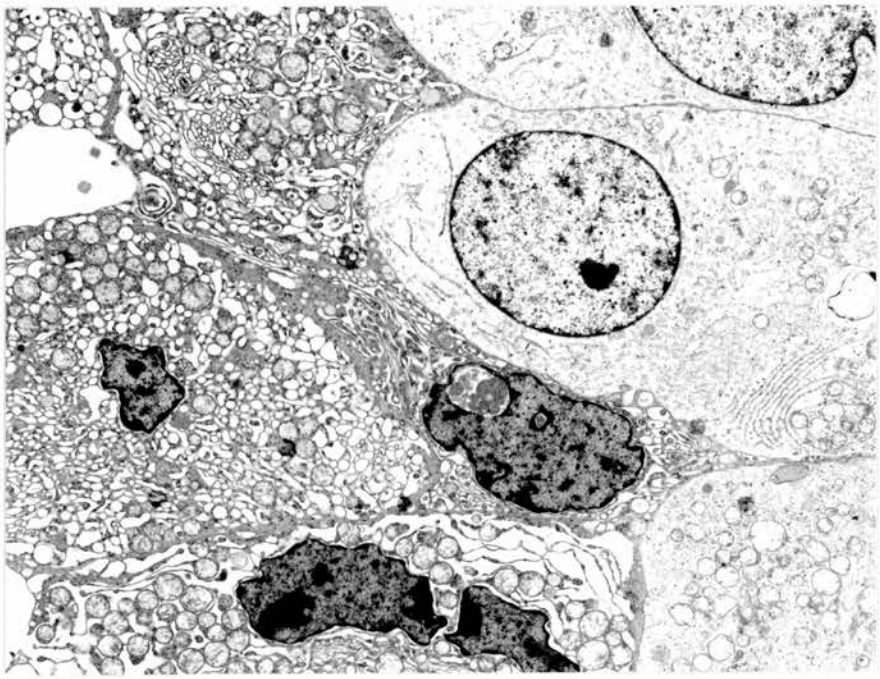

Figure 154a. Adrenal cortical carcinoma. There is a striking difference in the numbers of organelles among the tumor cells. x 6,200.

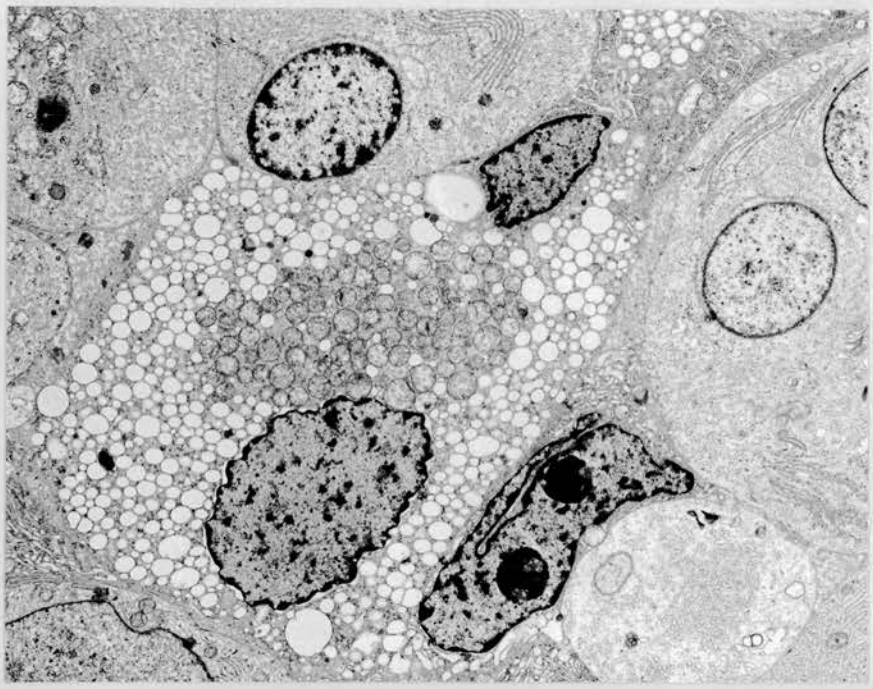

Figure 154b. Same tumor as figure 154. The central cell contains many smooth-surfaced vesicles while the surrounding cells have stacks of granular endoplasmic reticulum. x 8,400.

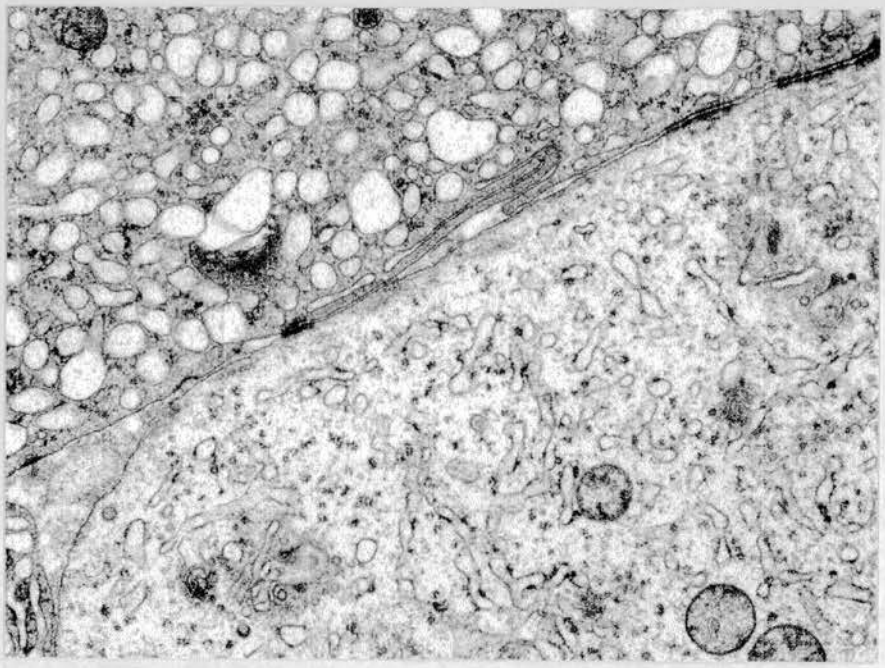

Figure 154c. Same tumor as figure 154 detailing the contrast between the slender tubules of predominantly smooth-surfaced endoplasmic reticulum and the larger vacuoles in the adjacent cell. Primitive cell junctions are present. x 14,600.

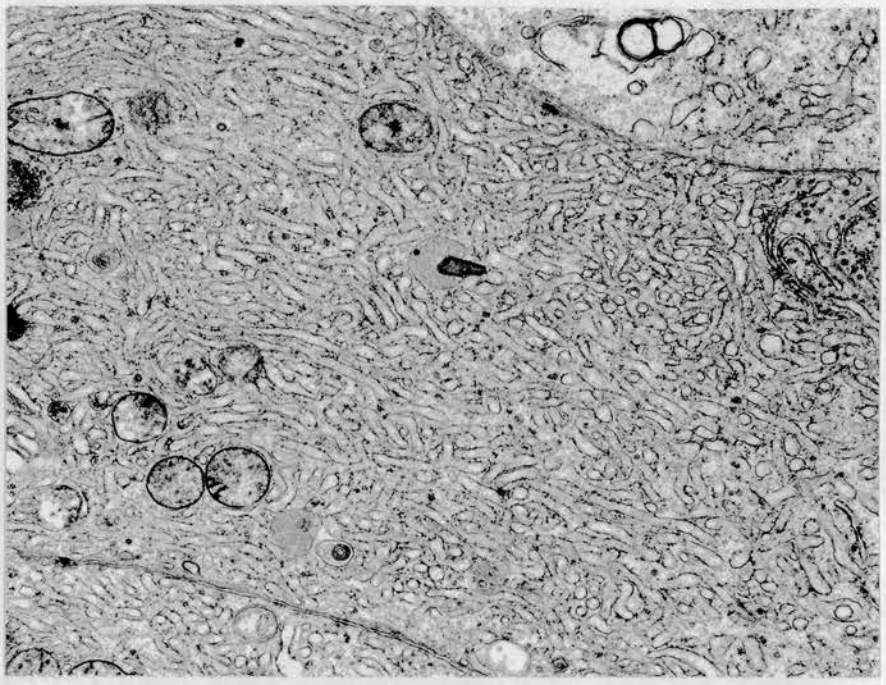

Figure 155a. Adrenal cortical carcinoma. The cell contains extensive tubules of smooth endoplasmic reticulum. x 11,200.

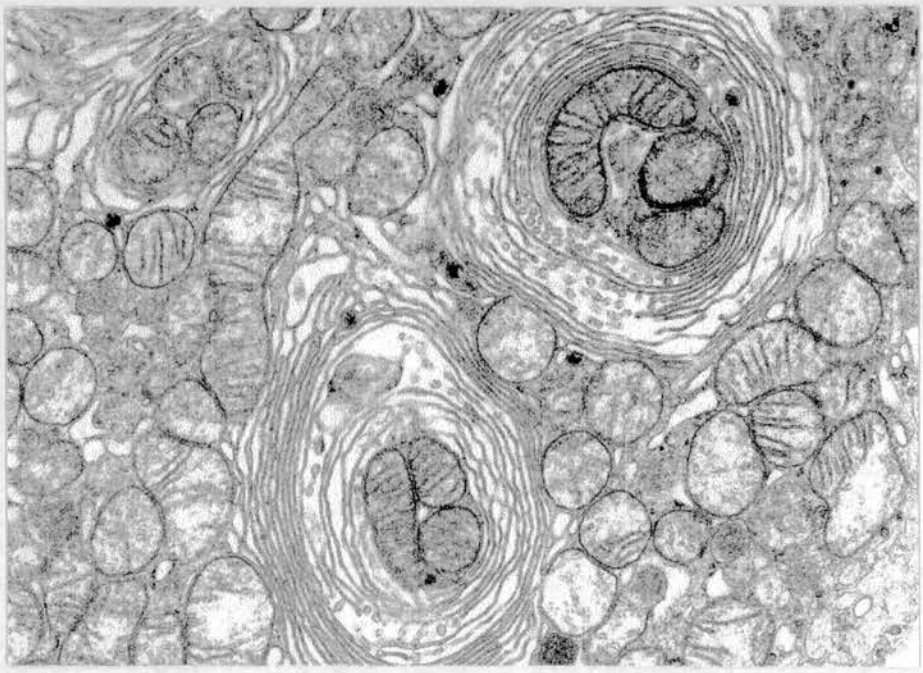

Figure 155b. Adrenal cortical carcinoma. Tubules of smooth endoplasmic reticulum encircle small groups of mitochondria. Much of the cytoplasm of the cell was occupied by mitochondria. x 17,500.

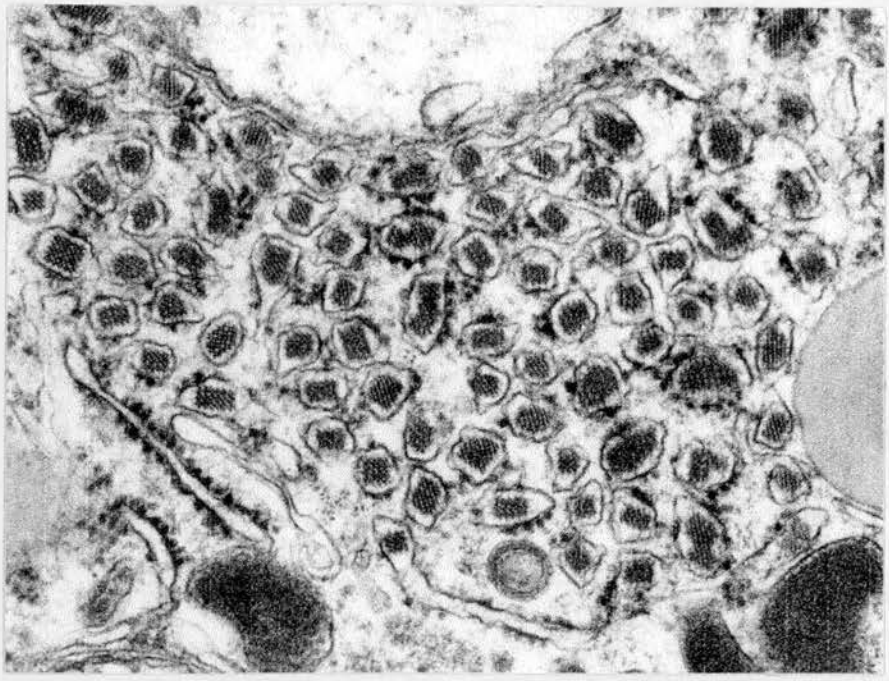

Figure 156. Adrenal cortical carcinoma cell with unusual crystalline aggregates in cisternae. x 19,000.

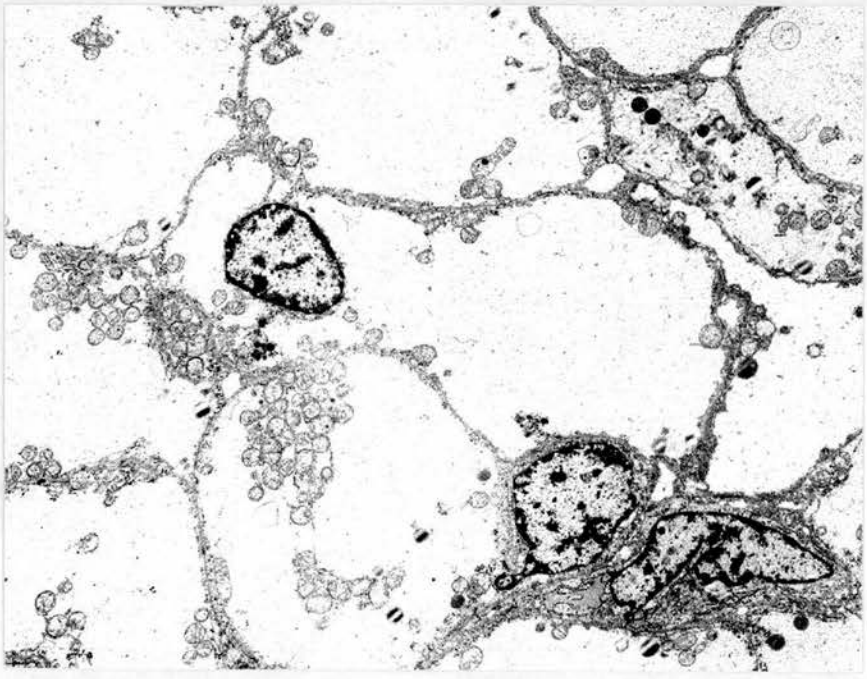

Figure 157. Adrenal cortical carcinoma, metastatic in lung. The cells contain large amounts of glycogen. x 3,800.

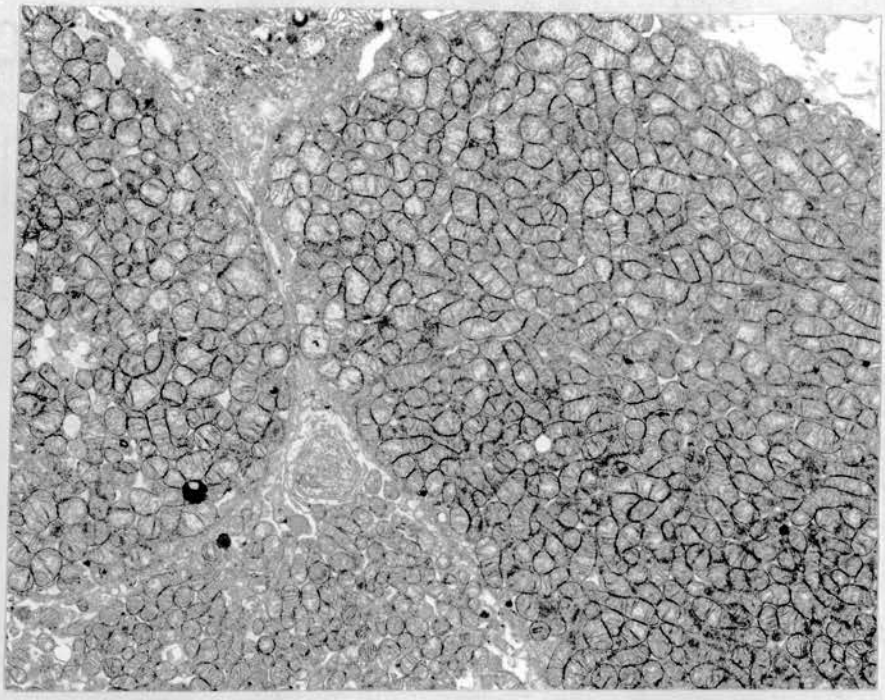

Figure 158. Adrenal cortical carcinoma. The tumor was composed of mitochondrion-rich cells. x 12,400.

Figure 159. Adrenal cortical carcinoma. The mitochondria have tubular cristae. x 17,000.

Mackay B. el-Naggar A. Ordonez NG. Ultrastructure of adrenal cortical carcinoma. Ultrastructural Pathology 18:181-190, 1994.
Additional cases brought the total of adrenocortical carcinomas to 30 and this study included comparison with adrenocortical adenomas, hyperplasias, and normal adrenal cortices. A broad range of ultrastructural appearances was seen among the carcinomas but the differences were mainly in the amount of cytoplasmic lipid, number of lysosomes, and quantity and architecture of the mitochondria and endoplasmic reticulum. Structural variants included tumors with lipid-rich, oncocytic, and glycogen-rich cells.

There were close similarities at the ultrastructural level between cells of the normal adrenal cortex and the hyperplastic and adenomatous glands. In hyperplasia, the tendency was for the cells to form diffuse sheets in which the closely apposed cells were intimately related to interspersed thin-walled vascular channels. The hyperplastic cells were often much larger than normal cortical cells but organelles were similar in appearance and usually also in their relative proportions. Mitochondrial cristae were tubulo-vesicular in most of the cells although sometimes they were small and inconspicuous. A number of the mitochondria contained large, round, dense inclusions comparable in size and appearance to those seen in oncocytic renal tumors. Lipid droplets were present in every cell and large lysosomes with angular and irregular profiles were common. Large cells were characteristic of hyperplasias but they were not a feature of the adenomas: the latter were composed of alveolar and cord-like formations alternating with nodules of closely packed cells. The organelles in the adenomas were however similar to those seen in the hyperplasias although there was more variation in their relative proportions. Some adenomas contained moderate numbers of mitochondria but no adenoma was truly oncocytic. The tubular cristae in mitochondria in the adenomas were often striking. Dense bodies, presumed to be lysosomes, were common in the perinuclear cytoplasm. Overall there was distinctly less lipid in the adenomas compared with the hyperplasias and normal glands. Tubules of smooth endoplasmic reticulum could always be found and they were generally slender and mixed with the other organelles. Two adenomas were composed of clear cells with abundant glycogen.

Approximately one third of the carcinomas failed to show convincing ultrastructural evidence of steroid cell differentiation. Lumens when present were narrow slits containing a few irregular short microvilli. In one third of the carcinomas, the mitochondria had the usual shelf-like cristae and large matrical densities were common. Smooth endoplasmic reticulum was conspicuous in some cells in two thirds of the carcinomas. All of the tumors contained ribosome-bearing cisternae which were often clustered in stacks. Different patterns of smooth endoplasmic reticulum were seen, ranging from slender tubular cisternae forming a loose branching network to larger more closely packed cisternae, vacuoles or concentric whorls. There did not appear to be a constant relationship between mitochondria with tubular cristae and smooth endoplasmic reticulum and one or the other usually predominated or was independently present. The slender rods within cisternae (figure 156) were only seen in one tumor. While adenomas can sometimes be related in their ultrastructure to zones of the normal cortex, this is not consistently feasible with the carcinomas, although a tumor with small cells and lamellar cristae may suggest the zona glomerulosa, larger cells with abundant lipid will recall the zona fasciculata, and smaller cells with less lipid but typical mitochondria can be reminiscent of the zone reticulata. Such a comparison has little practical value because cells of the zona fasciculata transform to those of the zona reticulata under the influence of corticotropin. We did not see convincing endocrine granules in any of the tumors. Five of the 30 carcinomas in this study contained many mitochondria with dense matrical inclusions. Intracytoplasmic crystalloids are a rare occurrence in tumors of the adrenal cortex[228]. None of the tumors which we studied contained spironolactone bodies[229]. (Kuramoto 85).

El-Naggar AK, Evans DB, Mackay B. Oncocytic adrenal cortical carcinoma. Ultrastructural Pathology 15:549-556, 1991.
An adrenocortical carcinoma was composed of mitochondrion-rich cells. The patient was a 56-year-old man who presented with acute abdominal pain. A CT scan revealed a 10 cm mass in the vicinity of the right adrenal gland. The tumor was invading the inferior vena cava and the liver but radical resection was achieved. The cells contained condensed zones and loose whorls of smooth endoplasmic reticulum, and crystalline matrical inclusions were present in some of the mitochondria while others contained round, homogeneous, dense matrical inclusions. Flow cytometry revealed a hyperdiploid cell line with a DNA index of 1.3.

This tumor is illustrated in figure 158. The adrenal gland is an unusual location for an oncocytic neoplasm[230]. The tumors have been called oncocytomas when they appeared to be nonfunctioning without evidence of recurrence or metastases: however, Sasano et al[231] were suitably guarded in presenting this conclusion in their report of three cases. Nguyen et al[232] found seven case reports in the literature and added a benign oncocytoma arising from retroperitoneal heterotopic adrenocortical tissue. I have seen two examples of oncocytic retroperitoneal neoplasms, both confirmed by EM, in patients without evidence of tumor in other locations, and I surmised but could not prove that they had arisen from ectopic adrenal cells. Although the majority of oncocytic endocrine tumors are benign, malignant examples include some Hurthle cell and salivary gland carcinomas. The tumor we report was infiltrating the inferior vena cava and liver and it was hyperdiploid. The reason for oncocytic transformation in cells has not been completely explained but the fact that the structure of the mitochondria is well maintained indicates that it is not a degenerative process. It has been described as a redifferentiation of the cells as they attempt to increase their output of high energy phosphate[233]. Many of the mitochondria in the virilizing oncocytic adrenal cortical adenoma reported by Erlandson[234] had tubulovesicular cristae and the smooth endoplasmic reticulum and golgi apparatus were well developed.

Katz RL, Patel S, Mackay B, Zornoza J. Fine needle aspiration cytology of the adrenal gland. Acta Cytologica 28:269-282, 1984.
Eight of the specimens obtained by fine needle aspiration biopsy from 22 patients with radiological evidence of an adrenal mass were studied by EM to evaluate the utility of ultrastructural study as an adjunct to routine light microscopic evaluation of the smears prepared from the fine needle aspiration.

Given good material and with skilled interpretation, fine needle aspiration biopsies (FNA) are an effective method with which to evaluate adrenal masses. In this study, my cytology colleagues found that the overall sensitivity of FNA in detecting the presence of malignancy was 85% while the number of patients correctly classified for all adrenal masses was 90%. The test was 100% specific for malignant lesions. In 15 of the patients, silent adrenal lesions were detected during radiologic surveys for metastatic disease and 53% had benign adrenal lesions treatable with a conservative approach. Features revealed by EM confirmed three of the four cases of adrenocortical carcinoma, two neuroblastomas, and three tumors metastatic to the adrenal gland.

Pheochromocytoma

The unique appearance of the cytoplasmic granules in pheochromocytoma prompted the following study. The morphometry was performed by Dr. Gomez.

Gomez RR, Osborne BM, Ordonez NG, Mackay B. Pheochromocytoma. Ultrastructural Pathology 15:557-562, 1991.
Fifty intra-adrenal and extra-adrenal neoplasms were studied to assess granule type and diameter. Twenty-seven of the tumors had been diagnosed by light microscopy as pheochromocytomas and most were intraadrenal tumors. Twenty-three had been called paragangliomas and these were extraadrenal neoplasms in various sites. In twenty of the pheochromocytomas and one paraganglioma, there was a clear predominance of granules with eccentric dense cores. One pheochromocytoma and 20 paragangliomas had only round granules with uniform round dense cores.

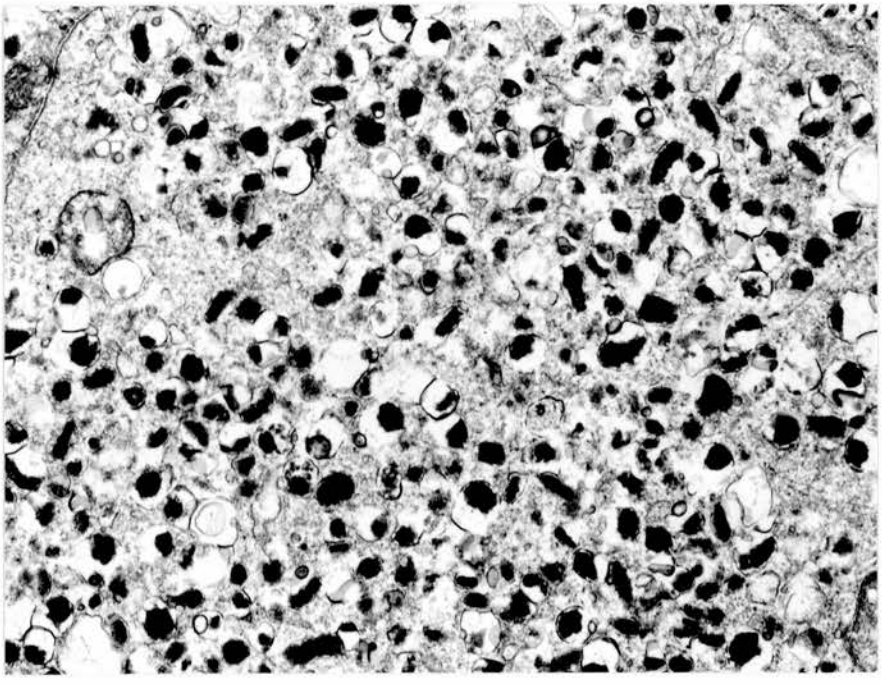

Figure 160. Pheochromocytoma, The cytoplasm of the tumor cell has a moth-eaten appearance at this magnification. x 9,800.

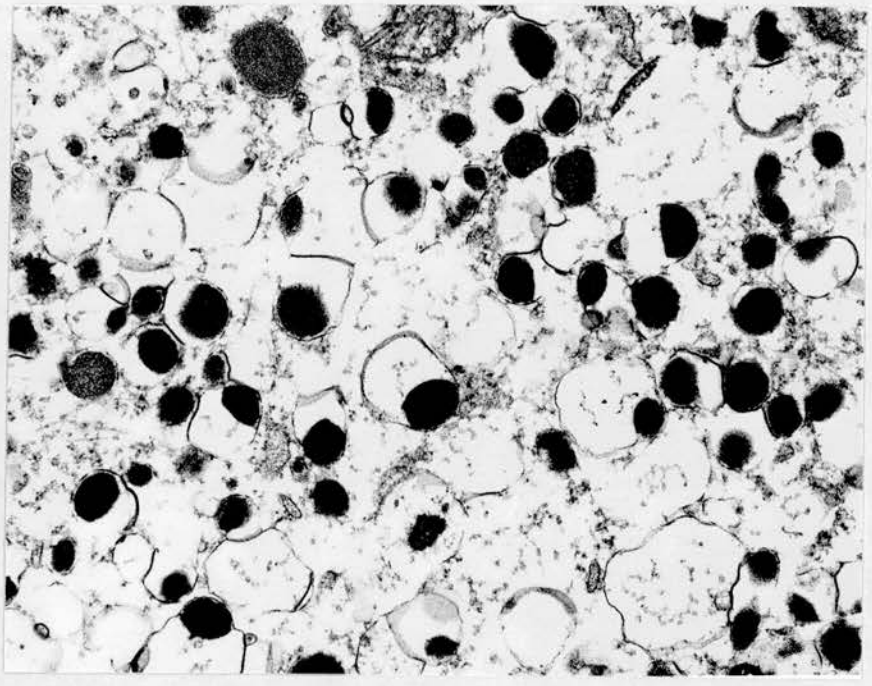

Figure 161. Same tumor as figure 160. The eccentric location of many of the dense cores is evident. x 32,000.

The cytoplasmic granules in adrenal pheochromocytomas were predominantly ovoid with loose-fitting membranes and eccentrically-positioned dense cores. The above study was prompted by the observation that similar granules were present in a recurrent tumor involving the organ of Zuckerkandl, suggesting that this tumor should be designated an extraadrenal pheochromocytoma rather than a paraganglioma. The irregular spaces in a pheochromocytoma cell give the impression at low magnification that the tissue has been poorly preserved (figure 160) but at higher power the spaces are seen to be within the secretory granules, and the appearance is produced by the peripheral location of the dense core within an ovoid limiting membrane (figure 161).

The terms pheochromocytoma and paraganglioma are often used loosely and even interchangeably, but some pathologists and clinicians reserve the designation of pheochromocytoma for a tumor of the adrenal medulla in a patient who presents with a syndrome of alpha and beta- adrenergic receptor stimulation due to secretion of epinephrine and norepinephrine. The term paraganglioma is usually applied to an extraadrenal neoplasm. A neoplasm arising from paraganglia that is associated with clinical evidence of catecholamine production may be termed an extraadrenal pheochromocytoma. Capella et al[235] observed a distinction between the two tumors and stated that tumors arising from the adrenal or extraadrenal chromaffin tissue are designated pheochromocytomas whereas tumors arising from nonchromaffin parasympathetic-related organs including chemoreceptors are termed nonchromaffin paragangliomas. An extraadrenal tumor may contain granules identical in appearance to those of an adrenal pheochromocytoma and we have seen examples in the urinary bladder[236].

Mihai et al[237] studied the number and type of secretory granules in 13 pheochromocytomas and 2 paragangliomas. Large round or elongated medium-density granules were adrenaline-type granules, whereas electron-dense granules lying in a vacuole were of noradrenaline

type. No correlation was found between noradrenaline output and the number or percentage of noradrenaline-type granules, although tumors with normal noradrenaline output had only a minority of this type of granule (less than 25 per cent). Adrenaline-type granules were predominant (77 per cent) in a tumor secreting only adrenaline, but the proportion of adrenaline-type granules in six tumors with normal adrenaline output varied significantly. Liu et al[238] found granules corresponding to epinephrine and norepinephrine granules in all 13 pheochromocytomas studied and did not observe a correlation with urinary catecholamine excretion.

From our EM study and the data in the literature, I conclude that pheochromocytoma and paraganglioma are not synonymous terms and that EM has value in identifying the two neoplasms.

Neuroblastoma

The following report drew attention to the value of electron microscopy in distinguishing pediatric neuroblastomas from other small round cell tumors.

> **Mackay B, Masse SR, King OY, Butler JJ. Diagnosis of neuroblastoma by electron microscopy of bone marrow aspirates. Pediatrics 56:1045-1049, 1975.** Three patients, aged 3 to 8 years, were reported in whom the diagnosis of neuroblastoma was made following EM of a bone marrow aspirate. The ultrastructural features demonstrated that this method could effectively distinguish neuroblastoma from other small round cell neoplasms with which it was often confused by routine light microscopy.

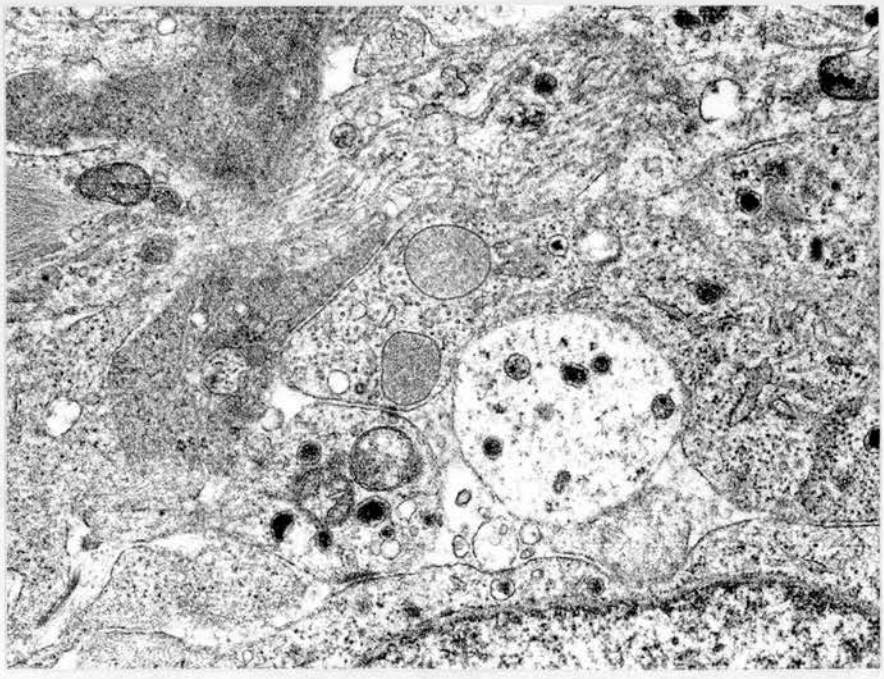

Figure 162. Neuroblastoma, metastatic in bone marrow of a three-year-old boy. Dendritic processes at the edge of a tumor cell are cut in different planes of section. Granules and microtubules are present. x 24,000.

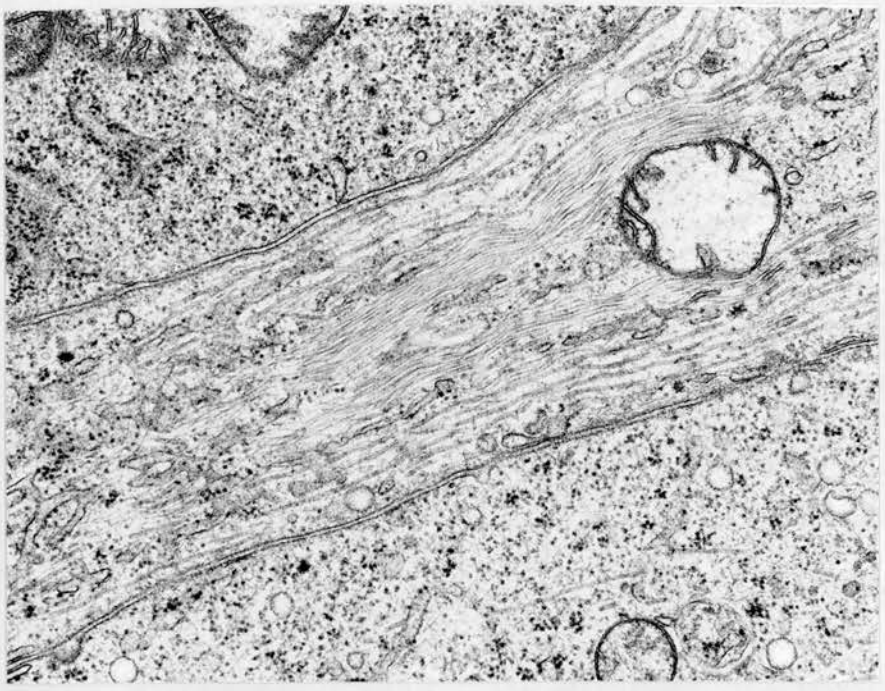

Figure 163. Neuroendocrine tumor cell process containing many microtubules. x 14,000.

Neuroblastoma cells are small and they and their nuclei are round to ovoid with smooth contours except where processes are arising. The dendritic processes of the tumor cells are typically numerous and they cluster, forming groups between cells or occupying the center of rosettes. The tumor cell in figure 162 has a thin band of cytoplasm that contains two small, membrane limited granules. Alongside the cell there are several dendritic processes cut in different planes of section, and one is attached by a primitive cell junction to the cell body. The processes contain numbers of granules, and in one that is obliquely sectioned, microtubules are also present. The longitudinal alignment of the microtubules in a neuroendocrine tumor cell process can be seen in figure 163.

Coexistence of neuroblastoma and rhabdomyosarcoma is unusual. The following case is described as an example. It was documented by EM performed on three sequential accessions.

> **Schmidt D, Mackay B, Osborne BM, Jaffe N. Recurring congenital lesion of the cheek. Ultrastructural Pathology 3:85-90, 1982.**
> A 3 cm purple area on the cheek of a newborn white female was biopsied revealing atypical cells in fibroadipose tissue. By 6 weeks, the lesion formed an irregular 6 cm paranasal mass compressing the nostril and depressing the corner of the mouth, and three small satellite masses were also present. A biopsy established the presence of a malignant neoplasm. Chemotherapy was given, and by six months the lesion was considerably smaller and firmer and the residual 3 cm, well circumscribed nodule was then excised. By 11 months, the lesion had recurred as a round, mobile nodule lateral to the previous surgical site, and the reexcision specimen revealed a firm, pale tan, 2 cm mass. Further chemotherapy was given but the child died at the age of 18 months.

Tissue was obtained for EM study at 6 weeks, 6 months and 11 months. At 6 weeks, both neuroblastic and skeletal muscle differentiation could be found in the small cells. At 6 months, ganglion cells were identified together with scattered neuroblasts and a small round cells contained cytoplasmic myofilaments. At 11 months, small round cells contained sparse organelles with no evidence of dendritic processes, myofilaments, microtubules or dense-core granules. This is an unusual case in my experience, but Tsokos[239] observed in 1992 that primitive tumors with overlapping neural and mesenchymal features were being identified more often than previously, and the term malignant ectomesenchymoma was introduced[240].

Although most patients with neuroblastoma are infants and young children, authentic examples are encountered in adults[241]. This 80-year-old patient is the oldest in whom it has been reported.

Salter JE Jr, Gibson D, Ordonez NG, Mackay B. Neuroblastoma of the anterior mediastinum in an 80-year-old woman. Ultrastructural Pathology 19:305-310, 1995.

A 7 cm anterior mediastinal tumor was detected in an 80-year-old woman. By light microscopy and EM, the tumor fulfilled criteria for neuroblastoma. Immunoreactivity for synaptophysin and chromogranin supported the diagnosis.

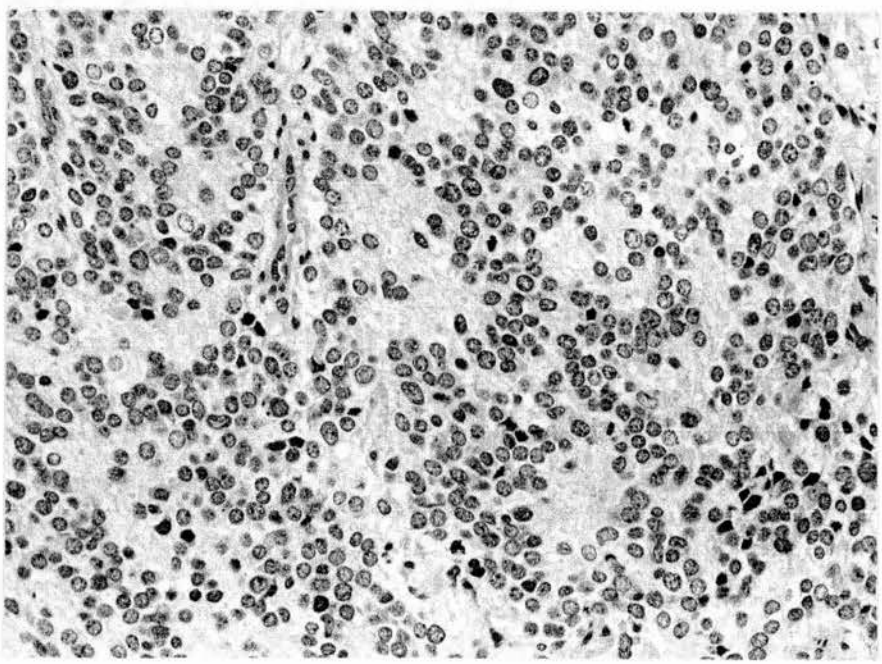

Figure 164. Neuroblastoma from the mediastinum. Hematoxylin and eosin.

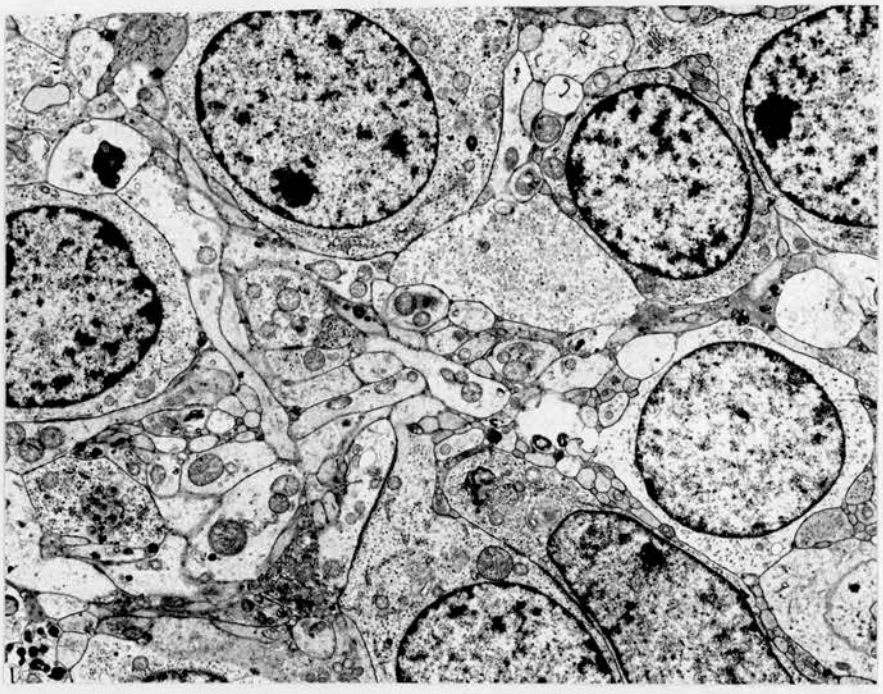

Figure 165. Same tumor as figure 164. A cluster of dendritic process is surrounded by the cell bodies of the tumor cells. x 4,000.

The light microscopic appearance was consistent with the diagnosis (figure 164) and EM and immunohistochemistry provided confirmation. Processes of the small cells tended to congregate in small groups (figure 165). A neuroblastoma in the anterior mediastinum of an adult is a particularly unusual combination that has rarely been recorded. Most intrathoracic neural tumors are in the posterior mediastinum and are benign peripheral nerve sheath neoplasms or ganglioneuromas[242]. Some of the tumors referred to in the past as adult neuroblastomas would now be called neuroendocrine carcinomas, but in this case, the pronounced rosette formation seen by light microscopy and the number of dendritic processes observed by EM merited the designation of neuroblastoma.

It is well known that neuroblastoma may mature to benign ganglioneuromas. The process of maturation in neuroblastic tumors was studied with EM. Dr. John Hicks participated in the electron microscopy.

Hicks MJ, Mackay B. Comparison of ultrastructural features among neuroblastic tumors: maturation from neuroblastoma to ganglioneuroma. Ultrastructural Pathology 19:311-322, 1995.
The study was conducted on 45 neuroblastic tumors (15 neuroblastomas, 15 ganglioneuroblastomas, 15 ganglioneuromas). Poorly differentiated neuroblastomas showed more frequent dendritic processes than the typical neuroblastomas, with sparse dense-core granules and immature schwann-like cells. Ganglioneuroblastomas possessed an admixture of cell types including immature ganglion cells without associated satellite cells together with intermediate cells and differentiating neuroblasts. The neuropil contained immature schwann cells encasing haphazardly arranged neuritic processes. Ganglioneuromas were composed of mature ganglion cells with occasional binucleation.

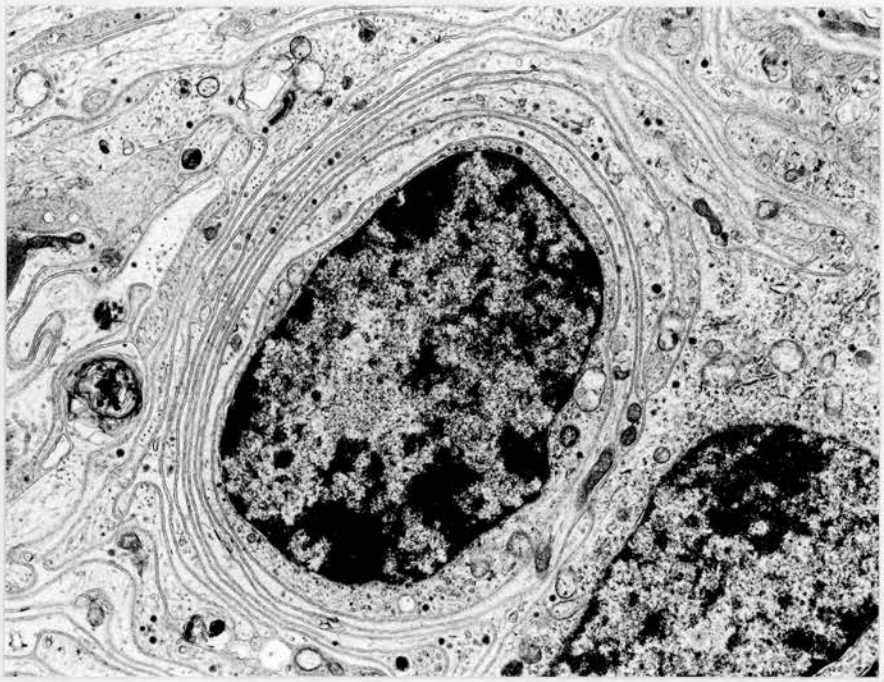

Figure 166. Neuroblastoma. Concentric cell processes at an early stage in maturation. x 8,800.

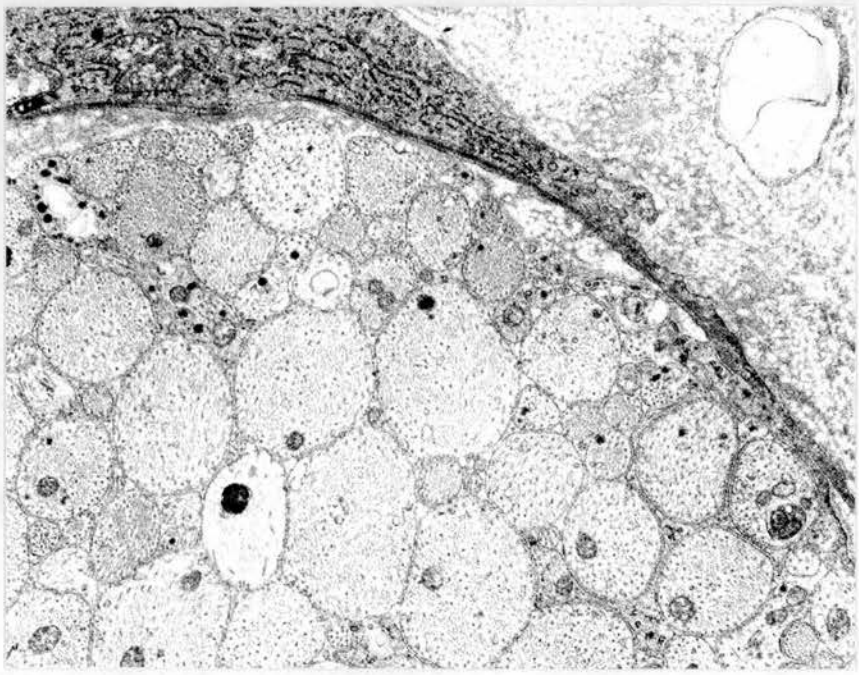

Figure 167. Ganglioneuroblastoma. A myofibroblast curves around the outside of a bundle of neural processes. x 6,400.

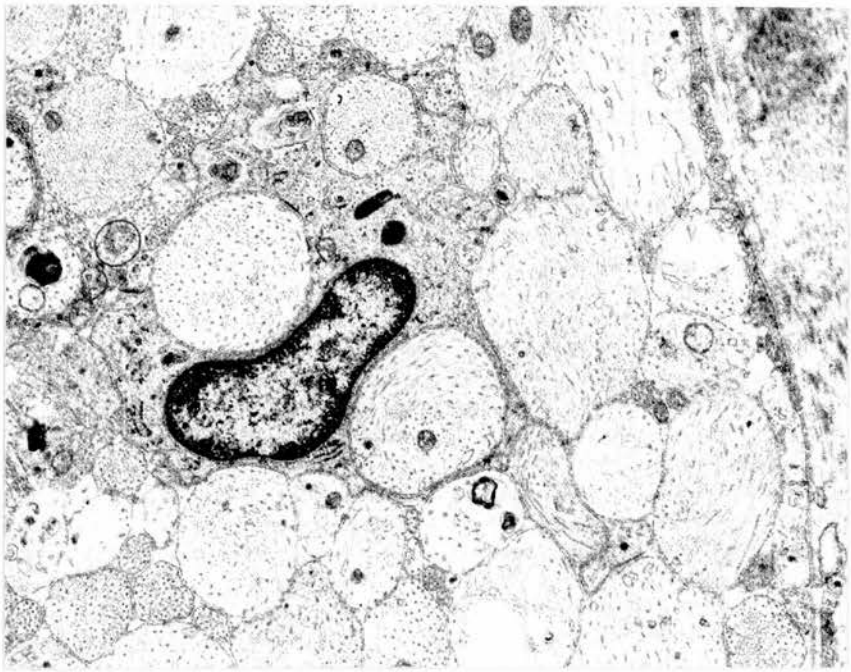

Figure 168. Same tumor as figure 167. A cell has infiltrated a bundle and is wrapping round some of the processes. x 6,600.

Neuroblastic tumors represent a continuum from undifferentiated neuroblastoma through ganglioneuroblastoma to the mature ganglioneuroma. They are derived from primordial neural crest cells which originate from the precursor cells that form the sympathetic nervous system, primarily composed of the adrenal medulla and paraspinal sympathetic ganglia. It is well recognized that neuroblastic tumors are capable of maturation from malignant to benign[243], and maturation can be spontaneous without intervention, or be induced by various chemotherapeutic agents or radiotherapy. The neural crest derived neuroblast has the unique ability to undergo gangliocytic and schwannian differentiation.

With maturation towards ganglion cells, the neuroblast cell size increases with a concomitant decrease in the nuclear to cytoplasm ratio. The neuroblast cell processes are initially haphazardly arranged but they increase in number and length and schwann cell cytoplasm begins to appear (figure 166). In ganglioneuroblastomas, varying views of the maturation process may be seen in EM specimens depending on the stage within the sequence and the areas of tumor sampled. Neuritic processes are often long but rarely grouped into orderly parallel bundles. Ganglioneuromas consist of mature ganglion cells with associated satellite cells in a background of well organized neuritic processes encased by mature schwann cells. The ganglion cell is the neoplastic cell, typified by its large size and the many neuritic processes extending from the cell body. The neuropil is composed of schwann cells and relatively abundant collagen, and the vast majority of neurites are unmyelinated. From our EM study, it appears that the schwann cells may arise from adjacent connective tissue, possibly by modification of fibroblasts. A myofibroblast can be seen alongside a bundle of neurites in figure 167, and it may be that stromal cells infiltrate a bundle to insinuate their cytoplasm between neurites and enwrap them with mesaxons (figure 168).